Fall 2014

Investigating and modeling tar-mats in a Kuwaiti carbonate reservoir and their role in understanding oil reserves and recovery economics

Abdullah Owidah Almansour

Department: Geosciences and Geological and Petroleum Engineering

INVESTIGATING AND MODELING TAR-MATS IN A KUWAITI CARBONATE RESERVOIR AND THEIR ROLE IN UNDERSTANDING OIL RESERVES AND RECOVERY ECONOMICS

by

ABDULLAH OWIDAH ALMANSOUR

A DISSERTATION

Presented to the Faculty of the Graduate School of the

MISSOURI UNIVERSITY OF SCIENCE AND TECHNOLOGY

In Partial Fulfillment of the Requirements for the Degree

DOCTOR OF PHILOSOPHY

in

PETROLEUM ENGINEERING

2014

Approved

Baojun Bai, Advisor

Ralph Flori, Co-Advisor

Waleed Al-Bazzaz, Co-Advisor

Mingzhen Wei

Parthasakha Neogi

ABSTRACT

Tar-mat columns exist in many carbonate reservoirs in the Middle East. Historically, tar-mats have been thought to impede primary oil extraction, thus necessitating further improved oil recovery (IOR) technology applications. However, this research considers tar-mats as potential sources for unlocking extremely difficult crude oil, less than 5 °API. The main objective of the study was to understand the qualitative physical and chemical properties of extremely viscous tar-mat oil and the quantitative potential of tar-mats to extract difficult oil.

The physical and chemical geneses of the tar-mat oil were analyzed utilizing several experimental geochemical techniques, including rock evaluation pyrolysis, liquid extracts (SARA analysis), and Pregl-Dumas (CHNSO) elemental analysis. The results showed that oil recovery increased significantly as the temperature increased, while the heavier compounds, Nitrogen, Sulfur, and Oxygen (NSO), decreased. The geochemical analysis results showed that the Kuwaiti carbonate reservoir under investigation was oil-prone and capable of oil/gas production. Most of the rock samples were thermally mature and good in terms of hydrocarbon generation. Additionally, the Hydrogen to Carbon (H/C) ratio increased as the API decreased. Toluene treatment produced the greatest oil recovery pattern at all tested temperatures, while surfactant and hot water yielded less oil recovery, respectively.

This research proposes a novel method for systematically characterizing and evaluating tar-mat reservoir rocks so that a greater quantity of non-conventional tar-mat oils can be added to the world market. This research also proposes a new model that can contribute to API gravity prediction for solid tar-mats.

ACKNOWLEDGMENTS

IN THE NAME OF GOD, MOST GRACIOUS, MOST MERCIFUL

First and foremost, praise and gratitude be to Allah, my God, the sole Creator and Sustainer of the Universe. His mercies and grace have brought me this far. Peace be upon his prophet Muhammad.

I am highly indebted to King Abdul-Aziz City for Science and Technology for the continued support they have accorded me to continue with my Ph.D. studies at the Missouri University of Science and Technology.

I would like to offer special gratitude to my dissertation committee chairman, Dr. Baojun Bai, for his beneficial help and invaluable guidance throughout this work. I am also thankful to other committee members, Dr. Ralph Flori, Dr. Neogi, and Dr. Wei, for their moral and professional support, as well as for their useful suggestions.

I specially thank Dr. Waleed Al-Bazzaz and Dr. Geetha for their assistance in the experiment, for providing me with the samples to accomplish my work, and for their general laboratory guidance, which was very helpful.

I express my deepest gratitude to my loving, caring, and supportive wife, for her encouragement during rough times. I also wish to heartily thank my entire family for their moral support, patience, and encouragement.

Lastly, I express many thanks to all my friends and colleagues at the university for our memorable and most cherished encounters.

TABLE OF CONTENTS

Page

LIST OF ILLUSTRATIONS

Figure Page

LIST OF TABLES

NOMENCLATURE

Symbol	Description
API	API Gravity of Tar-Mat Oil
BI	Bitumen Index (mgHC/g rock)
CII	Colloidal Instability Index
GP	Genetic Potential (mgHC/g rock)
HI	Hydrogen Index (mg HC/g TOC)
K	Core Permeability (mD)
OI	Oxygen Index (mg CO2/g TOC)
OIP	Oil in Place (cc)
PCI	Pyrolysable Carbon Index (mgHC/g rock)
PI	Productivity Index
QI	Quality Index (mgHC/g rock)
S1	Free Hydrocarbon (mgHC/g rock)
S2	Hydrocarbons Derived from Kerogen Pyrolysis (mgHC/g rock)
S3	CO_2 from Organic Source ($mgCO_2$/g rock)
T_{max}	Temperature at the Highest Yield of S2 Hydrocarbons (°C)
TOC	Total Organic Carbon (wt.%)
S1r	Light Oils of Hydrocarbons in the Range of C1-C22
S2a	Heavy Oils of Hydrocarbons in the Range of C22-C40
S2b	Resin + Asphaltene in the C40+ Range
RCr	Percentage of Residual Carbon in the TOC after Pyrolysis
%Ro	Vitrinite Reflectance (%)
ϕ	Porosity (%)

m_1	Weight of the Sample before Extraction (gm)
m_2	Weight of the Sample after Extraction (gm)
ρ_m	Density Mixture of (Grains + Fluids), (gm/cc)
ρ_{ma}	Matrix Density (gm/cc)

1. INTRODUCTION

1.1. STATEMENT AND SIGNIFICANCE OF THE PROBLEM

Tar-mats are extra heavy oil zones sandwiched between aquifers and adjoining oil columns that isolate an oil reservoir from its aquifer either partially or completely. The presence of tar-mats in oil reservoirs results in rapid pressure drops, prematurely high gas-oil ratios, and low primary oil recovery, all of which point to some form of pressure maintenance early in a field's life (Harouaka et al., 1991). Furthermore, tar-mats create several problems in the extraction of primary oil from carbonate reservoirs, as well as in the IOR application methods. In petroleum reservoirs, the column thickness of tar-mats can vary within the same reservoir and may reach a few hundred feet in thickness. They contain extra heavy oil or bitumen, typically have a gravity under 10° API and/or in-situ viscosity above 10,000 cp, and generally are located at the bottom of the oil column (Nascimento and Gomes, 2004). Asphaltenes are the hydrocarbon components in petroleum with the highest molecular weight, and due to the high asphaltene content, which is usually 20 to 60% of the weight, tar-mats have high gravity and viscosity (Wilhelms and Larter, 1994a). They usually are composed of various amounts of carbon (which contains 100 to 300 atoms per molecule), oxygen, sulfur, hydrogen and nitrogen components, and fractions of vanadium and nickel (Pineda-Flores and Mesta-Howard, 2001).

Several geochemical studies in the literature have discussed the causes of tar-mat formation extensively (Moor, 1984; Hirschberg, 1988). The most widely accepted theories attribute the formation of tar-mats to compositional differences in the oil column

or to the segregation of asphaltenes, either of which can lead to the difference in oil viscosity.

Recently, tar-mat zones at the base of oil columns in large carbonate reservoirs have been identified worldwide. The zones create a barrier, which has a close to zero permeability, that physically separates the high-pressure aquifer or, in other cases, the injection of water wells below the hydrocarbon reservoir, from the producing zones (Al-Umran et al., 2005). Tar-mat columns have been found in various parts of the world, but more so in Middle Eastern nations such as Saudi Arabia, Qatar, south Iraq, and Kuwait. For instance, in Saudi Arabia, in reservoirs such as those found in the Uthmaniya region, the tar-mats tend to stretch up to 15 miles, with a thickness of 500 feet (Al-kaabi et al., 1988).

A tar-mat impacts the neighboring aquifer's ability to support instantaneous removal from the oil zone that borders the aquifer. In severe cases in which the tar-mat totally surrounds the oil zone, the reservoir acts as a restricted lens; a rapid drop in pressure is immediately followed by an alarming rise in the production gas/oil ratio during primary depletion (Osman, 1985). In some instances in which the tar is moving, the pressure difference throughout the tar-mat could intensify to a level that could cause the tar seals to break down rather suddenly, allowing severe water deposition into adjacent wells.

In general, it is believed that tar mobility is the norm, and its extension over the aquifer can be either continuous or discontinuous. Bottom water drive may be hindered by the tar in certain reservoirs, thus completely isolating the oil zone from the aquifer (Bashbush et al., 1983; Al-Kaabi et al., 1988).

The success of initial and secondary oil recovery schemes may be hindered by discontinuous tar-mat obstructions that significantly reduce the vertical and horizontal permeability, which occurs as a result of the tortuous path and changing contact area of the fluid flow during the depletion phase (Richardson et al., 1978).

Tar may "break down" after a certain period of continuous production or injection, so separating the reservoir into a completely independent hydraulic unit using a continuous tar-mat may not be possible. This breakdown occurs as a result of the existence of vertical permeability that contrasts based on the physical characteristics of the tar itself (Osman, 1985). An excessive pressure drop in the oil zone caused by production, or a large pressure increase brought on by injection, can form permeable paths in the tar zone, leading to water coning and excessive water production (Al-Kaabi et al., 1988).

The objective of this study was to develop a quantitative measure by which to investigate the geochemical and petrophysical properties of tar-mats and their economic potential for several proposed EOR methodologies. Designing innovative techniques that can overcome the mobility difficulties worsened by the presence of tar-mats in petroleum reservoirs and measuring with deterministic scientific methods the amount of oil that can be extracted from the tar-mats are critical steps for oil recovery.

An economic tool was used to conduct a sensitivity study that highlighted the economic feasibility of these reservoirs. The results of this study help to reveal the adverse effects of the most influential tar-mat parameters. These results also indicate the importance of studying tar-mat properties and of using novel techniques and methods for the benefit of future hydrocarbon estimation and reservoir recovery.

1.2. OBJECTIVES

The overall objective of the study was to identify methods that can be used to both characterize and improve the oil recovery from tar-mat reservoir rocks. The results of this research could be used to understand the performance of tar-mats in carbonate reservoirs, and to select the best EOR methods for extracting extremely heavy oil from tar-mat reservoir rocks. Specifically, the objectives of the study were as follows:

- To characterize the extremely viscous oil in tar-mats and its recovery attributes using toluene, water, and surfactant injections.
- To study the physical and chemical geneses of tar-mat oil under several temperature variations.
- To integrate novel geochemical techniques to evaluate the in-situ potential of tar-mats.
- To develop a new process design or model for recommending strategies for producing difficult tar-mat oils.
- To understand the performance of tar-mat reservoirs.

1.3. RESEARCH SCOPE

Characterizing tar-mats in carbonate reservoirs begins with examining the rock to identify its physical and chemical properties and composition. Several tools are available for tar-mat characterization, such as geochemical rock pyrolysis using Rock Eval-6, CHNSO elemental analysis using Elementar 106, and conventional SARA analysis of extractable hydrocarbons from tar-mats. Rock–Eval 6 analysis has been used to characterize the varying species of organic matter in bulk samples of recent aquatic

sediments, as well as some reservoir properties, such as the API of tar-mats that cannot be characterized using conventional methods. It also can measure the quantity of CO and CO_2 generated during the pyrolysis and oxidation of samples in an attempt to quantify the extractable hydrocarbons under different conditions. Elementar investigates the presence and amount of carbon, hydrogen, nitrogen, oxygen, and sulfur in tar-mat samples. SARA analysis quantifies saturates, aromatics, resins and asphaltenes in these samples.

Integrating these tools in this study allowed for better characterizations of tar-mat fingerprints and for the following questions to be weighted, measured, and answered:

- Can the problem of oil mobility be overcome through the presence of tar-mats in carbonate reservoirs?
- What quantity of oil can be recovered from tar-mat layers?

Figure 1.1 illustrates the primary stages of the proposed research. The Research Methodology section includes an explanation of each task.

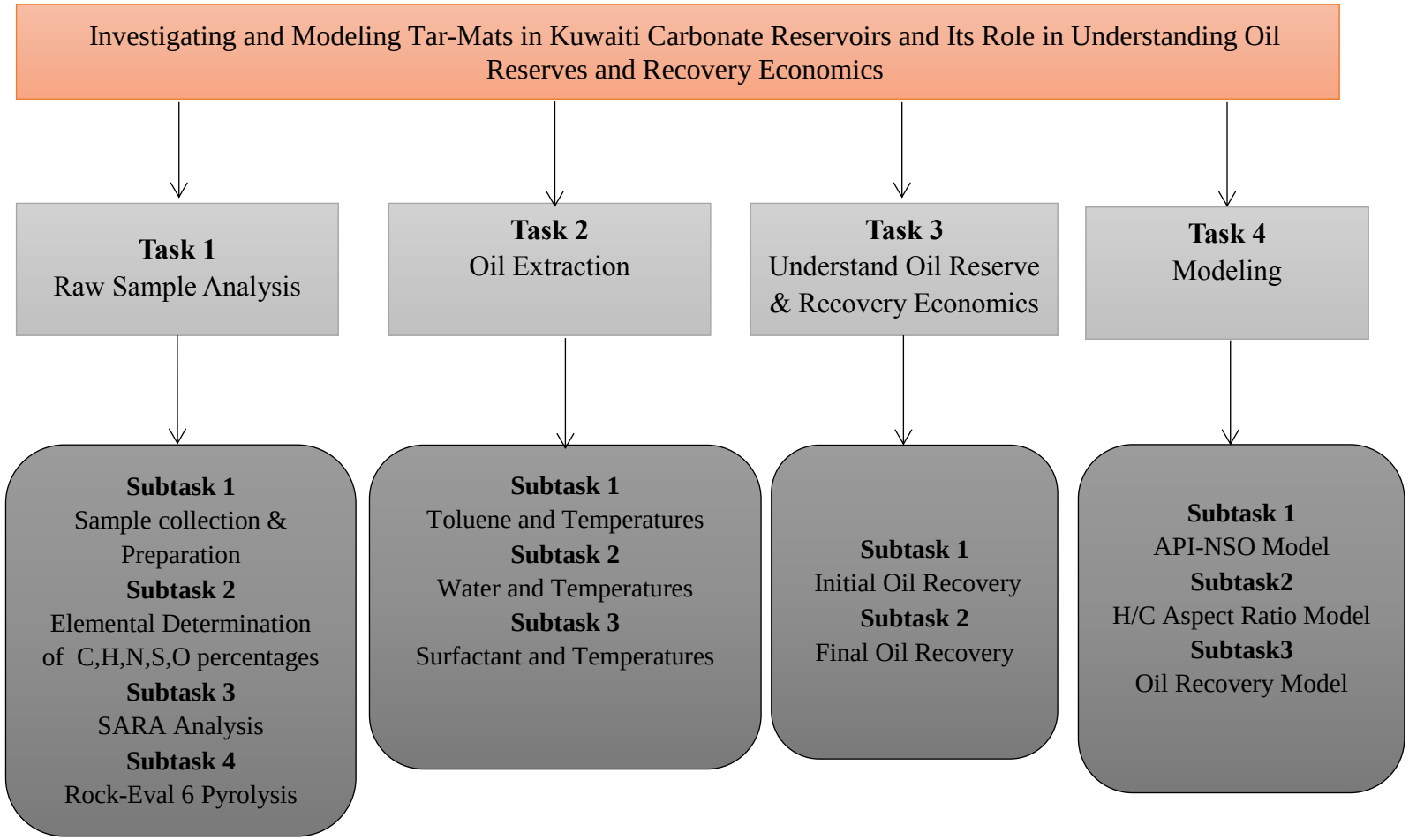

Figure 1.1. Planned Project Tasks

2. REVIEW OF THE LITERATURE ON ASSOCIATED TECHNOLOGIES

2.1. DEFINITION OF TAR-MAT

The definition of a tar-mat, which is a generic term for tar-mat and bitumen, varies across authors. However, a tar-mat typically can be described as an extra heavy oil zone sandwiched between an aquifer and an adjoining oil column, as depicted in Figure 2.1. It isolates an oil reservoir from its aquifer either partially or completely (Harouaka et al., 1991).

The definition of a tar-mat, as used in the field of organic geochemistry, was proposed by Wilhelms and Larter (1994a) as a "Reservoir zone containing petroleum strongly enriched in asphaltenes relative to the related oil leg petroleum. Tar-mats usually have a sharp boundary with the oil leg" (p. 441). Furthermore, "Tar mats can best be described as compositionally sharply defined zones of petroleum columns often close to geological discontinuities including, but not limited to, oil-water contacts (OWC) which are enriched in asphaltenes relative to the oil leg up to concentrations of around 20-60wt.% of the C15+ fraction of petroleum" (p. 418).

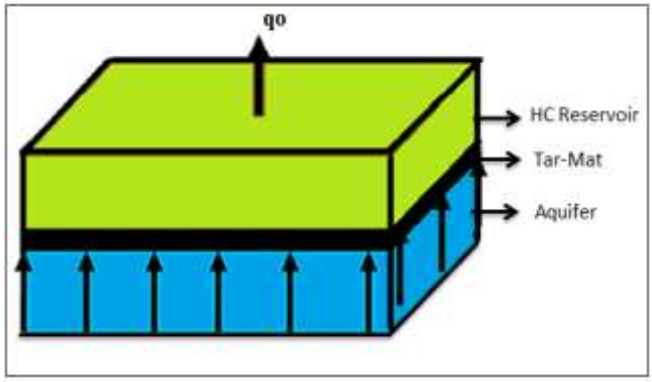

Figure 2.1. Tar-Mat Layer Occurs between Aquifer and HC Layers

2.2. TAR-MAT FORMATION AND DISTRIBUTION

2.2.1. Tar-Mat Formation. Moor (1994) contributed significantly to the tar-mat literature with his studies on the presence, distribution, and nature of tar-mats, as well as asphaltic sands and bitumen, in reservoirs. He identified the following four contributors to the formation of tar-mats:

1. Water Washing: A portion of light hydrocarbons is removed, allowing the asphaltic fraction to locate itself at the foundation of oil accumulation.
2. Gravity Segregation: The resistance attracts the heavier hydrocarbons towards the foundation, and the lighter hydrocarbons move upward.
3. Natural Deasphalting: Natural gases enter from the source rock and rise through the hydrocarbon column due to buoyancy, resulting in lower solubility and causing the asphaltic fraction to precipitate and rest at the foundation of the reservoir.
4. Biodegradation: Meteoric water moves beneath the pooled reservoir, transmitting bacteria that metabolize crude oil's lighter fraction. Thermal currents located in the reservoir distribute the lighter fraction to the oil/water located at the base, where the bacteria are active. As a result, tar-mats form near the foundation of the reservoir.

Compositional variation can be observed in many reservoirs (Hirschberg, 1988). In the case of light oil, strong compositional grading occurs if fluid is critical, while in the case of heavy oil, it occurs due to the isolation of asphaltenes. The biggest drawback of asphalt isolation is the resulting difference in oil viscosity and the production of tar-mats. The compositional grading of oil in reservoirs by gravity is due to the heavy polar mechanism. Asphaltene isolation has a more significant effect in the case of heavier oils.

A simple molecular model was designed to measure asphalt segregation and the effect of asphalt on crude viscosity.

2.2.2. Tar-Mat Distribution. Moor's research (1994) can be extended to other areas, such as the five different groups of subsurface tar seals that occur due to the level of concentration, continuation, and the structural position. The hydrocarbon distribution over entire bases or within individual traps is controlled by tar seals associated with unconformities. Additionally, tar seals occurring at unconformities are categorized into the following five different groups, as shown in Figure 2.2:

(i) Tar seals with four-way closures located above traps

(ii) Tar seals located alongside the margins of overly mature basins

(iii) Oil first trapped by tar seals and then reallocated through basin deformation

(iv) Oil trapped by tar seals and deeper structures

(v) Tar seals that advantageously trap oil

Reservoirs having many levels of these characteristics are known as tar-mat reservoirs. They can be found across the world but are located mainly in the Middle East (Moor, 1984).

To address the isothermal asphaltene compositional grading in a constant gravitational field, Panuganti et al. (2011) suggested an algorithm that makes use of the perturbed-chain statistical associating fluid model (PC-SAFT) equation of state (EoS). The concept has been proven by data from well logs and output information. Comparisons between the information collected from the well and the output data should inform decisions about calculating the reservoir divisions. Such comparisons also provide

an exact diagnostic answer that can help in the classification of compositional asphaltene, as a thermodynamic reaction to the solution emerges as well. In some cases, the way in which asphaltene composition has been categorized can lead to tar-mat formation. In research conducted by Panuganti et al. (2011), PC-SAFT asphaltene composition grading was extended to model the possibility of tar–mart formation as a result of the gravitational segregation of asphaltene.

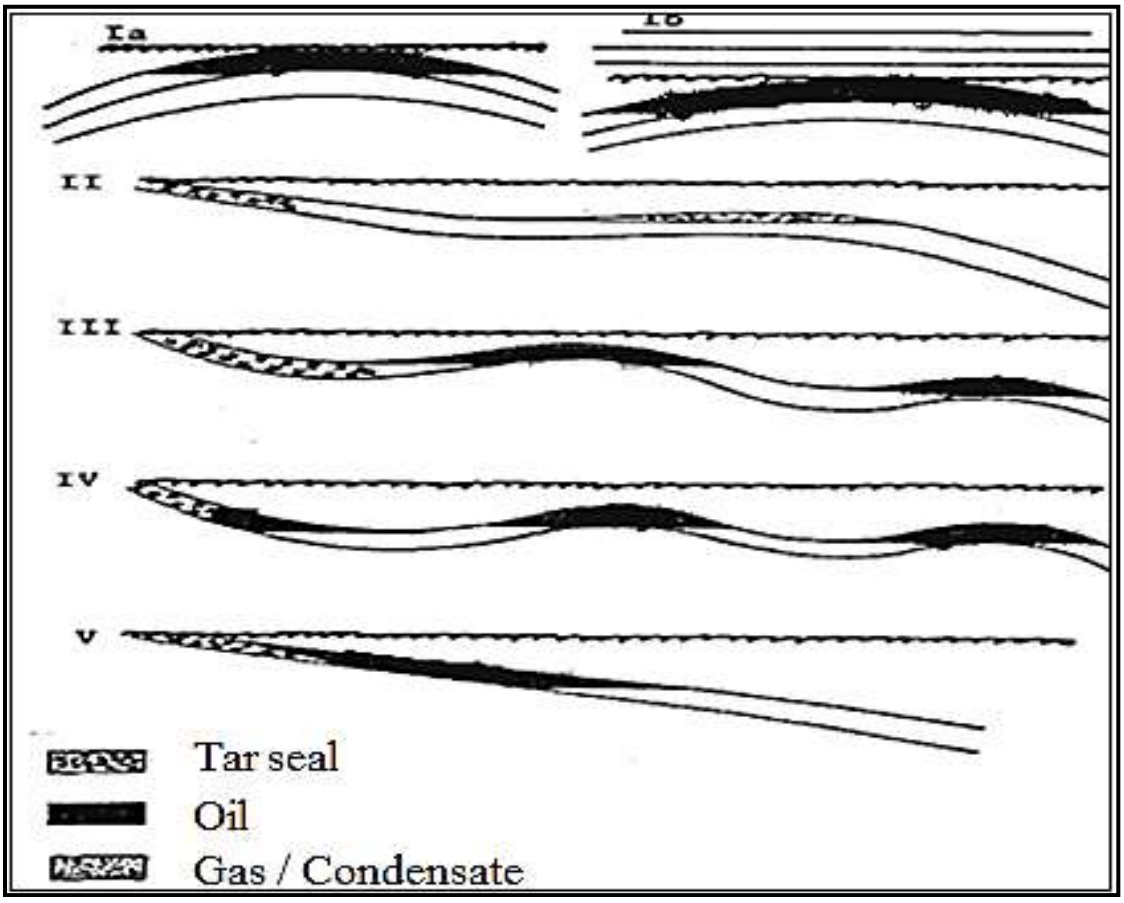

Figure 2.2. Tar Seal Classification (Moor, 1984)

2.3. TAR-MAT CHARACTERIZATION

Tripathy (1988) compared the two approaches that are often adopted to characterize tar-mat in a model. These entail characterizing tar in a model such as: 1) high-viscosity hydrocarbon fluid, or 2) relatively impermeable rock matrices. However, considering these approaches, it becomes evident that none of the models offer or even maintain unique adaptability of occurrence of the particular tar zone under study. This therefore suggests that it is not possible to rigorously characterize a tar zone in a model. However, it is quite possible to successfully apply the two approaches that have been discussed in this chapter to any field situation, as long as the suggestions listed below are considered.

i. A tar-mat at the lower end of the viscosity scale where the pressure is 100MPa's could be modeled sufficiently as hydrocarbon fluid. This is also a valid consideration in situations in which the high pressure could cause tar displacement. However, for high-viscosity tar, tar-mat modeling is only justified as a part of the aquifer system.

ii. A tar-mat that had previously been intact and that only broke down at a later time, or one that has a chance of breaking down on the basis of similar deposition information, should be modeled as part of the reservoir fluid system, irrespective of viscosity.

Waxman et al. (1980) conducted the first quantitative study investigating the dynamic characteristics and mobility of tar-mats under isothermal reservoir conditions. Their series of experiments focused on the Peace River and Berea cores in order to investigate the mobility of tar and brine.

The flow runs were conducted at temperatures between 380 ^{0}F and 389 ^{0}F, with a fluid backpressure of 400 psig and an overburden pressure held at 1500psig. In the flow studies, Waxman et al. (1980) employed two different approaches: 1) continuous single-phase (tar) recycle flow, and 2) a single pass-through with two-phase flow (tar/brine), including a permeability determination of a steady state.

Waxman et al. (1980) determined that the tar and brine mobilities of the Peace River core declined under the single-pass flow approach when they used thermally unaltered tar. However, the investigators were unable to obtain steady-state permeabilities in the Peace River flow runs. In the single-phase recycle flow approach with unaltered tar, the mobility of the tar largely decreased in the Peace River core, but the values continued to be at a steady state. Additionally, Waxman et al. (1980) discovered that the movement of inorganic fines can significantly impair permeability throughout the duration of recycle flows. The findings demonstrate that thermally altered tar, or regular tar mixed with even a small amount of thermally altered tar, is stable and highly mobile under both the single-pass and recycle-flow approaches.

2.3.1. Chemical Characterization of Tar-Mats. Harouaka et al. (1991) studied the chemical characterization of tar-mats in carbonate reservoirs in order to determine the mobility of the tar and to understand various ways of initiating contact between the water and oil zones. They used two different methods to extract a sample, including extracting it from the core and taking a bottom-hole fluid sample. In examining the sample, they used the high-performance liquid chromatography (HPLC) technique to quantify and separate the hydrocarbons from the tars. The results demonstrated that the tar properties

varied even if the depth and area were in the same field, and also that the carbon-to-hydrogen ratio increased systematically as the API gravity decreased.

2.3.2. Physical Characterization of Tar-Mats. Harouaka et al. (2002) researched the detailed physical characterization of tar-mat from a carbonate reservoir in Saudi Arabia to evaluate its mobility and methods of establishing contact between the lighter oil and its aquifer. They simulated reservoir pressure and temperature conditions at which to measure the density and viscosity of several tar samples.

Additionally, the simulated distillation, pour point, and penetration index were determined experimentally. The results showed that the physical properties of the tar depended on the depth and area of the same field. The density and viscosity gradually increased from the tar/oil contact towards the tar/water contact, with a much more significant increase in the neighborhoods of the tar/water contact. Lastly, the density and viscosity of tar diluted with toluene were quite similar to that of pure tar.

2.3.3. Nuclear Magnetic Resonance (NMR) and Conventional Logs. Nascimento and Gomes (2004) presented field examples of tar-mat characterization from Nuclear Magnetic Resonance (NMR) and conventional logs, supported by formation pressure measurements in the aquifer and oil leg. Despite a very clear continuity of the reservoir all along the aquifer and oil leg, with an obvious oil-water contact OWC, the pressure data showed evidence of depletion by production in the oil column, and no pressure drop was noted in the water zone.

Jedaan et al. (2007) studied tar-mat characterization in order to understand its formation mechanism, also evaluating its occurrence in wells and its type, thickness, and distribution in various rock types. They then propagated this distribution in a 3D reservoir

model for the entire field. Asphaltene was found to fill a significant part of the porous network. After correction using Jacob's formula, the measurement of the reflectance by white reflected light yielded a maturity between 0.76% and 0.83% Ro eq, which resembled the first half of the "oil window." Part of the bitumen was observed to be insoluble in organic solvents, even after a protracted extraction. The study concluded that the tar mat was not kerogen and not a result of the biodegradation of oil because bitumen deposits formed by biodegradation are usually soluble in organic solvents and would not cause the tar-mat to undergo thermal alteration.

To improve reservoir tar-mat research, asphaltene science and a new method, down-hole fluid analysis, have been merged to produce the industry's first predictive EoS for asphaltene concentration grading. This was accomplished using the asphaltene nanoscience model and the modified Yen model, also called the Yen-Mullins model (Zuo et al., 2012). The analysis combines FHZ EOS and the measurement of these gradients by using down-hole fluid analysis to effectively consider many reservoir properties, including the 0o fluid disequilibrium, reservoir connectivity, and viscosity gradients. One may decide to make the asphaltene concentration gradients large based on the gravity term and gas/oil ratio (GOR) gradients, as shown by the EOS model. FHZ EOS then reduces to a very concise form. This procedure also can be applied to calculate the asphaltene concentration gradients.

The following two types of tar-mats will be discussed: 1) a large, irregular increase in the asphaltene concentration at the base of the oil column, and 2) an uninterrupted increase in the asphaltene concentration at the base of a heavy oil column. In order to investigate the asphaltene concentration grading and tar-mat production in

reservoirs, a very powerful new approach is introduced through these methodologies by integrating the FHZ EOS with DFA technology and the Yen-Mullins model (Zuo et al., 2012).

2.4. EOR METHODS TO ENHANCE OIL RECOVERY FROM OIL RESERVOIRS WITH A TAR-MAT BARRIER

2.4.1. Water Flooding. Investigating oil recovery from a bottom water-drive reservoir with a tar barrier primarily involves determining the range of oil recoveries, implementing water flooding to recover oil, and increasing oil recovery by scattering tar using steam and solvents (Shamaldeen and Ali, 1985). Three models were used in the experiment, a vertical model (consisting of an oil zone, tar zone, and water zone), a cylindrical model (provides useful insights), and a rectangular model (also called a box model and used for detailed study). When the contact between the oil zone and the bottom water drive is very low, water flooding appears to be quite useful. Injecting solvent into a tar zone can improve the efficiency of tar mobility; dissolving the tar through steam injection is effective if this is a feasible option and if adequate injections are given.

Abu-Khamsin et al. (1993) used a tar-mat reservoir laboratory model to study the effects of tar viscosity, the thickness of a tar zone during oil recovery, and the pressure variation and average water saturation in the tar. Water flooding experiments were conducted in which the three adjacent oil, tar, and water zones were simulated by means of a berea composite core saturated with kerosene, a blend of asphalt and crude oil, and KCl brine, respectively. In each experiment, brine was injected at a constant rate into the water zone and was forced to penetrate the tar zone to flood the oil zone. The results

demonstrate that as the viscosity and the thickness of the tar zone increased, the oil recovery increased. However, at average water saturation in the tar zone, the opposite effect was found, meaning that as the thickness of the tar zone decreased, the rate of oil recovery increased. The injection pressure exceeded its previous maximum shortly after injection commenced and continued to increase as the tar viscosity and tar zone thickness increased. However, the effective permeability of water seemed to be smaller in tests in which the product of tar viscosity and thickness was higher. Finally, the water saturation distribution in the oil zone combined with the pressure behavior points caused water fingers to develop in both tar and oil zones.

2.4.2. Solvent and Hot Water. Tobey et al. (1993) studied the effect of extraction with several solvents on the permeability and porosity of core plugs from a tar zone in the Arab–D formation in order to understand how tar obstructs rock pores. Thin sections of the extracted rock were examined microscopically to determine where the tar was distributed and how that distribution corresponded with permeability and porosity data. The results demonstrated that while increasingly polar solvents continued to remove white organic matter, the permeability, which is controlled by the macropore system, showed very little improvement. However, the marginally accessible porosity was largely blocked by tar. In the larger scheme of the experiment, the results of the elemental and pyrolytic analysis of the core sample taken before and after the extraction indicated that the tar was not homogeneous and not uniformly distributed inside the well or from well to well. The results also indicated that certain components of tars are not soluble to any of the organic systems used.

Okasha et al. (1998) investigated and evaluated the role of combined solvent and hot water injections beneath the tar-mat in the improvement of aquifer support by displacing and dispersing tar, as shown in Figure 2.3. The results of their study show that while oil recovery from hot water displacement was lower than that from cold water displacement in the absence of tar, hot water led to the recovery of substantially more oil than cold water in the presence of a tar-mat. An optimum slug size exists for maximizing hydrocarbon recovery; however, dividing the optimal slug size into portions separated by small slugs of hot water further increased recovery. Lastly, an important factor affecting oil recovery was the injection rate for all hot water flooding schemes; lower injection rates increased oil recovery.

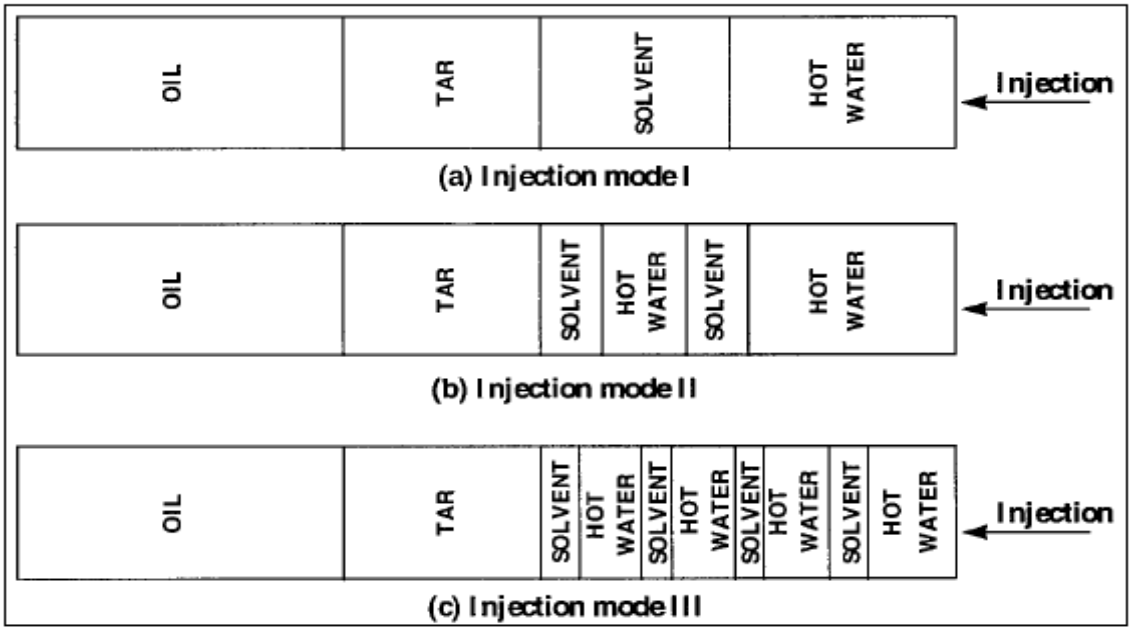

Figure 2.3. Different Injection Models (Okasha et al., 1998)

Al-Kaabi et al. (1988) focused on tar-mat reservoirs subject to bottom water drive. In order to study the behavior of the water oil ratio (WOR) and oil recovery, four different shapes of tar layers were simulated: 1) a square barrier beneath the well, 2) a disk beneath the well (Figure 2.4a), 3) a hollow square or disk beneath the well (Figure 2.4b), and 4) a half plane. The results of the study demonstrated that the earliest breakthrough occurred in the case of hollow tar-mat barriers, and a significant delay was observed in the tar-mat barrier shaped like a dish beneath the well. Unexpectedly, in the case of a half-plane tar-mat barrier, the WOR increased rapidly, becoming higher toward the end of the depletion in comparison to the other three cases. None of the no-barrier cases yielded the highest recovery, but the hollow tar-mat barrier yielded the lowest recovery.

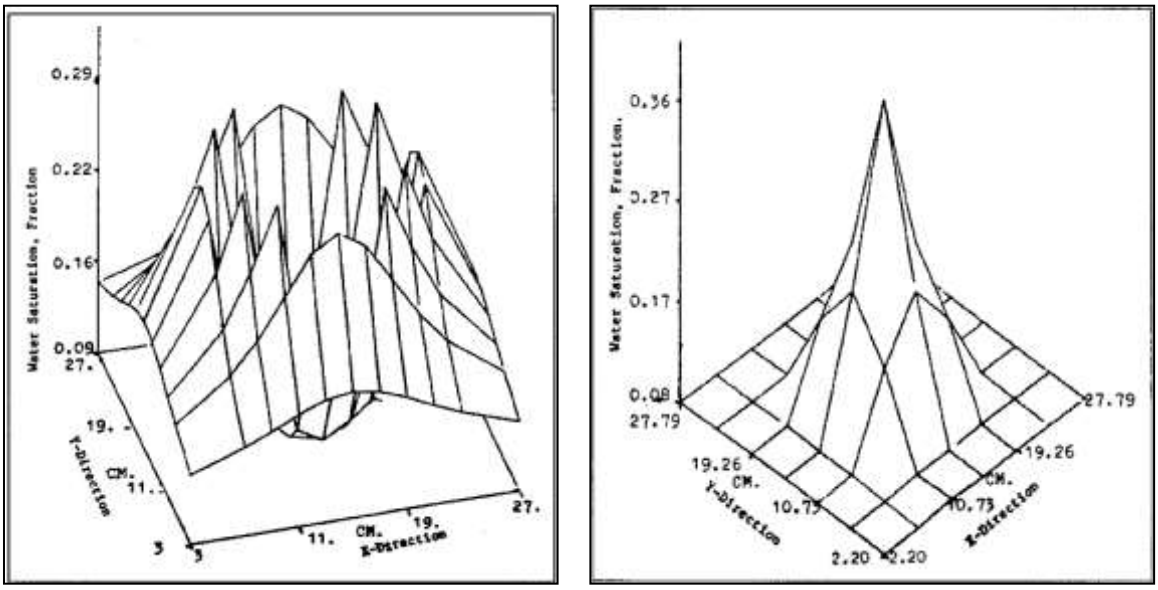

(a) (b)

Figure 2.4. 3D Plot of Water Saturation Distribution of Top Layer: a) before break-through-disk-barrier case, b) after break-through-disk–barrier case through-hollow-square-barrier case (Aziz Al-Kaabi et al., 1988)

2.5. METHODS TO OVERCOME POTENTIAL PROBLEMS CAUSED BY TAR-MAT ZONES

Al-Umran et al. (2005) addressed two strategies for overcoming potential problems caused by tar-mat zones. The first strategy involved drilling a tunnel well diagonally across the tar zone, thus connecting the water injection area (high-pressure area) with the oil production area (low-pressure area). The connection of these two areas improved production from the nearby wells and revived the dead wells. As a result, two formerly dead wells, as well as other producers, experienced a significant increase in oil production. A total of 4.8 MBD was gained as a result of drilling the tunnel.

Figure 2.5 and Figure 2.6 illustrate the connection of the two areas in more detail. The second strategy offered by Al-Umran et al. (2005) was a multi-stage matrix acid treatment applied during the power injection, which increased the production in the well and reduced functional hurdles. Both approaches showed the potential to be highly effective at decreasing the effects of the tar-mat zones depending upon the characteristics of the reservoirs.

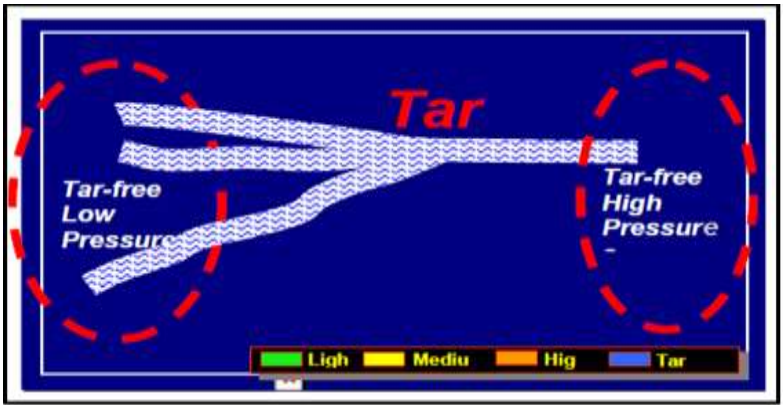

Figure 2.5. Transmitting Pressure from High-Pressure to Low-Pressure Zones (Al-Umran et al., 2005)

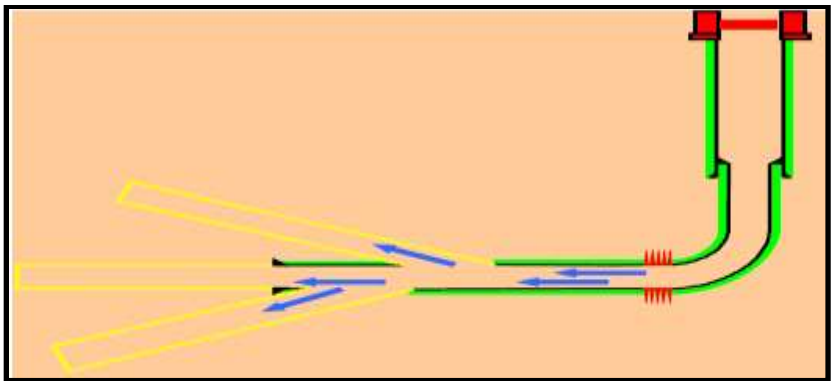

Figure 2.6. Sketch of Tunnel's Flow Path Well (Al-Umran et al., 2005)

Tripathy (1985) discussed the mobility of reservoir fluids across continuous tar zones that had been characterized to separate the oil reservoir from the aquifer tar zones through which water influx was viable in order to deliver partial pressure support to the producing oil column. He proposed optimum water-injection locations for a reservoir requiring additional pressure support. As a result, tar occupying the pore spaces in the 'tar zone' rock matrix was defined as a highly viscous reservoir fluid, representing an extension of the pressure-volume-temperature (PVT) characteristics of the oil column.

Tripathy (1985) also presented case studies utilizing a hypothetical cross-sectional reservoir model to characterize the identity of continuous tar zones. The influence of a large aquifer was simulated through external injectors located outside the tar column.

Combustion tube tests are conducted only when the manufactured tar and the original reservoir tar have the same chemical and physical properties. In a study conducted by Abu-Khamsin, (2002), Ottawa sand of 20-30 mesh size was used to prepare a tar-sand mixture having 37% porosity, 21-32% tar saturation, and 19-25% water saturation. Tar burns easily above 500C, but the oxidation property makes it challenging

to prolong combustion through a tar-saturated sand pack. Also, a large concentration of iron may impair the combustion performance. In this experiment, a minimum iron concentration of 2700 ppm proved effective for tar combustion.

Richardson et al. (1978) contributed to the tar-mat literature by developing a mathematical model used to describe the entrapment of oil above a physical barrier when oil is being displaced by gas, as shown in Figure 2.7. Their model consisted of the following equation developed by Richardson et al. (1978) that first and foremost calculates the time required for oil to drain from the barrier (Eq. 1):

$$(t - ti) = \frac{392.7 \mu o f (1 - Swi) E D b^2}{KH \Delta \rho} \left[\frac{1}{H} - \frac{1}{Hi} \right] \quad (1)$$

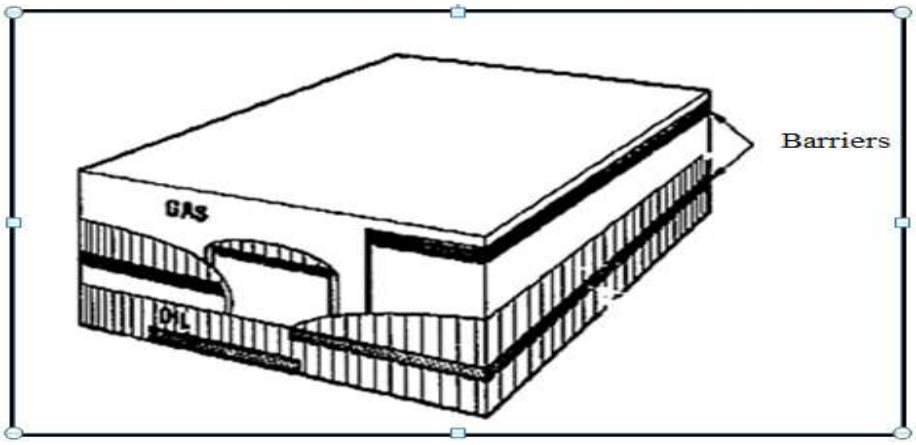

Figure 2.7. Oil Draining off Barriers (Richardson et al., 1978)

In the second part of their experiment, Richardson et al. (1978) designed a fine-grid computer model to investigate the effects of discontinuous barriers on oil recovery, with the primary objective of validating the mathematical computer model. Secondly, they developed a method by which to simulate the effect on oil recovery of small and discontinuous barriers located in simulators with large block sizes. They discovered that the wider the barrier, the smaller the recovery (Richardson et al., 1978).

Al-Ali (1988) conducted another study on tar-mat reservoirs and the different methods and strategies used to enhance oil recovery through their localized communication. An areal model of 19x34grids was used to simulate a typical Middle Eastern tar-mat. The grids varied in size depending on which zones they were in; for example, in the oil zone, the grid sizes were approximately 1 kilometer, whereas in the aquifer zone, they ranged in size up to several kilometers.

Additionally, Al-Ali assumed that the oil zone and the water zone were in complete isolation, which helped simulate the mobility of tar. Also, the transmissibility of tar blocks was reduced severely to help in the implementation of the simulation (Al-Ali, 1988).

Based on his experimental results, Al-Ali (1988) observed that oil recovery is enhanced through the gained potential of the intercommunication between oil and water zones and that while intercommunication helps, the size of the communication opening positively affects the amount of recovery. In other words, a small opening leads to lower recovery values, and combined with the high pressure in the tar and the unfavorable mobility of water, a high probability exists that coning will dominate (Al-Ali, 1988).

Al-Mutairi et al. (2012) discussed the consequences of acid and its worm-holing behavior on tar and on carbonate rock saturated with crudes having varying °API gravities. The results indicated that consistent and emulsified acids produced similar wormhole penetration in tar. Tar formations had difficulty exhibiting face dissolution at extremely low injection rates. In general, the penetration and benefit from emulsified acid decreased when higher °API oil saturated the rock, as shown in Figure 2.8. The wormhole breakthrough volume in a rock saturated with intermediate oil was less than that of a rock saturated with condensate oil. Condensate might have allowed better diffusion of acid droplets to react with the rock. This work provided essential insight that can help to overcome challenges in this area. In addition, these results are of special interest when long, horizontal injectors or producers are placed within the tar zones of conventional oil reservoirs.

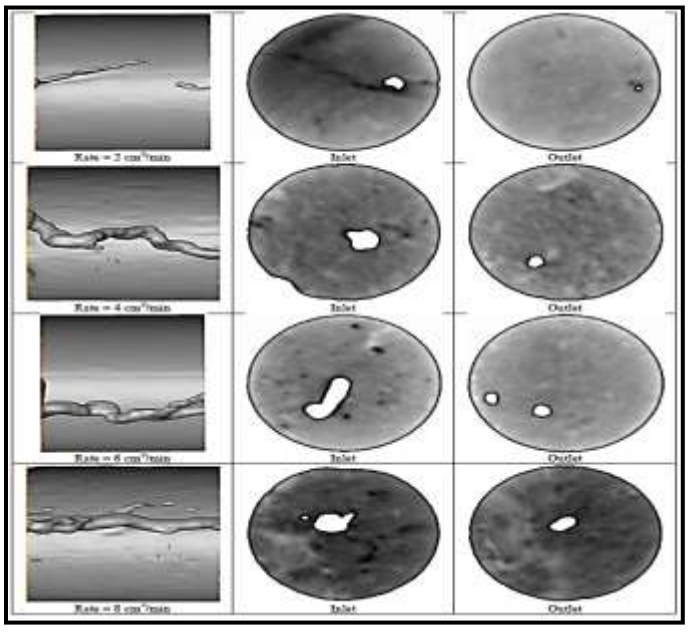

Figure 2.8. Wormholes in Plugs Saturated with Condensate Oil after Acidizing with Emulsified Acid (Al-Mutairi et al., 2012)

Illustrations of the quantitative geological control of fluid property variations show how petroleum geochemistry can be used to swiftly produce high-resolution fluid property images of tar, sand, and heavy oil reservoirs (Larter et al., 2006). In heavy oil reservoirs, the effect of viscosity disparities on production depends on the recovery method. Numerical thermal reservoir simulations have revealed that oil viscosity heterogeneity with a vertical viscosity profile in the reservoir decreases the oil production volumes from steam-assisted gravity drainage in geologically realistic reservoirs relative to results from corresponding model runs with constant normal viscosity profiles. Parallel outcomes have been found for the cyclic steam stimulation (CCS) process. In cases with viscosity profiles, the relatively high viscosity at the base of the reservoir slows the growth of steam chambers relative to that in uniform viscosity reservoirs. These cases also illustrate how the chemical fluid heterogeneities are able to foretell the oil viscosity from well cuttings and/or cores, and to de-mix produced oils into zonal contributions from varying parts of the well where production has taken place.

Haggag and Al-Yaaqoobi (2008) investigated the methodology used to evaluate the occurrence of bitumen in the well, its thickness, and its distribution across the field. Their results suggested that the evolution of bitumen’s structure is very important in tracing it in non-cored wells and defining its intervals in new wells. Overall, the paper contributed to a better understanding of reservoir performance in the presence of bitumen intervals and enhanced the reservoir history match of the 3D reservoir model. The results of this study have had a significant impact on the field; they currently are being used to inform several ongoing, full-field reservoir studies.

Acharya (1987) used two different approaches in his research, each on a different reservoir, A and B. In the first approach, he simulated the behavior of the tar, and in the second approach, he transformed the relative permeability. Both approaches yielded a good response and primarily showed that in both reservoirs, the tar-mat initially acted like a barrier; then, after production continued at the same ratio, the pressure differential in the aquifer and the oil zone increased and had enough power to break down the tar-mat layer.

Osman (1985) studied the Minagish field located in Kuwait, which represents a very typical case of tar-mat reservoirs in which tar exists at the OWC and usually has a thickness between 30 feet and 115 feet. Figure 2.9 presents the average rock properties and the structural cross-section of the MN-26 injector showing the tar-mat.

Initially, water flooding was to be conducted below the tar-mat in the Minagish field, which served as the impetus for discussing a possible tar-mat breakdown due to water flooding below the tar zone. Figure 2.10 illustrates the graphical method that Osman used to predict the different pressure rates at the tar-mats depending on the injection rate and time. Figure 2.11 depicts the curves of the differential pressure of the injected water versus the injection time depending on the distance of the injector. The most important result of Osman's study was the discovery that water injection had the biggest impact on differential pressure across tar-mats, followed by oil production. Lastly, Osman recommended a way to observe the response time at the well, which gives the operator time to switch the injection from below to above the tar-mat (Osman, 1985).

Osman's model serves as a very simplistic way to represent such a complicated problem. However, the paper contained the following questionable assumptions and

uncertainties. The tar-mat was considered a rigid barrier breaking at 15psi/foot as a pressure gradient. The pressure increase due to water injection was considered preeminent, but the pressure decrease due to oil production insignificant. The way in which the superposition theory was applied was unclear. The paper contained no mention of the rheology or other characteristics of the tar. Lastly, the paper did not provide or discuss a geometric description of the broken tar-mat.

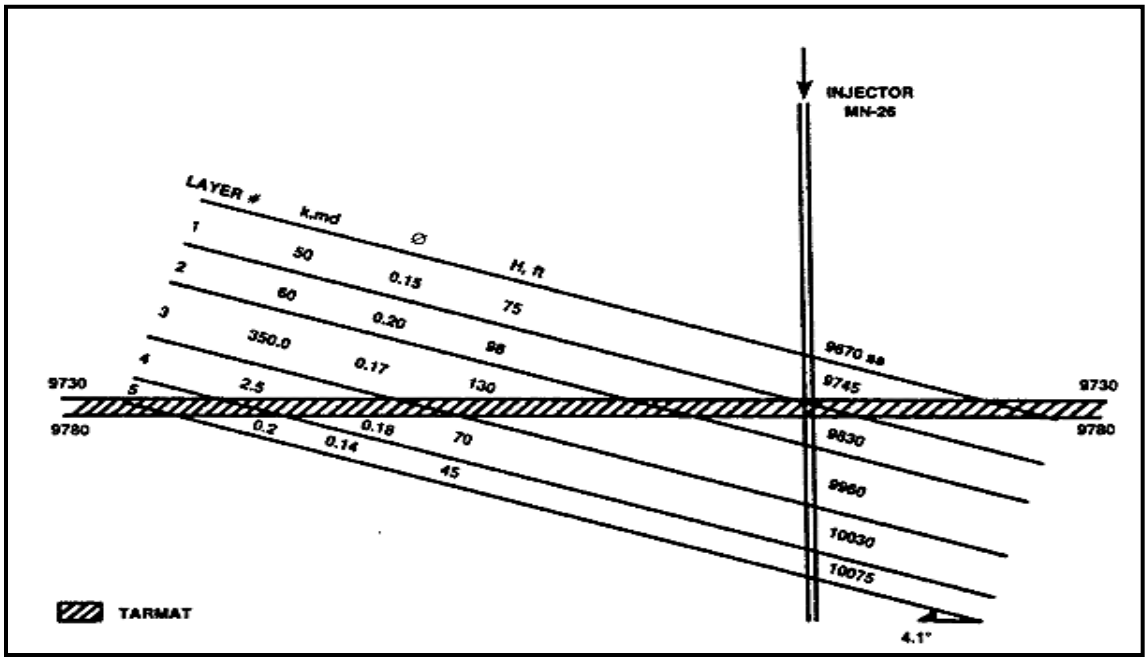

Figure 2.9. Structural Cross-Section of Northern Pilot Injector MN-26 (not to scale) (Osman, 1985)

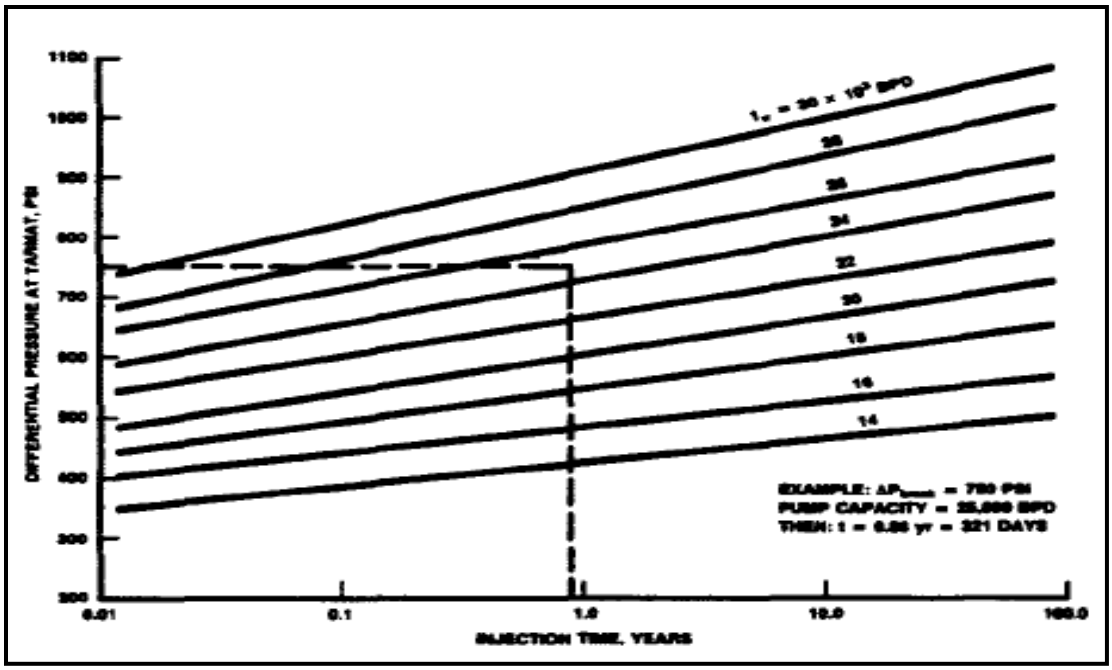

Figure 2.10. Differential Pressure vs. Injection Time for Different Injection Rates (Osman, 1985)

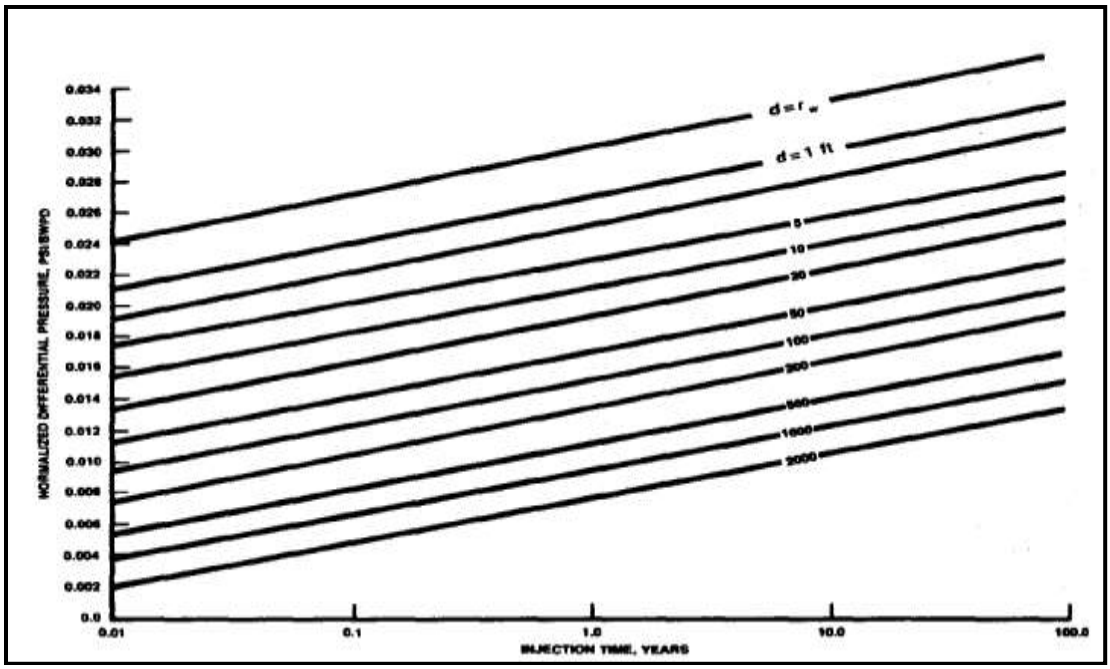

Figure 2.11. Differential Pressure vs. Injection Time for Different Distances of the Tar-Mat from the Injector (Osman, 1985)

An extension of Osman's work examined the results of having a sealing fault close to the water injection and the influence of the sealing fault on the behavior of the tar-mat (Osman, 1985). The study resulted in a technique that can calculate the time of the tar-mat breakdown, the response time at the nearest well, and the differential pressure at a tar-mat located anywhere in the reservoir (Osman, 1985).

Many researchers have discussed the tar-mat related problems that occur in reservoirs. Osman (1988) observed the following two major behaviors: 1) the behavior of a tar-mat given water injection by an injector with no faults, and 2) the behavior of a tar-mat given water injection by an injector with some faults. The case discussed by Osman (1988) contained two different faults, so the behavior of a tar-mat anywhere in the reservoir could be predicted graphically or analytically. Increasing the distance of the injector from the two faults decreased the effect of the injector on both faults or caused it to become very linear. A model was prepared to investigate all associated problems and to determine proper solutions. The model predicted that the tar-mat present at the OWC would act as a sealing barrier between the reservoir and the aquifer of the reservoir and would remain there until it broke down. Conservative predictions were made of the pressure differential of the tar-mat at the time when water injections went unnoticed. The intersecting faults were perpendicular to each other; the reservoir and its aquifer acted like a finite reservoir.

The opportunity to break down tar by injecting water below it, as well as the time needed to achieve this breakdown, has been discussed in detail (Osman, 1988). However, Osman did not describe the techniques used for tar breakdown or how the water enters the tar barrier and moves into the oil zone, possibly due to his intentional concentration

on the breakdown of the tar-mat. He importantly noted that it is the water injection, not oil production, which causes differential pressure. In some cases, he predicted that the pressure loss, which is the result of oil production, would be equivalent to the pressure gained after tar breakdown.

Al-Harthi et al. (2012) analyzed a case study and introduced an innovative, integrated methodology that uses static and dynamic data to determine the tar distribution and its sealing degree. They thoroughly analyzed data from before the subject field began to produce and then collected production and post-production data to refine the characterization. Additionally, the study highlighted the importance of conducting a Pyrolytic Oil Productivity Index (POPI) analysis and of using formation pressure during drilling to optimize the placement of the injector. Injectors were placed above the tar/oil contact (TOC) to provide effective pressure support and to ensure sufficient injectivity and reservoir sweep towards the producer well, as displayed in Figure 2.12. Lastly, Al-Harthi et al. (2012) used saturation and production logging tools to determine the presence of aquifer influx across the tar-mat, and the degree of influx was determined through material balance and reservoir simulation.

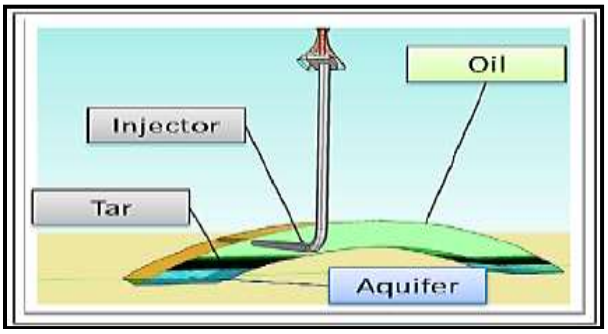

Figure 2.12. Well Placement above TOC (Al-Harthi, 2012)

2.6. DETECTION OF TAR-MAT ZONE

2.6.1. Logging While Drilling (LWD). Akkurt et al. (2008) discussed the petrophysical framework for a best-practice, real-time tar-mat detection workflow using Logging While Drilling (LWD) measurements. This methodology was implemented in two different carbonate fields in Saudi Arabia, demonstrating that with proper technologies and robust interpretation algorithms in place, real-time tar identification can be achieved efficiently and accurately. The results further confirmed that the existing LWD logging tools are reliable and capable of making accurate measurements.

2.6.2. Logging While Drilling (LWD) and NMR. The results of a study conducted in a Saudi Arabian carbonate field showed successful 6.25-in horizontal well placement by use of LWD and NMR devices. These two devices generally form a pressure tester that detects tar in complex, triple-combination density, resistivity, and neutron LWD logs.

Al-Shehri et al. (2011) detailed the successful real-time application of slim-hole NMR and the formation pressure measurements while drilling (FPWD) technologies to identify tar, optimally place water injectors, and solve the problem of pressure inadequacy arising due to impermeable tar barriers. Figure 2.13 illustrates the schematics of the NMR LWD tool and the sensor sub-arrangement. The viability of horizontal well drilling facilitated by the application of tar detection technologies has been evaluated in two different case studies conducted in Saudi Arabia in reservoirs characterized as clean carbonate reservoirs. These case studies relate to extended reach power injectors, as shown in Figure 2.14. In both case studies, the NMR and the FPWD proved effective in geosteering the horizontal wells, consequently achieving the objective. This success

indicated a breakthrough in handling and managing the challenges posed by tar in the exploitation of oil by petroleum engineers.

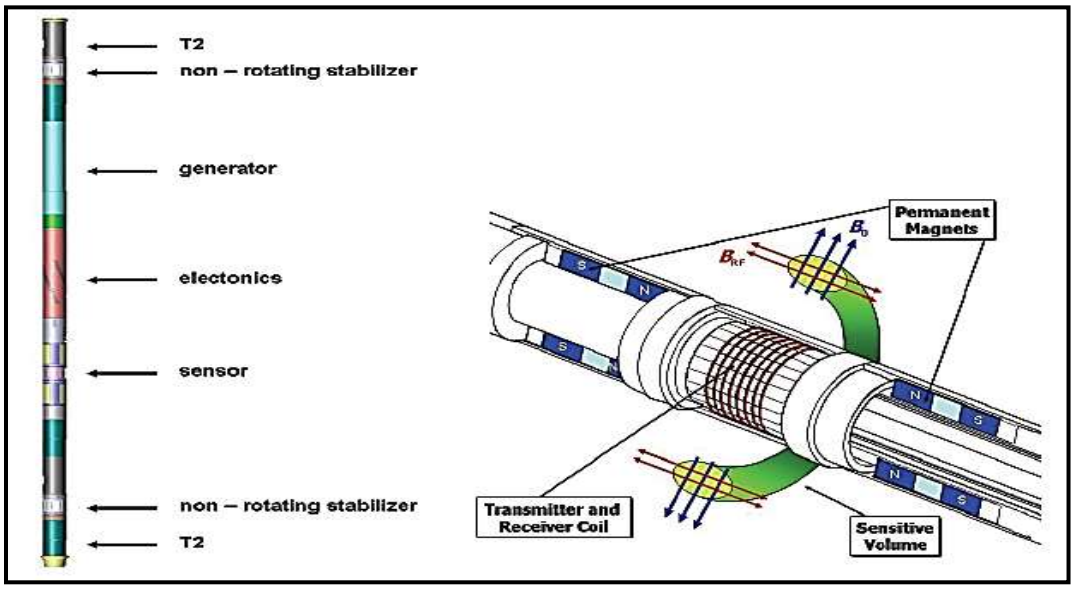

Figure 2.13. 4 ¾" NMR LWD Tool Assembly for 5 7/8", 6 /18" Hole Size Application and NMR LWD Sensor Arrangements (Al-Shehri et al., 2011)

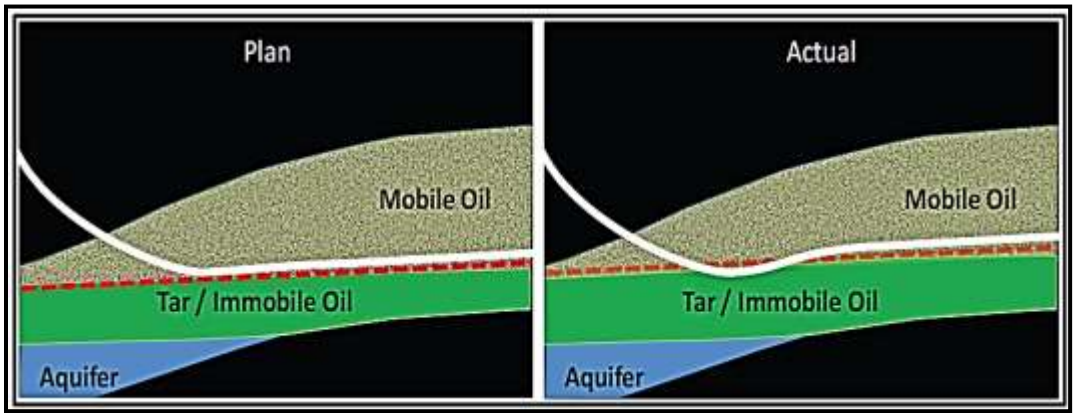

Figure 2.14. Planned Well Path and Actual Well Path Adjusted in Real Time for Tar (Al-Shehri et al., 2011)

2.6.3. Petrophysical Data, Rock Eval, and Electrical Log-derived Methods. Carpentier et al. (1998) assessed the continuity of the bitumen-rich interval and its role as an intra-reservoir permeability barrier responsible for the pressure anomalies recognized at the field scale during oil production. The investigators used three different methods, petrophysical data, Rock Eval, and electrical log-derived methods, to detect bitumen in 68 wells. The experiment produced 3D images of the tar-mat distribution on the field scale, which suggested no difference in the origins or maturity of the tar-mat or the overlying oil.

Carpentier et al. (1998) also conducted a thorough comparison of the bitumen location, sedimentological facies, petrophysical properties, field structural history, and present-day and paleo OWC used to decipher the process and timing of the tar-mat deposition. The overall results demonstrated that the bitumen-rich interval did not affect the pressure drop during production and did not act as a permeability barrier between the central and northern parts of the field.

The bitumen's distribution and continuity were recognized as a result of analyzing geochemical data, which usually entailed SARA composition and results of the Rock Eval analysis technique, particularly when integrated with wire-line log interpretation techniques (Carpentier et al., 2007). The ZADCO oil company arrived at this technique in its successful efforts to realize two types of bitumen-rich levels in the main field reservoir. One of these reservoirs corresponded to the main bitumen-rich reservoir intervals, which typically are associated with high oil saturation and high resistivity. Usually, these intervals are regarded as "tar-mats." The other reservoir corresponded to low oil saturation, usually regarded as "heavy oil residual."

Dessort et al. (2012) used a continuous power laser technology called the Laser Induced Pyrolysis System (LIPS) (Figure 2.15) to identify the presence of a tar-mat in a carbonate reservoir, which was affecting the assessment of reservoir quality, the GOIIP, the presence of permeability barriers, and the response of electric logs. This method has been applied successfully in numerous unconventional studies, yielding high-resolution, accurate quantitative measurements of the total organic carbon in oil shale and gas shale plays. With this data, the petroleum yield produced from oil shale pyrolysis can be estimated, and the quantity of the remaining petroleum potential of oil shale deeper in the basin can be extrapolated, modeled, and mapped. This technology greatly benefits mapping as it provides a very accurate tool with which to calibrate conventional well logs with respect to the distribution of the organic matter.

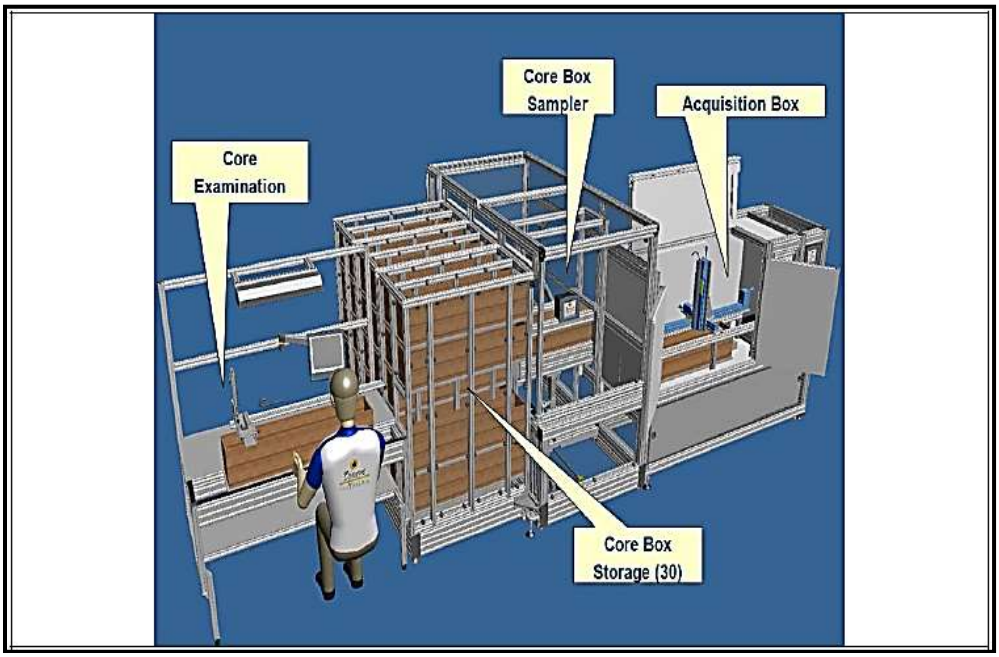

Figure 2.15. Laser Induced Pyrolysis System (LIPS) (Dessort et al., 2012)

3. EXPERIMENTAL METHODS AND PROCEDURES

3.1. EXPERIMENTAL MATERIALS

Various materials were used in this research, including five tar-mat cores, tin foil, and extraction fluids, such as toluene, hot water, and an anionic surfactant type of synthetic detergent (Lulu Soap), to extract the oil from the samples.

3.1.1. Tar-Mat Cores. Five tar-mat rock fragments were selected from five different depths in a Kuwaiti carbonate reservoir. Thirteen samples were collected from each segment; one of each of the 13 samples was used for the evaluation before the recovery/extraction, while the remaining 12 samples were used for testing after the recovery/extraction.

3.1.2. Preparation of Tar-Mat Cores. The tar-mat cores used in these experiments were prepared as follows:

1. The tar-mat rock fragments were broken into small pieces.
2. A manual marble grinder was used to crush the small pieces of the tar-mat rock samples until they became homogeneous powder, as shown in Figure 3.1.
3. Figure 3.2 a and b shows the tar-mat rock samples before and after being ground into homogenous powder.
4. The homogeneous powder was collected from the marble grinder and stored in glass containers, as displayed in
5. Figure 3.2 b, to prepare them for the next experiments.

Using a marble grinder and glass containers was important to avoid contamination and achieve accurate results.

Figure 3.1. Manual Marble Grinder

(a) Real Core Samples

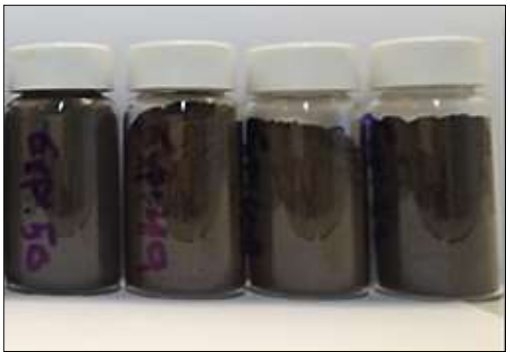

(b) Homogenous Powder

Figure 3.2. Tar-Mat Rock Samples Before and After Crushing

3.2. POROSITY MEASUREMENT

3.2.1. Helium Porosimeter (SCAL, Inc.). A helium porosimeter method was used to measure the porosity of the five tar-mat samples.

3.2.2. Equipment. The following equipment was used in this experiment:

- Porosimeter
- Helium
- Computer

3.2.3. Experimental Setup. Figure 3.3 and Figure 3.4 represent the method used to measure the porosity of the five tar-mat samples. The apparatus consisted of a helium cylinder, a core holder, and a PC. The helium cylinder was connected to the core holder, which likewise was connected to the PC.

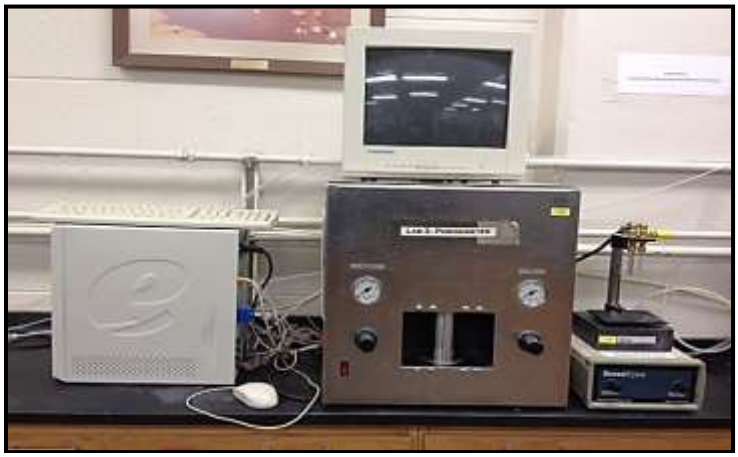

Figure 3.3. Helium Porosimeter Apparatus

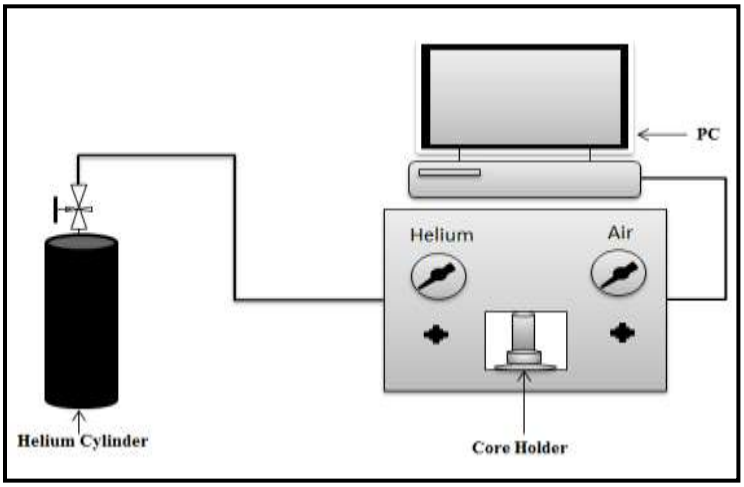

Figure 3.4. Schematic of a Helium Porosimeter

3.2.4. Experimental Procedures. The procedures for measuring the porosity in the experiments were as follows:

1. The tar-mat samples were processed into cuboid shapes, as shown in Figure 3.5.
2. Oil was extracted from the samples using toluene.
3. The samples were heated in the oven at 110 °C to remove moisture.
4. The effective porosity of the samples was measured using a helium porosimeter, as shown in Figure 3.3.
5. The sample was loaded into the sample cell, the reference cell was filled with helium at a certain pressure and then released into the sample cell;
6. The pressure was monitored before and after the valve opened.
7. Finally, the porosity was calculated using the pressure data under Boyle's law.

Figure 3.5. Cuboid Shapes of Tar-Mat Samples

3.3. PERMEABILITY MEASUREMENT

3.3.1. CoreLab Ultra-Perm 600. A CoreLab Ultra-Perm 600 was used to measure the permeability of the five tar-mat samples.

3.3.2. Equipment. The following equipment was used to perform this experiment:

- Gas Permeameter: CoreLab Ultra-Perm 600
- Core Holder
- Pump: ISCO 500D
- Nitrogen tank
- Vernier caliper

3.3.3. Experimental Setup. Figure 3.6 represents the method used to measure the permeability of the tar-mat samples. The apparatus consisted of a nitrogen tank, core holder, pump, gas permeameter, and PC. The nitrogen tank was connected to a core holder and a gas permeameter; the gas permeameter was connected to the PC. The pump was used to confine the pressure.

3.3.4. Experimental Procedures. The following procedures were used to measure the permeability:

1. The tar-mat samples were processed into cuboid shapes and dried in an oven.
2. The samples were taken out of the oven after water vaporized at 100+°C.
3. The dry, cuboid-shaped samples were coated with viscous epoxy in a 1 in ID acrylic tube, as shown in Figure 3.7.
4. Each instrument was powered on. The Winperm and Rosemount PC software were opened, and then “Connect” and “Start monitoring” were clicked in order to begin monitoring in low and high Rosemount windows.

5. The dimensions of each core were measured using the Vernier caliper. Three readings each were taken on the length and diameter.
6. The sample was placed in the core-holder, and the connections were assembled.
7. The effective confining pressure was set at 400psi.
8. Winperm>File>New were clicked, the file name was input, the temperature was changed to Fahrenheit, and the unit was changed to inches;
9. The sample ID, length (inches), diameter (inches), Bar. Pressure (14.7), Temperature, number of pressure measurements (15), and confining pressure (400psi) were input, Klinkenberg was chosen, and "Measure perm" was clicked.
10. The gas tank was opened, and the pressure was adjusted to the desired test pressure on the gauge using the adjustment knob.
11. The confining pressure was increased to (400+Pm) psia.
12. The kg was recorded until it changed only slightly.
13. The screen was printed, the figure was saved, and "Proceed to Next Pres." was clicked.
14. Steps 8-11 were repeated for the next pressure, for at least 4 pressures.
15. Excel was used to analyze the data and give the absolute permeability for the sample.

3.3.5. Permeability Calculation. Table 3.1 shows the input data for permeability calculation.

- Diameter: D1= , D2= , D3= , $\overline{D}$ =
- Length: L1= , L2= , L3= , $\overline{L}$ =
- Cross-Sectional Area A (cm2) = _____
- μg = 0.01781cp.

- Create a plot of gas permeability, kg (Y-axis) versus the average of two pressures 1/pm (x-axis);
- Draw a line to fit the data points and get the fitting equation. From the intercept with the Y-axis, read the absolute permeability, ka;
- Discuss the relationship between 1/pm and kg;

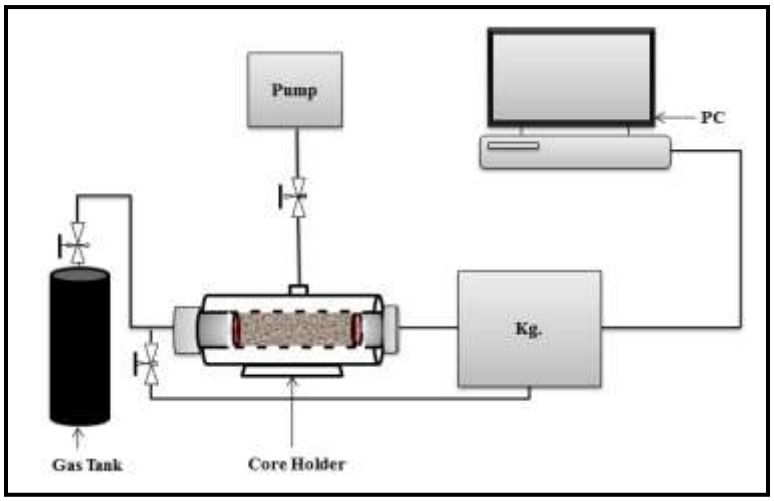

Figure 3.6. Schematic of Gas Permeameter: CoreLab Ultra-Perm 600

Figure 3.7. Cuboid-Shaped Samples Coated with Viscous Epoxy in a 1 in ID Acrylic Tube

Table 3.1. Data Sheet for Permeability Calculation

P1	P2	P1(atm)	P2 (atm)	Q1	Pm	Pm (atm)	1/Pm	Ka
94.61	13.51	6.440	0.920	0.44	54.06	3.68	0.272	0.903
134.64	13.65	9.165	0.929	0.64	74.15	5.05	0.198	0.878
153.99	13.73	10.483	0.935	0.74	83.86	5.71	0.175	0.878
184.08	13.83	12.531	0.941	0.89	98.95	6.74	0.148	0.869
205.62	13.89	13.997	0.946	1.00	109.76	7.47	0.134	0.870
178.20	13.76	12.131	0.937	0.86	95.98	6.53	0.153	0.875

3.4. ELEMENTAL ANALYSIS TO DETERMINE THE % OF C, H, N, AND S FROM TAR-MAT SAMPLES

3.4.1. CHNSO Elemental Analysis. Tar-mat characteristics help to clarify the natural properties of tar-mats present in carbonate reservoirs. Elemental analysis aids in the detailed chemical characterization of tar-mats and can be used to investigate the presence and amount of carbon, hydrogen, nitrogen, oxygen, and sulfur in tar-mat samples.

3.4.2. Equipment. The following equipment was used to perform these experiments:

- Macro Elemental Analyzer 106
- Analytical balance
- Helium and oxygen cylinders
- Computer

3.4.3. Experimental Setup. Figure 3.8 and Figure 3.9 illustrate the experimental setup, which consisted of the macro elemental analyzer, peripheral equipment, computer, and printer (for control and evaluation). The peripheral instruments were connected via the supplied cables to the appropriate sockets at the back of the elemental analyzer.

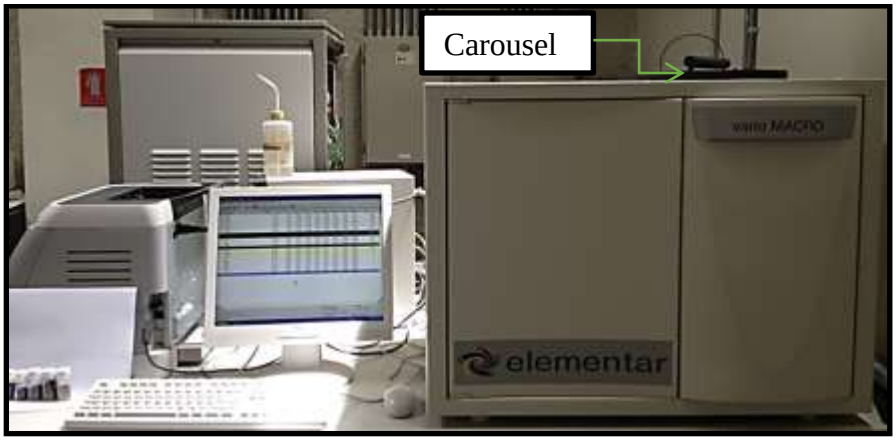

Figure 3.8. Macro Elemental Analyzer Apparatus

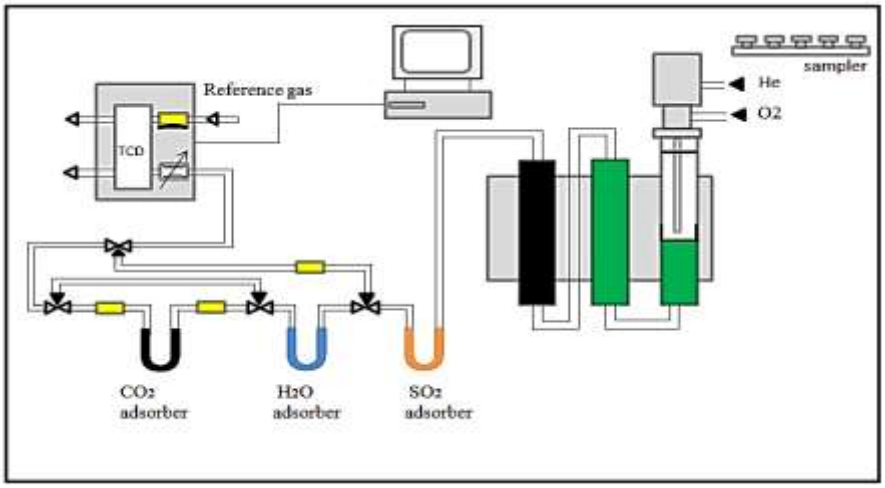

Figure 3.9. Schematic of Macro Elemental Analyzer

3.4.4. Experimental Procedures. The following steps were completed to determine the amount of C, H, N, S, and O in the tar-mat samples:

1. The samples were weighed manually using the analytical balance, as illustrated in Figure 3.10.
2. The homogenized samples then were packed in tin foil and placed into the carousel of the automatic sample feeder, as shown in Figure 3.8, Figure 3.11, andFigure 3.12.
3. The weight of each sample was varied from 40-45 mg in order to achieve accurate results.
4. The weights of the samples were input into the PC either through the online balance via an interface or manually using the keyboard.
5. The sample names and the matrix-specific oxygen dosing were allocated to the sample weight.
6. After inputting the sample data and identifying the methods of analysis, the analysis began.
7. At the start of each analysis, the auto-zero adjusts of the measuring signal were passed through the detector. Then, the ball valve was opened with a 180° displacement of the blind-hole ball. Next, the carousel was moved up one position, and the sample was dropped into the ball valve's blind hole. The ball valve then was turned 90° into a flush position, and the apparatus was sealed. The atmospheric nitrogen that had entered was flushed out with 0.3 bar pre-pressure at approximately 300 ml/min. The sample then was dropped into the combustion tube's ash finger through another 90° turning of the ball valve.

8. Finally, the results were uploaded to the software and were ready for reading, as displayed in Table 3.2 and Figure 3.8

Figure 3.10. Analytical Balance Apparatus

Figure 3.11. Tin Foil Apparatus

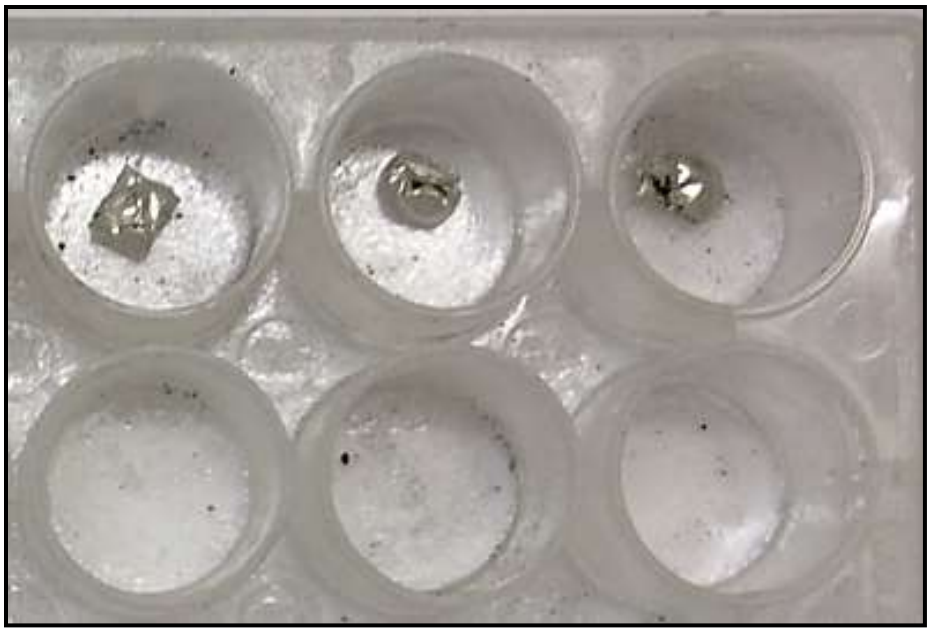

Figure 3.12. Tin Foil Containing Samples

Table 3.2. Summarized List of the Elemental Analysis Output

NO	Name	Weight	Date	Time	C (%)	H (%)	N (%)	S (%)
1	AB1	41.363	12.06.12	11:32	24.27	2.541	0.706	7.961
2	AB2	41.363	12.06.12	11:46	18.85	0.863	0.441	0.902
3	AB3	41.363	12.06.12	12:00	18.69	0.879	0.473	0.747
4	AB4	41.363	12.06.12	12:14	18.04	0.853	0.448	0.716
5	AB5	41.363	12.06.12	12:28	30.76	2.666	0.821	5.241

3.5. GEOCHEMISTRY PYROLYSIS ANALYSIS

3.5.1. Rock-Eval 6 Pyrolysis. Rock-Eval pyrolysis is used extensively for characterizing the quality, quantity, and thermal maturity of organic matter in sedimentary rocks, essential parameters for assessing the petroleum potential of sedimentary basins (Issler et al., 2012). Table 3.3 summarizes the output of the Rock-Eval 6 analysis.

Table 3.3. Summary of Rock-Eval 6 Analysis Output

Rock Eval Peaks and Their Significance		
Parameter	Unit	Name
S1	mgHC/g rock	Free Hydrocarbons
S2	mgHC/g rock	Oil Potential
Tmax	^{o}C	Source Rock Maturity
S3	mgCO_2/g rock	CO_2 from Organic Source
S3’	mgCO_2/g rock	CO_2 from Mineral Source
TpS3’	^{o}C	Temperature for Maximum of Surface S3’
S3CO	mgCO/g rock	CO from Organic Source
TpS3CO	^{o}C	Temperature for Maximum of Surface S3CO
S3’CO	mgCO/g rock	CO from Organic and Mineral Sources
S4-CO_2	mgCO_2/g rock	CO_2 from Organic Source
S4-CO	mgCO/g rock	CO from Organic Source
S5	mgCO_2/g rock	CO_2 from Mineral Source
Source Rock Screening		
TOC	% wt	Total Organic Carbon
PI	S1/(S1+S2)	Production Index
PC	% wt	Pyrolysable Carbon Organic
RC CO	% wt	Residual Carbon Organic (CO)
RC CO_2	% wt	Residual Carbon Organic (CO_2)
RC	% wt	Residual Carbon Organic
HI	mg HC/g TOC	Hydrogen Index
(OI) CO_2	mg CO_2/g TOC	Oxygen Index (OI) CO_2
(OI) CO	mg CO/g TOC	Oxygen Index CO
PyroMinC	% wt	Pyrolysis Mineral Carbon
OxiMinC	% wt	Oxidation Mineral Carbon
MinC	% wt	Mineral Carbon

3.5.2. Equipment. The following equipment was used in this experiment:

- Rock-Eval 6
- Helium
- Computer

3.5.3. Materials and Methods. Five tar-mat rock fragments were selected from five different depths in a Kuwaiti carbonate reservoir. Thirteen samples were collected from each segment to characterize the quality, quantity, and thermal maturity of organic matter in sedimentary rocks through Rock-Eval 6 pyrolysis. One of each of the 13 samples was used for the evaluation before the recovery/extraction, and the remaining 12 samples were used for testing after the recovery/extraction. Figure 3.13 shows the main steps and outputs of the Rock–Eval 6 pyrolysis.

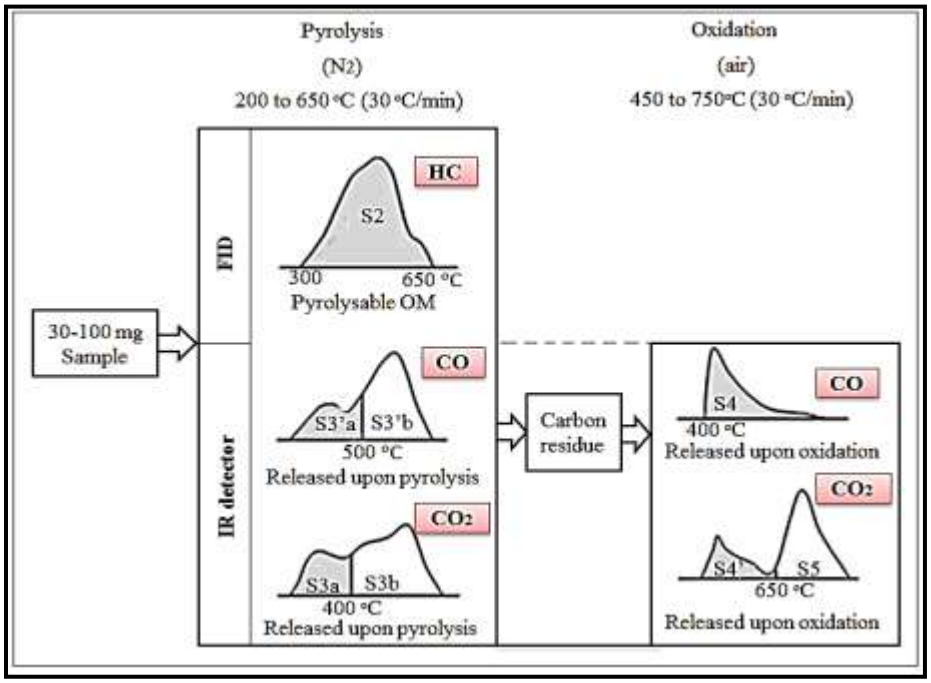

Figure 3.13. Main Steps and Outputs of Rock–Eval 6 Pyrolysis (Saenger et al., 2013)

3.5.4. Experimental Procedures. The procedures for the geochemical pyrolysis experiments were as follows:

1. After being crushed to a fine powder, the tar-mat samples were measured manually using the analytical balance and varied from 40-45 mg.
2. The samples were packed in the sample container, as shown in Figure 3.14.
3. The sample containers were packed into the carousel of the automatic sample feeder, also shown in Figure 3.14.
4. The software was run to begin the Rock-Eval 6 experiment; it took approximately 30 minutes to generate the results for each sample, as shown in Figure 3.15.
5. The results of this experiment were uploaded automatically to the software.

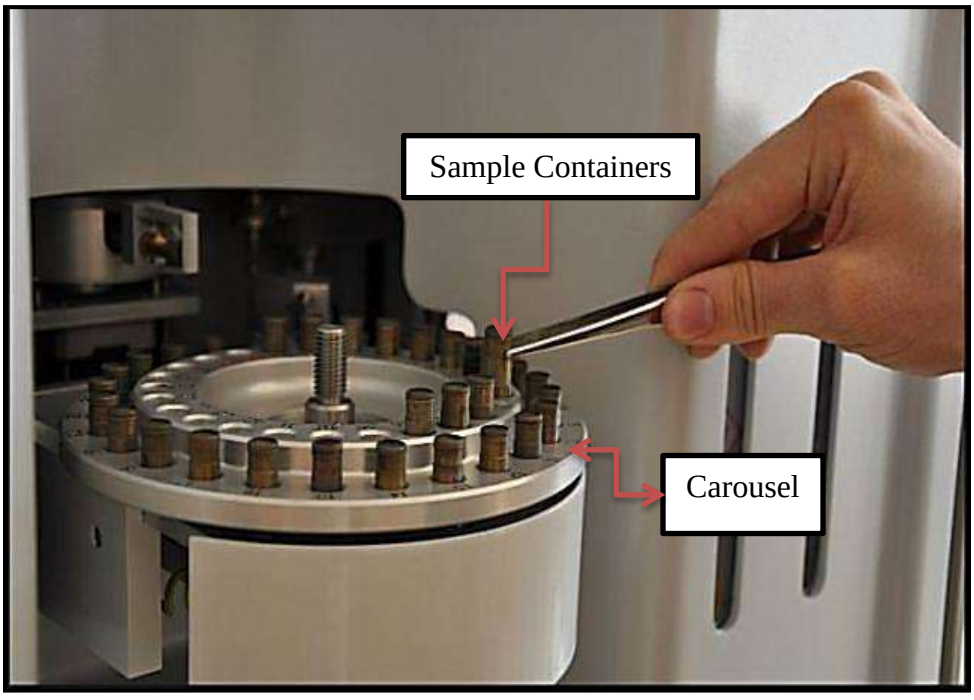

Figure 3.14. Sample Containers and Carousel

Figure 3.15. Rock-Eval 6 Apparatus

3.6. OIL EXTRACTION

3.6.1. Soxhlet Apparatus. The Soxhlet extractor was used to extract the oil from the tar-mat samples. Three types of fluids, toluene, water (H_2O), and surfactant solution, were used in this experiment to extract oil from the homogeneous powder samples.

3.6.1.1 Equipment. The equipment used to perform these experiments included the following:

- Analytical balance to measure the homogenous samples
- Electrical heater to heat the fluids
- One boiling flask to contain both the fluid and the sample

- Glass beam to raise the sample from the bottom of the boiling flask
- Siphon arm to allow vapor to pass through for circulation
- Extraction thimbles
- Condenser

3.6.1.2 Experimental setup. The experimental setup consisted of a Soxhlet Extractor Mantle Heater (electric), water condenser, and flash evaporator. Figure 3.16 and Figure 3.17 show the experimental setup of the Soxhlet extractor.

3.6.1.3 Experimental procedures. The procedures for extracting oil from the homogeneous powder samples in the toluene, hot water, and surfactant solution experiments were as follows:

1. The weight of the homogenous powder sample was measured before the experiment began. The amount of homogeneous powder used for this experiment varied between 20 to 21 grams from each sample.
2. Each homogeneous powder sample was wrapped in a piece of cloth to keep the sample from dispersing in the liquid during the oil extraction experiment.
3. 450 ml of toluene was placed in the flask as an extraction fluid.
4. The glass beads were placed at the bottom of the flask to raise the sample in order to avoid heat from the high temperature.
5. A piece of cloth containing the homogeneous powder sample to be extracted was dipped in the flask of toluene.
6. Each homogeneous powder sample was dipped in the toluene and heated for six hours at different temperatures of 25, 135, 225, and 315 ^{o}C.

7. As the toluene boiled, its vapors rose and were condensed by a condenser. The condensed toluene then filled up the thimble. Any excess toluene automatically siphoned back down into its original container. This process repeated until all of the material to be extracted from the homogeneous tar-mat powder sample in the flask was extracted into the toluene.
8. The procedures for extracting oil from the homogeneous powder sample using 450 ml of water (H_2O) and a combination of 400 ml of water and 50 ml of Lulu soap (surfactant) were the same as those used for the toluene experiment.
9. Finally, the toluene containing oil was placed back into the beaker for the next experiment, which involved isolating the toluene from the oil, as shown in Figure 3.18.

Figure 3.16. Soxhlet Extractor Apparatus

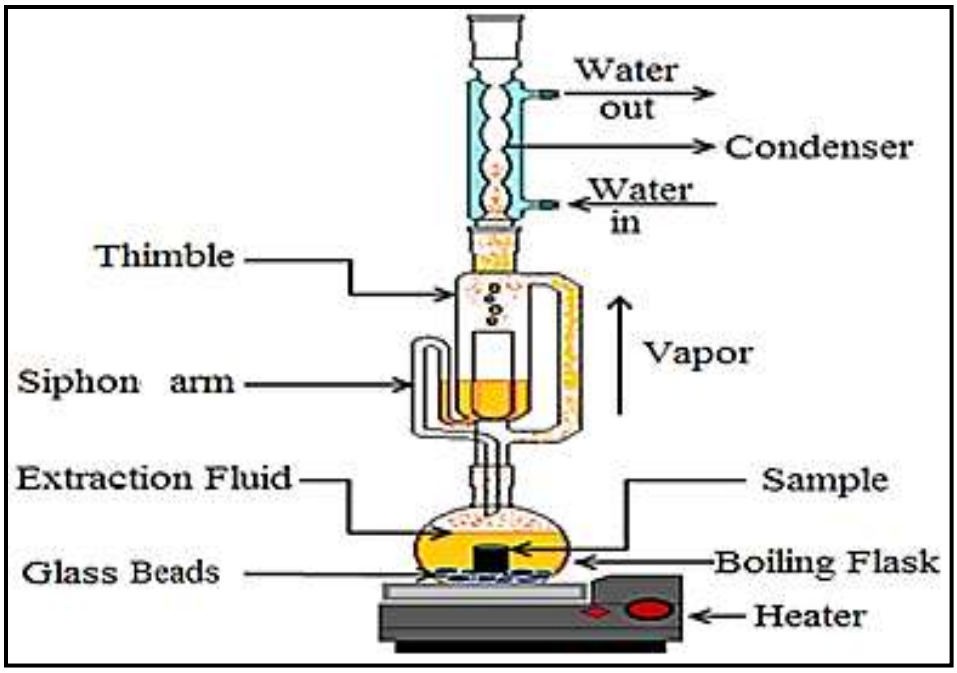

Figure 3.17. Soxhlet Extractor Schematic

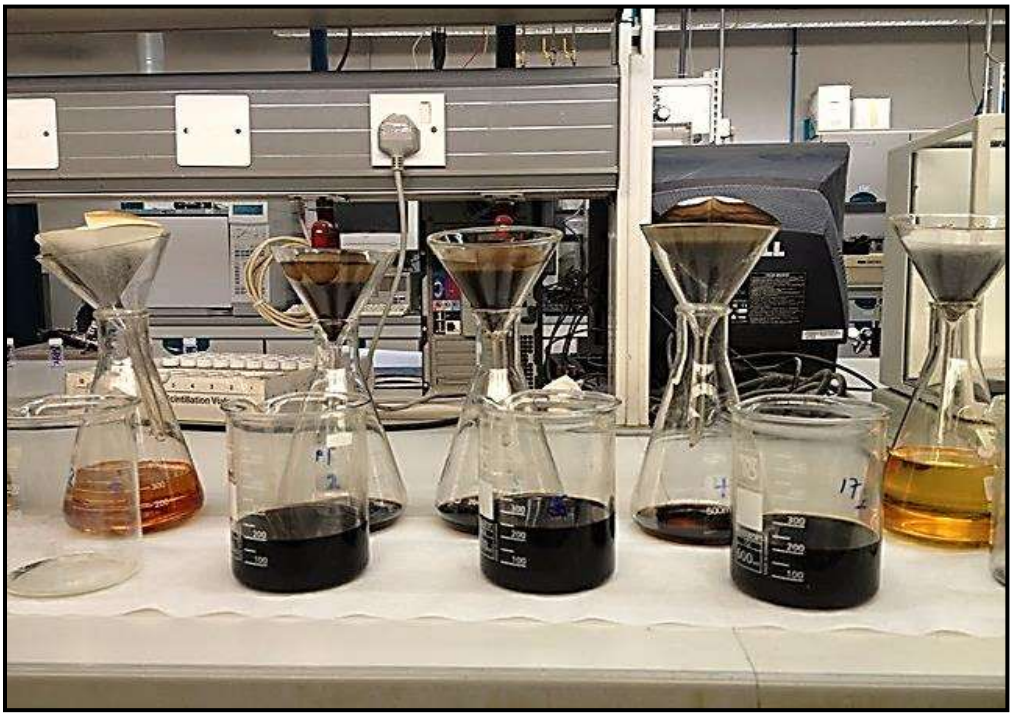

Figure 3.18. Apparatus for Filtering Dirt out of Oil

3.6.2. Isolating the Oil from the Extraction Fluids. After the extraction, the oil was separated from the toluene and dirt. This oil was used for the SARA analysis experiments.

3.6.2.1 Equipment. The following equipment was used to isolate the oil from the extraction fluids (toluene) and filter the dirt out of the oil:

- Electronic heater
- Hot bath
- Evaporator flask
- Collecting flask
- Condenser
- Heating circulator
- Vacuum
- Oven
- Filtrate paper
- Filtrate funnel
- Beaker
- Oven

3.6.2.2 Experimental setup. Figure 3.19, Figure 3.20, and Figure 3.21 represent the experimental setup, which consisted mainly of an electronic heater with a hot bath, a condenser containing evaporate, and a collecting flask. These pieces of equipment were connected to the heating circulator. The hot bath contained water used for heating the evaporate flask. The condenser held two flasks; the evaporate flask was dipped into the hot bath, and the other flask was used to collect the extraction fluid. The heating

circulator was used to circulate the evaporate flask. Furthermore, the filtrate paper, filtrate funnel, and beaker were used to isolate the oil from any dirt that it may have contained.

3.6.2.3 Experimental procedures. The procedures for isolating the extraction fluids from the oil samples were as follows:

1. The oil samples containing the extraction fluids (toluene) were placed in the evaporate flask and dipped into the hot bath.
2. The electronic heater was used to heat the water in the hot bath that contained the evaporate flask.
3. The evaporate flask in the hot bath was circulated by the heat circulator for a period of time.
4. The condenser containing the evaporate flask and the collecting flask was vacuumed to separate the evaporate extraction fluids from the oil samples; the fluids were placed in the collecting flask.
5. The oil sample was placed in the oven for approximately one hour to evaporate any extraction fluids remaining in the oil samples, as shown in Figure 3.22.
6. The filtrate paper, filtrate funnel, and beaker were used to separate out any dirt that the oil may have contained.

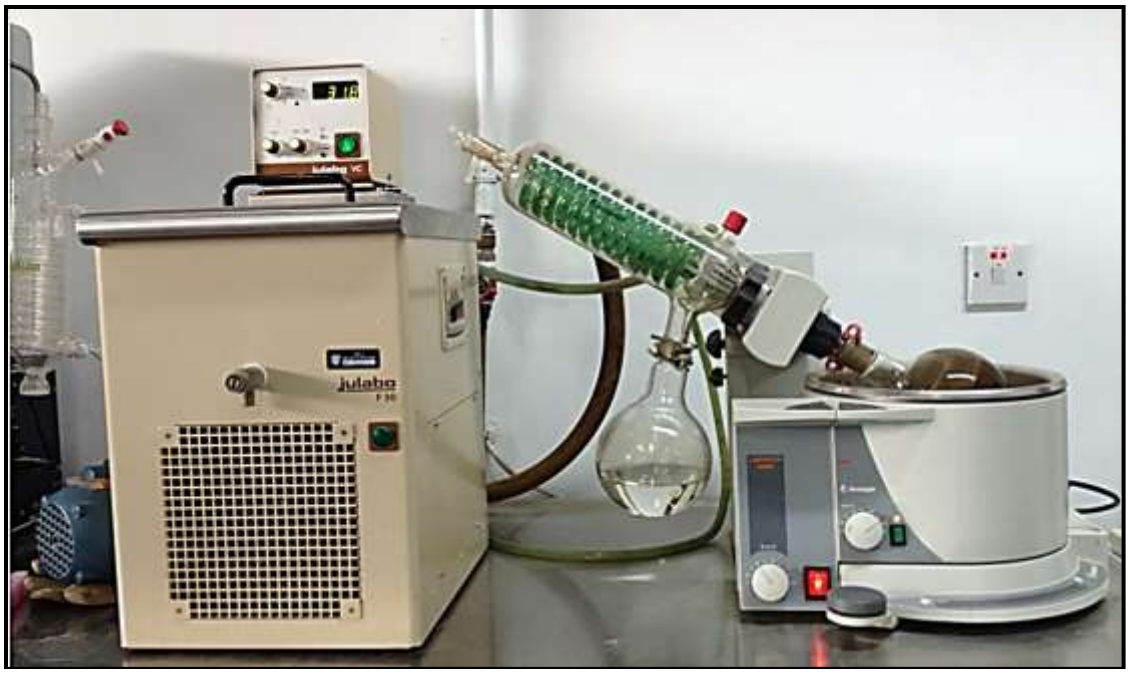

Figure 3.19. Apparatus for Separating Oil from Extraction Fluids

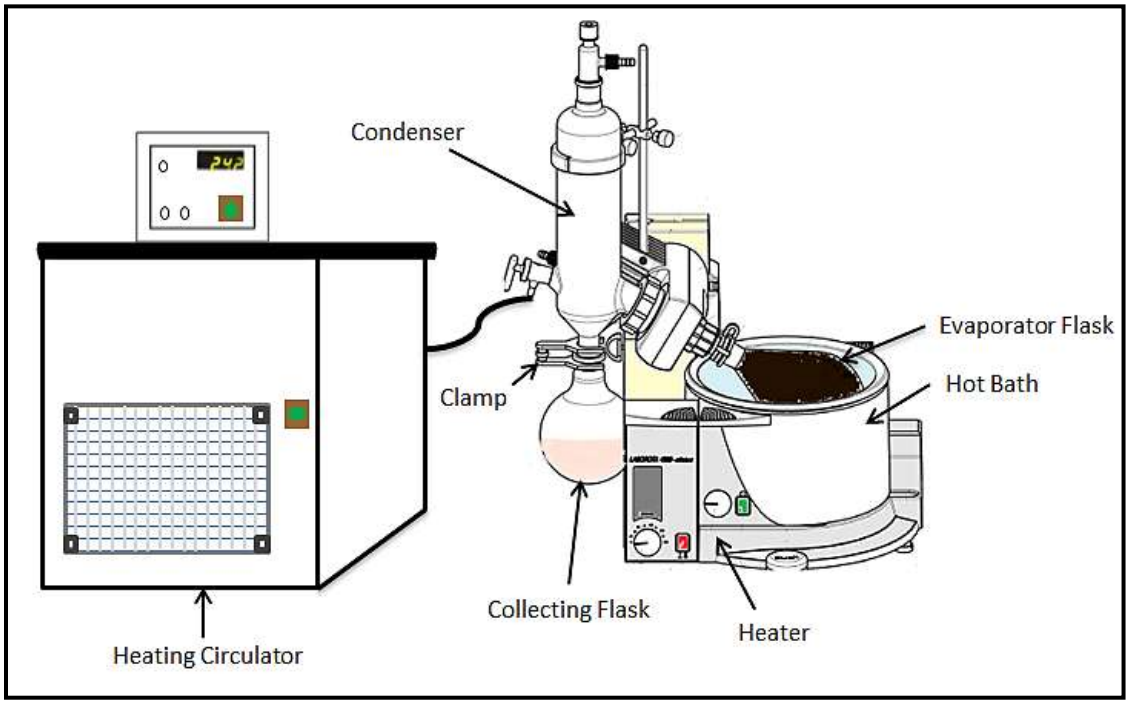

Figure 3.20. Schematic of Separating Oil from Extraction Fluids

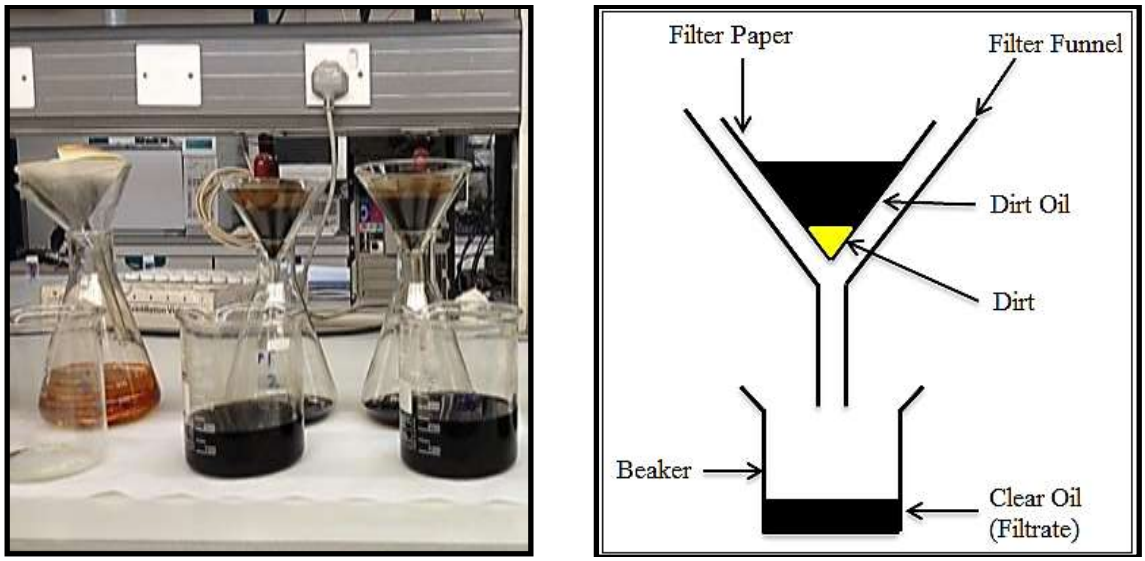

Figure 3.21. Apparatus and Schematic of Filtrating Oil from Dirt

Figure 3.22. Oven Apparatus

3.7. SARA ANALYSIS

3.7.1. SARA Analysis Method. SARA analysis was one of the methods used to characterize the oil samples. SARA oil testing measures the percentage of saturates, asphaltenes, resins, and aromatics in heavy crude oil and tar-mat samples.

3.7.2. Experimental Materials. The main components of SARA were 10 ml of dichloromethane and a 0.1 g oil sample. In addition, three types of solvent were used for each tank; the first one contained 70 ml of either n-Hexane or n-Heptane according to the type of sample, the second one contained 70 ml of toluene, and the last one contained 70 ml of a mixture of two solvents (95% dichloromethane + 5% methanol).

3.7.3. Experimental Setup. Figure 3.23 shows the setup of this experiment.

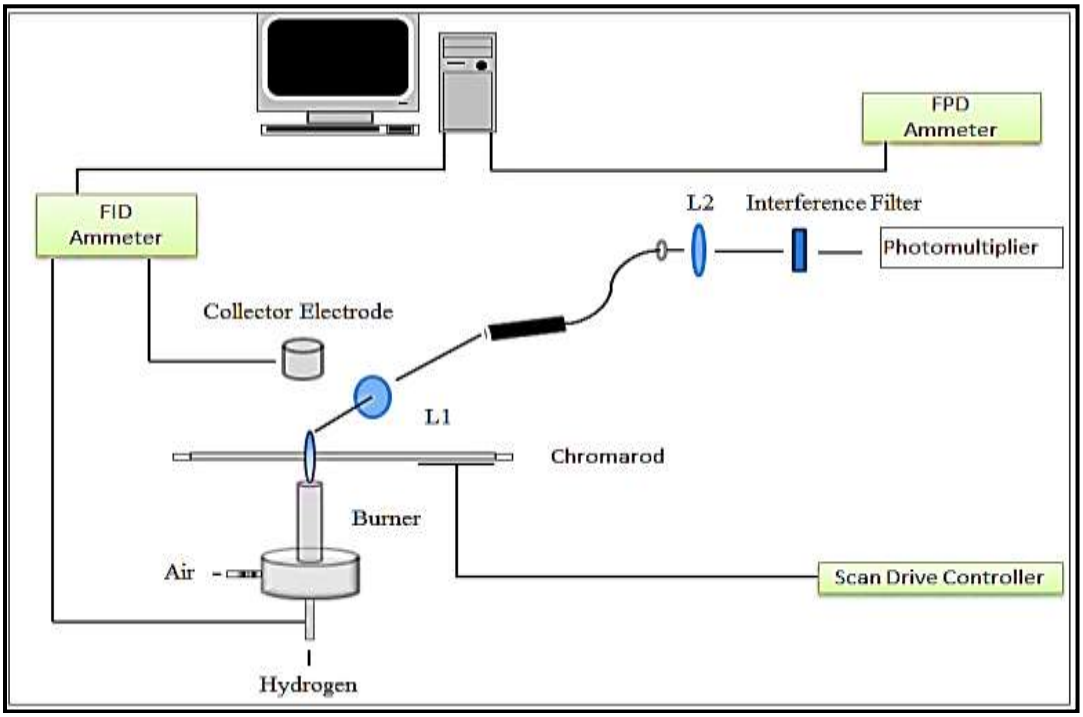

Figure 3.23. IATROSCAN MK-6 Diagram

3.7.4. Equipment. Figure 3.24 through Figure 3.29 show the equipment used for SARA analysis experiment.

Figure 3.24. Development Tank DT-150

Figure 3.25. Chromarod Apparatus

Figure 3.26. Chromarod Storage Chamber

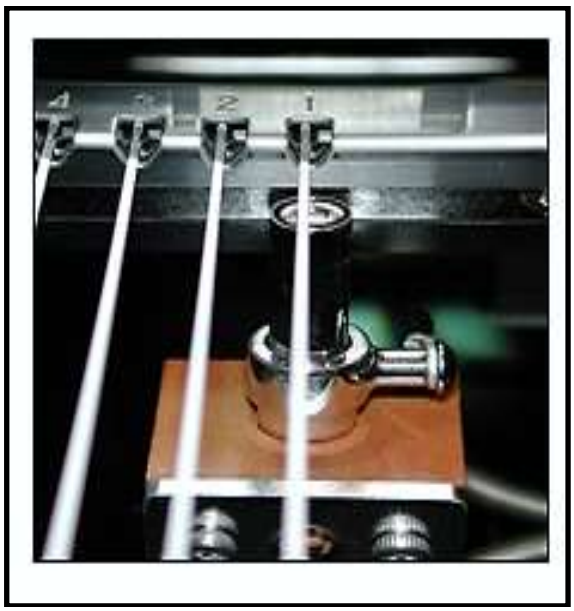

Figure 3.27. Hydrogen Flame

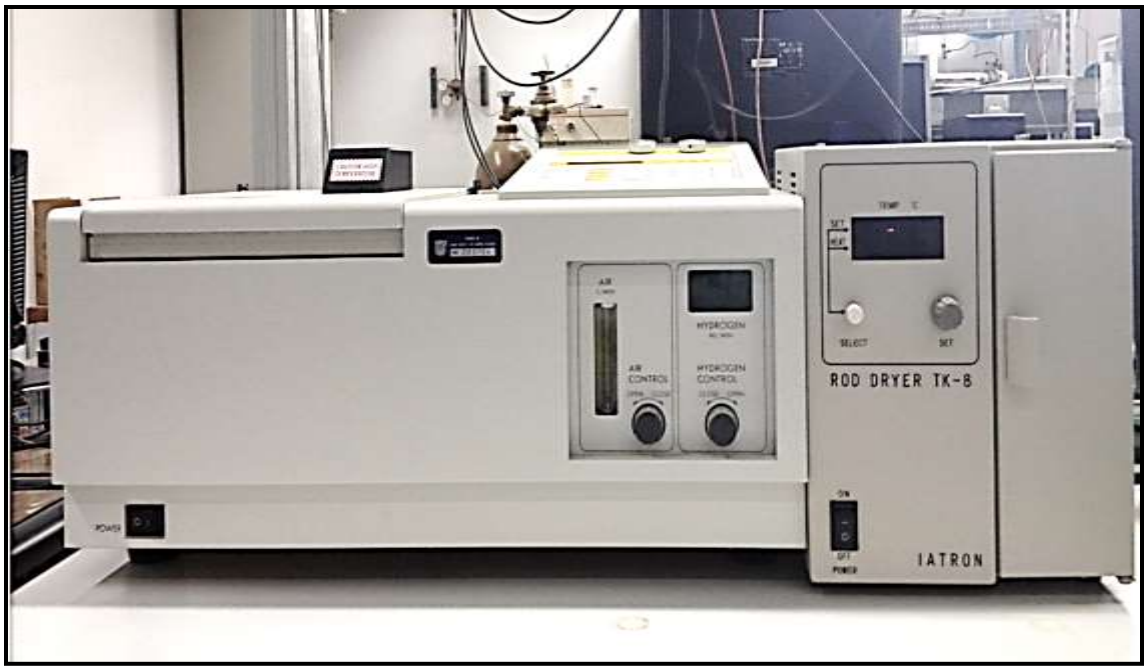

Figure 3.28. Chromarod Dryer TK-8 Apparatus

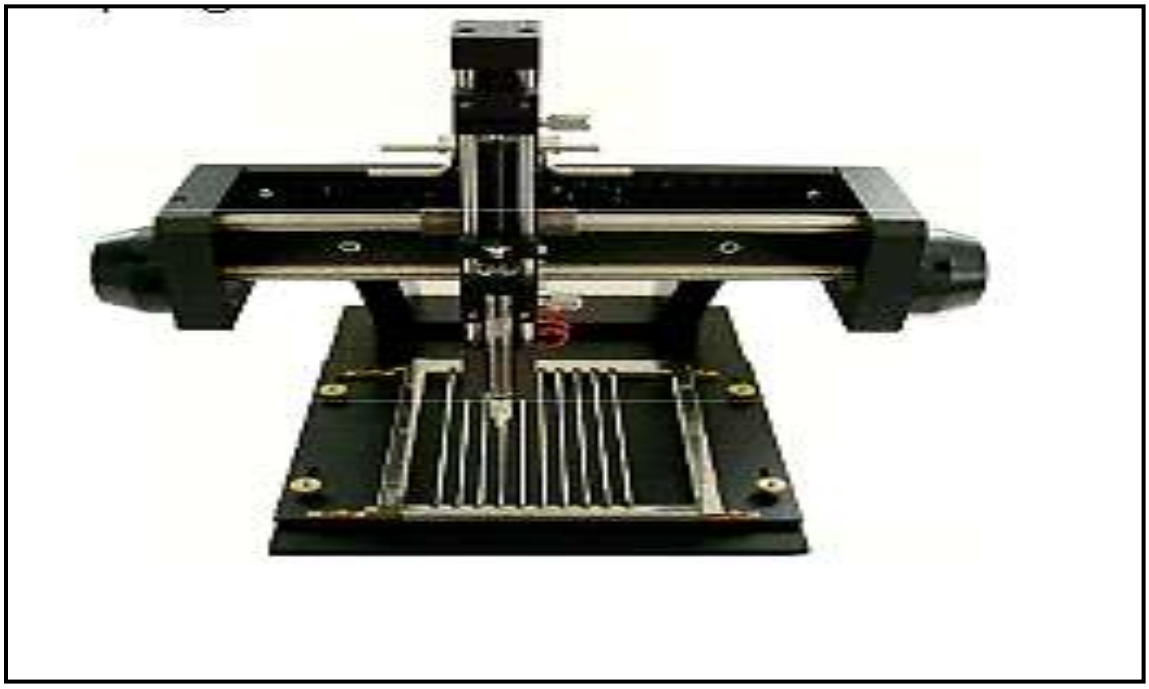

Figure 3.29. Blank Scanning Apparatus

3.7.5. Experimental Procedures. The following instructions were followed to determine the percentage of saturates, asphaltenes, resins, and aromatics in heavy crude oil and tar-mat samples:

A) Preparation of the Sample Development Tank and Rods

1. Weigh a 0.1 g oil sample and place it in the volumetric flask. (Before taking the sample, make sure it is homogeneous by heating and shaking it.)
2. Add 10 ml of dichloromethane to the oil sample in order to adjust the concentration of the sample to 10-20 mg/ml.
3. Put this flask (sample + dichloromethane) in the sonic bath for 10 min or more for mixing.
4. Prepare three tanks, each containing one type of solvent (70 ml of n-Hexane or n-Heptane, according to the type of sample; 70 ml of toluene; and 70 ml of a mixture of two solvents (95% dichloromethane + 5% Methanol)). The third tank should be prepared after finishing the development in the second tank in order to prevent the volatilization of the solvent.
5. Before putting the solvents in their tanks, each tank should be equipped with one L-shaped filter paper to increase the evaporation of the liquid within. (Make sure to set the development tanks far from direct sunlight and air turbulence.)
6. Take fresh or cleaned Chromarods and set them in the empty rod holder. (The rods are very sensitive. Do not touch them with your hand; use tongs to set them in the rod holder.)
7. Put the filled frame on the spotting guide for sample spotting.

B) Sample Spotting & Development

1. Before sample spotting, conduct one or two blank scans to make sure the Chromarods are cleaned and activated.
2. Take the prepared sample from the sonic bath, and, using a micro-dispenser, take 1µ of the sample and put it on the rod at the intersection point; repeat this step for all rods. (Before spotting, clean the micro-dispenser with dichloromethane and then with the sample itself.)
3. During spotting, touch the Chromarod with the tip of the micro-dispenser to ensure that the entire sample has transferred from the dispenser to the Chromarod, but do not pressurize the Chromarod; it is fragile and dangerous if broken.
4. Before development, make sure the solvents are highly pure; they should be prepared newly every day.
5. Execute the development work as quickly as possible upon completing the sample spotting to prevent any errors associated with air humidity.
6. Take the spotted frame and put it in the first tank, which contains either n-Hexane or n-Heptane. (Make sure to wet a filter paper thoroughly with solvent to homogenize the vapor in the tank prior to development.)
7. The first tank is responsible for developing the sample up to 70 mm, which takes approximately 24 min. (The temperature of the development tanks should be constant at approximately 20 ^{o}C.)
8. Take the sample out and dry it manually by air or in the oven (Chromarod Dryer TK-8) for 2 min before putting it in the desiccator for 3 min or more in order to absorb the humidity in the Chromarod. (Make sure the silica in the desiccator is activated.)

9. Put the sample in the second tank, which is responsible for developing the sample up to 45 mm; this takes approximately 6 min. Then, take it out and dry it for 2 min before putting it in the desiccator for 3 min or more.
10. Put the sample in the third tank, which is responsible for developing the sample up to 20 mm; this takes approximately 1.5 min. Then, take it out and dry it for 2 min before putting it in the desiccator for 3 min or more.

C) Scanning and Analyzing the Sample

1. Open the hydrogen valve and switch on the Iatroscan device; then, ignite the burner using a lighter.
2. Adjust the hydrogen flow to 160 mL/min and the air flow to 2 L/min.
3. Set the scanning speed to 30 sec/scan by clicking SCAN SPEED and then 2 → ENTRY.
4. Set the number of rods used to 10 by clicking Rod No. and then 1 → ENTRY → 10 → ENTRY.
5. Fix the spotted frame after development in the three tanks in the Iatroscan device.
6. Click NORMAL SCAN to scan the spotted rods.
7. Ensure that the system is level at the zero position; if not, click AUTO ZERO to re-zero the level.
8. Click AUX SGN to connect the computer with the Iatroscan device.
9. Before clicking START, make sure the screen shows both 30 and 1-10. (Do not click START until the software setup is finished.)
10. Open the SIC-480 II program and click Run to specify the sample and scanning condition; click Continue.

11. Click CH A for SARA analysis or CH B for sulfur analysis.
12. Name the file to identify it after finishing the scan.
13. Specify the scan speed and number of rods (scan speed = 0.5 min/scan, rods = 10); click Next.
14. Add more information about the sample in the description cell, and then click ↓ to start.
15. After finishing the scan, click Exit → Yes.
16. Click Postrun twice to select the required file, and then press OK.
17. Four peaks will appear on the screen. To achieve the best results (components percentage), follow these steps:
18. Click Force Integration to specify the area under the curve.
19. Go back to ensure that there are no more than four peaks. If any extra peaks exist, delete them by clicking Delete; specify the undesirable peaks and then click Delete again.
20. Click Back to return to the main screen.
21. Click Excel to transfer the data from the SIC-480 II program to Microsoft Excel. (Make sure to open Microsoft Excel before transferring the data.) In Excel:
22. Choose peak data by putting a √ in front of it.
23. Select the number of Sheets and Rows.
24. Select the required information by putting a √ before Peak Area and Peak Area %, and then press OK.
25. To go to another file, click Load, and then choose the required file; press OK.

D) Cleaning and Activating Chromarods

1. In the process of scanning the sample, the Chromarod is automatically cleaned and reactivated. Therefore, in most cases, it can be reused immediately after scanning. However, after finishing scanning, the Chromarod may be contaminated by organic compounds or metallic salts from some sample in the origin (spotting point).
2. To clean the contaminated Chromarods, first immerse them in the solvent until reaching 100 mm in order to move the contaminants from the tail end of the Chromarod into a position higher than the burning position. After that, vaporize the solvent, and then put it in the SARA scanning device. (Conduct two blank scans to remove contaminants.)
3. To employ an alternative cleaning method, follow these steps:
    a. Wash the Chromarods lightly in deionized water.
    b. Soak them in the concentrated sulfuric acid throughout the night.
    c. Upon removing the Chromarods from the concentrated sulfuric acid, thoroughly rinse them with deionized water.
    d. Remove the water by drying the Chromarods for 1 hour at 120 ^{o}C or by conducting two blank scans after drying them for 3 min at 120 ^{o}C.
4. As an alternative, clean the Chromarods according to the previous steps, but employ nitric acid instead of sulfuric acid.
5. Place the Chromarod in a storage chamber to protect it from air humidity and dust.

4. RESULTS AND DISCUSSION OF TAR-MAT SAMPLE CHARACTERIZATION

4.1. INTRODUCTION

This chapter includes extensive systematic characterization of tar-mat samples results using three methods, including Elemental analysis, SARA analysis, and Rock-Eval pyrolysis. These results are importance to investigate the physical and chemical characterization and the quality, quantity, thermal maturity from tar-mat samples.

4.2. PHYSICAL ASPECTS OF TAR-MAT SAMPLES

Five tar-mat rock fragments were selected from five different depths in a Kuwaiti carbonate reservoir. Thirteen samples were collected from each segment. One of each of the 13 samples was used for the evaluation before the recovery/extraction, and the remaining 12 samples were used for testing after the recovery/extraction. These samples were crushed until they became fine powder. Toluene, hot water, and an anionic surfactant type of synthetic detergent (Lulu Soap) were used as extraction fluid agents to extract the oil from the samples. The effective porosity and absolute permeability of the five tar-mat rock fragments were measured in the lab. The °API gravity from the five tar-mat cores was calculated based on the method provided by Cubitt et al. (2004).

Table 4.1 lists the physical properties of the tar-mat samples. Clearly, the API gravity values decreased as the depth increased, as shown in Figure 4.1. Also, most of the samples had low permeability and API gravity; this indicates that they were tight, which would make it difficult to produce oil from them.

Table 4.1. Physical Properties of Tar-Mat Samples

Zone	Depth (ft.)	°API	Ø (%)	K (md)
AB1	2674	1.34	34.9	0.2
AB2	2703	5.17	28.3	0.84
AB3	2723	4.1	35	7.3
AB4	2755	3.76	35.7	5.2
AB5	2782	1.72	9.8	0.5

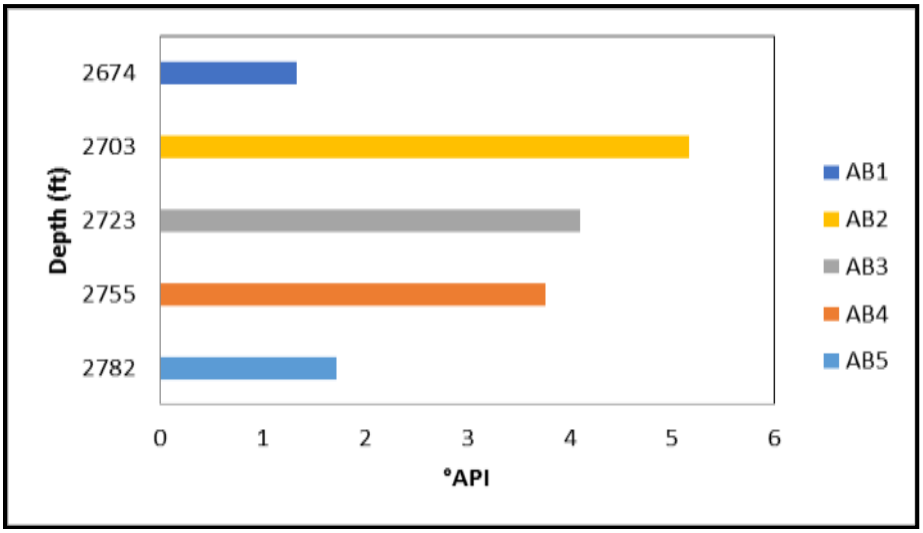

Figure 4.1. Histogram Showing the Distribution of API with Depth

Figure 4.2 compares Missouri heavy oil and tar-mat oil. The viscosity of Missouri heavy oil was 24343 cp at 20 °C, and the °API gravity was 17.1 °API (Rabia et al., 2010). This comparison shows that the Missouri heavy oil was mobile, while the tar-mat oil was

immobile, like a solid. Furthermore, this comparison indicates that this tar-mat contained extremely heavy oil with high viscosity and low °API gravity values.

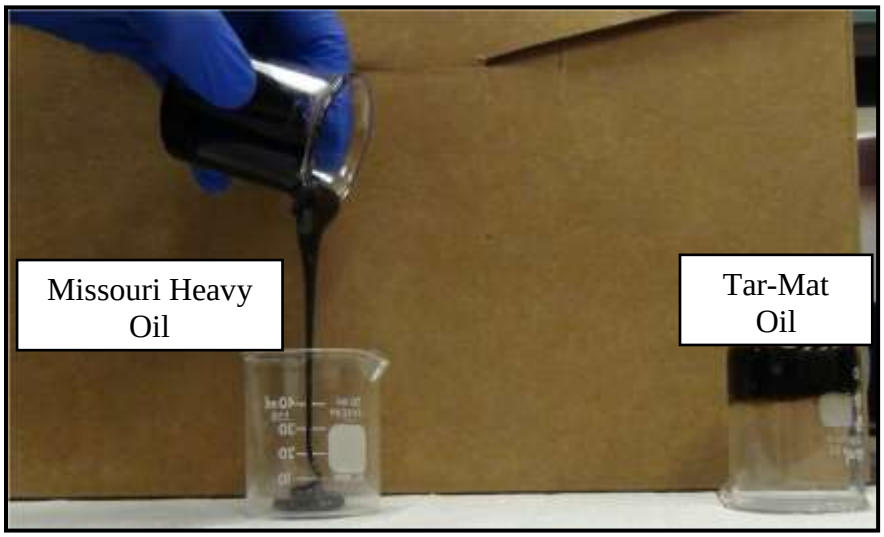

Figure 4.2. Comparison between Missouri Heavy Oil and Tar-Mat Oil

4.3. RAW SAMPLE ANALYSIS TO CHARACTERIZE TAR-MAT SAMPLES

Characterizing a tar-mat in a carbonate reservoir begins with examining the components of the rock, such as its physical and chemical properties and composition. Therefore, several tools are integrated to achieve tar-mat characterization, such as geochemistry rock pyrolysis using Rock Eval-6 and CHNSO elemental analyses using Elemental 106, as well as the conventional SARA analysis of extractable hydrocarbons from the tar-mat.

4.3.1. CHNSO Elemental Analysis from Original Tar-Mat Cores before the Extraction. The amount of carbon, hydrogen, nitrogen, and sulfur present in the five tar-mat samples from different depths was determined directly using vario-macro elemental analysis, as shown in Table 4.2. The oxygen content was obtained by subtracting the sum of the carbon, hydrogen, nitrogen, sulfur, and ash content from 100%.

The data summarized in Table 4.2 indicate that the total concentrations of the analyzed elements (CHNOS) varied with depth. Figure 4.3 shows that the H/C ratio of these five tar-mat samples increased as the API gravity decreased. Figure 4.4 depicts the nearly random variation of carbon content in the tar-mat samples with depth. Similarly, the hydrogen, nitrogen, and sulfur also exhibited variations with depth. The percentages of these elements (C, H, N, S) in the tar-mat samples increased and decreased greatly over very short vertical distances. Furthermore, Figure 4.5 shows that the percentages of C, H, N, and S were relatively higher in samples AB1 and AB5 than in the other three samples.

Table 4.2. Results of Vario-Macro Elemental Analysis from Tar-Mat Samples before the Extraction

Sample	Depth (ft.)	Wt.(mg)	C (%)	H (%)	N (%)	S (%)	O (%)	H/C	Total (%)
AB1	2674	43.00	24.27	2.54	0.71	7.96	64.52	1.26	100
AB2	2703	42.01	18.85	0.86	0.44	0.90	78.94	0.55	100
AB3	2723	42.60	18.69	0.88	0.47	0.75	79.21	0.56	100
AB4	2755	41.45	18.04	0.85	0.45	0.72	79.94	0.57	100
AB5	2782	40.12	30.76	2.67	0.82	5.24	60.51	1.04	100

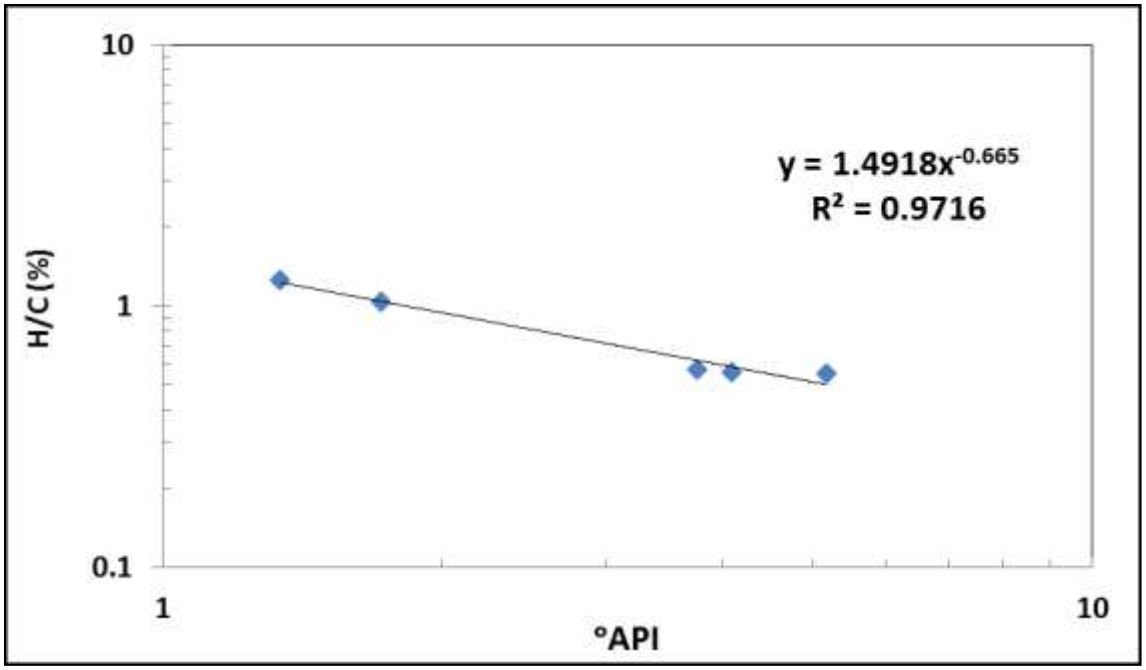

Figure 4.3. Distribution of H/C Ratio from Five Tar-Mat Samples with °API Gravity

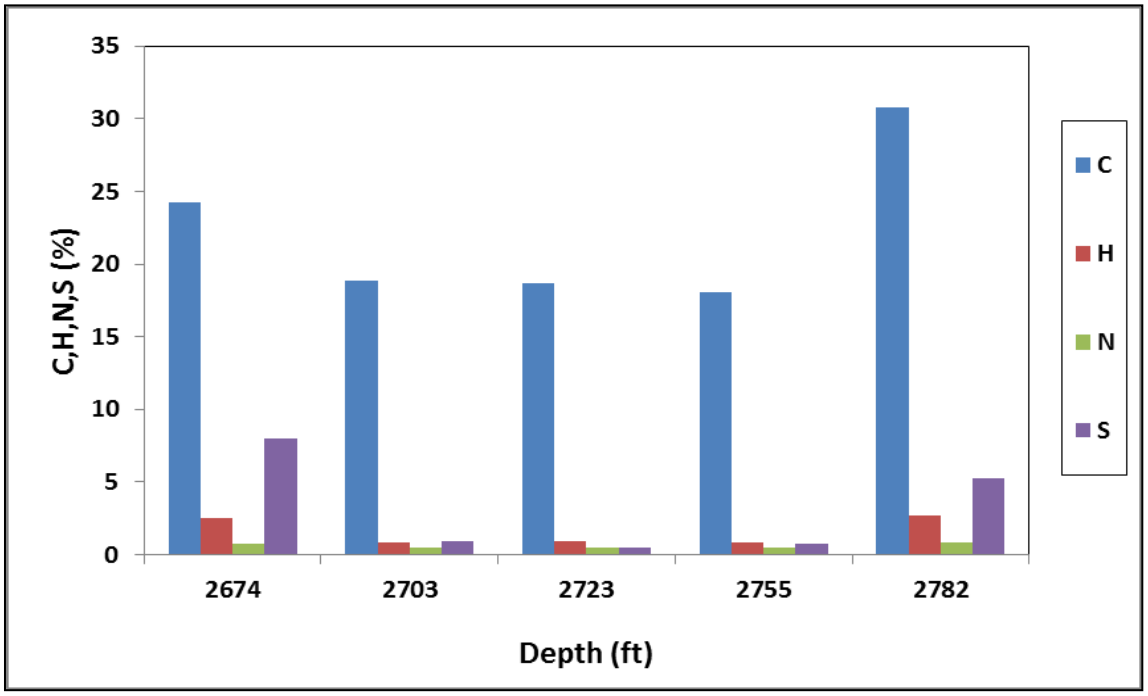

Figure 4.4. Distribution of C, H, N, and S from Five Tar-Mat Samples with Depth

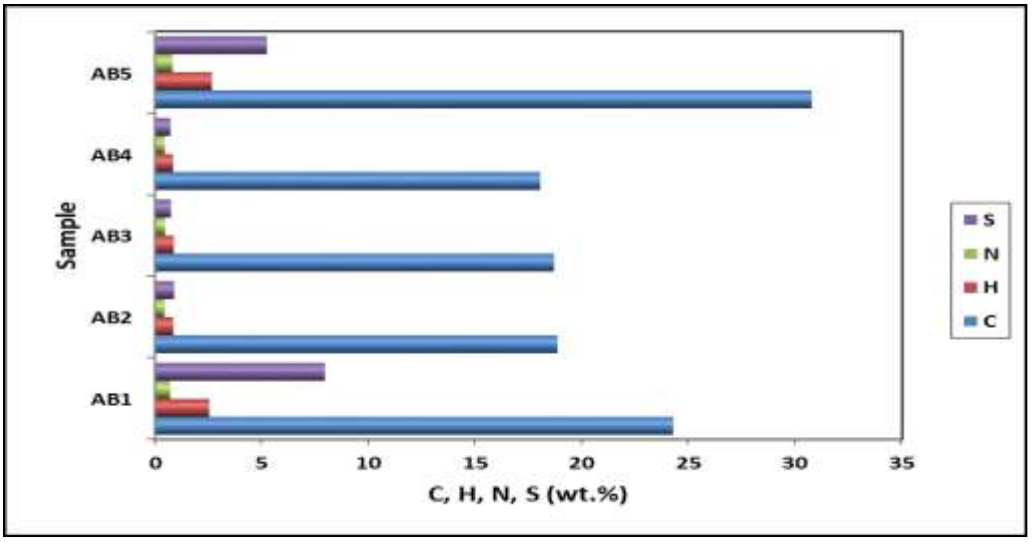

Figure 4.5. Histogram Showing the C, H, N, S Contents of Five Tar-Mat Samples

4.3.2. Effect of Toluene, Hot Water, and Surfactant Solution on C, H, N, S, and H/C from Tar-Mat Samples after the Extraction. Table 4.3 through Table 4.5 provide the results from the tar-mat samples after the extraction by toluene, hot water, and surfactant solution. Table 4.3 indicates that the amount of C, H, N, S, and the H/C ratio obtained from the tar-mat samples after the extraction by toluene decreased as the temperature increased. The most significant reductions occurred in samples AB2, AB3, and AB4, which had API gravity greater than 3 API. On the other hand, samples AB1 and AB5, which had API gravity less than 2 API, showed only slight reductions. Furthermore, a comparison of the properties of samples AB1, AB2, AB3, AB4, and AB5 indicated that these properties varied with depth. Table 4.6 and Table 4.7 show that the amount of C, H, N, S, and the H/C ratio decreased slightly after extraction using hot water and surfactant solution under different temperatures.

Table 4.3. Result of Elemental Analysis from Tar-Mat Samples after the Extraction by Toluene

Sample	Solvent	Temp. (˚C)	wt (g)	C (%)	H (%)	N (%)	S (%)	H/C (%)
AB1	Original	24.5	41.36	24.27	2.54	0.71	7.96	1.26
	Toluene	25	41.36	22.75	2.83	0.66	7.37	1.49
		135	41.36	22.55	2.23	0.66	6.39	1.19
		225	41.36	25.24	2.48	0.67	9.06	1.18
		315	41.36	26.26	2.58	0.71	7.84	1.18
AB2	Toluene	25	41.36	16.22	0.456	0.438	1.067	0.34
		135	41.36	14.21	0.171	0.42	0.872	0.14
		225	41.36	14.41	0.148	0.413	0.81	0.12
		315	41.36	14.41	0.167	0.427	0.81	0.14
AB3	Toluene	25	41.36	19.91	0.95	0.48	2.06	0.57
		135	41.36	19.59	0.94	0.48	2.32	0.57
		225	41.36	19.58	0.93	0.48	2.37	0.57
		315	41.36	18.17	0.86	0.43	6.26	0.57
AB4	Toluene	25	41.36	16.28	0.496	0.456	1.503	0.37
		135	41.36	13.99	0.125	0.433	0.345	0.11
		225	41.36	13.6	0.156	0.427	0.507	0.14
		315	41.36	14.3	0.156	0.461	0.377	0.13
AB5	Toluene	25	41.36	29.76	2.55	0.80	4.35	1.03
		135	41.36	36.36	2.96	0.87	4.79	0.98
		225	41.36	31.19	2.54	0.81	5.78	0.98
		315	41.36	32.77	2.74	0.82	4.68	1.00

Table 4.4. Result of Elemental Analysis from Tar-Mat Samples after the Extraction by Hot Water

Sample	Solvent	Temp. (˚C)	wt (g)	C (%)	H (%)	N (%)	S (%)	H/C (%)
AB1	Original	24.5	41.36	24.27	2.54	0.71	7.96	1.26
	Water	25	41.36	22.84	2.60	0.67	7.13	1.37
		135	41.36	30.29	2.80	0.83	6.47	1.11
		225	41.36	23.04	2.73	0.70	6.27	1.42
		315	41.36	23.76	2.80	0.67	6.86	1.41
AB2	Water	25	41.36	19.43	0.89	0.45	3.53	0.55
		135	41.36	19.19	0.92	0.46	4.30	0.57
		225	41.36	19.28	0.90	0.45	3.08	0.56
		315	41.36	19.32	0.91	0.44	3.55	0.56
AB3	Water	25	41.36	19.91	0.95	0.48	2.06	0.57
		135	41.36	19.59	0.94	0.48	2.32	0.57
		225	41.36	19.58	0.93	0.48	2.37	0.57
		315	41.36	18.17	0.86	0.43	6.26	0.57
AB4	Water	25	41.36	13.33	0.07	0.42	0.35	0.06
		135	41.36	19.38	0.90	0.45	1.64	0.55
		225	41.36	18.88	0.89	0.47	1.54	0.56
		315	41.36	17.96	0.84	0.44	2.80	0.56
AB5	Water	25	41.36	30.36	2.79	0.82	5.23	1.10
		135	41.36	23.84	2.66	0.69	4.23	1.34
		225	41.36	31.03	2.868	0.84	4.737	1.11
		315	41.36	27.59	2.571	0.76	5.235	1.12

Table 4.5. Result of Elemental Analysis from Tar-Mat Samples after the Extraction by Surfactant Solution

Sample	Solvent	Temp. (˚C)	wt. (g)	C (%)	H (%)	N (%)	S (%)	H/C (%)
AB1	Original	24.5	41.36	24.27	2.54	0.71	7.96	1.26
	Surfactant	25	41.36	22.35	2.62	0.64	7.27	1.41
		135	41.36	22.67	2.73	0.64	5.41	1.44
		225	41.36	21.15	2.74	0.64	5.04	1.55
		315	41.36	21.85	2.75	0.64	4.61	1.51
AB2	Surfactant	25	41.36	18.02	0.85	0.43	3.60	0.56
		135	41.36	18.05	0.83	0.43	2.56	0.55
		225	41.36	17.76	0.82	0.41	2.64	0.56
		315	41.36	18.07	0.84	0.43	3.16	0.56
AB3	Surfactant	25	41.36	18.43	0.89	0.45	2.15	0.58
		135	41.36	18.58	0.90	0.46	2.18	0.58
		225	41.36	18.17	0.88	0.46	2.25	0.58
		315	41.36	18.21	0.88	0.45	2.31	0.58
AB4	Surfactant	25	41.36	18.08	0.89	0.45	1.48	0.59
		135	41.36	17.76	0.85	0.43	2.13	0.57
		225	41.36	17.95	0.86	0.44	1.91	0.57
		315	41.36	17.65	0.84	0.43	1.63	0.57
AB5	Surfactant	25	41.36	27.97	2.62	0.75	3.45	1.12
		135	41.36	29.09	2.83	0.77	4.35	1.17
		225	41.36	29.21	2.79	0.76	3.55	1.15
		315	41.36	29.58	2.97	0.77	3.53	1.20

4.4. PYROLYSIS ANALYSIS

According to Tissot and Welte (1984), any rock that was or is capable of generating petroleum can be considered a petroleum source rock. Hunt et al. (1996) added that such a rock's capacity to generate petroleum depends on several factors, such as its quantity (TOC), the thermal maturity of its organic matter, and its quality. Pyrolysis analysis has become the most preferred and thus the most frequently used technique for recognizing and describing petroleum source rocks (Peters, 1986; Spiro, 1991; Sykes and Snowdon, 2002).

4.4.1. Rock-Eval 6 Pyrolysis and Organic Matter Types. Rock–Eval 6 analysis was used to characterize the varying species of organic matter in the sedimentary rock, as well as some reservoir properties, such as the API of the tar-mat, that are impossible to characterize using conventional methods. The quantity, quality, and thermal maturity of the tar-mat rock samples were evaluated from the total organic carbon (TOC) content and Rock-Eval 6 pyrolysis data. Four important parameters can be obtained from pyrolysis analysis: (1) the total free hydrocarbons that can decompose under heat (from S1 peaks); (2) the hydrocarbons derived from kerogen pyrolysis obtained by heating during pyrolysis (from S2 peaks); (3) the organic carbon dioxide (CO2) released by heating organic matter (from S3 peaks); and (4) the temperature at the highest yield of S2 hydrocarbons (T_{max}) (Tissot and Welte, 1984).

The use of thermal volatilization, which mostly entails keeping the sediments at a constant temperature of 300°C for three minutes and gradually increasing it to 500°C, yields the S1 and S2 characteristics. In this case, S1 is the amount of free hydrocarbons, such as oil and gas, in the test sample measured in milligrams of hydrocarbon per one gram of rock; S2 is the amount of hydrocarbons generated when nonvolatile organic

matter is cracked thermally. Table 4.6 summarizes the parameters that can be obtained from Rock-Eval 6.

Table 4.6. Summarized List of Rock-Eval 6 Analysis Output

Parameter	Unit	Name
S1	mg HC/g rock	Free Hydrocarbons
S2	mg HC/g rock	Oil Potential
T_{max}	^{o}C	Source Rock Maturity
S3	mgCO2/g rock	CO2 from Organic Source
S3’	mgCO2/g rock	CO2 from Mineral Source
S3CO	mg CO/g rock	CO from Organic Source
S3’CO	mg CO/g rock	CO from Organic and Mineral Sources
Source Rock Screening		
TOC	% wt.	Total Organic Carbon
PI		Production Index
PC	% wt.	Pyrolysable Carbon Organic
RC	% wt.	Residual Carbon Organic
HI	mg HC/g TOC	Hydrogen Index
OI	mg CO2/g TOC	Oxygen Index
PyroMinC	% wt.	Pyrolysis Mineral Carbon
OxiMinC	% wt.	Oxidation Mineral Carbon
MinC	% wt.	Mineral Carbon

The following parameters can be calculated through the relationship between the S1, S2, and TOC values obtained from the Rock-Eval 6 pyrolysis analysis:

- HI: Hydrogen Index, (S2/TOC)×100 [mg HC/g TOC]
- BI: Bitumen Index, (S1/TOC)×100 [mg HC/g TOC]
- QI: Quality Index, ([S1+S2]/TOC)×100 [mg HC/g TOC]
- PI: Productivity Index (transformation ratio), S1/[S1+S2]
- GP: Genetic potential, (S1+S2) [mg HC/g rock]
- PCI: Pyrolyzable Carbon Index, [0.83 x (S1+S2)]

When evaluating rocks to determine which ones have the potential to produce petroleum, three factors must be employed, which are based solely upon the parameters of the Rock-Eval test, specifically, the guidelines for quality, quantity and thermal maturity, as noted previously (adapted from Ghasemi-Nejad, 2008 and Peters and Cassa, 1994; Table 4.7):

1. S1, S2, and TOC are the factors upon which the quantity, in this case, the potential quantity, is based.
2. The H1 and S2/S3 ratio provide the criterion for determining the type of produced hydrocarbon.
3. P1 and T_{max} determine the level of thermal maturity of the petroleum generated.

The results from the five initial tar-mat samples and from the other 60 samples (12 samples collected from each tar-mat core) after extraction were analyzed and interpreted according to Espitalié et al. (1977), Avramidis and Zelilidis (2007), and Peters and Cassa (1994) using the guidelines shown in Table 4.7.

Table 4.7. Guidelines for Pyrolysis of Quality, Quantity, and Thermal Maturity (from Peters and Cassa, 1994)

Quantity	TOC (wt. %)	S1 (mg HC/g rock)	S2 (mg HC/g rock)
Poor	0-0.5	0-0.5	0-2.5
Fair	0.5-1	0.5-1	2.5-5
Good	1-2	1-2	5-10
Very Good	2-4	2-4	10-20
Excellent	>4	>4	>20
Quality	HI (mg HC/g TOC)	S2/S3	Kerogen type
None	<50	<1	IV
Gas	50-200	1-5	III
Gas and Oil	200-300	5-10	II/III
Oil	300-600	10-15	II
Oil	>600	>15	I
Maturation	Ro (%)	T_{max} (°C)	PI
Immature	0.2-0.6	<435	<10
Mature	-	-	-
Early	0.6-0.65	435-445	0.10-0.15
Peak	0.65-0.9	445-450	0.25-40
Late	0.9-1.35	450-470	>40
Postmature	>1.35	>470	-

The Rock-Eval 6 pyrolysis results from the five original tar-mat samples before the extraction are summarized in Table 4.8. The results from the tar-mat samples after the extraction by toluene, hot water, and surfactant are summarized in Table 4.9 through Table 4.11.

Table 4.8. Results of Total Organic Carbon (TOC) and Rock-Eval 6 Pyrolysis Data from Tar-Mat Samples before the Extraction

Sample	Depth (ft.)	wt. (mg)	T_{max}	HI	S1	S2	S3	TOC	OI	S2/S3	BI	QI	PI	GP	PCI	Ro Cal. (%)
AB1	2674	45.4	428	214	3.3	54	4.4	25.3	17	12.2	13.2	227.0	0.06	57.3	47.6	0.54
AB2	2703	45.4	465	514	18.2	38.9	0.3	7.6	4	114.4	240.6	754.9	0.32	57.1	47.4	1.21
AB3	2723	45.8	467	520	17.6	40.3	0.4	7.8	5	115.1	226.8	746.8	0.30	57.9	48.0	1.25
AB4	2755	45.8	468	577	16.9	43.9	0.3	7.6	4	141.6	221.4	798.4	0.28	60.8	50.4	1.26
AB5	2782	45.3	438	214	9.5	73.5	4.7	34.3	14	15.5	27.7	242.2	0.11	83.0	68.9	0.72

Table 4.9. Results of Total Organic Carbon (TOC) and Rock-Eval 6 Pyrolysis Data from Tar-Mat Samples after the Extraction by Toluene

Sample	Solvent	T (°C)	wt. (g)	T_{max}	HI	S1	S2	S3	TOC	S1+S2	S2/S3	BI	QI	PI	PG	PCI
AB1	Raw	24.5	45.4	428	214	3.3	54	4.4	25.3	57.3	12.2	13.2	227	0.06	57.3	47.6
	Toluene	25	45.5	428	177	4.5	54.5	4.5	30.8	59.1	12.1	14.7	191.8	0.08	59.1	49
		135	45.5	429	161	7.7	48.9	4.7	30.3	56.6	10.5	25.4	186.6	0.14	56.6	47
		225	45.4	428	114	7.7	49.3	4.8	43.1	57.1	10.3	17.9	132.3	0.14	57.1	47.4
		315	45.8	430	164	7.3	47.3	4.7	28.8	54.6	10	25.1	189.3	0.13	54.6	45.3
Sample	Solvent	T (°C)	wt. (g)	T_{max}	HI	S1	S2	S3	TOC	S1+S2	S2/S3	BI	QI	PI	PG	PCI
AB2	Raw	25	45.4	465	514	18.2	38.9	0.3	7.6	57.1	12.2	240.6	754.9	0.32	57.1	47.4
	Toluene	25	45.8	464	440	8.9	20.5	0.4	4.7	29.4	58.5	191.6	631.6	0.3	29.4	24.4
		135	45.2	463	284	1.2	5.8	0.2	2	7	26.3	59.3	343.1	0.17	7	5.8
		225	45.6	459	196	0.8	4.9	0.3	2.5	5.7	17	31.5	227.5	0.14	5.7	4.7
		315	45.4	455	192	0.6	5.7	0.5	3	6.3	12.2	19.1	211.1	0.09	6.3	5.2
Sample	Solvent	T (°C)	wt. (g)	T_{max}	HI	S1	S2	S3	TOC	S1+S2	S2/S3	BI	QI	PI	PG	PCI
AB3	Raw	24.5	45.8	467	520	17.6	40.3	0.4	7.8	57.9	115.1	226.8	746.8	0.3	57.9	48
	Toluene	25	45.4	463	442	8.9	23.4	0.5	5.3	32.3	47.7	168.2	610.4	0.28	32.3	26.8
		135	45.4	460	294	0.5	5.8	0.4	2	6.3	14.5	23.9	317.8	0.08	6.3	5.2
		225	45.3	458	264	1	7	0.4	2.7	8	19.4	36.2	300.4	0.12	8	6.6
		315	45.4	461	247	0.5	5.1	0.3	2.1	5.6	15	23.2	270	0.09	5.6	4.6
Sample	Solvent	T (°C)	wt. (g)	T_{max}	HI	S1	S2	S3	TOC	S1+S2	S2/S3	BI	QI	PI	PG	PCI
AB4	Raw	24.5	45.9	468	577	16.9	43.9	0.3	7.6	60.8	141.6	221.4	798.4	0.28	60.8	50.4
	Toluene	25	45.9	465	501	9	22.6	0.4	4.5	31.6	64.6	198.9	700.2	0.28	31.6	26.2
		135	45.4	464	275	0.5	3	0.3	1.1	3.6	9.5	49.1	324.5	0.15	3.6	3
		225	45.7	464	284	0.6	3.9	0.3	1.4	4.5	13	46.7	330.7	0.14	4.5	3.8
		315	45.4	464	175	0.3	2.1	0.3	1.2	2.4	6.9	21.3	195.9	0.11	2.4	2
Sample	Solvent	T (°C)	wt. (g)	T_{max}	HI	S1	S2	S3	TOC	S1+S2	S2/S3	BI	QI	PI	PG	PCI
AB5	Raw	24.5	45.3	438	214	9.5	73.5	4.7	34.3	83	15.5	27.7	242.2	0.11	83	68.9
	Toluene	25	45.3	437	184	8.8	71.9	4.9	39	80.7	14.7	22.4	206.9	0.11	80.7	67
		135	45.4	438	173	11.2	66.5	5.3	38.5	77.7	12.6	29	202.1	0.14	77.7	64.5
		225	45.3	440	176	8.3	63.4	5.6	36	71.6	11.3	22.9	198.8	0.12	71.6	59.5
		315	45.6	440	166	10.5	63.5	5.4	38.2	74	11.7	27.4	193.6	0.14	74	61.4

Table 4.10. Results of Total Organic Carbon (TOC) and Rock-Eval 6 Pyrolysis Data from Tar-Mat Samples after the Extraction by Hot Water

Sample	Solvent	T (°C)	wt. (g)	T_{max}	HI	S1	S2	S3	TOC	S1+S2	S2/S3	BI	QI	PI	PG	PCI
AB1	Raw	24.5	45.4	428	214	3.3	54	4.4	25.3	57.3	12.2	13.2	227	0.06	57.3	47.6
	Water	25	45.2	428	182	3.6	57.6	4.3	31.6	61.2	13.3	11.3	193.5	0.06	61.2	50.8
		135	45.8	438	217	8.6	73.9	5.6	34	82.5	13.2	25.3	242.5	0.1	82.5	68.5
		225	45.6	428	240	2.9	59.4	4.7	24.7	62.3	12.6	11.9	252.2	0.05	62.3	51.7
		315	45.6	428	262	2.8	58.6	4.5	22.4	61.4	12.9	12.3	273.8	0.04	61.4	51
Sample	Solvent	T (°C)	wt. (g)	T_{max}	HI	S1	S2	S3	TOC	S1+S2	S2/S3	BI	QI	PI	PG	PCI
AB2	Raw	25	45.4	465	514	18.2	38.9	0.3	7.6	57.1	12.2	240.6	754.9	0.32	57.1	47.4
	Water	25	45.7	464	545	19.3	38.6	0.4	7.1	57.9	91.9	272.3	817.4	0.33	57.9	48
		135	45.3	467	620	17.6	44.8	0.4	7.2	62.3	127.9	243.4	863.2	0.28	62.3	51.7
		225	45.9	465	600	18.9	40.1	0.3	6.7	59	143.3	282.2	882.6	0.32	59	48.9
		315	45.1	466	624	18.8	39.6	0.3	6.4	58.4	146.7	296.1	919.7	0.32	58.4	48.5
Sample	Solvent	T (°C)	wt. (g)	T_{max}	HI	S1	S2	S3	TOC	S1+S2	S2/S3	BI	QI	PI	PG	PCI
AB3	Raw	24.5	45.8	467	520	17.6	40.3	0.4	7.8	57.9	115.1	226.8	746.8	0.3	57.9	48
	Water	25	45.3	464	512	18.3	41.2	0.6	8	59.5	69.7	228.3	740.7	0.31	59.5	49.4
		135	45.3	465	585	18.5	43.8	0.4	7.5	62.3	125.1	247.5	832	0.3	62.3	51.7
		225	45.6	465	583	17.2	41.1	0.5	7	58.3	82.1	244.3	827.7	0.3	58.3	48.4
		315	45.3	465	599	17.3	42	0.4	7	59.3	100	246.4	845.8	0.29	59.3	49.2
Sample	Solvent	T (°C)	wt. (g)	T_{max}	HI	S1	S2	S3	TOC	S1+S2	S2/S3	BI	QI	PI	PG	PCI
AB4	Raw	24.5	45.9	468	577	16.9	43.9	0.3	7.6	60.8	141.6	221.4	798.4	0.28	60.8	50.4
	Water	25	45.3	467	580	17.3	44.2	0.4	7.6	61.5	113.3	226.9	807	0.28	61.5	51
		135	45.6	465	601	18.7	41.8	0.3	7	60.4	134.7	268.5	869.2	0.31	60.4	50.1
		225	45.1	468	647	16.7	44.1	0.3	6.8	60.8	147	244.8	892.2	0.27	60.8	50.4
		315	45.7	468	642	16.7	43.9	0.3	6.8	60.6	146.4	243.4	885.7	0.27	60.6	50.3
Sample	Solvent	T (°C)	wt. (g)	T_{max}	HI	S1	S2	S3	TOC	S1+S2	S2/S3	BI	QI	PI	PG	PCI
AB5	Raw	24.5	45.3	438	214	9.5	73.5	4.7	34.3	83	15.5	27.7	242.2	0.11	83	68.9
	Water	25	45.2	438	215	9.8	76.1	5.4	35.3	85.9	14.2	27.7	243.1	0.11	85.9	71.3
		135	45.7	424	243	3.4	60	4.5	24.7	63.4	13.3	13.7	256.7	0.05	63.4	52.6
		225	45.5	438	256	8.6	75	5.5	29.3	83.5	13.6	29.3	285.2	0.1	83.5	69.3
		315	45.2	439	264	8.4	73	5.6	27.7	81.4	13.2	30.3	293.9	0.1	81.4	67.5

Table 4.11. Results of Total Organic Carbon (TOC) and Rock-Eval 6 Pyrolysis Data from Tar-Mat Samples after the Extraction by Surfactant Solution

Sample	Solvent	T (°C)	wt. (g)	T_{max}	HI	S1	S2	S3	TOC	S1+S2	S2/S3	BI	QI	PI	PG	PCI
AB1	Raw	24.5	45.4	428	214	3.3	54	4.4	25.3	57.3	12.2	13.2	227	0.06	57.3	47.6
	Surfactant	25	45.2	426	274	5.7	60.3	4.4	22	66	13.7	26	300.4	0.09	66	54.8
		135	45.8	426	221	6.7	63.7	4.5	28.8	70.4	14.2	23.3	244.8	0.1	70.4	58.4
		225	45.2	427	210	9	65.6	4.5	31.3	74.6	14.6	28.7	238.4	0.12	74.6	61.9
		315	45.3	429	209	8	63.3	4.2	30.3	71.2	15.2	26.2	234.8	0.11	71.2	59.1
Sample	Solvent	T (°C)	wt. (g)	T_{max}	HI	S1	S2	S3	TOC	S1+S2	S2/S3	BI	QI	PI	PG	PCI
AB2	Raw	25	45.4	465	514	18.2	38.9	0.3	7.6	57.1	12.2	240.6	754.9	0.32	57.1	47.4
	Surfactant	25	45.7	468	561	18.3	40	0.4	7.1	58.3	99.9	257.3	818.4	0.31	58.3	48.4
		135	45.5	466	565	16.8	38.9	0.3	6.9	55.6	117.8	243.5	808.4	0.3	55.6	46.2
		225	45.5	469	552	14.6	38.2	0.4	6.9	52.7	90.9	210.3	762.1	0.28	52.7	43.8
		315	45.5	467	553	14.2	36.9	0.4	6.7	51.1	97	213.2	766.7	0.28	51.1	42.4
Sample	Solvent	T (°C)	wt. (g)	T_{max}	HI	S1	S2	S3	TOC	S1+S2	S2/S3	BI	QI	PI	PG	PCI
AB3	Raw	24.5	45.8	467	520	17.6	40.3	0.4	7.8	57.9	115.1	226.8	746.8	0.3	57.9	48
	Surfactant	25	45.7	467	565	18.4	42	0.7	7.4	60.4	64.7	246.6	811.6	0.3	60.4	50.1
		135	45.3	466	528	17.7	43	0.8	8.2	60.8	52.5	217.5	745.4	0.29	60.8	50.4
		225	45.6	469	506	15.4	41.9	0.7	8.3	57.3	62.6	185.3	691.1	0.27	57.3	47.6
		315	45.3	466	437	15.7	40.6	0.8	9.3	56.3	48.4	168.8	606.1	0.28	56.3	46.7
Sample	Solvent	T (°C)	wt. (g)	T_{max}	HI	S1	S2	S3	TOC	S1+S2	S2/S3	BI	QI	PI	PG	PCI
AB4	Raw	24.5	45.3	438	214	9.5	73.5	4.7	34.3	83	15.5	27.7	242.2	0.11	83	68.9
	Surfactant	25	45.4	468	599	16.8	41.3	0.5	6.9	58.1	84.3	243.1	842.5	0.29	58.1	48.2
		135	45.7	468	562	16.3	44.3	0.8	7.9	60.6	55.4	207	769.2	0.27	60.6	50.3
		225	45.6	467	553	15.3	43.9	0.6	8	59.3	77.1	192.8	745.4	0.26	59.3	49.2
		315	45.1	467	460	15.2	42.1	0.7	9.2	57.3	59.3	165.9	625.7	0.27	57.3	47.5
Sample	Solvent	T (°C)	wt. (g)	T_{max}	HI	S1	S2	S3	TOC	S1+S2	S2/S3	BI	QI	PI	PG	PCI
AB5	Raw	24.5	45.3	438	214	9.5	73.5	4.7	34.3	83	15.5	27.7	242.2	0.11	83	68.9
	Surfactant	25	45.6	436	247	12.6	77.7	5.3	31.5	90.3	14.6	39.9	286.7	0.14	90.3	74.9
		135	45.6	440	198	12.1	80.7	5.6	40.8	92.8	14.4	29.7	227.5	0.13	92.8	77.1
		225	45.7	438	205	12.9	86.1	5.8	41.9	98.9	14.9	30.7	236.2	0.13	98.9	82.1
		315	45.8	440	141	12.6	84.9	5.8	60.1	97.5	14.6	21	162.4	0.13	97.5	80.9

4.4.2. Total Organic Carbon (TOC). The TOC content can be considered a direct expression of the amount of combined kerogen and bitumen present in petroleum source rock; it represents the amount of organic matter in a rock sample (Peters and Cassa, 1994).

Before the extraction, five rock samples were analyzed to determine their TOC (wt.%) in order to evaluate the Kuwaiti formation quantitatively. The results of the TOC wt. % for the five initial tar-mat rock samples (AB1, AB2, AB3, AB4, and AB5), as determined by Rock-Eval 6, appear in Table 4.6. The TOC values of the samples, respectively, were 25.25, 7.56, 7.75, 7.61, and 34.29. AB1 and AB2 had the highest TOC wt.% content, while AB2, AB3, and AB4 had the lowest. The average TOC was 16.49%. Considering these values and applying Peters and Cassa's (1994) classification indicates that the tar-mat rock was rich in organic matter and had very good to excellent potential for hydrocarbon production because the TOC was more than 4%, as shown in

Figure 4.6 Figure 4.7 gives the results of the TOC values under the varied conditions, namely, the use of water, toluene, and surfactant, for all of the samples under the various operating temperatures. Following the extraction using toluene, the TOC values decreased in samples AB2, AB3, and AB4, which had API gravity values greater than 3 API. Due to the high API, the three samples were considered to be light tar-mats.

The value of TOC decreased toward good and very good source rock after the extraction of toluene in samples AB2, AB3, and AB4, as displayed in Figure 4.7. This indicates that toluene had a greater impact on these samples after the extraction, while surfactant and hot water had only a slight impact on them.

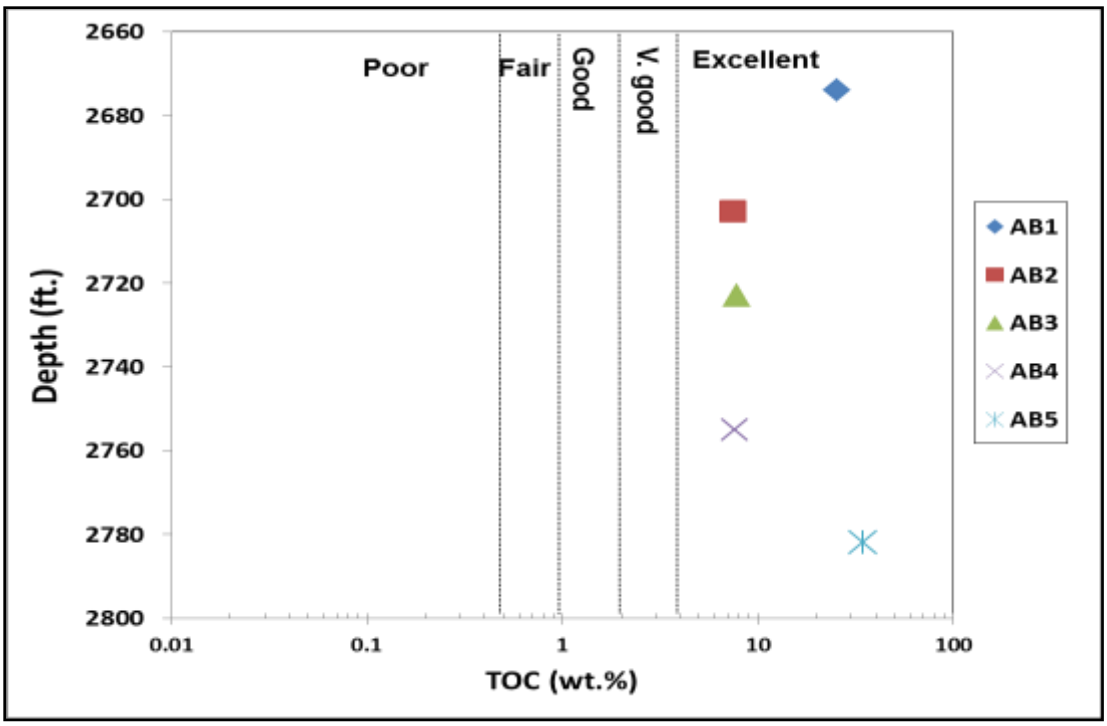

Figure 4.6. Source Rock Characteristics of Tar-Mat Samples before the Extraction

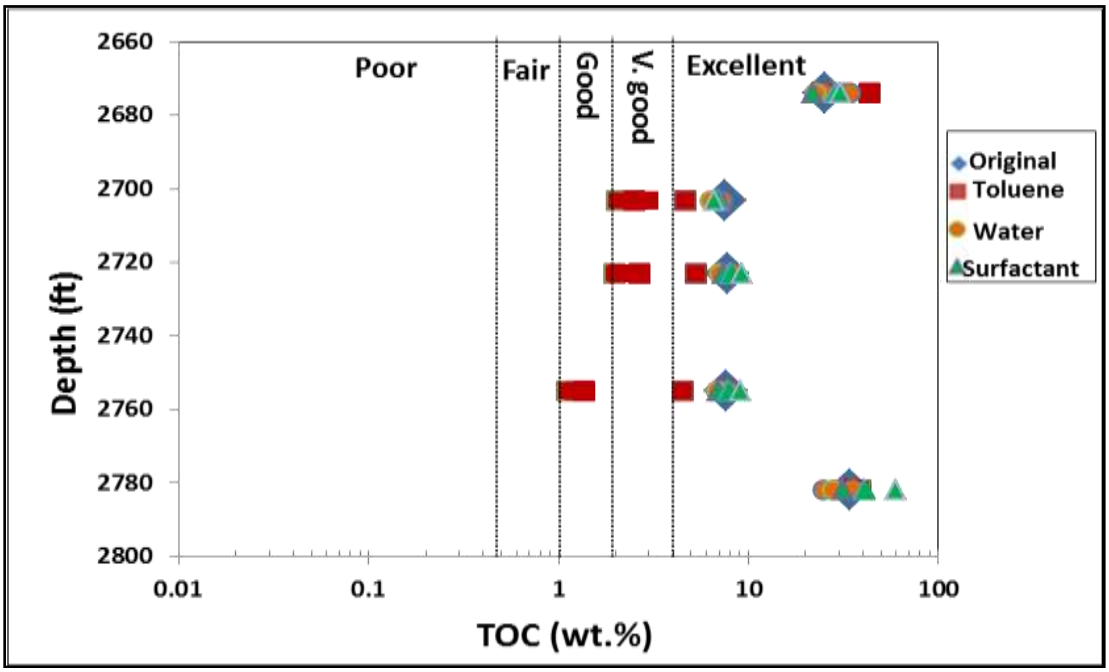

Figure 4.7. Source Rock Characteristics of Tar-Mat Samples after the Extraction

4.4.3. Quantity of Organic Matter from Tar-mat Samples. The quantity of organic matter from the tar-mat samples was determined based on parameters obtained from the Rock-Eval pyrolysis, such as the GP, TOC, S1, and S2.

4.4.3.1 Genetic potential (GP). Table 4.12 shows the classification used to evaluate the quantity of organic matter from tar-mat samples based on the genetic potential values. Generally, a sample's total genetic potential (GP) is the sum of the quantity of free hydrocarbon that has already been generated in the rock, usually denoted as S1, and the quantity of remaining hydrocarbon in the source rock, which usually has not been converted into hydrocarbon yet (S2). Generally, an evaluation of the quality of prospective organic matter in a source rock employs the GP.

Table 4.8 showed the GP of the five tar-mat samples before the extraction. The GP values (GP=S1+S2) fell between 57.07 and 83.04 mg HC/g of rock, with an average of 63.22 mg HC/g of rock. According to the classification given by Tissot and Welte (1984), GP values above 6 mg HC/g of rock indicate good source rock potential (Figure 4.8). After the extraction, toluene had a greater impact on the tar-mat samples, indicating their position as fair to good source rock for generating hydrocarbon. On the other hand, hot water and surfactant solution had only a slight impact on the tar-mat samples, as shown in Figure 4.9.

Table 4.12. Quantity of Organic Matter Based on Genetic Potential Value and Comparable Source Rock Quality According to Tissot and Welte (1984)

Source Potential	Genetic Potential (GP) Value
Poor source rock	<2
Moderate source rock	2-6
Good source rock	>6

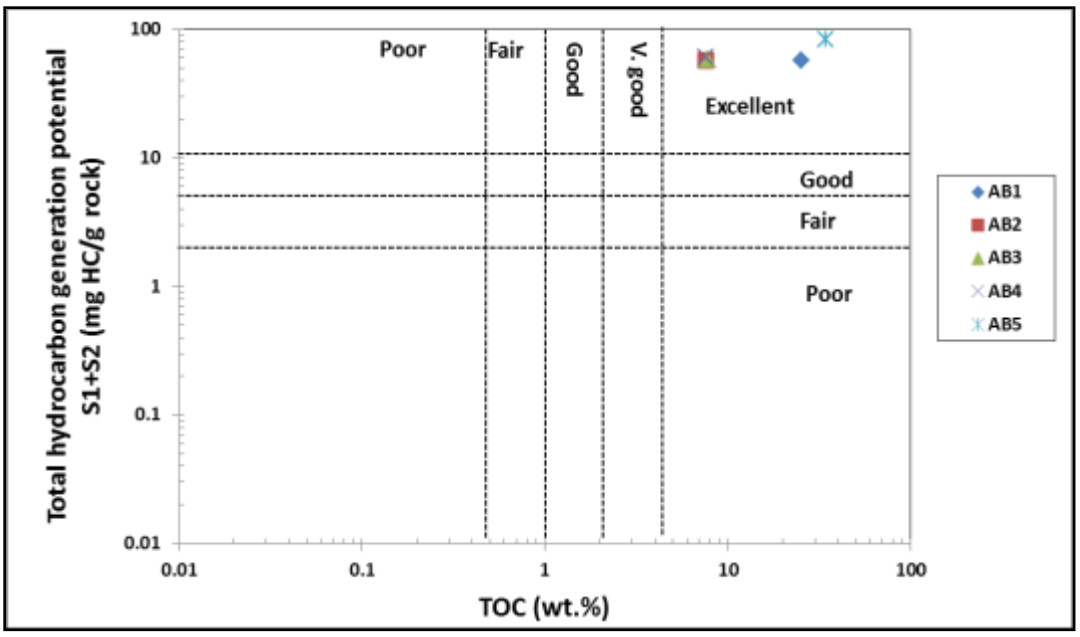

Figure 4.8. Crossplots of TOC vs. GP (S1+S2) Values Showing the Potential Quantity of Produced Hydrocarbon from Tar-Mat Samples before the Extraction

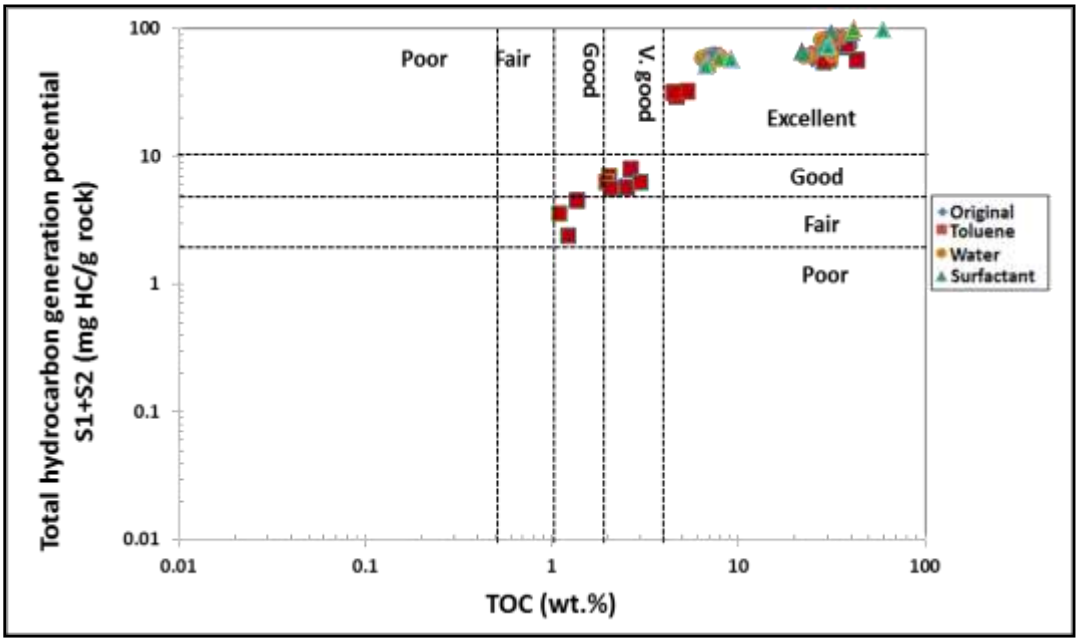

Figure 4.9. Crossplots of TOC vs. GP (S1+S2) Values Showing the Potential Quantity of Produced Hydrocarbon from Tar-Mat Samples after the Extraction

4.4.3.2 TOC versus S1 and S2. The potentiality of the source rock was determined by plotting the pyrolysis S1 and S2 values versus the TOC. For samples AB1 through AB5, the S1 value was between 3.33 and 18.19 mg HC/g of rock. The average value of S1 was 13.01 mg HC/g of rock (Table 4.6). These obtained S1 values indicate a very good to excellent potential source rock for hydrocarbon generation (Figure 4.10).

The S2 value for the same samples was between 38.88 and 73.54 mg HC/g of rock. The mean value was 50.13 mg HC/g of rock (Table 4.6). These values, depicted in Figure 4.12, indicate excellent hydrocarbon generation. When water, surfactant, and toluene were used in the extraction, the 12 samples collected from each tar-mat core recorded reduced S1 and S2 values. Figure 4.11and Figure 4.13 depict the S1 and S2 value reductions after extraction using toluene and indicate fair to good potential source rock for hydrocarbon generation.

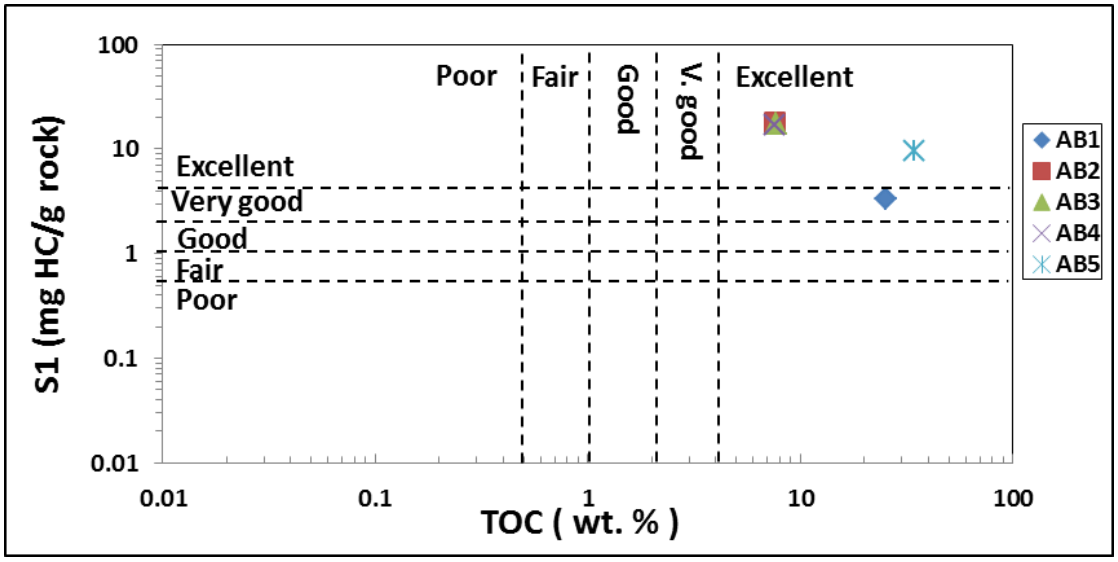

Figure 4.10. Crossplots of TOC vs. Rock-Eval Pyrolysis S1 Values Showing the Potential Quantity of Produced Hydrocarbon from Tar-Mat Samples before the Extraction

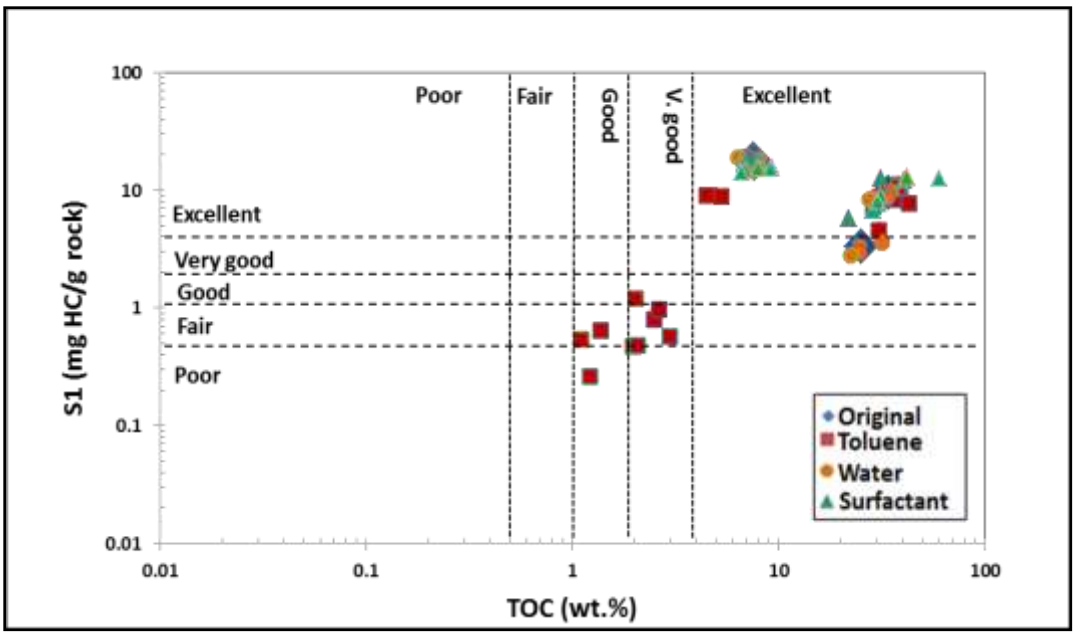

Figure 4.11. Crossplots of TOC vs. Rock-Eval Pyrolysis S1 Values Showing the Potential Quantity of Produced Hydrocarbon from Tar-Mat Samples after the Extraction

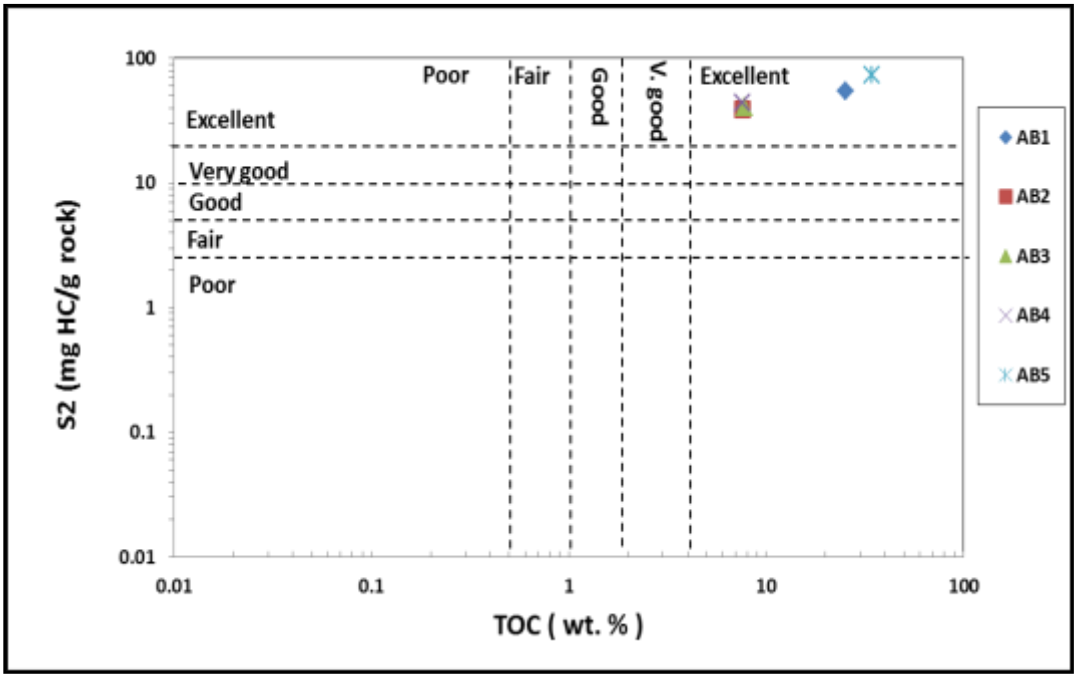

Figure 4.12. Crossplots of TOC vs. Rock-Eval Pyrolysis S2 Values Showing the Potential Quantity of Produced Hydrocarbon from Tar-Mat Samples before the Extraction

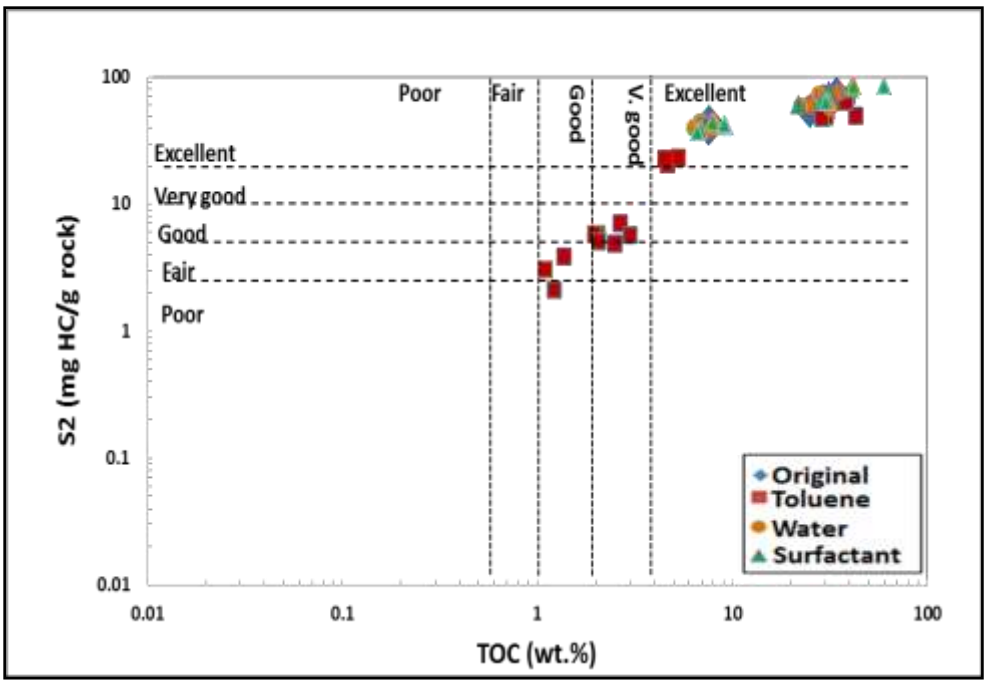

Figure 4.13. Crossplots of TOC vs. Rock-Eval Pyrolysis S2 Values Showing the Potential Quantity of Produced Hydrocarbon from Tar-Mat Samples after the Extraction

Figure 4.14 and Figure 4.15 illustrate that the TOC and S1 contents after the extraction by toluene decreased as the temperature increased. This reduction were more pronounced in samples AB2, AB3, and AB4, which had API gravity greater than 3 API. On the other hand, the TOC and S1 contents from samples AB1 and AB5 increased, probably due to the entrapment of toluene with tar and their low API gravity. Furthermore, Figure 4.16 shows that the S2 contents decreased as the temperature increased in all of the samples after the extraction by toluene. On the other hand, the TOC, S1, and S2 contents decreased slightly after the extraction by hot water and surfactant solution.

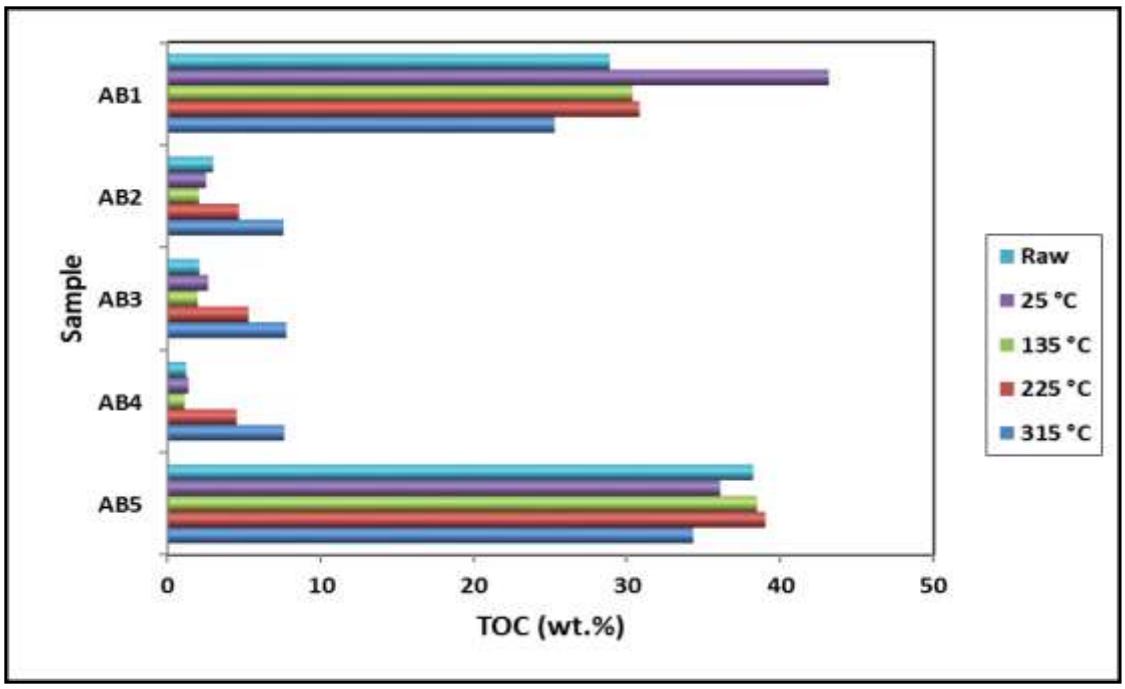

Figure 4.14. Effect of Toluene Recovery on Tar-Mat TOC with Increased Temperature

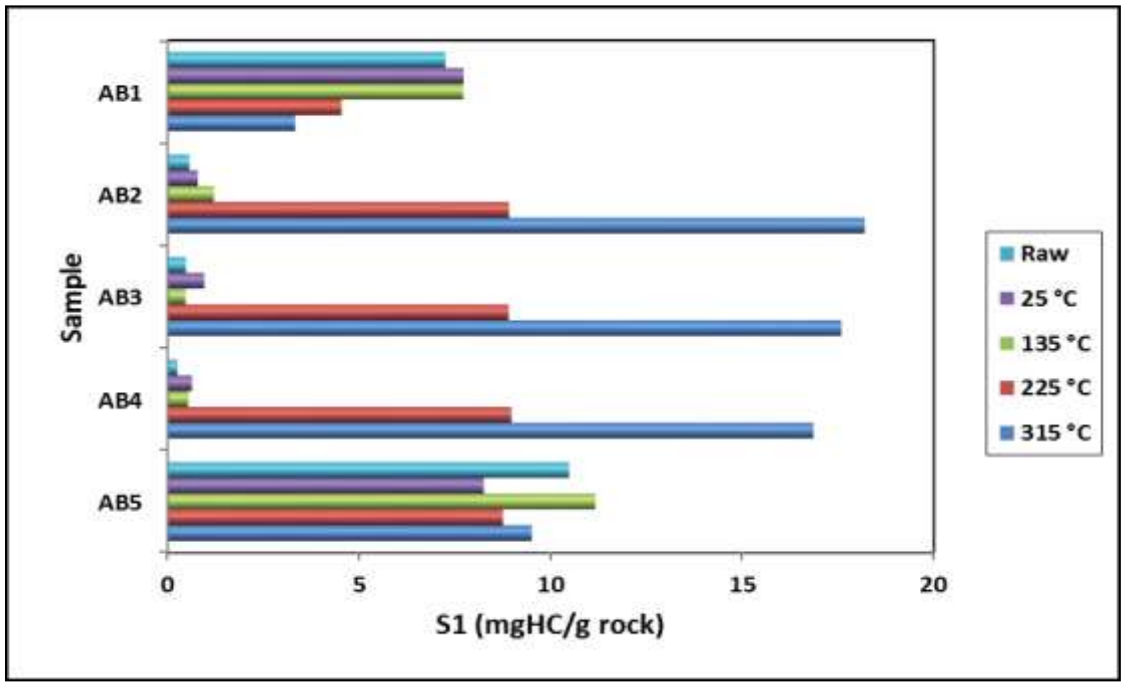

Figure 4.15. Effect of Toluene Recovery on Tar-Mat S1 with Increased Temperature

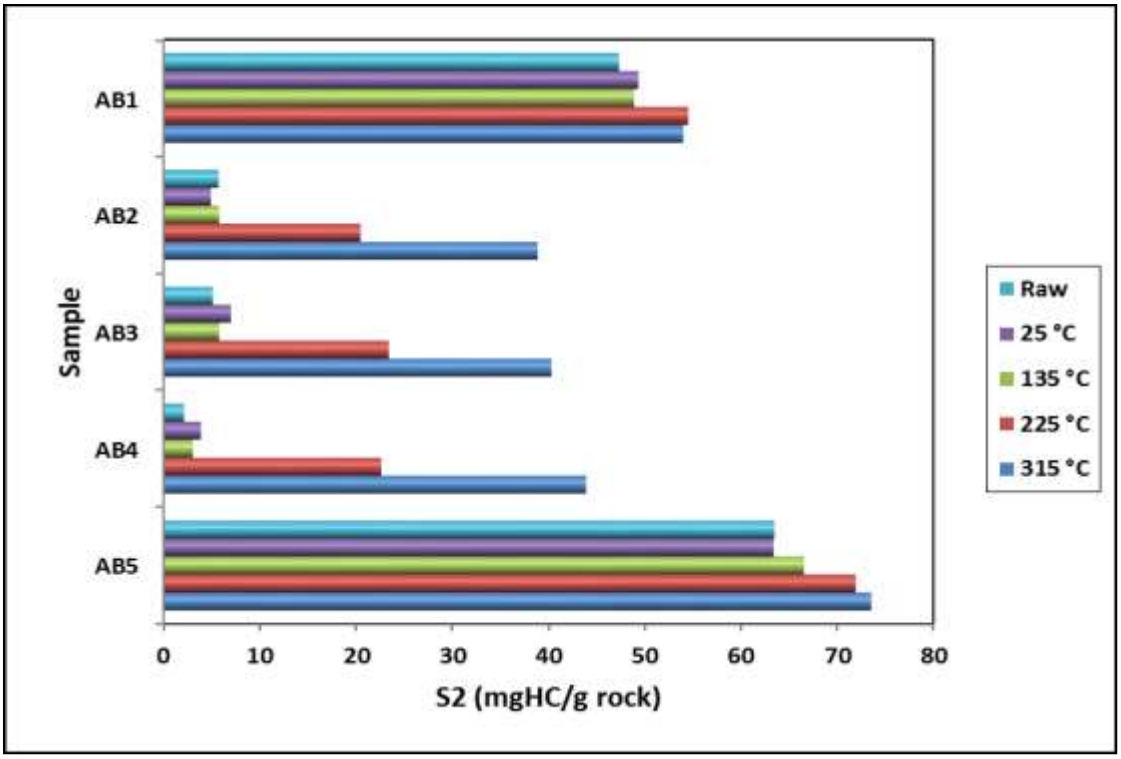

Figure 4.16. Effect of Toluene Recovery on Tar-Mat S2 with Increased Temperature

4.4.4. Quality of Organic Matter (Kerogen Type). The quality of organic matter from tar-mat samples can be determined based on parameters obtained from the Rock-Eval 6 pyrolysis, such as HI, OI, T_{max}, S1, S2/S3, and PCI.

4.4.4.1 Hydrogen and oxygen indices (HI and OI). The hydrogen index (HI) and oxygen index (OI) usually compare to the accrued total of the content of these tow gases within the kerogen. Both indices serve as useful parameters for describing the origin of organic matter. In this regard, it is important to appreciate that it is the hydrogen index that is widely used to measure or determine a rock's potential to generate oil. Oxygen cannot serve as the criterion for this determination because some oxygen is released from the organic matter due to the oxidation of the kerogen or carbonate in a

rock. Mathematically, the hydrogen index and oxygen index are expressed as [(100 x S2) /TOC] and [(100 x S3) /TOC], respectively, (Tissot and Welte, 1984; Peters and Cassa, 1994; Hunt 1996).

At early stages of thermal maturity:

a. Type I kerogen usually contains HI values >600 mg HC/g TOC and OI values <50 mg CO2/g TOC; Type II kerogen usually contains HI values 300–600 mg HC/g TOC and OI values <50 mg CO2/g TOC; and Type III kerogen usually contains HI values 50–200 mg HC/g TOC and OI values of 5–100 mg CO2/g TOC;
b. A combination of Type II and Type III kerogen has a low HI of approximately 200–300 mg HC/g TOC;
c. Type IV kerogen contains HI values of <50 mg HC/g TOC (Tissot and Welte, 1984; Peters and Cassa, 1994).

The HI values for the initial five tar-mat cores, AB1 through AB5, before the extraction were 214, 514, 520, 577, and 577 mgHC/g of TOC, respectively. The mean was 407.8 mgHC/g of TOC. According to Peters and Cassa's (1994) classification, these values indicate that samples AB1 and AB5 contained Type II/III kerogen of either land or marine origin capable of emitting oil and gas. The other samples, AB2 through AB4, contained Type II kerogen of marine origin, which is rich in hydrogen and poor in oxygen. Combining these characteristics with the good S2 hydrocarbon of samples AB2, AB3, and AB4 yielded 39, 40, and 44 mg HC/g of rock, respectively (Table 4.8). The OI ranged from 4 to 17 mg CO2/g of TOC, with an average of 8.8 mg CO2/g of TOC.

Comparing the HI versus the OI indicated that two of the samples were kerogen Type II/III (AB1, AB5), and three of the samples were kerogen Type II (AB2, AB3, and AB4), as shown in Figure 4.17.

After the extraction by toluene, hot water, and surfactant solution, the HI vs. OI diagrams showed that the samples lying on the curves mainly consisted of kerogen Types II and II/III (Figure 4.18).

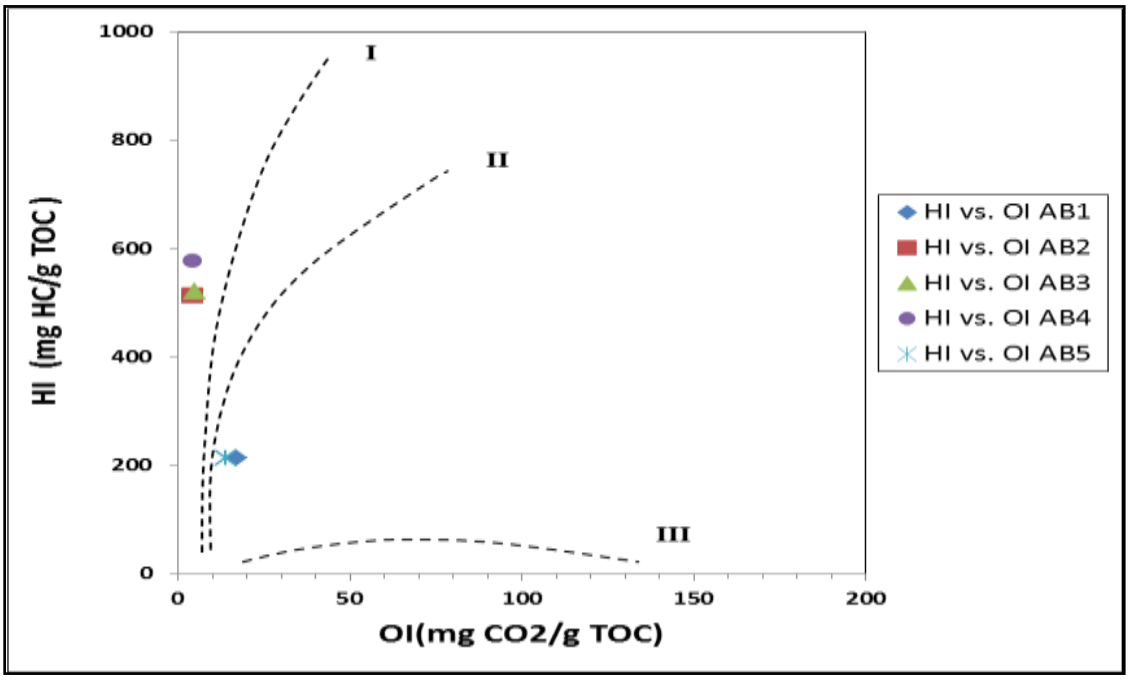

Figure 4.17. Van Krevelen-Type Diagram of HI vs. OI to Determine Organic Matter Type Found in Kuwaiti Carbonate Reservoir Tar-Mat Samples before the Extraction (Van Krevelen, 1993)

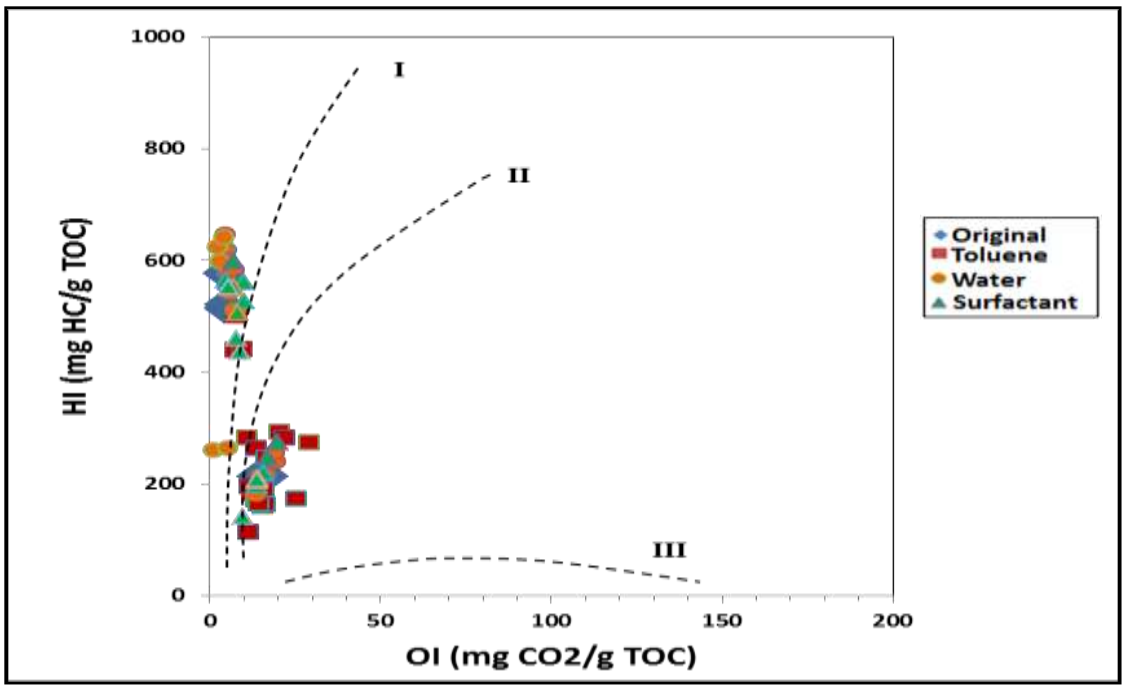

Figure 4.18. Van Krevelen-Type Diagram of HI vs. OI to Determine Organic Matter Type Found in Kuwaiti Carbonate Reservoir Tar-Mat Samples after the Extraction (Van Krevelen, 1993)

4.4.4.2 Hydrogen index (HI) and T_{max}. HI versus T_{max} commonly is used to determine and evaluate the type of kerogen while avoiding the influence of the OI. Tables 4.8, 4.9, and 4.10 show the results of HI and T_{max} obtained by Rock-Eval pyrolysis. The maximum temperature (T_{max}) was between 428 and 468 °C, with an average of 453.2 °C. As shown in Table 4.8, the organic geochemical results were plotted along the curves HI vs. T_{max} in order to evaluate the type of kerogen in the five samples before the extraction. The HI vs. T_{max} diagrams show that the samples lying on the curves mainly consisted of kerogen Types II and II/III (Figure 4.19 and Figure 4.20).

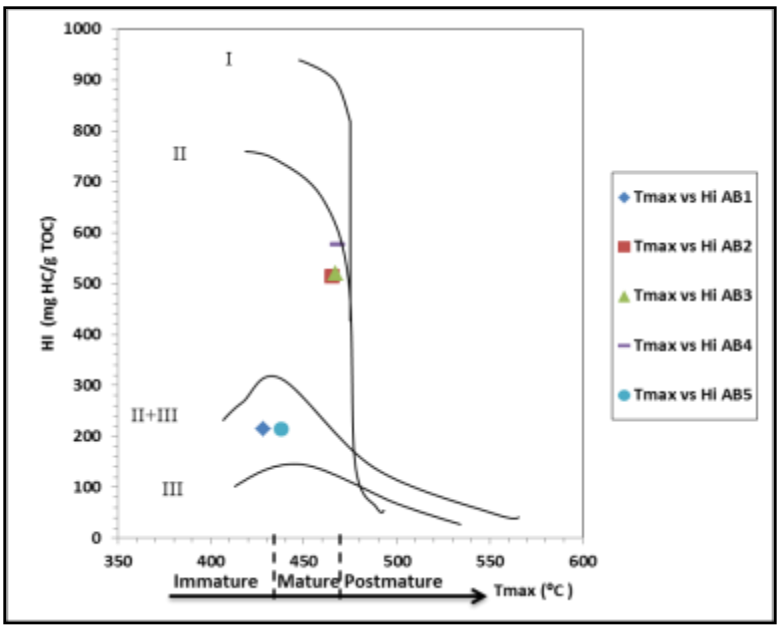

Figure 4.19. Crossplots of T_{max} vs. HI to Determine Organic Matter Type Found in Kuwaiti Carbonate Reservoir Tar-Mat Samples before the Extraction (Van Krevelen, 1993)

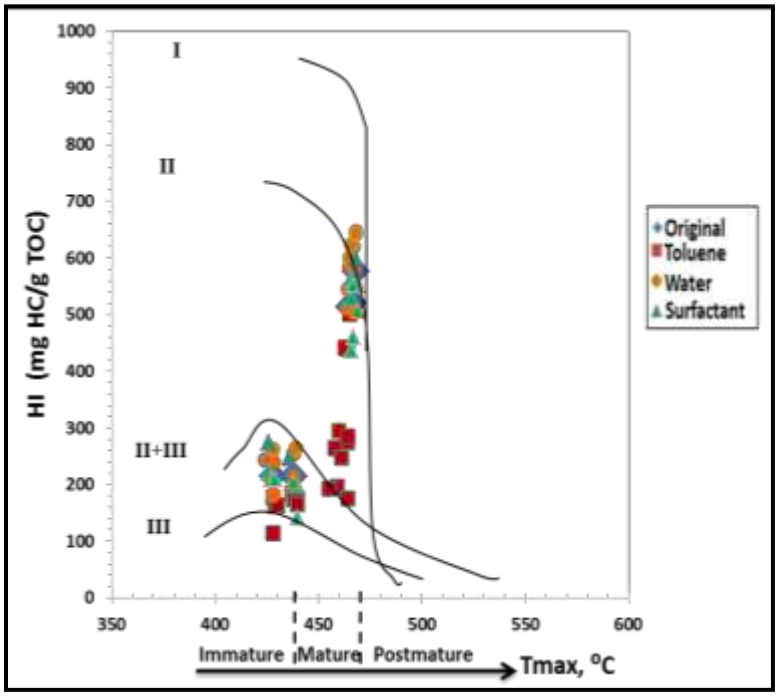

Figure 4.20. Crossplots of T_{max} vs. HI to Determine Organic Matter Type Found in Kuwaiti Carbonate Reservoir Tar-Mat Samples after the Extraction (Van Krevelen, 1993)

4.4.4.3 S2/S3 ratio. The S2/S3 ratio, which represents the hydrocarbon type index, was used by Clementz et al. (1979) and Groune et al. (2013) to determine the kerogen type. The hydrocarbon type index (S2/S3) values of samples AB1 and AB5 were 12 and 15, respectively. Values ranging from 10-15 indicate Type II kerogen (Table 4.7). The S2/S3 values of samples AB2, AB3, and AB4 were 114, 115, and 141, respectively; values greater than 15 (>15) may indicate kerogen Type I (Peters and Cassa, 1994).

According to Peters and Cassa's (1994) classification, given the HI and S2/S3 values from the five tar-mat samples in Table 4.7, samples AB2, AB3, and AB4 were oil prone, while samples AB1 and AB5 were a mixture of oil and gas prone, as shown in Figure 4.21. The diagram of S2/S3 versus TOC can be used to determine the quality and hydrocarbon content that can be produced from the source rocks (Peters and Cassa, 1994), as shown in Figure 4.22 for this study. The samples (AB1-AB5) were in the zone considered excellent for oil generation.

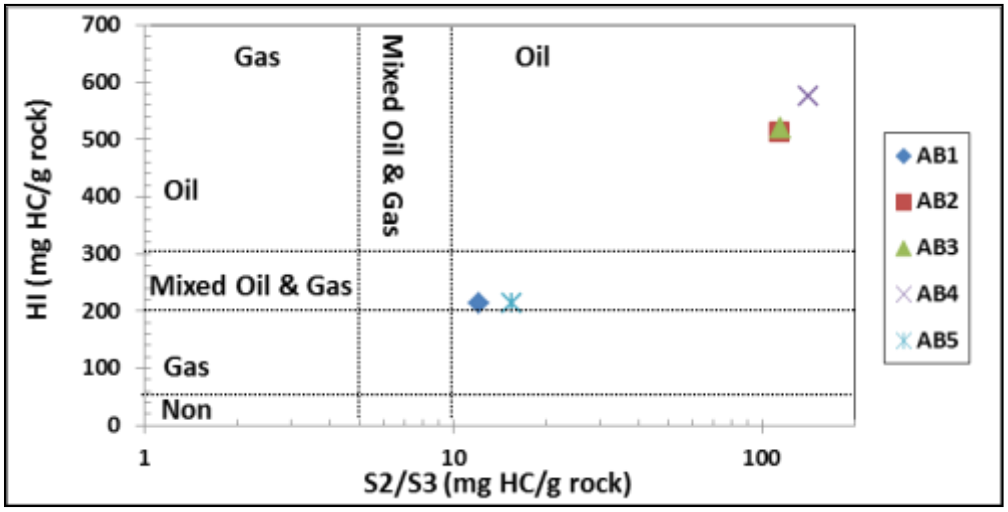

Figure 4.21. Crossplots of Hydrogen Index (HI) vs. Rock-Eval S2/S3 Values Showing the Quality and Hydrocarbon Content of Oil Produced from Tar-Mat Samples

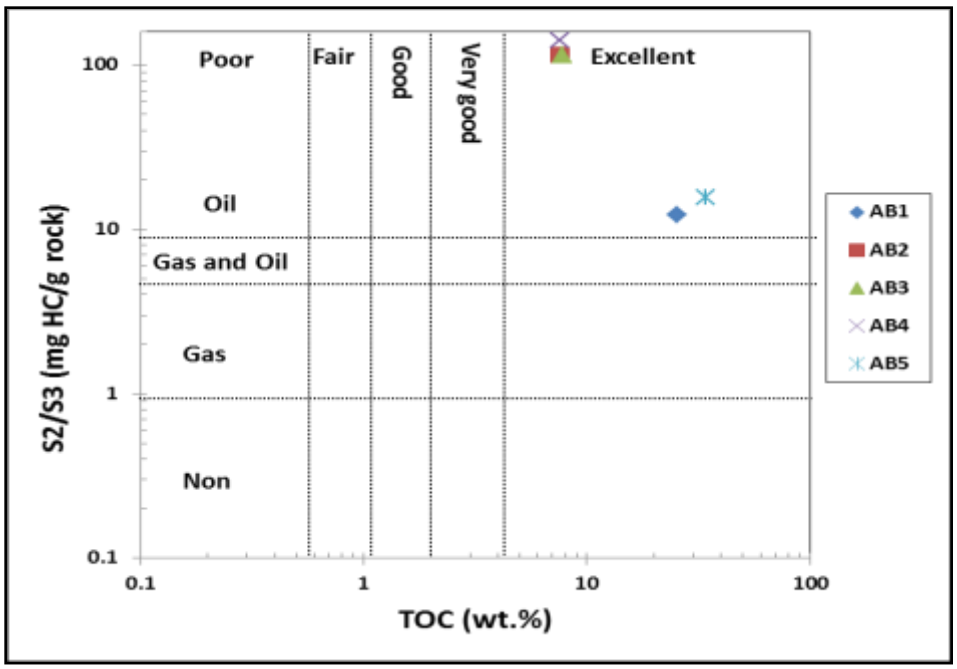

Figure 4.22. Crossplots of TOC vs. Rock-Eval S2/S3 Values Showing the Quality and Hydrocarbon Content of Oil Produced from Tar-Mat Samples

4.4.4.4 Pyrolyzable carbon index (PCI). The pyrolyzable carbon index (PCI) indicates the maximum amount of hydrocarbon that a sample generates during the analysis. The PCI is another parameter that can be used to determine the kerogen type and its hydrocarbon potential. PCI values ≥75 indicate Type I; values from 40–50 indicate Type II; and values <15 indicate Type III (Reed and Ewan, 1986; Shaaban et al., 2006). The expression for obtaining the PCI from the initial five tar-mat samples and from the 60 samples collected from these five initial tar-mats was suggested to be (Reed and Ewan, 1986; Geologic Materials Center, 1990; Shaaban et al., 2006):

$$PCI=0.83\times(S1+S2) \quad (2)$$

The plot of PCI versus TOC before the extraction from the five initial samples shows that samples AB1 through AB4 were kerogen Type II, and sample AB5 was a mix of kerogen Type I/II (Figure 4.23). Also, Figure 4.24 shows the results of the 60 samples after the extraction using toluene, water, and surfactant solution. The results indicate that toluene had a greater impact on these samples, especially AB2 through AB4 (Figure 4.24).

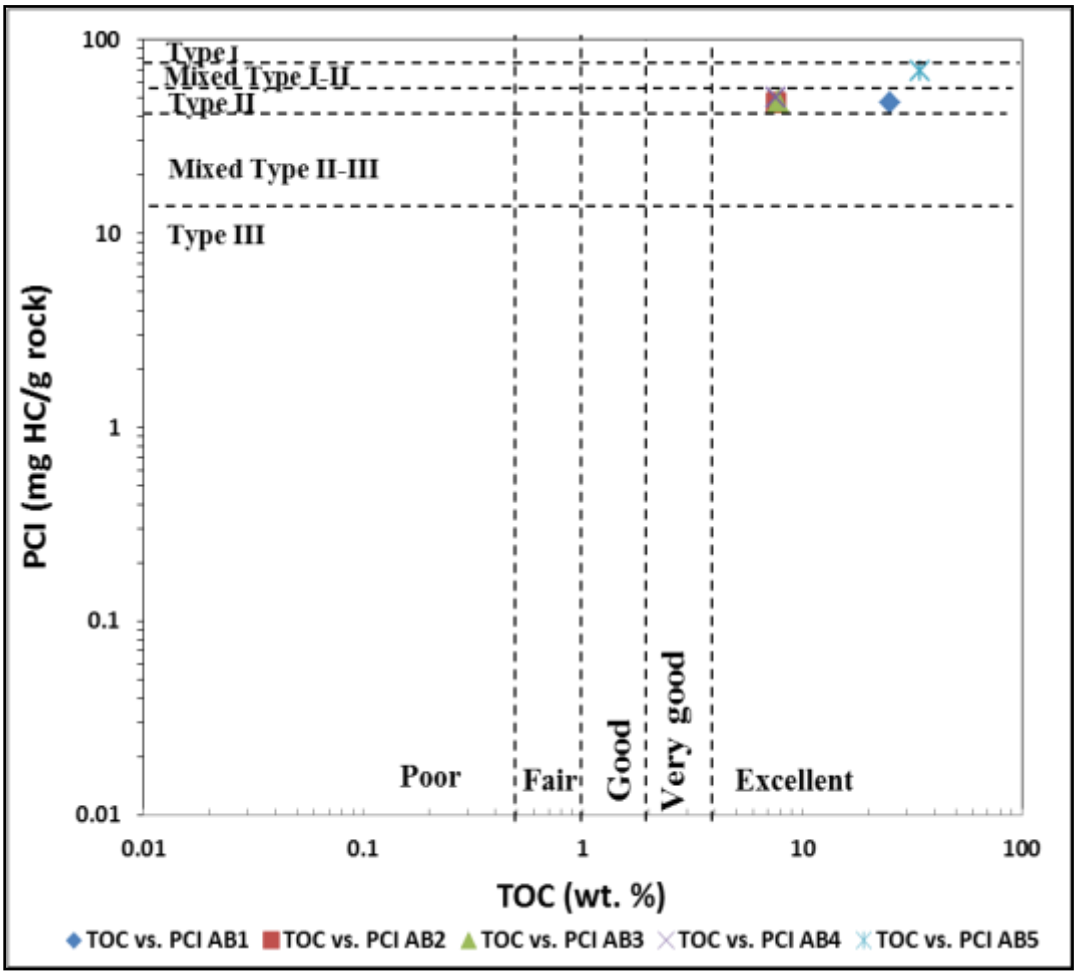

Figure 4.23. Crossplots of TOC vs. PCI Indicating the Quality and Kerogen Type of Tar-Mat Samples from Kuwaiti Carbonate Reservoir before the Extraction

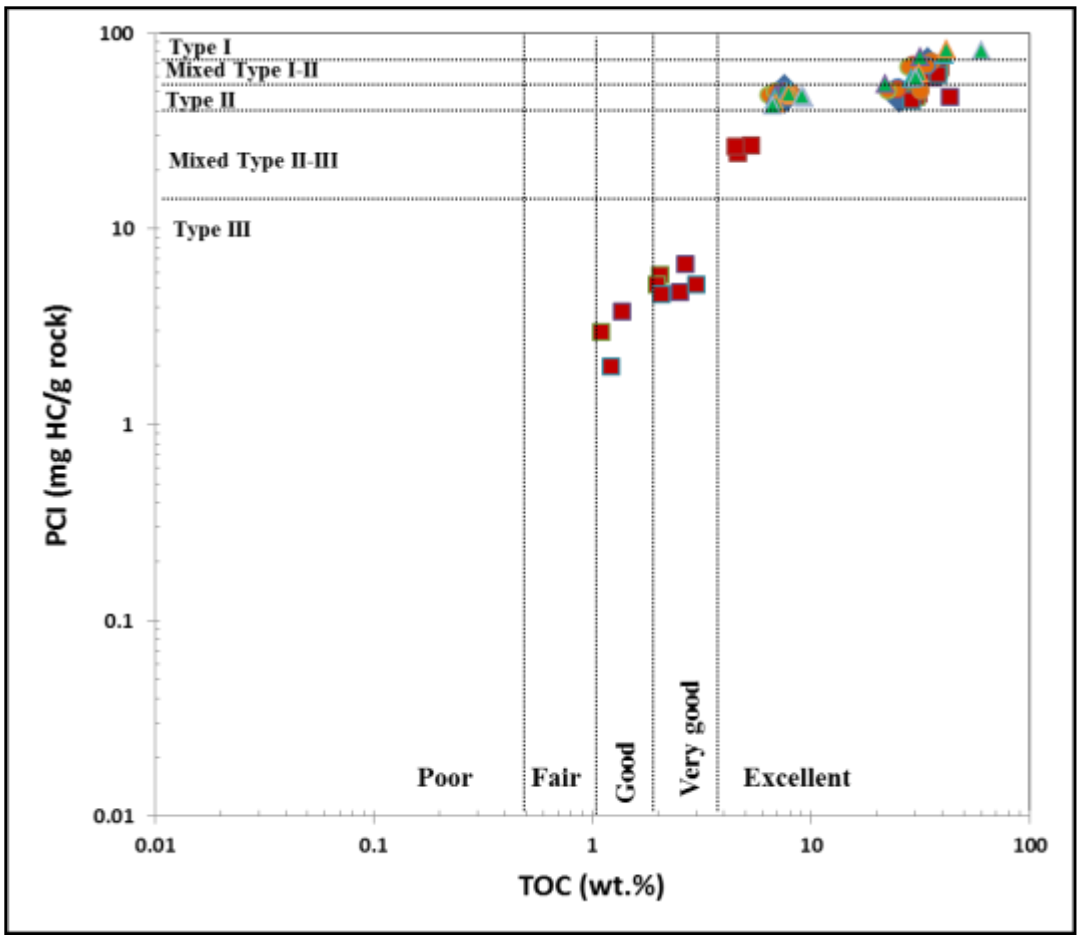

Figure 4.24. Crossplots of TOC vs. PCI Indicating the Quality and Kerogen Type of Tar-Mat Samples from Kuwaiti Carbonate Reservoir after the Extraction

4.4.4.5 Migrated and non-migrated hydrocarbons. Plotting S1 versus the TOC can help to differentiate between the migrated and non-migrated hydrocarbons. When S1 is high and the TOC is low, this indicates migrated hydrocarbon (Hunt, 1996). The dividing line on the plot is where S1/TOC = 1.5. Non-indigenous hydrocarbons have higher values than this, while indigenous hydrocarbons have lower values (Hunt, 1996).

Figure 4.25 and Figure 4.26 show that all of the analyzed tar-mat samples contained both migrated and non-migrated hydrocarbons.

Clearly, the Kuwaiti carbonate reservoir formation is characterized by localized intervals with the capacity to generate both oil and mixed oil/gas. The oil-prone source rock intervals from samples AB2, AB3, and AB4 were characterized by very high TOC (7.56-7.75%) and excellent potential to generate oil, as indicated by their high HI (pyrolysis S2 yields from 38.9 to 43.9 mg HC/g of rock, and HI mostly >500 mg HC/g of TOC). The mixed-prone source rock intervals from samples AB1 and AB5 were characterized by high TOC (25.25-34.29%) and fair to very good potential to generate oil and gas, as indicated by their high HI (pyrolysis S2 yields from 54-73.5 mg HC/g of rock, and HI mostly >200 mg HC/g of TOC).

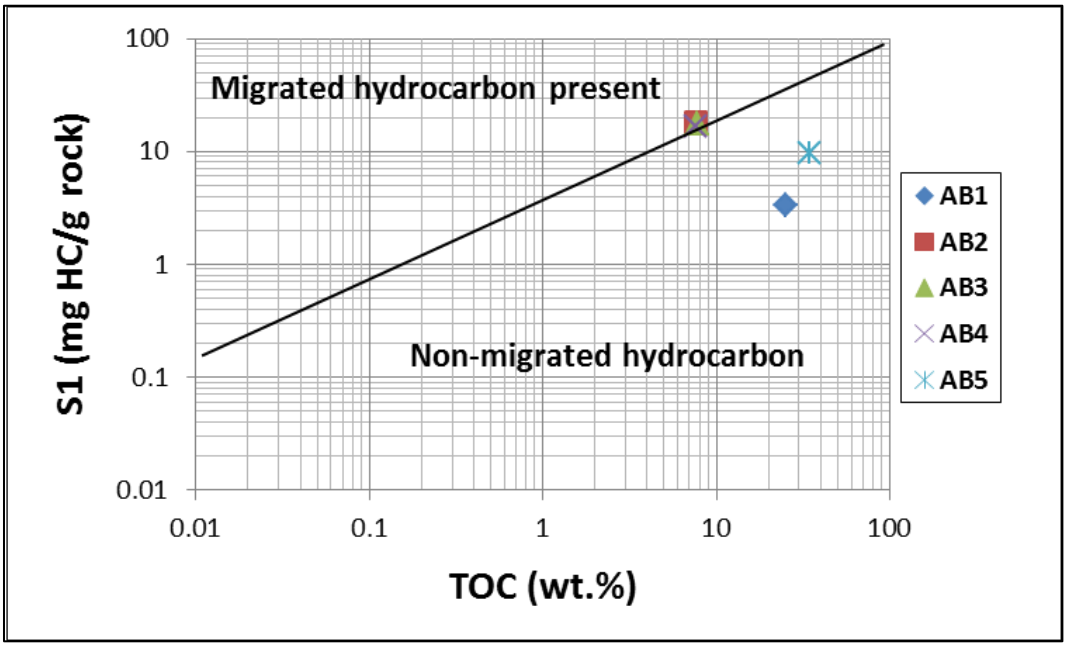

Figure 4.25. S1 vs. TOC to Identify Migrating and Non-Migrating Hydrocarbons from Tar-Mat Samples before the Extraction

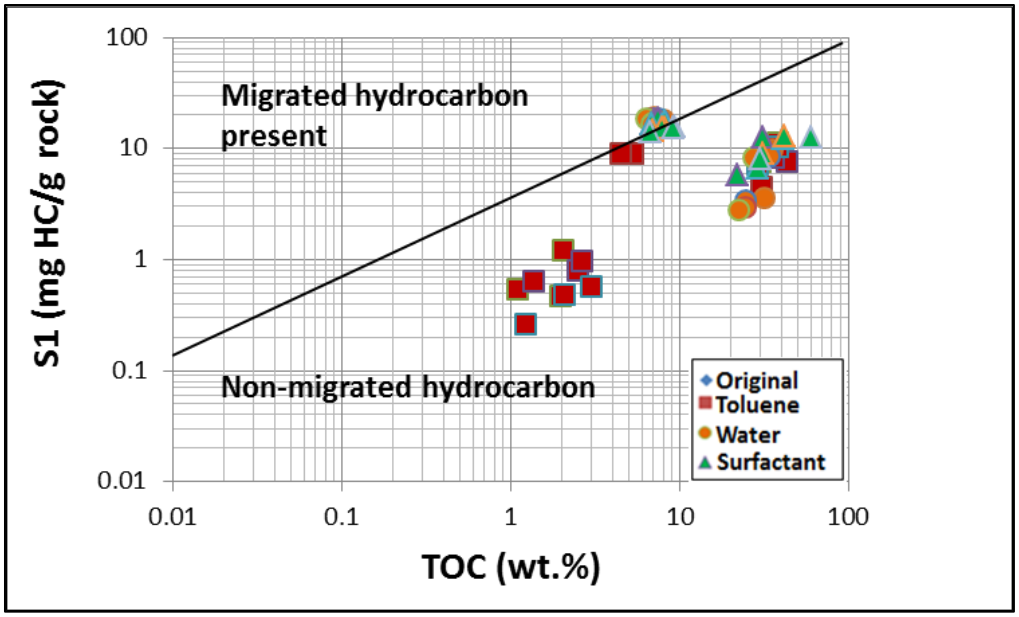

Figure 4.26. S1 vs. TOC to Identify Migrating and Non-Migrating Hydrocarbons from Tar-Mat Samples after the Extraction

4.4.5. Thermal Maturity of Organic Matter. The thermal maturity of organic matter from tar-mat samples can be determined based on parameters obtained from Rock-Eval pyrolysis, such as T_{max}, PI, and %Ro.

4.4.5.1 T_{max} vs. PI. The best way to determine the thermal maturity of organic matter usually involves determining and combining the relationships between the essential Rock-Eval parameters, such as T_{max}, and the calculated Rock-Eval parameter, the production index (PI). Both T_{max} and PI, otherwise known as the transformation ratio, can be used to determine the thermal maturity of the organic material from the tar-mat samples. Before the extraction, PI ranged from 0.03 to 0.32, with an average of 0.21 (Table 4.8). The plot of T_{max} versus PI for samples AB1 and AB5 indicates a stage of immature oil formation (Figure 4.27). The values for the other three samples indicate a

stage of late–mature oil formation. Figure 4.28 shows the results of T_{max} versus PI after the extraction by toluene, water, and surfactant under different temperatures.

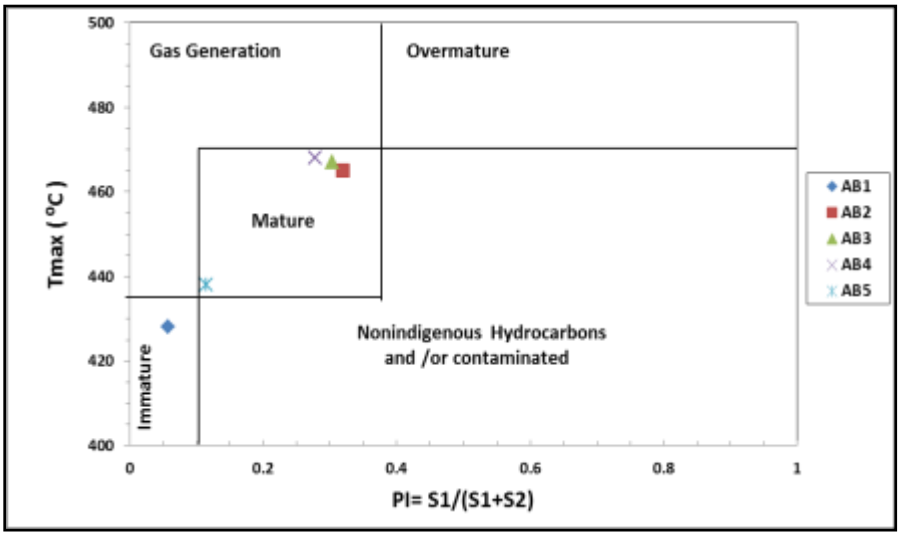

Figure 4.27. T_{max} vs. PI Diagram of the Investigated Tar-Mat Samples from Kuwaiti Carbonate Reservoir before the Extraction

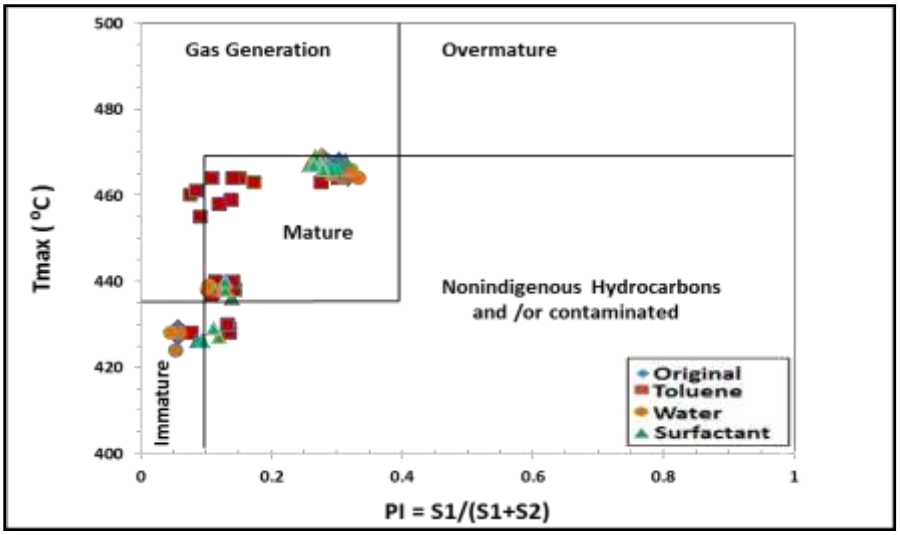

Figure 4.28. T_{max} vs. PI Diagram of the Investigated Tar-Mat Samples from Kuwaiti Carbonate Reservoir after the Extraction

The plot of the Rock-Eval parameter PI versus depth can be used to determine the boundary depth between mature and immature zones in the Kuwaiti formation. Figure 4.29 clearly shows that the discontinuous red line identifies the boundary between the immature zone and the mature zone from tar-mat samples. As seen in Figure 4.29, it can be obvious that the mature zone is located 2700 feet below sea level.

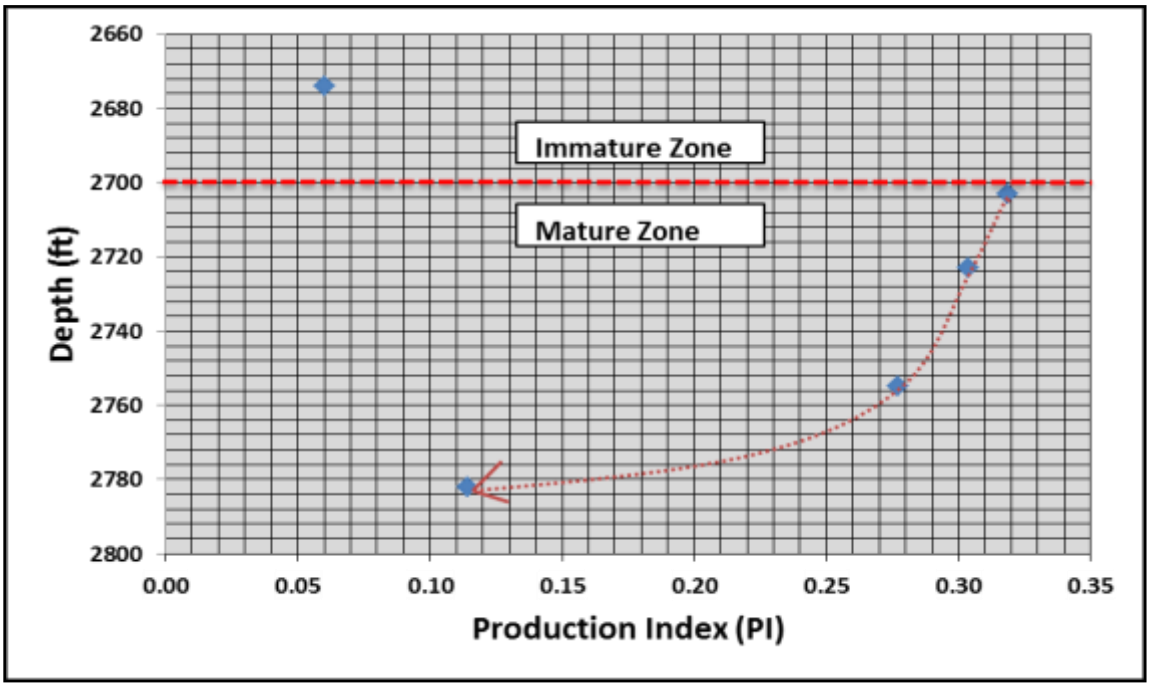

Figure 4.29. Crossplot of Production Index (PI) Versus Depth (adapted from Huc and Hunt, 1980)

4.4.5.2 T_{max} vs. %Ro. Vitrinite reflectance is an optical method for measuring the maturity of a source rock (Tissot and Welte, 1984). The method makes use of materials derived from vascular plants (Hunt, 1996). The reflectance (Ro) of a light increases as the maturity of the organic matter increases. The T_{max} parameter of Rock-Eval pyrolysis serves as an indicator of thermal maturity, so it is therefore possible to convert T_{max} into Ro (Dembicki Jr, 2009).

Similarly, the vitrinite reflectance (%Ro) value can be used to precisely determine the level of maturity of organic matter. This value can be calculated for kerogen Types II and III. The expression for obtaining %Ro, as suggested by Jarvie et al. (2001), is:

$$\%RO = (0.0180 \times Tmax) - 7.16 \quad (3)$$

Also, reasonable Ro data were obtained when the equation was not applied to samples with S2 values smaller than 0.5 mg HC/g of rock and with T_{max} <420°C or >500°C.

The results of the Ro% analysis of the five tar-mat samples before the extraction appear in Table 4.6. As Figure 4.30 depicts, the Ro% values, which ranged from 0.54% to 1.26%, with an average of 1.0%, indicate that this formation ranges from immature to mature. Figure 4.31 shows the results of %Ro versus depth from 60 samples after the extraction by toluene, water, and surfactant under different temperatures.

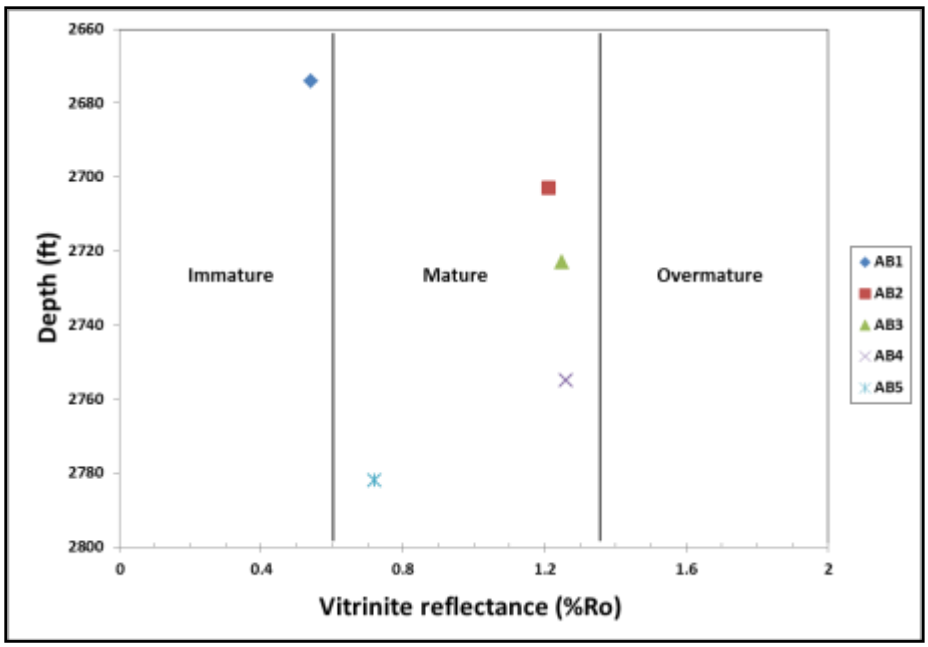

Figure 4.30. Plot of Ro vs. Depth to Explain the Maturation Stage of Tar-Mat Samples from Kuwaiti Carbonate Reservoir before the Extraction

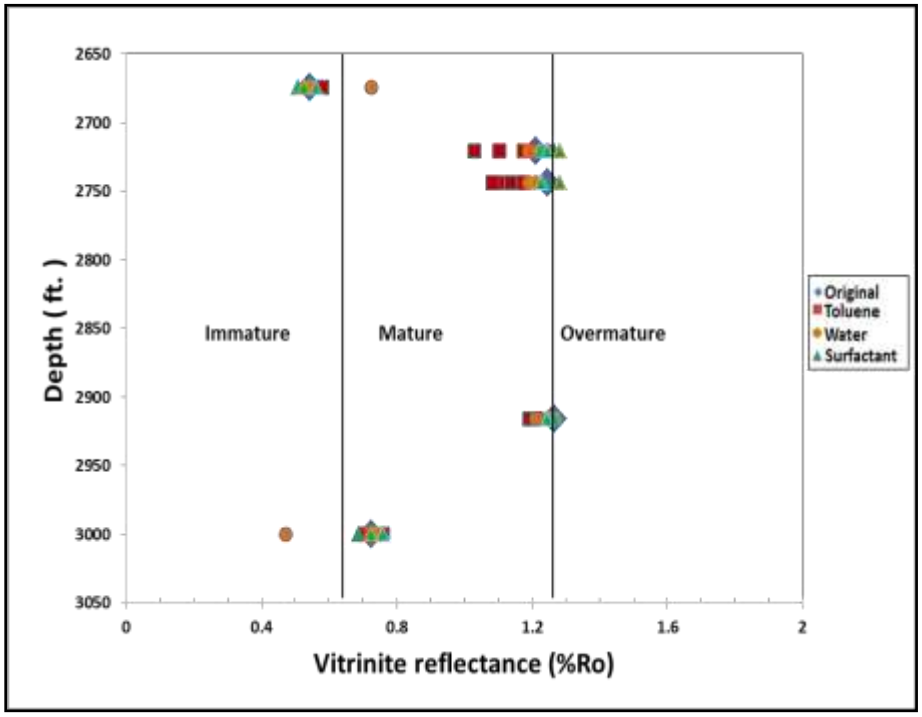

Figure 4.31. Plot of Ro vs. Depth to Explain the Maturation Stage of Tar-Mat Samples from Kuwaiti Carbonate Reservoir after the Extraction

The results of the Rock-Eval 6 analysis (Table 4.8) revealed that the values of 10 parameters obtained from the tar-mat samples (HI, QI, BI, PI, PCI, PG, T_{max}, S1+S2, and S1) increased as the thermal maturity of the organic materials in the tar-mat samples increased during the initial stage of thermal maturation. This increase was more noticeable in the mature tar-mat samples AB2, AB3, AB4, and AB5.

The results and conclusions summarized from the Rock-Eval 6 pyrolysis data indicating the quality, quantity, and thermal maturity of the five tar-mat samples appear in Table 4.13. The samples were rich in organic matter, were composed of Types II and II/III kerogen of either land or marine origin capable of emitting oil and gas, and contained both mature and immature fluids.

Table 4.13. Summary of Results and Conclusions from Rock-Eval 6 Pyrolysis Data

Sample No.	**AB1-AB5**					
Type of kerogen / Method	**I**	**II**	**I+II**	**III**	**II+III**	**IV**
HI vs. OI	0	3	0	0	2	0
HI vs. Tmax	0	3	0	0	2	0
PCI	0	3	2	0	0	0
S2/S3	4	1	0	0	0	0
HI value	0	3	0	0	2	0
Maturity / Method	**Immature**	**Mature**	**Postmature**	**N/A**		
PI Range	2	3	0	0		
Tmax Range	1	4	0	0		
Tmax vs. PI	1	4	0	0		
Ro (Calculated)	1	4	0	2		
Oil or Gas Prone / Method	**Oil**	**Oil+Gas**		**Gas**		
HI Range	3	2		0		
S2/S3	5	0		0		
Quality of Organic Matter / Method	**Poor**	**Fair**	**Good**	**Very Good**	**Excellent**	
PCI vs. TOC	0	0	0	0	5	
TOCvs. S1	0	0	0	1	4	
S2 vs. TOC	0	0	0	0	5	
Genetic Potential / Method	**Poor**		**Moderate**	**Good**		
Genetic Potential Value	0		0	5		

4.5. SARA ANALYSIS

The tar-mat samples were characterized based on the SARA analysis method. Five tar-mat reservoir rocks were used to determine the saturates, aromatics, resins, and asphaltenes of the tar-mat samples.

4.5.1. Tar-Mat Sample AB1. Table 4.14 and Figure 4.32 through Figure 4.35 summarize the results of the SARA analysis from tar-mat sample AB1. The content of saturates and aromatics in the initial raw sample was 54.71%, the resin content was 36.06%, and the asphaltene content was 8.69%.

The SARA analysis yielded a novel discovery; a middle peak between the resin peak and the asphaltene peak was identified, which represented the resin-to-asphaltene peak. This peak, a tar-mat signature, appeared in each treatment under all tested temperatures. This resin-to-asphaltene peak will be referred to as the RAS peak. The weight percentage result of the RAS component of sample AB1 was 0.54 %. This peak is unusual in typical SARA analyses but repeatedly reported in tar-mat analyses. As shown in Figure 4.32, this important observation added a fifth parameter to consider in the SARA analysis of tar-mat recovery. No RAS peak has been reported previously in the literature for other extracts. Because it was located between the heavier ends of the resin and asphaltene side of the tar-mat oil, it was presumed to be an annex to the asphaltene peak. However, when monitored individually, it was seen that the RAS peak correlated with mobility improvement and, therefore, oil recovery.

The RAS peak was first reported in tar-mat sample AB1, so naturally, no fundamental knowledge of its impact on total reservoir performance exists. However, evidence from observation points to its important role in recovery enhancement for each recovery method at each temperature. Mobility improved as the RAS weight percent

increased. For each recovery method, the immobile asphaltene particles may have transformed into less viscous resin particulates during the RAS process, hence improving the recovery of tar-mat oil. Toluene recovery improved the RAS from 0.54% to 7.4% at 225 °C, which was the most significant improvement. The water recovery method improved the RAS from 0.54% to 10.28% at 225 °C. The surfactant solution improved the RAS from 0.54% to 16.21% at room temperature. Clearly, each method contributed to the oil recovery improvement through this RAS evolution.

According to the SARA analysis results (Table 4.14), sample AB1 contained very low saturates (8.85 wt.%), high NSOs (44.74 wt.%) and a low saturates/aromatics ratio (0.19). These results confirmed the presence of a tar-mat in sample AB1 (Almansour et al., 2014). Figure 4.33 through Figure 4.35 also indicate that more NSO was produced as the temperature increased.

Table 4.14. SARA Analysis from Tar-Mat Oil Sample AB1

Sample	Temperature (˚C)	Saturates (wt. %)	Aromatics (wt. %)	Resins (wt. %)	RAS (wt. %)	Asphaltenes (wt. %)	Total (wt. %)	Sat./Aro.	NSO [Res. + Asph.] (wt. %)
AB1-Raw	Raw Tar-Mat	8.85	45.86	36.06	0.54	8.69	100	0.19	44.74
Toluene	25 ˚C	31.01	14.86	42.87	2.43	8.83	100	2.09	51.7
	135 ˚C	20.63	18.95	36.68	2.03	21.71	100	1.09	58.39
	225 ˚C	18.16	15.96	30.57	7.4	27.91	100	1.14	58.48
	315 ˚C	21.2	38.87	24.65	6.56	8.72	100	0.55	33.37
Water	25 ˚C	27.42	33.12	27.15	8.13	4.15	100	0.83	31.3
	135 ˚C	9.45	26.12	53.72	5.55	5.17	100	0.36	58.89
	225 ˚C	33.48	23.84	28.43	10.28	3.96	100	1.4	32.39
	315 ˚C	19.58	11	40.95	5.71	22.76	100	1.78	63.71
Surfactant	25 ˚C	24.33	27.37	24.54	16.21	7.55	100	0.89	32.09
	135 ˚C	25.8	20.45	35.47	5.05	13.23	100	1.26	48.7
	225 ˚C	32.61	15.93	47.33	2.49	1.63	100	2.05	48.96
	315 ˚C	11.94	10.32	59.7	5	13.04	100	1.16	72.74

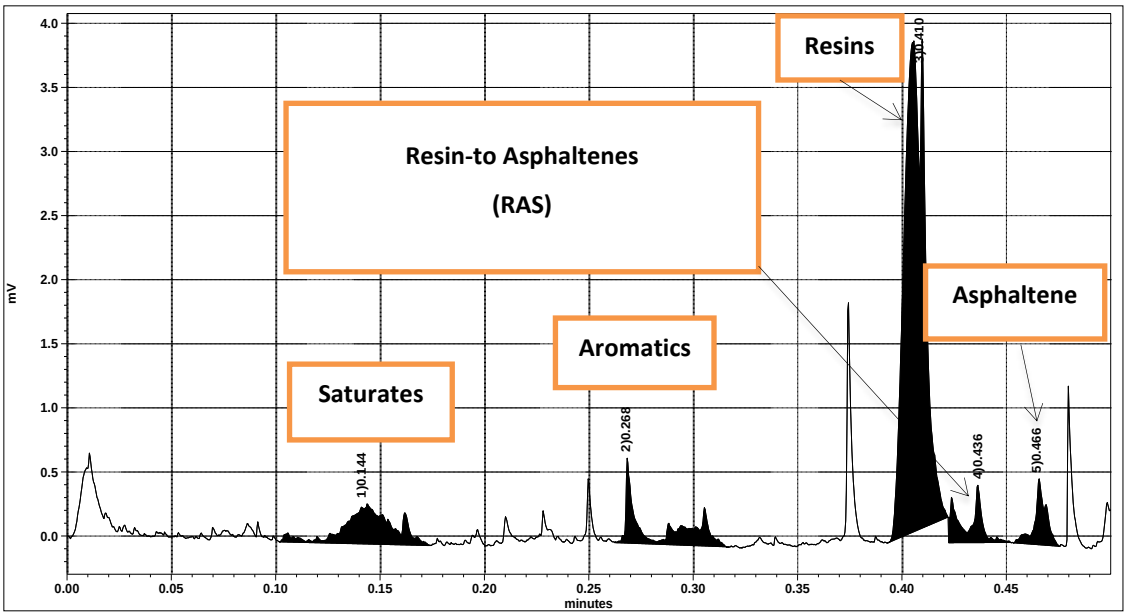

Figure 4.32. New SARA Analysis Peak Discovered between Resins and Asphaltenes

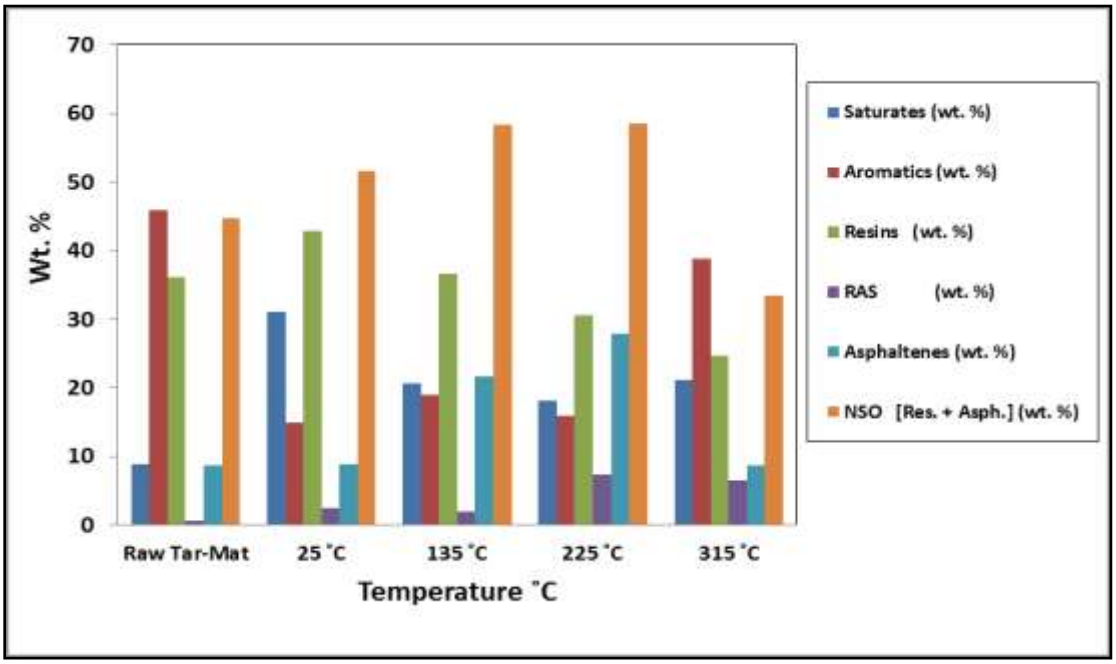

Figure 4.33. SARA Analysis for Toluene Recovery at Various Temperatures (Sample AB1)

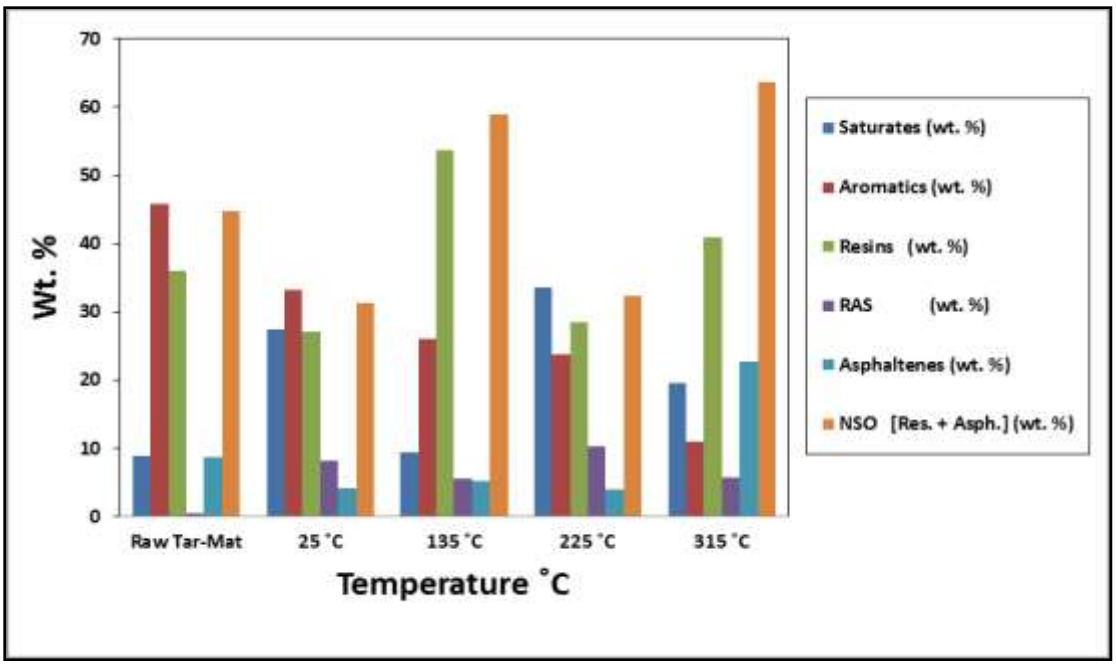

Figure 4.34. SARA Analysis for Hot Water Recovery at Various Temperatures (Sample AB1)

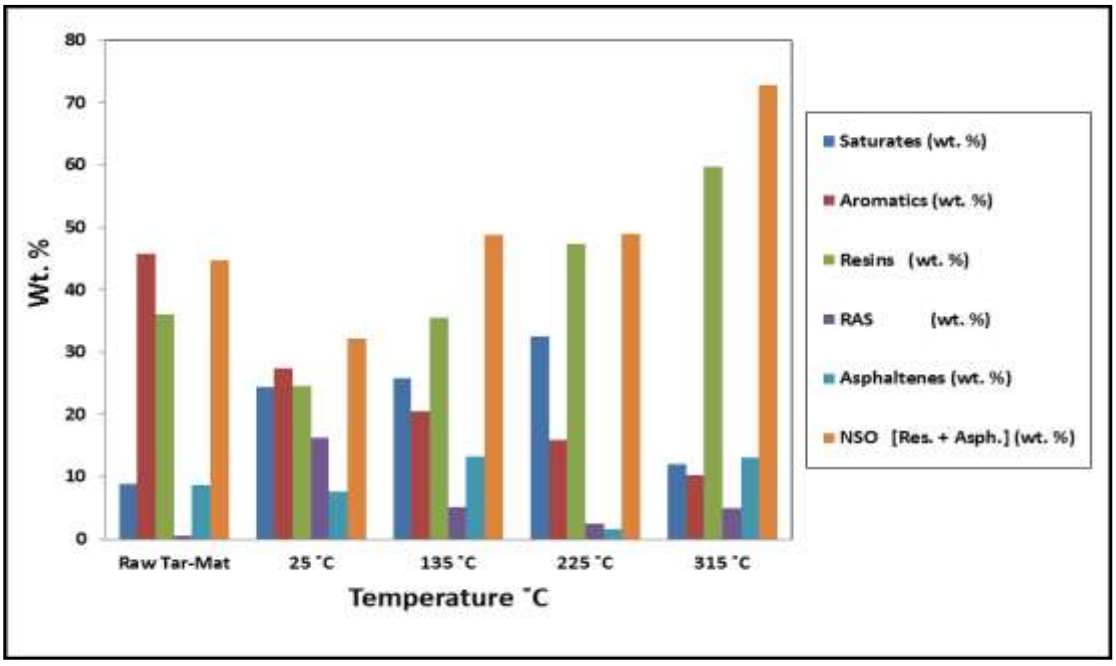

Figure 4.35. SARA Analysis for Surfactant Solution Recovery at Various Temperatures (Sample AB1)

4.5.2. Tar-Mat Sample AB2. Table 4.15 summarizes the SARA analysis results for sample AB2. The initial contents were 23.82%, 7.72%, 65.15%, and 2.04% of saturates, aromatics, resins, and asphaltenes, respectively. The weight percentage result of the RAS component of sample AB2 was 1.28%.

The toluene recovery method improved the RAS from 1.28% to 25.02%% at 135 °C, which was the most significant improvement. The water recovery method improved the RAS from 1.28% to 4.98 % at 225 °C. The surfactant solution showed slightly improvement where improved the RAS was improved from 1.28% to 6.31% at 315 °C.

Figure 4.36 through Figure 4.38 support that NSO production increased as the temperature increased. Clearly, each method contributed to the oil recovery improvement through this RAS evolution.

Table 4.15. SARA Analysis from Tar-Mat Oil Sample AB2

Sample	Temperature (˚C)	Saturates (wt. %)	Aromatics (wt. %)	Resins (wt. %)	RAS (wt. %)	Asphaltenes (wt. %)	Total (wt. %)	Sat./Aro.	NSO [Res. + Asph.] (wt. %)
AB2-Raw	Raw Tar-Mat	23.82	7.72	65.15	1.28	2.04	100	3.08	67.18
Toluene	25 ˚C	21.74	9.70	64.62	1.99	1.55	100	2.24	66.17
	135 ˚C	16.22	11.93	45.02	25.02	1.8	100	1.36	46.82
	225 ˚C	11.72	21.84	48.65	9.95	7.84	100	0.54	56.49
	315 ˚C	21.31	37.29	26.17	7.67	7.56	100	0.57	33.73
Water	25 ˚C	22.08	11.94	60.61	4.34	1.4	100	1.85	62.01
	135 ˚C	10.12	17.36	66.28	2.34	3.9	100	0.58	70.18
	225 ˚C	30.95	11.24	49.90	4.98	2.93	100	2.75	52.83
	315 ˚C	28.15	16.64	47.46	4.68	3.07	100	1.69	50.53
Surfactant	25 ˚C	21.40	12.39	57.33	5.84	3.05	100	1.73	60.38
	135 ˚C	25.47	14.96	55.64	1.42	2.5	100	1.70	58.14
	225 ˚C	14.37	10.42	66.42	1.78	7.02	100	1.38	73.44
	315 ˚C	10.85	11.95	65.35	6.31	5.54	100	0.91	70.89

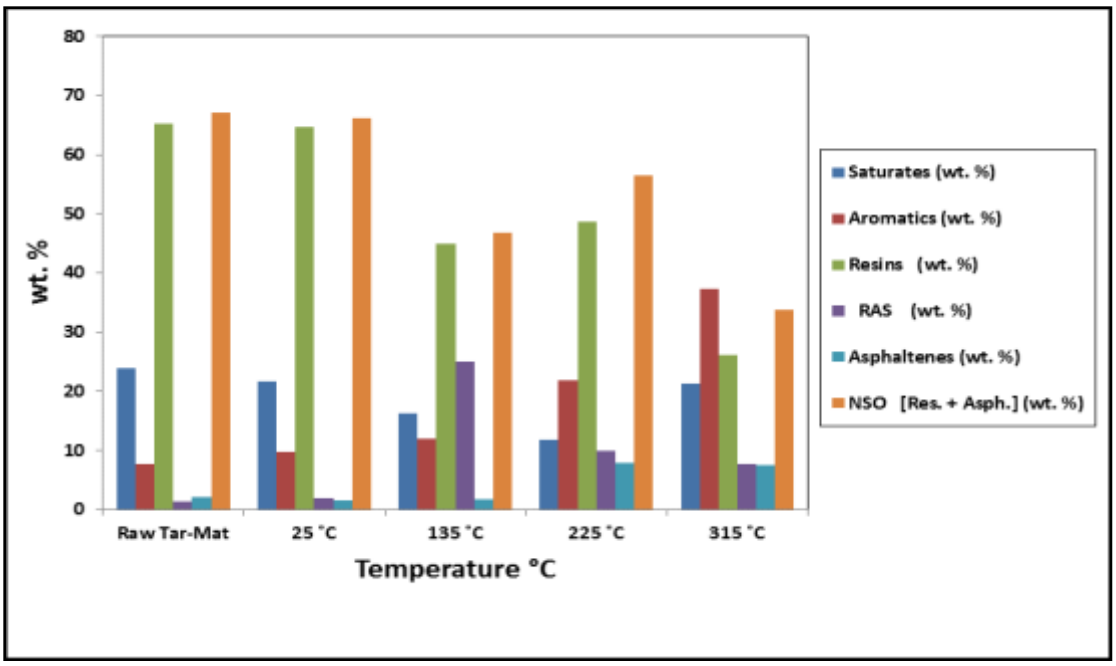

Figure 4.36. SARA Analysis for Toluene Recovery at Various Temperatures (Sample AB2)

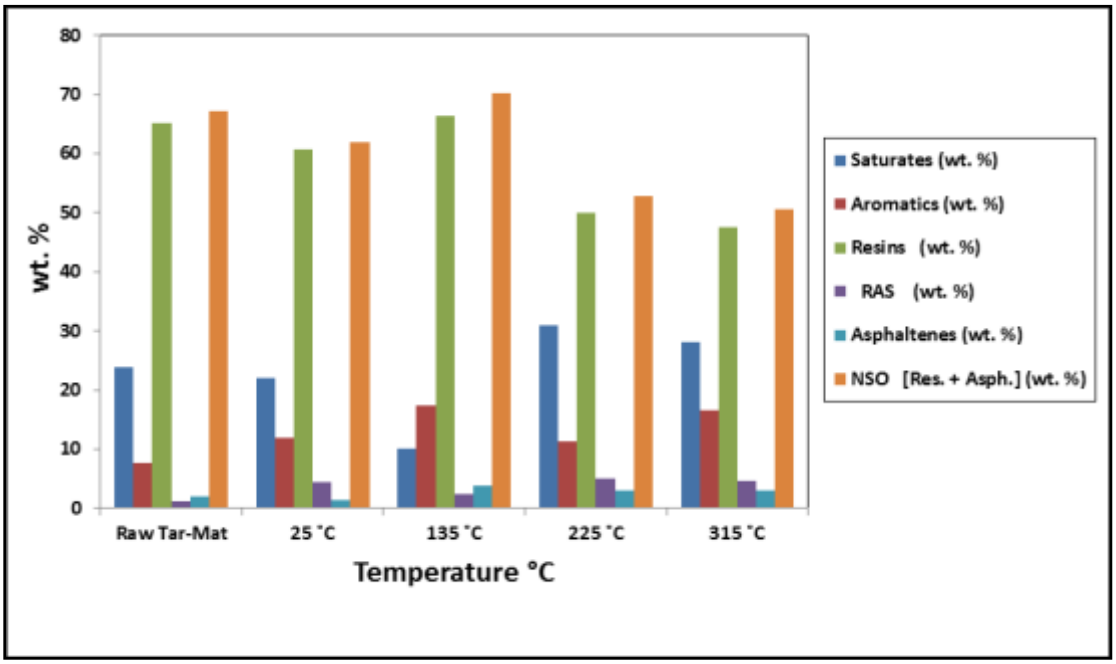

Figure 4.37. SARA Analysis for Hot Water Recovery at Various Temperatures (Sample AB2)

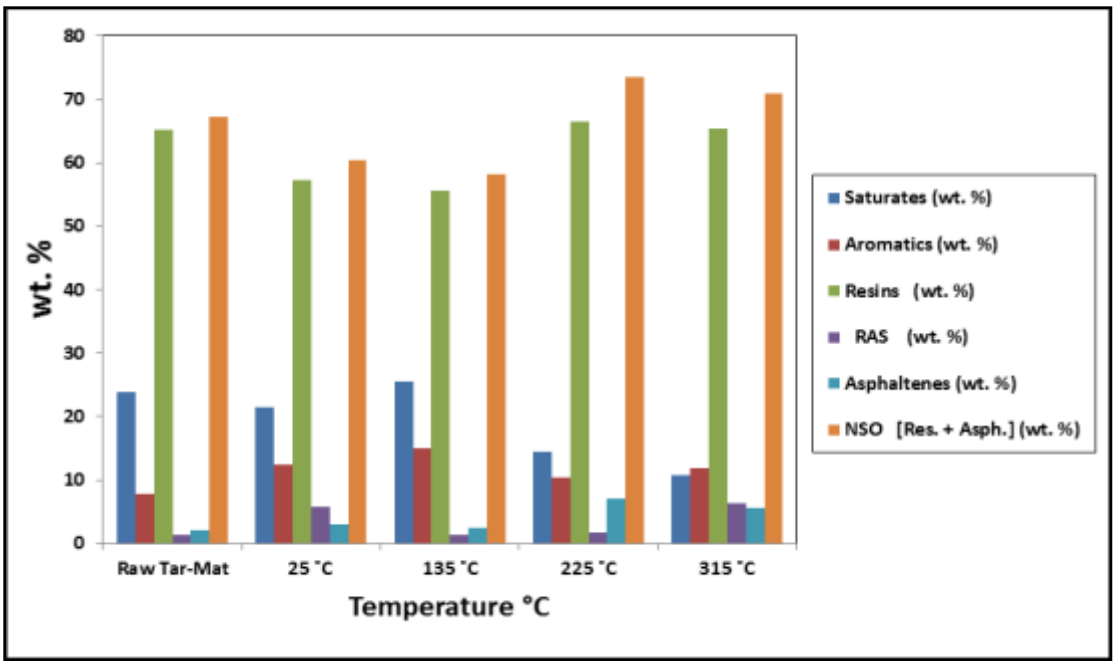

Figure 4.38. SARA Analysis for Surfactant Solution Recovery at Various Temperatures (Sample AB2)

4.5.3. Tar-Mat Sample AB3. The results of the analysis from tar-mat sample AB3 are summarized in Table 4.16 and Figure 4.39 through Figure 4.41. The content of saturates, aromatics, resins, and asphaltenes in the initial raw sample was 16.11%, 6.98%, 72.51%, and 2.03%, respectively.

The toluene recovery method improved the RAS from 2.03% to 6.40% at 225 °C, which was the most significant improvement. The water recovery method improved the RAS from 2.03% to 8.30% at 315 °C. The surfactant solution slightly improved the RAS from 2.03% to 3.12% at 135 °C.

NSO production increased as the temperature increased, as well as after the extraction with toluene and hot water, as shown in Figure 4.39 through Figure 4.41.

Table 4.16. SARA Analysis from Tar-Mat Oil Sample AB3

Sample	Temperature (˚C)	Saturates (wt. %)	Aromatics (wt. %)	Resins (wt. %)	RAS (wt. %)	Asphaltenes (wt. %)	Total (wt. %)	Sat./Aro.	NSO [Res. + Asph.] (wt. %)
AB3-Raw	Raw Tar-Mat	16.11	6.98	72.51	2.03	2.36	100	2.31	74.87
Toluene	25 ˚C	12.64	29.36	48.84	2.57	6.59	100	0.43	55.43
	135 ˚C	33.36	15.25	46.72	2.86	1.81	100	2.19	48.53
	225 ˚C	26.55	22.91	25.25	6.40	18.9	100	1.16	44.15
	315 ˚C	27.77	36.23	22.83	4.63	8.53	100	0.77	31.36
Water	25 ˚C	15.41	10.42	66.78	5.13	2.25	100	1.48	69.03
	135 ˚C	12.80	11.27	66.86	5.31	3.76	100	1.14	70.62
	225 ˚C	32.31	10.10	50.07	4.83	2.69	100	3.20	52.76
	315 ˚C	33.09	12.19	41.06	8.30	5.36	100	2.72	46.42
Surfactant	25 ˚C	15.78	6.83	38.49	1.95	36.95	100	2.31	75.44
	135 ˚C	17.53	26.94	46.20	3.12	6.21	100	0.65	52.41
	225 ˚C	10.81	9.15	60.67	0.81	18.56	100	1.18	79.23
	315 ˚C	15.00	13.46	66.82	0.48	4.24	100	1.11	71.06

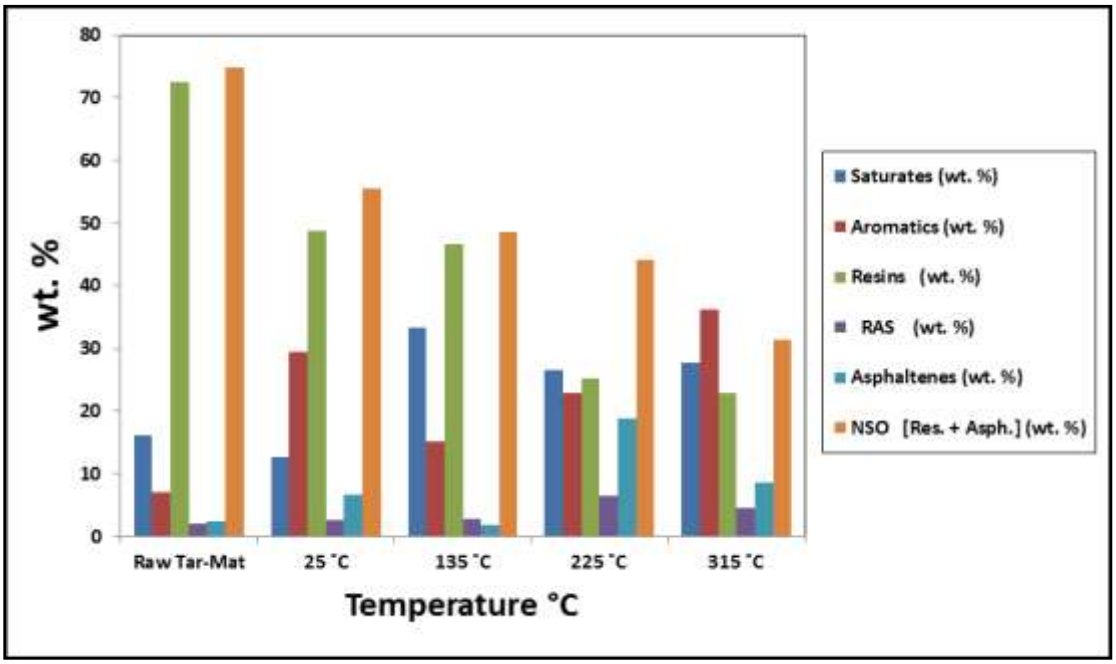

Figure 4.39. SARA Analysis for Toluene Recovery at Various Temperatures (Sample AB3)

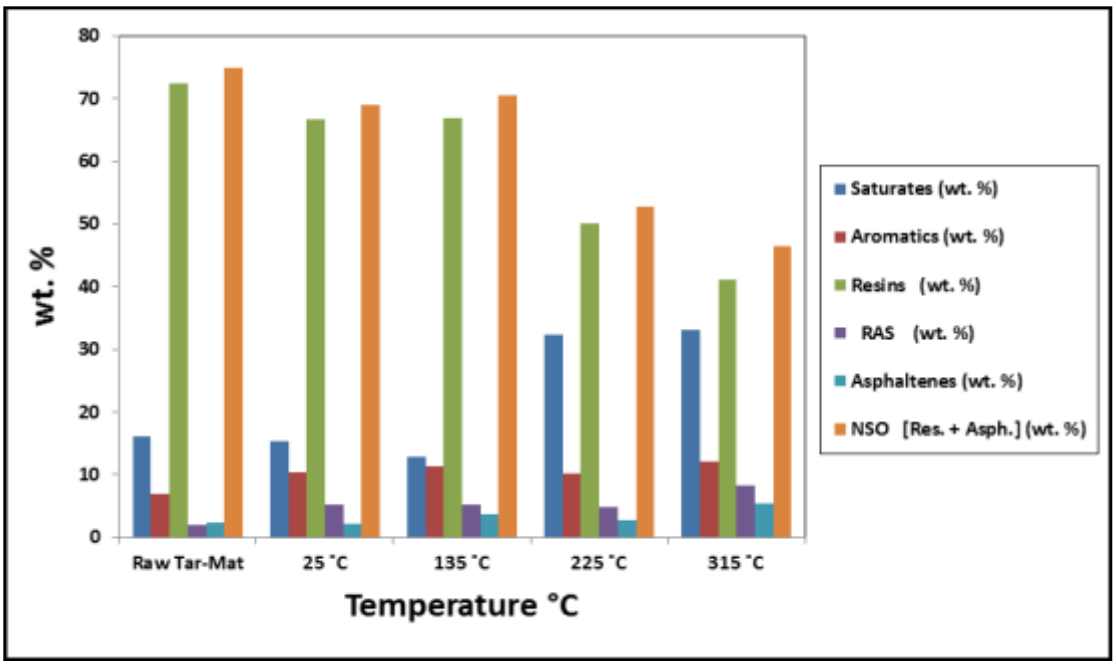

Figure 4.40. SARA Analysis for Hot Water Recovery at Various Temperatures (Sample AB3)

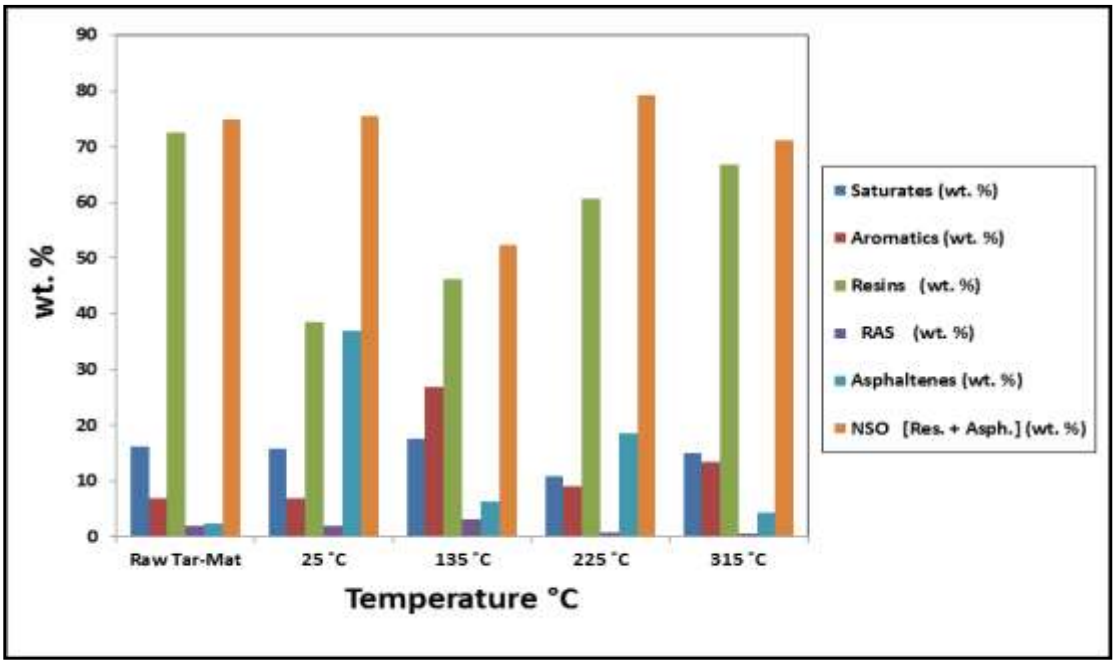

Figure 4.41. SARA Analysis for Surfactant Solution Recovery at Various Temperatures (Sample AB3)

4.5.4. Tar-Mat Sample AB4. The content of saturates, aromatics, resins, asphaltenes, and RAS of sample AB4, as obtained from SARA analysis, is summarized in Table 4.17. Toluene recovery improved the RAS from 5.82% to 9.42% at 225 °C, which was the most significant improvement.

Figure 4.42 through Figure 4.44 indicate that NSO production increased as the temperature increased, particularly after the extraction with toluene. The surfactant solution improved the RAS from 5.82% to 6.59% at 25 °C, while the water recovery method failed to improve the RAS in sample AB4.

Table 4.17. SARA Analysis from Tar-Mat Oil Sample AB4

Sample	Temperature (˚C)	Saturates (wt. %)	Aromatics (wt. %)	Resins (wt. %)	RAS (wt. %)	Asphaltenes (wt. %)	Total (wt. %)	Sat./Aro.	NSO [Res. + Asph.] (wt. %)
AB4-Raw	Raw Tar-Mat	26.50	4.45	58.21	5.82	5.02	100	5.95	63.23
Toluene	25 ˚C	24.05	7.34	55.51	2.28	10.82	100	3.28	66.33
	135 ˚C	33.40	9.03	44.11	5.05	8.42	100	3.70	52.53
	225 ˚C	32.83	19.90	22.05	9.42	15.81	100	1.65	37.86
	315 ˚C	50.44	24.44	14.65	6.34	4.13	100	2.06	18.78
Water	25 ˚C	11.30	11.07	72.35	3.40	1.88	100	1.02	74.23
	135 ˚C	14.36	14.80	63.54	3.99	3.3	100	0.97	66.84
	225 ˚C	17.86	11.54	63.39	4.60	2.62	100	1.55	66.01
	315 ˚C	14.36	21.86	56.79	2.17	4.82	100	0.66	61.61
Surfactant	25 ˚C	26.57	10.45	50.13	6.59	6.26	100	2.54	56.39
	135 ˚C	11.93	13.53	66.66	1.36	6.53	100	0.88	73.19
	225 ˚C	13.24	9.88	66.58	0.98	9.31	100	1.34	75.89
	315 ˚C	11.44	7.19	71.31	1.00	9.07	100	1.59	80.38

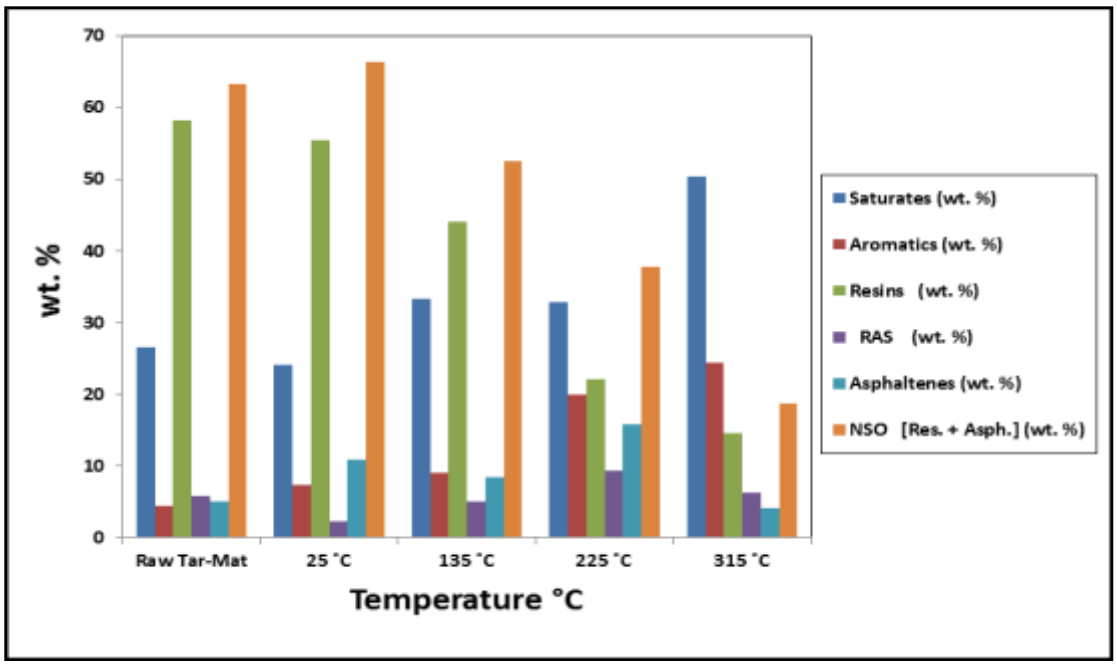

Figure 4.42. SARA Analysis for Toluene Recovery at Various Temperatures (Sample AB4)

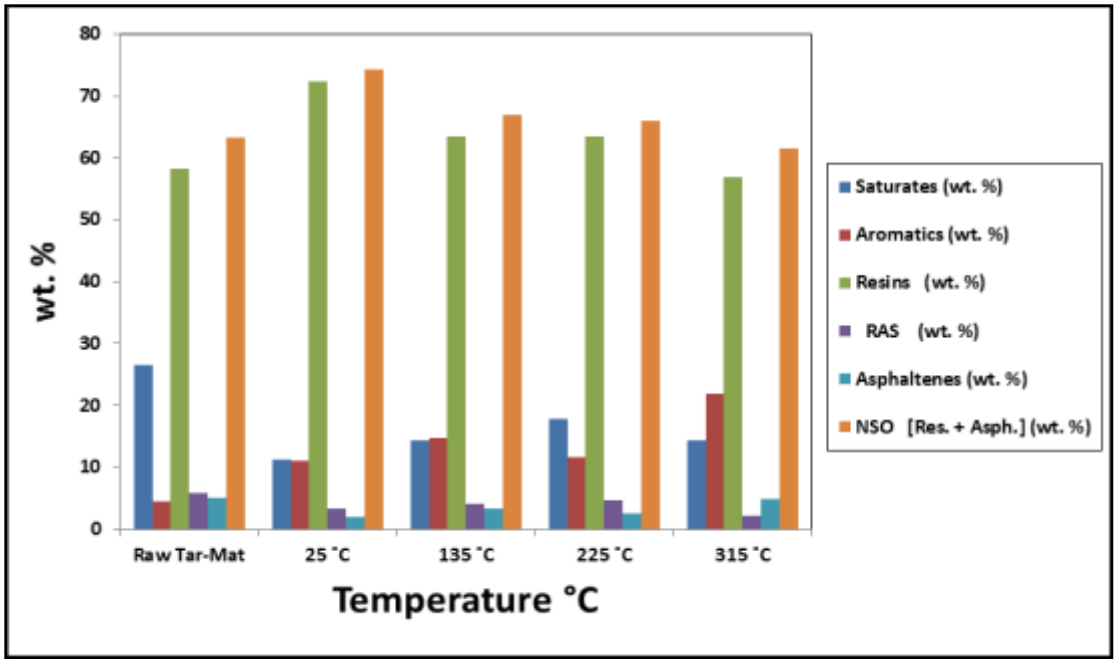

Figure 4.43. SARA Analysis for Hot Water Recovery at Various Temperatures (Sample AB4)

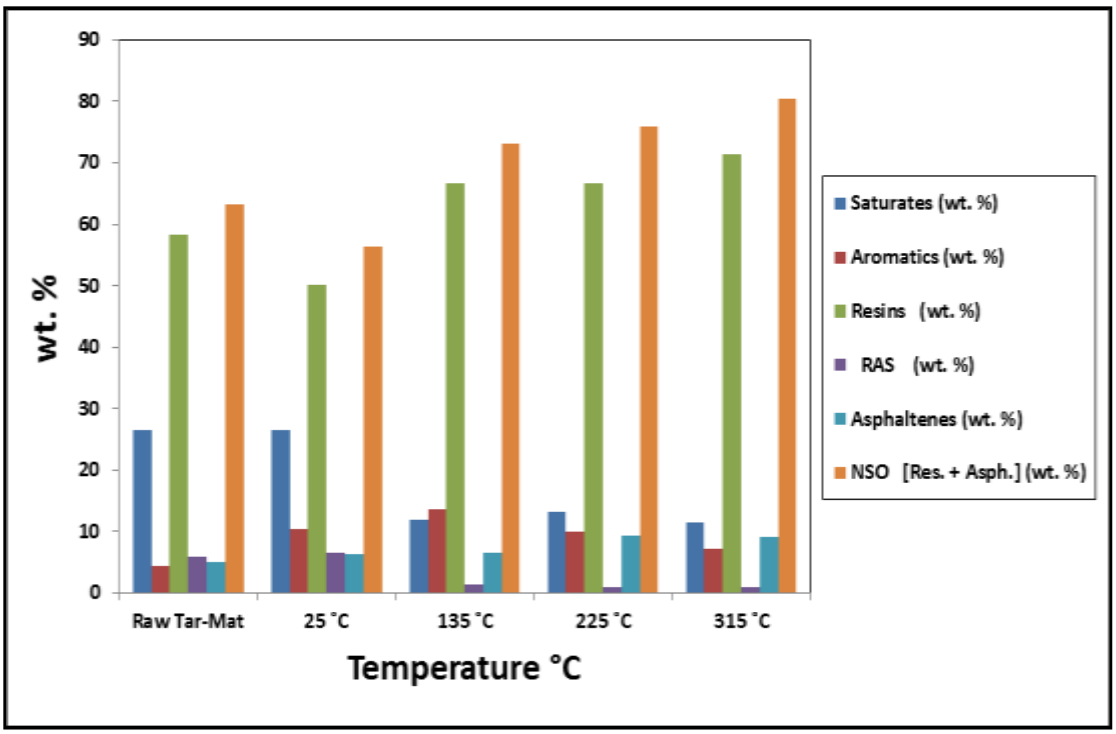

Figure 4.44. SARA Analysis for Surfactant Solution Recovery at Various Temperatures (Sample AB4)

4.5.5. Tar-Mat Sample AB5. The results of the SARA analysis obtained from tar-mat sample AB5 are summarized in Table 4.18 and Figure 4.45 through Figure 4.47. The toluene and hot water methods improved the RAS from 1.33% to 10.62% and from 1.33% to 13.36%, respectively, at 315 °C. Figures 4.45 also indicate that NSO production increased as the temperature increased, particularly after the extraction with toluene and hot water. The surfactant solution improved the RAS from 1.33% to 7.33% at 315 °C.

Table 4.18. SARA Analysis from Tar-Mat Oil Sample AB5

Sample	Temperature (˚C)	Saturates (wt. %)	Aromatics (wt. %)	Resins (wt. %)	RAS (wt. %)	Asphaltenes (wt. %)	Total (wt. %)	Sat./Aro.	NSO [Res. + Asph.] (wt. %)
AB5-Raw	Raw Tar-Mat	10.36	6.55	62.45	1.33	19.31	100	1.58	81.76
Toluene	25 ˚C	31.56	13.16	32.12	5.84	17.33	100	2.40	49.45
	135 ˚C	20.62	21.07	43.22	5.50	9.59	100	0.98	52.81
	225 ˚C	15.96	29.02	29.84	9.54	15.65	100	0.55	45.49
	315 ˚C	20.63	27.12	26.98	10.62	14.64	100	0.76	41.62
Water	25 ˚C	5.91	3.44	17.56	3.43	69.65	100	1.72	87.21
	135 ˚C	19.59	17.03	44.87	8.99	9.52	100	1.15	54.39
	225 ˚C	35.12	21.45	29.93	8.53	4.97	100	1.64	34.90
	315 ˚C	22.89	20.99	25.64	13.36	17.13	100	1.09	42.77
Surfactant	25 ˚C	29.09	16.89	25.81	6.11	22.1	100	1.72	47.91
	135 ˚C	14.65	16.87	60.23	4.34	3.91	100	0.87	64.14
	225 ˚C	9.89	12.33	59.25	7.17	11.36	100	0.80	70.61
	315 ˚C	14.28	12.07	63.38	7.33	2.94	100	1.18	66.32

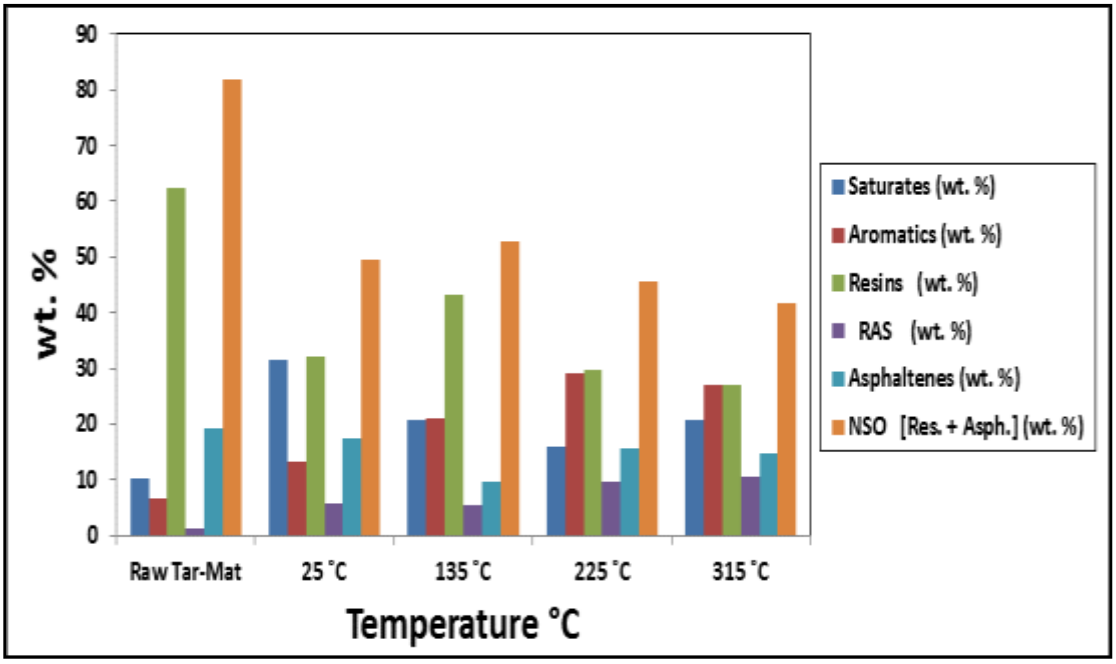

Figure 4.45. SARA Analysis for Toluene Recovery at Various Temperatures (Sample AB5)

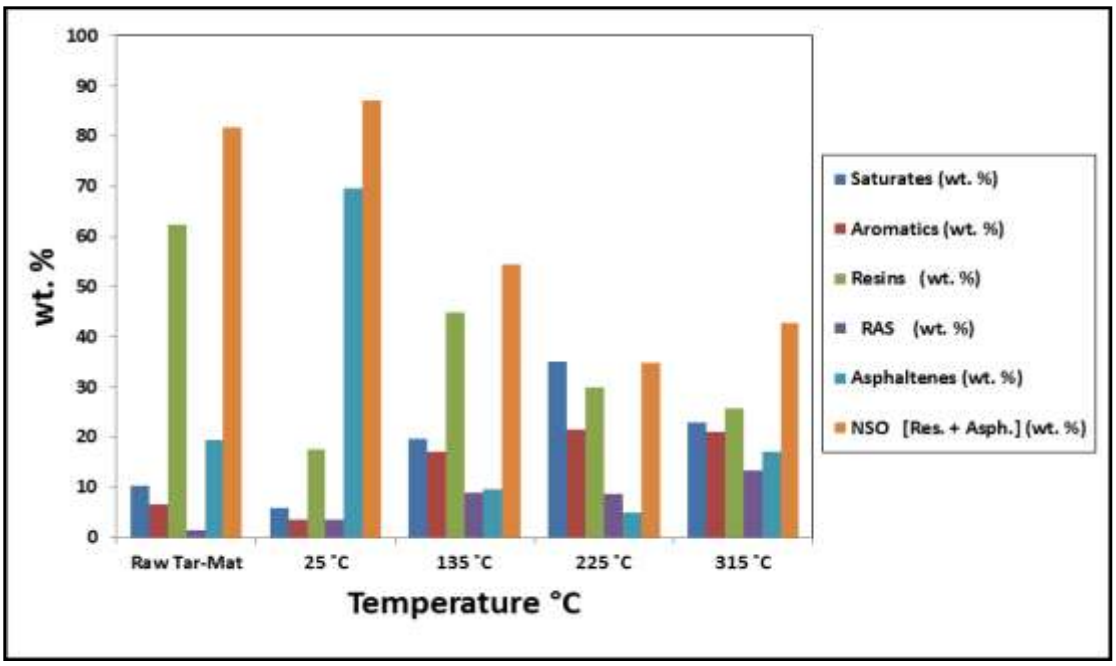

Figure 4.46. SARA Analysis for Hot Water Recovery at Various Temperatures (Sample AB5)

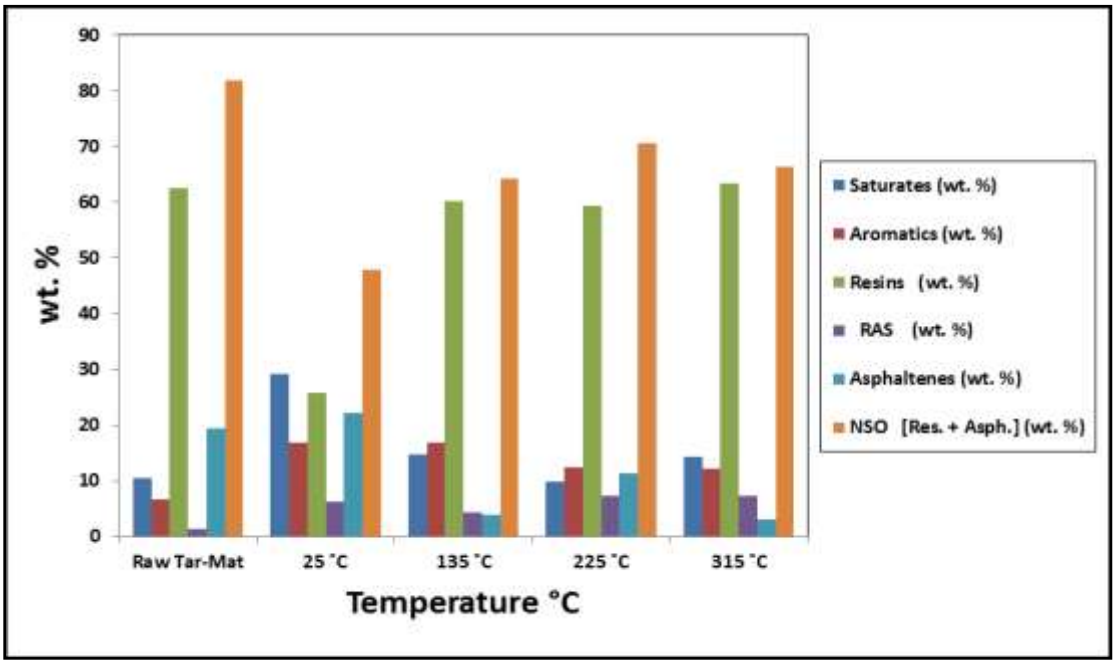

Figure 4.47. SARA Analysis for Surfactant Solution Recovery at Various Temperatures (Sample AB5)

Within the scope of the samples analyzed, a noticeable difference existed in the SARA fraction distribution when comparing samples at various depths from the same well. Also, the tar-mat samples had higher concentrations of resins and asphaltenes than of saturates and aromatics. Some of the tar-mat samples, such as AB1 and AB5, showed high asphaltene concentrations (8% to 20% in weight).

According to the SARA analysis results (Table 4.19), the Kuwaiti carbonate reservoir formation at 2674 feet (sample AB1) contains very low saturates (8.85 wt.%), high NSOs (44.75 wt.%), and a low saturates/aromatics ratio (0.19). These results indicate the presence of a tar-mat.

Figure 4.48 depicts the nearly random variation of asphaltene content in the tar-mat samples with depth. Similarly, the saturates, aromatics, and resins also exhibited variations with depth. The asphaltene content of the tar-mat samples increased and decreased greatly over very short vertical distances.

4.5.6. Prediction of Crude Oil Stability. The Colloidal Instability Index (CII) can be used to predict the stability of crude oil. This approach is based on the results obtained through SARA analysis. The CII values for the five tar-mat cores were calculated as in Eq. 4 (Newberry and Barkere, 2000):

$$\text{CII} = \frac{\text{Saturates} + \text{Asphaltenes}}{\text{Aromatics} + \text{Resins}} \tag{4}$$

CII values below and above 0.9 indicate stable and unstable crude oil, respectively (Yen et al., 2001; Chaogang et al., 2013). Table 4.19 shows the CII results of the five tar-mat oil samples. The CII values of all five samples were less than 0.9 due to their higher content of aromatics and resins and lower content of saturates and

asphaltenes, indicating the stability of their oils. Figure 4.48 shows that the asphaltene deposition sequence of the five tar-mat oil samples was AB5>AB1>AB4>AB3>AB2.

Table 4.19. Results of SARA Analysis from Initial Tar-Mat Samples

Sample No.	Sat. (wt.%)	Aro. (wt.%)	Res. (wt.%)	Asph. (wt.%)	Sat./Ar. (wt.%)	CII	Stability	NSO Res.+Asph.(wt.%)
AB1	8.85	45.86	36.06	8.69	0.19	0.21	Stable <0.9	44.75
AB2	23.82	7.72	65.15	2.04	3.08	0.35	Stable <0.9	67.19
AB3	16.11	6.98	72.51	2.36	2.31	0.23	Stable <0.9	74.87
AB4	26.50	4.45	58.21	5.02	5.95	0.50	Stable <0.9	63.23
AB5	10.36	6.55	62.45	19.31	1.58	0.43	Stable <0.9	81.76

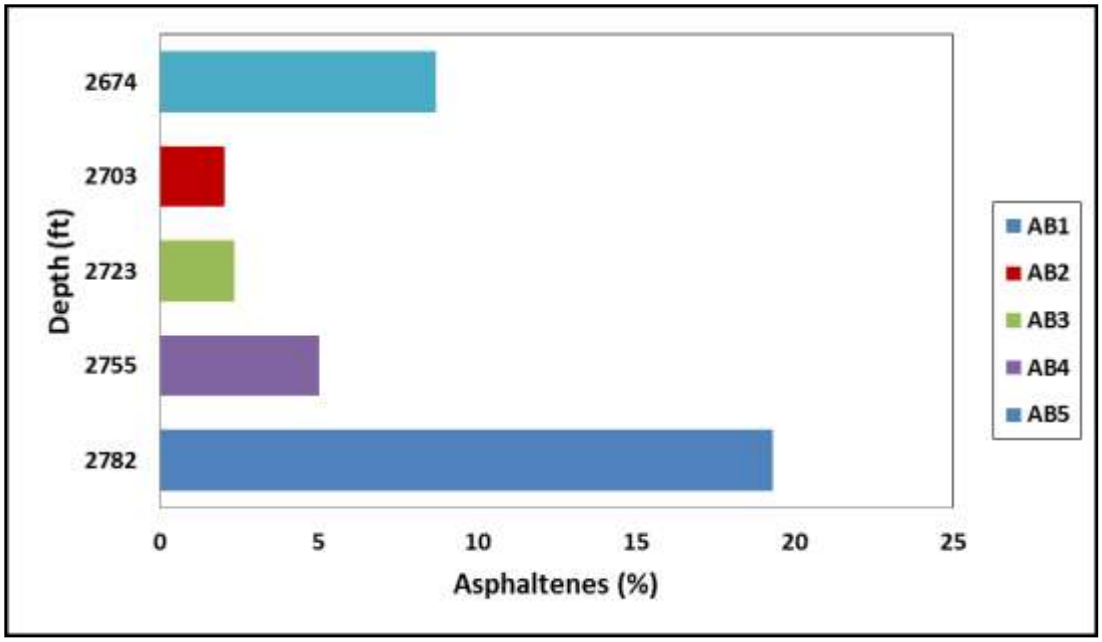

Figure 4.48. Asphaltene Versus Depth of Tar-Mat Samples, Indicating Large Variation of Asphaltene Content with Small Intervals of Height

4.6. API CALCULATION

A rapid method was employed to inexpensively estimate the API gravities of small crude oil samples, tars, reservoir rocks, and solid bitumen using the Rock-Eval 6 instrument. As Dow et al. (2002) and Cubitt et al. (2004) explained, this inexpensive method employs subjecting rock reservoir samples (usually small samples) to pyrolysis. Alternatively, the process can employ a freeing criterion for isothermal hydrocarbons, which involves sustaining a temperature of 180°C for 10 minutes. Thereafter, the temperature is increased to 650°C at a rate of approximately 10°C per minute. However, this pyrolysis phase liberates three peaks representing free hydrocarbons in the range of C1 to C21 (S1r), C22 to C40 (S2a), and C40+ (S2b), respectively. At 650°C, the samples are oxidized, which helps to determine the residual carbon (RC). Rock-Eval 6 offers the most reliable RC values because it can determine the CO and CO2 values. Once the necessary data are obtained, they are used to determine the API gravity coefficient "X," as shown in Eq. 5 (Cubitt et al., 2004):

$$X = \frac{(S1r + S2a)}{(S1r + S2a + NSO)} \tag{5}$$

NSO represents the asphaltenes in the equation and can be calculated mathematically as:

$$NSO = S2b + (RCr / 0.09) \tag{6}$$

Where:

S1r represents light oils of hydrocarbons in the range of C1-C22.

S2a represents heavy oils of hydrocarbons in the range of C22-C40.

S2b is an equivalent of resin + asphaltene in the C40+ range.

RCr represents the percentage of residual carbon in the TOC after pyrolysis.

In the pyrolysis of the five tar-mat core samples, an unacceptable RC variability was observed, which possibly can be attributed to the decomposition of the mineral carbonates. In order to correlate the results of Rock-Eval 6 pyrolysis to the petroleum density, a Y coefficient was adopted (Eq. 7), as given by Cubitt et al. (2004):

$$Y = \frac{(S1r + S2a)}{(S1r + S2a + S2b)} \tag{7}$$

Table 4.20 shows the results from the five tar-mat cores. Thereafter, the exponential fit equation (Eq. 8) was used to calculate the predicted API gravity for petroleum in the five cores, as illustrated in Figure 4.49.

$$API = 0.92448 \times e\,\wedge\,(4.0679 \times Y) \tag{8}$$

Table 4.20. Rock-Eval Pyrolysis Data from Five Tar-Mat Reservoir Rocks

Sample No.	S1r (mgHC/g rock)	S2a (mgHC/g rock)	S2b (mgHC/g rock)	RCr (%)	NSO (mg/g)	Y	°API Calc.
AB1	0.77	4.44	51.86	28.56	369.19	0.0913	1.34
AB2	5.46	16.85	30.43	3.31	67.21	0.4231	5.17
AB3	7.12	14.55	37.47	3.48	76.14	0.3664	4.10
AB4	5.57	15.53	40.04	3.09	74.37	0.3451	3.76
AB5	3.11	9.17	68.31	36.65	475.53	0.1524	1.72

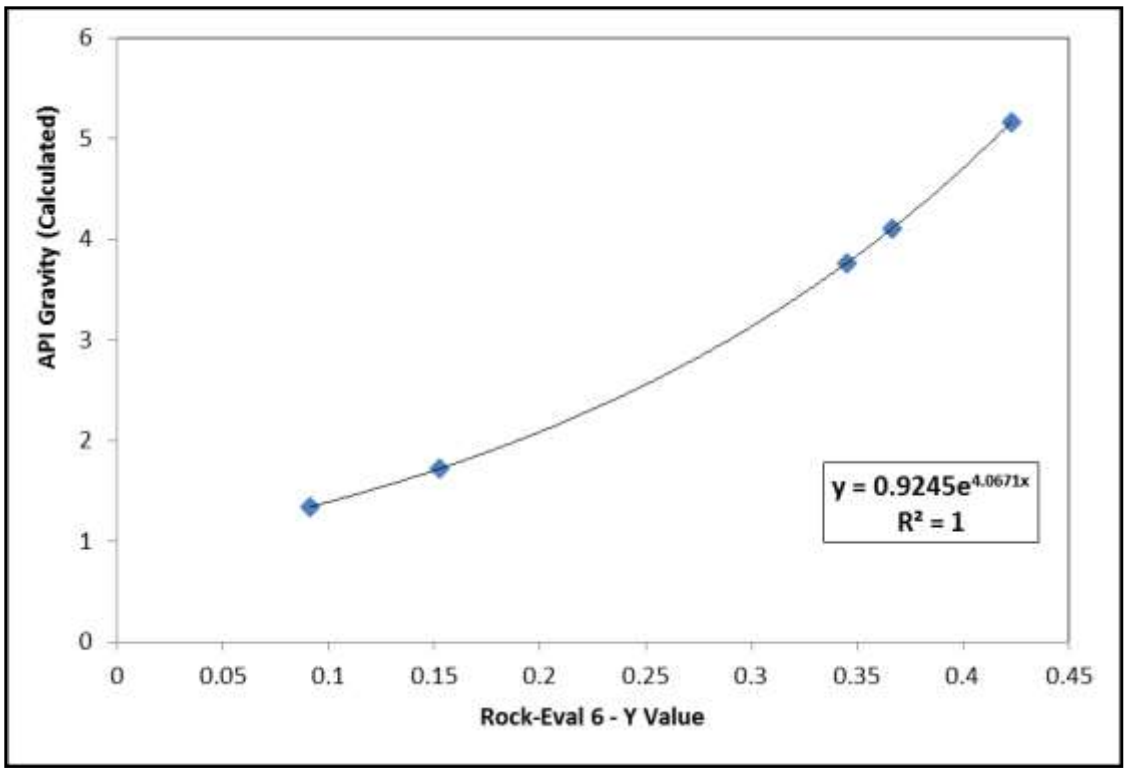

Figure 4.49. Calibration Curve Relating Rock-Eval 6 Y Factor Versus Calculated API Gravity

5. OIL RECOVERY BASED ON SOXHLET EXTRACTOR AND GEOCHEMISTRY PYROLYSIS ANALYSIS

5.1. RECOVERY SCENARIO SETTING FOR SOXHLET EXTRACTOR

Sixty samples were collected from five tar-mat cores from a carbonate reservoir (12 samples from each core). Of these, 20 were extracted by toluene, 20 by hot water, and 20 by surfactant solution. These extractions were conducted at different temperatures (25 °C, 135 °C, 225 °C, and 315°). Oil was extracted from powdered tar-mat samples of approximately 20 to 21g, on average, using a Soxhlet apparatus. The matrix density was 2.71 gm/cc for calcite and 2.87 gm/cc for dolomite. The extraction took approximately six hours. The oil recovery from all samples was calculated based on Eqs. 9 through 13:

$$\text{Weight of fluid before extraction (OIP)} = \frac{m_1}{\rho_m} \times \phi \tag{9}$$

$$\rho_m = \phi \times \rho_{oil} + (1-\phi) \times \rho_{ma} \tag{10}$$

$$\text{Weight of fluid after extraction } (m_2) = \frac{m_2}{\rho_m} \times \phi \tag{11}$$

$$\text{Oil Produced (Qo)} = \text{weight before extraction (OIP)} - \text{weight after extraction} \tag{12}$$

$$\text{Oil Recovery Factor (ORF)} = \frac{Qo}{OIP} \times 100 \tag{13}$$

Where:

m_1 represents the weight of the sample before the extraction, (gm).

ρ_m represents the density mixture of (grains + fluids), (gm/cc).

Ø represents the porosity, (%).

ρ_{ma} represents the matrix density, (gm/cc).

OIP represents the oil in place, (cc).

5.1.1. Effect of Toluene and Temperature on Oil Recovery. Table 5.1 presents the oil recovery results. Figure 5.1 illustrates the oil recovery results by toluene from all samples at four different temperatures, showing that the oil recovery increased as the temperature increased. The highest recoveries occurred in samples AB4, AB3, and AB2 at 315 °C, in that order, while samples AB1 and AB5 had the lowest oil recovery values. The incremental oil recovery of sample AB4 exceeded 47.1% at 315 °C.

The results indicate that the samples with high permeability and an API gravity value greater than 3 ˚API, as in samples AB2, AB3, and AB4, experienced the highest recovery by toluene, while samples with low permeability and API gravity less than 2 ˚API experienced less oil recovery. These results were due to the enhanced displacement efficiency caused by the improved tar and oil mobilities and reduced tar-mat and oil viscosities as the temperature increased.

5.1.2. Effect of Hot Water and Temperature on Oil Recovery. Table 5.2 shows the results of oil recovery from the tar-mat samples. Figure 5.2 shows the results of oil recovery from water extraction at different temperatures, indicating that the oil recovery increased as the temperature increased. Samples AB2 at 225 °C and AB4 at 315 °C experienced the highest recovery. This clearly occurred as a result of reduced tar-mat and oil viscosities with temperature. Also, increasing the temperature reduces the interfacial tension, which further reduces the effect of the capillary forces. The reduction of capillary forces reduces the residual oil saturation, which increases the oil recovery (Okasha et al., 1998).

As illustrated in Figure 5.2, oil recovery from samples AB2, AB3, and AB4 increased greatly at 25 and 135°C, and even more dramatically at 225 and 315°C. Samples AB1 and AB5, which had ˚API gravity less than 2 ˚API, showed slight oil recovery at 315°C.

5.1.3. Effect of Surfactant Solution and Temperature on Oil Recovery. The results of oil recovery from the tar-mat samples appear in Table 5.3. Figure 5.3 provides the results of oil recovery from surfactant extraction, indicating that the oil recovery increased as the temperature increased. Samples AB2, AB3, and AB4, which had API values greater than 3 ˚API at 315 °C, experienced the highest recovery. The other samples, AB1and AB5, which had API values lower than 2 ˚API, yielded low oil recovery, as shown in Figure 5.3.

Using surfactant solution at various temperatures to extract oil reduced the tar-mat and oil viscosity, which decreased the interfacial tension and thus the effect of the capillary forces; this, in turn, decreased the residual oil saturation.

Figure 5.3 indicates that samples AB2, AB3, and AB4 experienced the highest oil recovery at 135, 225, and 315°C, while the oil recovery from samples AB1 and AB5 increased slightly at 135, 225, and 315°C.

Table 5.1. Results of Oil Recovery from 20 Samples Extracted by Toluene under Various Temperatures

Sample No.	Temp. ˚C	Weight Before Extraction (g)	Weight After Extraction (g)	Ø %	Oil Density (g/cc)	ρ_{ma} (g/cc)	OIP (cc)	Weight of Fluid After Extraction (cc)	Oil Produced (cc)	RF %
AB1	25	20.06	19.72	0.349	1.065	2.240	3.125	3.072	0.053	1.69
	135	20.07	19.542	0.349	1.065	2.240	3.127	3.045	0.082	2.63
	225	20.14	19.412	0.349	1.065	2.240	3.138	3.024	0.113	3.61
	315	20.13	18.807	0.349	1.065	2.240	3.136	2.930	0.206	6.57
AB2	25	20.04	17.262	0.283	1.035	2.351	2.413	2.078	0.334	13.86
	135	20.03	17.082	0.283	1.035	2.351	2.411	2.057	0.355	14.72
	225	20.12	16.76	0.283	1.035	2.351	2.422	2.018	0.405	16.70
	315	20.05	16.65	0.283	1.035	2.351	2.414	2.004	0.409	16.96
AB3	25	20.03	16.68	0.35	1.044	2.127	3.296	2.745	0.551	16.72
	135	20.06	15.426	0.35	1.044	2.127	3.301	2.538	0.763	23.10
	225	20.2	15.386	0.35	1.044	2.127	3.324	2.532	0.792	23.83
	315	20.1	14.207	0.35	1.044	2.127	3.308	2.338	0.970	29.32
AB4	25	20.05	16.98	0.357	1.046	2.116	3.383	2.865	0.518	15.31
	135	20.1	15.196	0.357	1.046	2.116	3.391	2.564	0.827	24.40
	225	20.13	14.106	0.357	1.046	2.116	3.396	2.380	1.016	29.93
	315	20.22	10.7	0.357	1.046	2.116	3.411	1.805	1.606	47.08
AB5	25	20.1	19.94	0.098	1.062	2.693	0.732	0.726	0.006	0.80
	135	20.08	19.583	0.098	1.062	2.693	0.731	0.713	0.018	2.48
	225	20.08	19.374	0.098	1.062	2.693	0.731	0.705	0.026	3.52
	315	20.107	18.883	0.098	1.062	2.693	0.732	0.687	0.045	6.09

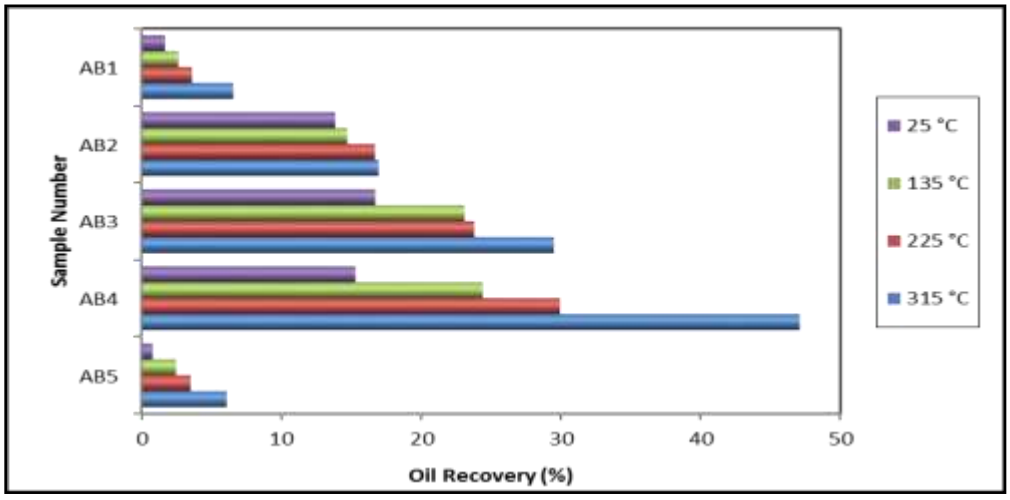

Figure 5.1. Effect of Temperature on Oil Recovery (Extracted by Toluene)

Table 5.2. Results of Oil Recovery from 20 Samples Extracted by Hot Water under Various Temperatures

Sample No.	Temp. ˚C	Weight Before Extraction (g)	Weight After Extraction (g)	Ø %	Oil Density (g/cc)	ρ_{ma} (g/cc)	OIP (cc)	Weight of Fluid After Extraction (cc)	Oil Produced (cc)	RF %
AB1	25	20.04	19.91	0.349	1.065	2.240	3.12	3.10	0.020	0.65
	135	20.12	19.84	0.349	1.065	2.240	3.13	3.09	0.044	1.42
	225	20.03	19.72	0.349	1.065	2.240	3.12	3.07	0.049	1.57
	315	20.10	19.63	0.349	1.065	2.240	3.13	3.06	0.074	2.38
AB2	25	20.11	19.90	0.283	1.035	2.351	2.42	2.40	0.025	1.04
	135	20.10	19.46	0.283	1.035	2.351	2.42	2.34	0.077	3.19
	225	20.11	19.27	0.283	1.035	2.351	2.42	2.32	0.101	4.17
	315	20.10	19.27	0.283	1.035	2.351	2.42	2.32	0.100	4.12
AB3	25	20.13	19.75	0.35	1.044	2.127	3.31	3.25	0.062	1.87
	135	20.21	19.54	0.35	1.044	2.127	3.33	3.22	0.110	3.32
	225	20.07	19.32	0.35	1.044	2.127	3.30	3.18	0.123	3.73
	315	20.10	19.35	0.35	1.044	2.127	3.31	3.18	0.123	3.71
AB4	25	20.24	19.48	0.357	1.046	2.116	3.41	3.29	0.128	3.75
	135	20.14	19.27	0.357	1.046	2.116	3.40	3.25	0.148	4.34
	225	20.14	19.08	0.357	1.046	2.116	3.40	3.22	0.179	5.28
	315	20.15	18.90	0.357	1.046	2.116	3.40	3.19	0.212	6.23
AB5	25	20.11	20.01	0.098	1.062	2.693	0.73	0.73	0.004	0.48
	135	20.11	19.88	0.098	1.062	2.693	0.73	0.72	0.008	1.16
	225	20.13	19.69	0.098	1.062	2.693	0.73	0.72	0.016	2.17
	315	20.20	19.75	0.098	1.062	2.693	0.74	0.72	0.016	2.22

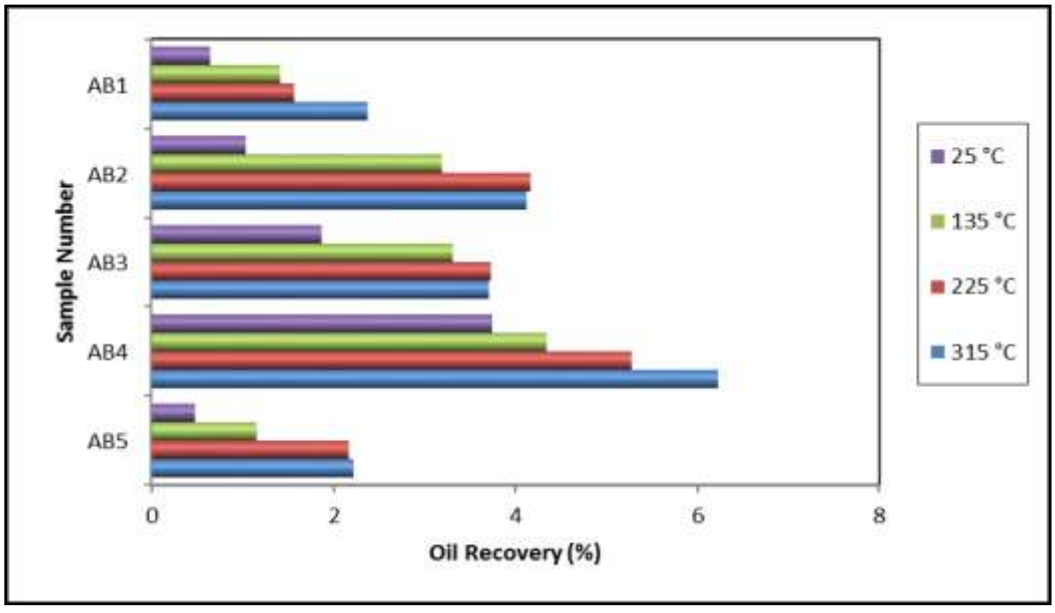

Figure 5.2. Effect of Temperature on Oil Recovery (Extracted by Hot Water)

Table 5.3. Results of Oil Recovery from 20 Samples Extracted by Surfactant Solution under Various Temperatures

Sample No.	Temp. ˚C	Weight Before Extraction (g)	Weight After Extraction (g)	Ø %	Oil Density (g/cc)	ρ_{ma} (g/cc)	OIP (cc)	Weight of Fluid After Extraction (cc)	Oil Produced (cc)	RF %
AB1	25	20.09	19.88	0.349	1.065	2.240	3.13	3.10	0.033	1.07
	135	20.08	19.67	0.349	1.065	2.240	3.13	3.06	0.065	2.07
	225	20.08	19.42	0.349	1.065	2.240	3.13	3.03	0.102	3.27
	315	20.16	19.49	0.349	1.065	2.240	3.14	3.04	0.104	3.30
AB2	25	20.17	19.71	0.283	1.035	2.351	2.43	2.37	0.055	2.28
	135	20.14	19.22	0.283	1.035	2.351	2.42	2.31	0.111	4.58
	225	20.22	19.01	0.283	1.035	2.351	2.43	2.29	0.146	5.98
	315	20.23	19.23	0.283	1.035	2.351	2.44	2.32	0.120	4.92
AB3	25	20.14	19.57	0.35	1.044	2.127	3.31	3.22	0.093	2.82
	135	20.04	19.25	0.35	1.044	2.127	3.30	3.17	0.131	3.96
	225	20.15	19.15	0.35	1.044	2.127	3.32	3.15	0.164	4.96
	315	20.15	19.07	0.35	1.044	2.127	3.32	3.14	0.178	5.36
AB4	25	20.11	19.24	0.357	1.046	2.116	3.39	3.25	0.147	4.33
	135	20.14	19.01	0.357	1.046	2.116	3.40	3.21	0.190	5.61
	225	20.10	18.77	0.357	1.046	2.116	3.39	3.17	0.224	6.61
	315	20.14	18.63	0.357	1.046	2.116	3.40	3.14	0.255	7.50
AB5	25	20.12	19.97	0.098	1.062	2.693	0.73	0.73	0.006	0.76
	135	20.25	19.89	0.098	1.062	2.693	0.74	0.72	0.013	1.76
	225	20.05	19.57	0.098	1.062	2.693	0.73	0.71	0.017	2.38
	315	20.17	19.54	0.098	1.062	2.693	0.73	0.71	0.023	3.12

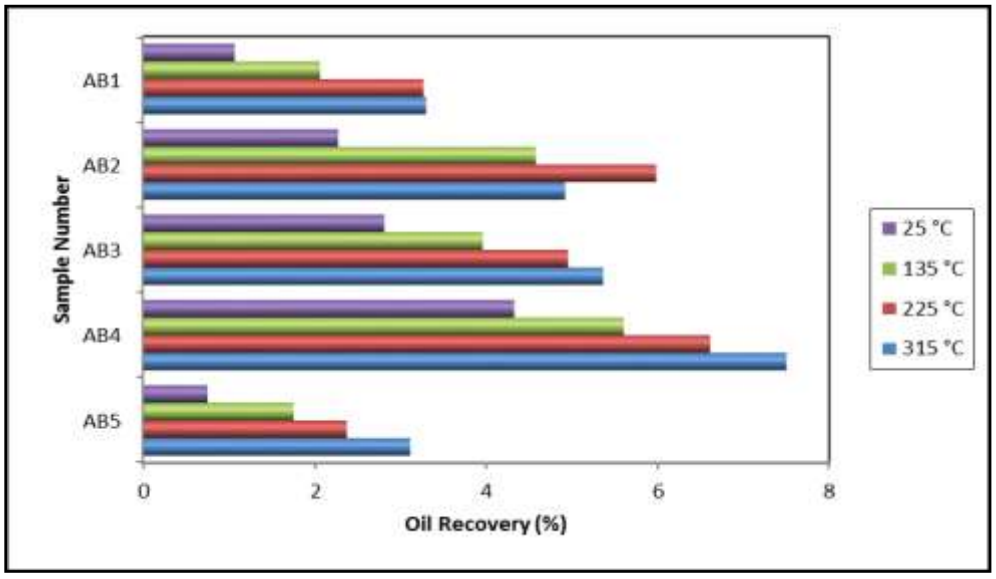

Figure 5.3. Effect of Temperature on Oil Recovery (Extracted by Surfactant Solution)

5.2. RECOVERY BASED ON GEOCHEMISTRY PYROLYSIS ANALYSIS

5.2.1. Pyrolysis Analysis Method. A pyrolysis test was conducted on powdered rock samples AB1 through AB5 under a temperature program called the reservoir method. The automatic temperature program first was defined in order to distinguish the different classes of hydrocarbons, such as free hydrocarbons, potential hydrocarbons, light oil, heavy oil, and NSO, that are released during pyrolysis. The final pyrolysis temperature applied to the pure organic matter was 650 °C. This temperature program method was developed to characterize oil and tars encountered in the reservoir. The cycle began at an initial temperature of 180 °C for 10 minutes to release the free-to-light oil (C1-C15). Light-to-medium oil (C15-C40) was detected when the temperature was between 320 °C and 380 °C. Heavy oils and NSOs were detected from 380 °C to 650 °C, which was the maximum temperature reached by the end of the program. Following the guidelines set forth by Cubitt et al. (2004), a Y coefficient was adopted (Eq. 20); then, a correlation was developed for this particular reservoir. Using Eq.19, the API gravities of samples AB1 through AB5 were calculated as 1.34, 5.17, 4.10, 3.76, and 1.72, respectively. This modified Cubitt approach (Eq. 19) did an excellent job of predicting the API gravity of extreme heavy oils (<5 API), such as the tar-mats in this reservoir.

5.2.2. Formulation of Models. Rock pyrolysis analysis was used to characterize the different species of organic matter in rock samples AB1 through AB5, as well as the reservoir properties, such as the API of the tar-mat, which usually are impossible to characterize using conventional methods. Table 5.4 shows the parameters obtained from the rock pyrolysis analysis.

Table 5.4. Parameters Obtained from the Rock Pyrolysis Analysis

Parameter	Name	Unit
S1r	Free-to-Light Hydrocarbon (C1-C15)	mg HC/g rock
S2a	Light-to-Medium Oil (C15-C40)	mg HC/g rock
S2b	Heavy Oil + NSO Compounds	mg HC/g rock
TOC	Total Organic Carbon	wt. %
PI	Production Index	-
PC	Pyrolysable Organic Carbon	wt. %
RC	Residual Organic Carbon	wt. %
Y	Cubitt's Coefficient	
API	Oil Gravity	°API

The following equations were solved using the rock analysis data and then used to calculate the oil recovery from the tar-mat samples:

$$\text{Oil}\,(\text{mg}/\text{g}) = \text{S1r} + \text{S2a} \tag{14}$$

Where:

S1r represents light oils of hydrocarbons in the range of C1-C15.

S2a represents heavy oils of hydrocarbons in the range of C15-C40.

$$\text{NSO or Kerogen}\left(\text{mg}/\text{g}\right) = \text{S2b} + \left(\text{RCr}/0.09\right) \tag{15}$$

Where:

S2b represents resin + asphaltene in the C40+ range.

RCr represents the percentage of residual carbon in the TOC after pyrolysis.

$$\text{OIS2b}\left(\text{Oxygen Index}\right) = \text{S3} / \text{TOC} \tag{16}$$

Where:

S3 represents CO2 from an organic source.

TOC stands for the total organic carbon.

$$\text{HI S2b}\left(\text{Hydrogen Index}\right) = \text{S2b} / \text{TOC} \tag{17}$$

$$\text{Total Production Index TPIr} = \left(\text{S1r} + \text{S2a}\right) / \left(\text{S1r} + \text{S2a} + \text{S2b}\right) \tag{18}$$

The following equations were used to calculate the API gravity based on the method provided by Cubitt et al. (2004):

$$\text{Estimated API Index} = 0.9245 \times e^{(4.0671 \times \text{Y})} \tag{19}$$

Where:

$$\text{Y} = \frac{(\text{S1r} + \text{S2a})}{(\text{S1r} + \text{S2a} + \text{S2b})} \tag{20}$$

The following equations were used to calculate the oil recovery from the tar-mat samples based on the rock pyrolysis analysis:

$$\text{API Method Recovery \%} = \text{ABS}\left[\left(\left(\text{APImethod} - \text{APIRaw}\right) / \text{APIRaw}\right) * 100\right] \tag{21}$$

$$\text{Residual Recovery}\left(\text{Potential Theoretical or Absolute}\right)\% = \frac{\text{Producible Carbon}}{\text{Total Organic Carbon}} \tag{22}$$

$$\text{Extractable Recovery}\left(\text{Recovery of Movable Oil C1 - C40}\right)\% = \frac{\text{Movable Carbon}}{\text{Total Organic Carbon}} \tag{23}$$

$$\text{Remaining Recovery}\left(\text{Recovery of Immobile Oil} > \text{C40}\right)\% = \frac{\text{Residual Carbon}}{\text{Extractable Carbon}} \quad (24)$$

$$\text{Method C1 - C40 Recovery}\%\left(\text{Improvement of recovery for the producible / movable carbon only}\right) = \frac{\text{Extractable recovery}}{\text{Total Organic Carbon}} \quad (25)$$

$$\text{Method} > \text{C40 Recovery}\%\left(\text{Improvement of recovery for the unproducible / residual carbon only}\right) = \frac{\text{Remaining recovery}}{\text{Total Organic Carbon}} \quad (26)$$

5.3. RESULTS AND DISCUSSION OF GEOCHEMESTRY PYROLYSIS

5.3.1. Recovery Scenario Setting. The results shown in Table 5.5 through Table 5.14 indicate that the tar-mat characterization revealed four distinct fluids that made up the complete composition mix: 1) Type I fluid consisting of free-to-light crude oil (C1-C15), 2) Type II fluid consisting of light-to-medium crude oil (C15-C40), 3) Type III fluid consisting of heavy crude oil (>C40), and 4) Type IV insoluble and immobile extreme heavy oil (NSO). Combining all four types of crude oil yields the total organic crude oil (TOC), or the estimated oil-in-place, of the tar-mat. Using pyrolysis analysis, the TOC was estimated to make up 33.51 wt.% of sample AB1, and the remaining 66.49% of the sample included the reservoir's other solid rock materials (inorganic carbon, water, trace metals, and other rare earth minerals).

Furthermore, the TOC was estimated to make up 7.70, 8.41, 8.19, and 43.57 wt.% of samples AB2 through AB5, respectively, and the remaining 92.3, 91.59, 91.81, and 56.43 wt.% of samples AB2 through AB5, respectively, included the reservoir's other solid rock materials. For all native-state tar-mat samples, the Type IV (insoluble NSO)

portion of the tar-mat oil was greater than the Type III (heavy oil >C40) portion; the Type III portion was greater than the Type II (light-to-medium C15-C40) portion; and the Type II portion was greater than the Type I (free-to-light C1-C15) portion. This result was repeated for all tar-mat samples, making this observation generalizable, with 100% confidence, as a new upgrade for the existing tar-mat definitions, especially from those rich in asphaltenes to rich in NSO. Therefore, to characterize tar-mat oil all over the world, the following pattern must be identified:

Type IV (insoluble NSO) > Type III (heavy oil >C40) > Type II (light-to-medium C15-C40) > Type I (free-to-light C1-C15).

Each type of fluid has a unique flow regime that dictates the nature of the flow and, hence, the type of recovery. The weight of the raw tar-mat samples (AB1-AB5) was approximately 40 mg each, and they had three distinct physical flow regimes, as shown in Table 5.5, Table 5.7, Table 5.9, Table 5.11, and Table 5.13. The first flow regime combines Type I and Type II fluids (C1-C40) and is referred to as extractable recovery or movable oil (Eq. 5.15). These free-light-medium hydrocarbons mixed with medium-density hydrocarbons can be recovered naturally without applying an aided-recovery method.

5.3.2. Tar-Mat Sample AB1. For sample AB1, the results of the geochemical characterization are summarized in Table 5.5 and Table 5.6. This regime yielded small quantities of movable oil (5.21 mg/g, 0.52% by carbon weight, 1.55% of the tar-mat's total mix). The second flow regime, Type III fluid, was the remaining recovery (>C40) (Eq. 24), referred to as producible carbon or immobile oil. This type of heavy oil requires an enhancement method to facilitate the movement of the dense materials in order to

achieve recovery. This flow regime yielded more oil than the free-light-medium hydrocarbon regime (51.86 mg/g, 4.95% by carbon weight, 14.77% of the tar-mat's total mix). The combined light and heavy fluid flow from both regimes yielded 57.07 mg/g, 5.47% by carbon weight, 16.32% of the tar-mat's total mix; this combination is referred to as residual (Eq. 22), theoretical, or potential recovery, which benefits from economical, conventional EOR recovery methods. These two flow regimes were the target of this study, which applied toluene, water, and surfactant solution recovery methods at different temperatures. The third flow regime includes the insoluble hydrocarbons (or NSOs) that give the tar-mat its extremely heavy density (<5 °API) and solid-like viscosity. NSO availability in significant amounts (quantitative) and complicated nitrogen, sulfur, and oxygen compounds (qualitative) serves as a distinct fingerprint for tar-mat oils. NSO availability in the tar-mat oil mix makes carbon residue difficult to extract and will enhance powerful attraction forces on the mineral crystals of carbonate grain. The NSO bond to carbon is highly likely to create a heavy carbon-NSO molecule that will cause the NSO to bond to the rock's surface. In this study, the insoluble regime is referred to as unproducible carbons or insoluble NSO. This regime yielded the highest quantity of oil (369.19 mg/g, 28.56% by carbon weight, 83.68% of the tar-mat's total mix). This result suggests that the greatest portion of tar-mats cannot be recovered economically using mild or conventional recovery techniques. This locked Type IV oil is not the subject of this study but will be researched further in future studies focusing on using unconventional higher temperatures, aggressive chemicals, or any combination of these two approaches.

Table 5.5. Sample AB1 Raw Geochemical Results with Type I (C1-C15), Type II (C15-C40), Type III (>C40), and Type IV Insoluble NSO - Detailed Amounts for Every Recovery Agent at All Temperature Variations

Reservoir Method	Temperature Setting	C1-C15 mg/g S1r	C15-C40 mg/g S2a	>C40 mg/g S2b	Insolubles mg/g NSO	C1-C40 mg/g Movable Oil	C1-C40 % Movable Oil	Producible Carbon (%) PCr	Unproducible Carbon (%) RCr	Total Organic Carbon (wt.%) TOC
Toluene	**Raw Tar-Mat**	**0.8**	**4.4**	**51.9**	**369.2**	**5.2**	**0.52**	**5.0**	**28.6**	**33.5**
	25°C	2.4	4.4	50.9	372.1	6.7	0.67	5.0	28.9	33.9
	135°C	9.4	3.6	44.1	428.9	13.0	1.30	4.9	34.6	39.6
	225°C	7.9	4.0	46.8	520.9	11.9	1.19	5.1	42.7	47.8
	315°C	6.7	4.1	46.2	1530.7	10.8	1.08	4.9	133.6	138.6
Water	**Raw Tar-Mat**	**0.8**	**4.4**	**51.9**	**369.2**	**5.2**	**0.52**	**5.0**	**28.6**	**33.5**
	25°C	0.8	4.9	53.7	355.6	5.6	0.56	5.1	27.2	32.3
	135°C	2.4	9.0	69.1	454.1	11.4	1.14	6.9	34.7	41.6
	225°C	0.4	4.0	54.4	354.6	4.5	0.45	5.1	27.0	32.1
	315°C	0.5	4.1	56.8	465.1	4.6	0.46	5.3	36.8	42.1
Surfactant	**Raw Tar-Mat**	**0.8**	**4.4**	**51.9**	**369.2**	**5.2**	**0.52**	**5.0**	**28.6**	**33.5**
	25°C	1.2	7.2	59.2	455.0	8.4	0.84	5.8	35.6	41.4
	135°C	0.8	7.5	59.5	340.8	8.3	0.83	5.8	25.3	31.2
	225°C	2.8	13.5	78.9	358.7	16.4	1.64	8.2	25.2	33.3
	315°C	1.3	10.2	61.9	258.1	11.5	1.15	6.3	17.7	23.9

Table 5.6. Sample AB1 Recovery Schemes for Toluene, Water, and Surfactant at Different Temperatures

Reservoir Method	Temperature Setting	Tar-Mat Density API	API-Toluene Recovery %	Residual Recovery %	Extractable Recovery %	Remaining Recovery %	C1-C40 Recovery %	> C40 Recovery %	Total Recovery %
Toluene	**Raw Tar-Mat**	**1.34**	**0.01**	**14.77**	**1.55**	**13.22**	**0.00**	**0.00**	**0.00**
	25°C	1.49	10.94	14.72	1.99	12.73	0.06	0.38	0.43
	135°C	2.33	74.01	12.48	3.28	9.20	0.08	0.23	0.32
	225°C	2.11	57.66	10.68	2.50	8.18	0.05	0.17	0.22
	315°C	2.00	49.07	3.57	0.78	2.79	0.01	0.02	0.03
Water	**Raw Tar-Mat**	**1.34**	**0.01**	**14.77**	**1.55**	**13.22**	**0.00**	**0.00**	**0.00**
	25°C	1.36	1.50	15.88	1.74	14.14	0.05	0.44	0.49
	135°C	1.64	22.56	16.67	2.73	13.93	0.07	0.34	0.40
	225°C	1.26	6.09	15.88	1.39	14.49	0.04	0.45	0.49
	315°C	1.26	6.18	12.65	1.10	11.54	0.03	0.27	0.30
Surfactant	**Raw Tar-Mat**	**1.34**	**0.01**	**14.77**	**1.55**	**13.22**	**0.00**	**0.00**	**0.00**
	25°C	1.54	14.57	14.04	2.04	12.01	0.05	0.29	0.34
	135°C	1.52	13.38	18.74	2.66	16.08	0.09	0.52	0.60
	225°C	1.86	38.77	24.45	4.91	19.54	0.15	0.59	0.73
	315°C	1.74	30.21	26.23	4.78	21.45	0.20	0.90	1.10

5.3.3. Tar-Mat Sample AB2. The results of the geochemical characterization are summarized in Table 5.7 and Table 5.8. This regime yielded large quantities of oil (22.31 mg/g, 2.23% by carbon weight, 28.97% of the tar-mat's total mix). The second flow regime, as described in Section 5.3.1.1, yielded more heavy oil than the light hydrocarbon regime (30.43 mg/g, 4.39% by carbon weight, 57.01% of the tar-mat's total mix). The combined light and heavy fluid flow from both regimes, the residual recovery described in Section 5.3.1.1, yielded 52.74 mg/g, 6.62% by carbon weight, 85.98% of the tar-mat's total mix. The third flow regime, as described in Section 5.3.1.1, yielded the most oil (67.21 mg/g, 3.31% by carbon weight, 14.02% of the tar-mat's total mix). This result suggests that the greatest portion of tar-mats can be recovered economically using mild or conventional recovery techniques.

Table 5.7. Sample AB2 Raw Geochemical Results with Type I (C1-C15), Type II (C15-C40), Type III (>C40), and Type IV Insoluble NSO - Detailed Amounts for Every Recovery Agent at All Temperature Variations

Reservoir Method	Temperature Setting	C1-C15 mg/g S1r	C15-C40 mg/g S2a	>C40 mg/g S2b	Insolubles mg/g NSO	C1-C40 mg/g Movable Oil	C1-C40 % Movable Oil	Producible Carbon (%) PCr	Unproducible Carbon (%) RCr	Total Organic Carbon (wt.%) TOC
Toluene	**Raw Tar-Mat**	**5.46**	**16.85**	**30.43**	**67.21**	**22.31**	**2.23**	**4.39**	**3.31**	**7.70**
	25°C	3.49	8.04	18.87	48.87	11.53	1.15	2.53	2.70	5.23
	135°C	0.45	1.32	5.86	36.64	1.77	0.18	0.65	2.77	3.42
	225°C	0.18	0.83	4.67	34.78	1.01	0.10	0.48	2.71	3.19
	315°C	0.52	1.45	5.23	197.45	1.97	0.20	0.61	17.30	17.91
Water	**Raw Tar-Mat**	**5.46**	**16.85**	**30.43**	**67.21**	**22.31**	**2.23**	**4.39**	**3.31**	**7.70**
	25°C	5.56	15.15	33.15	65.37	20.71	2.07	4.48	2.90	7.38
	135°C	5.66	15.26	39.84	70.28	20.92	2.09	5.06	2.74	7.80
	225°C	5.81	16.14	35.64	62.86	21.95	2.20	4.79	2.45	7.24
	315°C	5.76	16.02	36.52	72.19	21.78	2.18	4.86	3.21	8.07
Surfactant	**Raw Tar-Mat**	**5.46**	**16.85**	**30.43**	**67.21**	**22.31**	**2.23**	**4.39**	**3.31**	**7.70**
	25°C	5.99	15.77	35.01	73.23	21.76	2.18	4.73	3.44	8.17
	135°C	5.59	15.00	34.31	57.53	20.59	2.06	4.57	2.09	6.66
	225°C	4.83	13.72	34.73	55.06	18.55	1.86	4.44	1.83	6.27
	315°C	4.59	13.47	34.85	56.52	18.06	1.81	4.42	1.95	6.37

Table 5.8. Sample AB2 Recovery Schemes for Toluene, Water, and Surfactant at Different Temperatures

Reservoir Method	Temperature Setting	Tar-Mat Density API	API-Toluene Recovery %	Residual Recovery %	Extractable Recovery %	Remaining Recovery %	C1-C40 Recovery %	> C40 Recovery %	Total Recovery %
Toluene	**Raw Tar-Mat**	**5.17**	**0.10**	**57.01**	**28.97**	**28.04**	**0.00**	**0.00**	**0.00**
	25°C	4.32	16.38	48.37	22.05	26.33	4.22	5.03	9.25
	135°C	2.37	54.06	19.01	5.18	13.83	1.51	4.04	5.56
	225°C	1.91	63.15	15.05	3.17	11.88	0.99	3.72	4.72
	315°C	2.81	45.59	3.41	1.10	2.31	0.06	0.13	0.19
Water	**Raw Tar-Mat**	**5.17**	**0.10**	**57.01**	**28.97**	**28.04**	**0.00**	**0.00**	**0.00**
	25°C	4.42	14.58	60.70	28.06	32.64	3.80	4.42	8.23
	135°C	3.75	27.46	64.87	26.82	38.05	3.44	4.88	8.32
	225°C	4.36	15.74	66.16	30.32	35.84	4.19	4.95	9.14
	315°C	4.22	18.29	60.22	26.99	33.23	3.34	4.12	7.46
Surfactant	**Raw Tar-Mat**	**5.17**	**0.10**	**57.01**	**28.97**	**28.04**	**0.00**	**0.00**	**0.00**
	25°C	4.39	15.00	57.89	26.63	31.26	3.26	3.83	7.09
	135°C	4.25	17.80	68.62	30.92	37.70	4.64	5.66	10.30
	225°C	3.81	26.32	70.81	29.59	41.23	4.72	6.58	11.29
	315°C	3.71	28.34	69.39	28.35	41.04	4.45	6.44	10.89

5.3.4. Tar-Mat Sample AB3. Table 5.9 and Table 5.10 summarize the results of the geochemical analysis for sample AB3. This regime yielded large quantities of oil (21.67 mg/g, 2.17% by carbon weight, 25.77% of the tar-mat's total mix). The Type III fluid flow regime yielded more heavy oil than the light hydrocarbon regime (37.47 mg/g, 4.93% by carbon weight, 58.62% of the tar-mat's total mix). The combined light and heavy fluid flow from both regimes yielded 59.14 mg/g, 7.1% by carbon weight, 84.39% of the tar-mat's total mix. The third flow regime yielded the most oil (76.14 mg/g, 3.48% by carbon weight, 15.61% of the tar-mat's total mix). These results show that tar-mat oil can be recovered using conventional recovery techniques.

Table 5.9. Sample AB3 Raw Geochemical Results with Type I (C1-C15), Type II (C15-C40), Type III (>C40), and Type IV Insoluble NSO - Detailed Amounts for Every Recovery Agent at All Temperature Variations

Reservoir Method	Temperature Setting	C1-C15 mg/g S1r	C15-C40 mg/g S2a	>C40 mg/g S2b	Insolubles mg/g NSO	C1-C40 mg/g Movable Oil	C1-C40 % Movable Oil	Producible Carbon (%) PCr	Unproducible Carbon (%) RCr	Total Organic Carbon (wt.%) TOC
Toluene	**Raw Tar-Mat**	**7.12**	**14.55**	**37.47**	**76.14**	**21.67**	**2.17**	**4.93**	**3.48**	**8.41**
	25°C	3.57	7.60	22.54	55.32	11.17	1.12	2.81	2.95	5.76
	135°C	0.14	0.51	5.85	36.07	0.65	0.07	0.55	2.72	3.27
	225°C	0.26	0.97	6.80	39.80	1.23	0.12	0.68	2.97	3.65
	315°C	0.12	0.39	4.65	23.98	0.51	0.05	0.45	1.74	2.19
Water	**Raw Tar-Mat**	**7.12**	**14.55**	**37.47**	**76.14**	**21.67**	**2.17**	**4.93**	**3.48**	**8.41**
	25°C	6.80	14.45	37.23	76.67	21.25	2.13	4.87	3.55	8.42
	135°C	6.65	14.81	38.68	74.01	21.46	2.15	5.01	3.18	8.19
	225°C	5.97	14.36	37.44	73.00	20.33	2.03	4.81	3.20	8.01
	315°C	6.29	15.68	41.11	87.33	21.97	2.20	5.26	4.16	9.42
Surfactant	**Raw Tar-Mat**	**7.12**	**14.55**	**37.47**	**76.14**	**21.67**	**2.17**	**4.93**	**3.48**	**8.41**
	25°C	7.35	15.21	38.57	86.01	22.56	2.26	5.10	4.27	9.37
	135°C	5.42	15.13	40.73	66.95	20.55	2.06	5.11	2.36	7.47
	225°C	6.10	14.37	39.41	66.08	20.47	2.05	4.99	2.40	7.39
	315°C	5.31	13.50	39.22	62.44	18.81	1.88	4.84	2.09	6.93

Table 5.10. Sample AB3 Recovery Schemes for Toluene, Water, and Surfactant at Different Temperatures

Reservoir Method	Temperature Setting	Tar-Mat Density API	API-Toluene Recovery %	Residual Recovery %	Extractable Recovery %	Remaining Recovery %	C1-C40 Recovery %	> C40 Recovery %	Total Recovery %
Toluene	**Raw Tar-Mat**	**4.10**	**0.07**	**58.62**	**25.77**	**32.85**	**0.00**	**0.00**	**0.00**
	25°C	3.56	13.23	48.78	19.39	29.39	3.37	5.10	8.47
	135°C	1.39	66.14	16.82	1.99	14.83	0.61	4.54	5.14
	225°C	1.72	57.96	18.63	3.37	15.26	0.92	4.18	5.10
	315°C	1.38	66.29	20.55	2.33	18.22	1.06	8.32	9.38
Water	**Raw Tar-Mat**	**4.10**	**0.07**	**58.62**	**25.77**	**32.85**	**0.00**	**0.00**	**0.00**
	25°C	4.05	1.16	57.84	25.24	32.60	3.00	3.87	6.87
	135°C	3.95	3.75	61.17	26.20	34.97	3.20	4.27	7.47
	225°C	3.87	5.66	60.05	25.38	34.67	3.17	4.33	7.50
	315°C	3.81	7.04	55.84	23.32	32.52	2.48	3.45	5.93
Surfactant	**Raw Tar-Mat**	**4.10**	**0.07**	**58.62**	**25.77**	**32.85**	**0.00**	**0.00**	**0.00**
	25°C	4.15	1.15	54.43	24.08	30.35	2.57	3.24	5.81
	135°C	3.62	11.81	68.41	27.51	40.90	3.68	5.47	9.16
	225°C	3.71	9.44	67.52	27.70	39.82	3.75	5.39	9.14
	315°C	3.45	15.73	69.84	27.14	42.70	3.92	6.16	10.08

5.3.5. Tar-Mat Sample AB4. The results of the geochemical characterization for sample AB4 are summarized in Table 5.11 and Table 5.12. This regime yielded large quantities of oil (21.10 mg/g, 2.11% by carbon weight, 25.76% of the tar-mat's total mix). The Type III fluid yielded more oil than the light hydrocarbon regime (40.04 mg/g, 5.10% by carbon weight, 62.27% of the tar-mat's total mix). The combination of light and heavy oil yielded 61.14 mg/g, 7.21% by carbon weight, and 88.03% of the tar-mat's total mix. These two flow regimes were the target of this study. The third flow regime yielded the most oil (74.37 mg/g, 3.09% by carbon weight, 11.97% of the tar-mat's total mix). The results indicate that the greatest amount of oil can be recovered using mild or conventional recovery techniques.

Table 5.11. Sample AB4 Raw Geochemical Results with Type I (C1-C15), Type II (C15-C40), Type III (>C40), and Type IV Insoluble NSO - Detailed Amounts for Every Recovery Agent at All Temperature Variations

Reservoir Method	Temperature Setting	C1-C15 mg/g S1r	C15-C40 mg/g S2a	>C40 mg/g S2b	Insolubles mg/g NSO	C1-C40 mg/g Movable Oil	C1-C40 % Movable Oil	Producible Carbon (%) PCr	Unproducible Carbon (%) RCr	Total Organic Carbon (wt.%) TOC
Toluene	**Raw Tar-Mat**	**5.57**	**15.53**	**40.04**	**74.37**	**21.10**	**2.11**	**5.10**	**3.09**	**8.19**
	25°C	3.10	7.86	20.47	46.36	10.96	1.10	2.62	2.33	4.95
	135°C	0.17	0.47	2.65	15.76	0.64	0.06	0.29	1.18	1.47
	225°C	0.16	0.55	3.59	26.81	0.71	0.07	0.37	2.09	2.46
	315°C	0.12	0.29	2.16	10.83	0.41	0.04	0.23	0.78	1.01
Water	**Raw Tar-Mat**	**5.57**	**15.53**	**40.04**	**74.37**	**21.10**	**2.11**	**5.10**	**3.09**	**8.19**
	25°C	5.78	14.98	37.45	69.78	20.76	2.08	4.85	2.91	7.76
	135°C	6.22	15.94	34.70	60.59	22.16	2.22	4.73	2.33	7.06
	225°C	5.34	15.29	39.61	67.17	20.63	2.06	5.02	2.48	7.50
	315°C	5.74	16.01	41.88	76.44	21.75	2.18	5.29	3.11	8.40
Surfactant	**Raw Tar-Mat**	**5.57**	**15.53**	**40.04**	**74.37**	**21.10**	**2.11**	**5.10**	**3.09**	**8.19**
	25°C	6.30	15.98	40.00	80.11	22.28	2.23	5.19	3.61	8.80
	135°C	5.18	14.74	38.99	62.66	19.92	1.99	4.91	2.13	7.04
	225°C	4.61	14.28	39.14	63.36	18.89	1.89	4.83	2.18	7.01
	315°C	4.41	13.82	38.47	61.36	18.23	1.82	4.72	2.06	6.78

Table 5.12. Sample AB4 Recovery Schemes for Toluene, Water, and Surfactant at Different Temperatures

Reservoir Method	Temperature Setting	Tar-Mat Density API	API-Toluene Recovery %	Residual Recovery %	Extractable Recovery %	Remaining Recovery %	C1-C40 Recovery %	> C40 Recovery %	Total Recovery %
Toluene	**Raw Tar-Mat**	**3.76**	**0.06**	**62.27**	**25.76**	**36.51**	**0.00**	**0.00**	**0.00**
	25°C	3.82	1.54	52.93	22.14	30.79	4.47	6.22	10.69
	135°C	2.04	45.76	19.73	4.35	15.37	2.96	10.46	13.42
	225°C	1.81	51.88	15.04	2.89	12.15	1.17	4.94	6.11
	315°C	1.77	52.96	22.77	4.06	18.71	4.02	18.53	22.55
Water	**Raw Tar-Mat**	**3.76**	**0.06**	**62.27**	**25.76**	**36.51**	**0.00**	**0.00**	**0.00**
	25°C	3.94	4.87	62.50	26.75	35.75	3.45	4.61	8.05
	135°C	4.51	19.97	67.00	31.39	35.61	4.45	5.04	9.49
	225°C	3.72	1.01	66.93	27.51	39.43	3.67	5.26	8.92
	315°C	3.71	1.27	62.98	25.89	37.08	3.08	4.41	7.50
Surfactant	**Raw Tar-Mat**	**3.76**	**0.06**	**62.27**	**25.76**	**36.51**	**0.00**	**0.00**	**0.00**
	25°C	3.96	5.34	58.98	25.32	33.66	2.88	3.82	6.70
	135°C	3.66	2.73	69.74	28.30	41.45	4.02	5.89	9.91
	225°C	3.47	7.60	68.90	26.95	41.95	3.84	5.98	9.83
	315°C	3.42	9.09	69.62	26.89	42.73	3.97	6.30	10.27

5.3.6. Tar-Mat Sample AB5. The results from sample AB5 appear in Table 5.13 and Table 5.14. This regime yielded large quantities of oil (12.28 mg/g, 1.23% by carbon weight, 2.82% of the tar-mat's total mix). The Type III fluid yielded more heavy oil than the light hydrocarbon regime (68.31 mg/g, 6.92% by carbon weight, 15.88% of the tar-mat's total mix). The combined light and heavy fluid flow from both regimes yielded 80.59 mg/g, 8.15% by carbon weight, 18.7% of the tar-mat's total mix. The third flow regime yielded the most oil (475.53 mg/g, 36.65% by carbon weight, 81.3% of the tar-mat's total mix). This result suggests that the greatest portion of tar-mats cannot be recovered economically using mild or conventional recovery techniques.

Table 5.13. Sample AB5 Raw Geochemical Results with Type I (C1-C15), Type II (C15-C40), Type III (>C40), and Type IV Insoluble NSO - Detailed Amounts for Every Recovery Agent at All Temperature Variations

Reservoir Method	Temperature Setting	C1-C15 mg/g S1r	C15-C40 mg/g S2a	>C40 mg/g S2b	Insolubles mg/g NSO	C1-C40 mg/g Movable Oil	C1-C40 % Movable Oil	Producible Carbon (%) PCr	Unproducible Carbon (%) RCr	Total Organic Carbon (wt.%) TOC
Toluene	**Raw Tar-Mat**	**3.11**	**9.17**	**68.31**	**475.53**	**12.28**	**1.23**	**6.92**	**36.65**	**43.57**
	25°C	4.22	8.09	68.22	584.89	12.31	1.23	6.91	46.50	53.41
	135°C	12.52	5.45	62.43	562.32	17.97	1.80	6.92	44.99	51.91
	225°C	7.73	4.37	60.68	1509.12	12.10	1.21	6.30	130.36	136.66
	315°C	13.31	4.07	59.07	407.74	17.38	1.74	6.59	31.38	37.97
Water	**Raw Tar-Mat**	**3.11**	**9.17**	**68.31**	**475.53**	**12.28**	**1.23**	**6.92**	**36.65**	**43.57**
	25°C	2.96	9.35	69.56	441.23	12.31	1.23	7.04	33.45	40.49
	135°C	0.52	4.28	54.03	354.03	4.80	0.48	5.09	27.00	32.09
	225°C	2.32	8.94	70.74	452.85	11.26	1.13	7.06	34.39	41.45
	315°C	2.26	9.09	70.84	598.62	11.35	1.14	7.08	47.50	54.58
Surfactant	**Raw Tar-Mat**	**3.11**	**9.17**	**68.31**	**475.53**	**12.28**	**1.23**	**6.92**	**36.65**	**43.57**
	25°C	3.71	12.17	74.47	322.58	15.88	1.59	7.73	22.33	30.06
	135°C	2.89	13.37	78.43	327.21	16.26	1.63	8.10	22.39	30.49
	225°C	2.71	13.92	81.58	341.25	16.63	1.66	8.40	23.37	31.77
	315°C	2.65	13.98	82.39	330.06	16.63	1.66	8.47	22.29	30.76

Table 5.14. Sample AB5 Recovery Schemes for Toluene, Water, and Surfactant at Different Temperatures

Reservoir Method	Temperature Setting	Tar-Mat Density API	API-Toluene Recovery %	Residual Recovery %	Extractable Recovery %	Remaining Recovery %	C1-C40 Recovery %	> C40 Recovery %	Total Recovery %
Toluene	**Raw Tar-Mat**	**1.72**	**0.11**	**15.88**	**2.82**	**13.06**	**0.00**	**0.00**	**0.00**
	25°C	1.72	0.09	12.94	2.30	10.63	0.04	0.20	0.24
	135°C	2.29	33.40	13.33	3.46	9.87	0.07	0.19	0.26
	225°C	1.82	5.69	4.61	0.89	3.72	0.01	0.03	0.03
	315°C	2.33	35.49	17.36	4.58	12.78	0.12	0.34	0.46
Water	**Raw Tar-Mat**	**1.72**	**0.11**	**15.88**	**2.82**	**13.06**	**0.00**	**0.00**	**0.00**
	25°C	1.70	0.93	17.39	3.04	14.35	0.08	0.35	0.43
	135°C	1.29	25.10	15.86	1.50	14.37	0.05	0.45	0.49
	225°C	1.62	6.05	17.03	2.72	14.32	0.07	0.35	0.41
	315°C	1.62	5.75	12.97	2.08	10.89	0.04	0.20	0.24
Surfactant	**Raw Tar-Mat**	**1.72**	**0.11**	**15.88**	**2.82**	**13.06**	**0.00**	**0.00**	**0.00**
	25°C	1.89	9.86	25.72	5.28	20.43	0.18	0.68	0.86
	135°C	1.86	8.06	26.57	5.33	21.23	0.17	0.70	0.87
	225°C	1.84	7.02	26.44	5.23	21.21	0.16	0.67	0.83
	315°C	1.83	6.42	27.54	5.41	22.13	0.18	0.72	0.90

5.4. EFFECT OF TOLUENE, HOT WATER, AND SURFACTANT AT DIFFERENT TEMPERATURES ON OIL RECOVERY BASED ON PYROLYSIS ANALYSIS

5.4.1. Toluene. Toluene was applied at different temperatures to recover the oil from the tar-mat samples in this study.

5.4.1.1 Effect of toluene and temperature on oil recovery from sample AB1. In the toluene recovery scheme provided in Figure 5.4 and Table 5.15, the residual recovery is the amount of producible carbon (PCr) available in the TOC, and this portion of the tar-mat is the absolute or theoretical amount that can be produced using conventional recovery methods. This residual quantity can be made to flow economically using conventional criteria. AB1 had a residual recovery of 14.77%, which was divided into two categories. The first category, movable light oil (C1-C40), was a combination of Type I and Type II oils that can be produced with a simple enhancement agent other than temperature or dry heat; it will be referred to as extractable recovery. For AB1, it was measured to be only 1.55%. The other category, heavy oils (>C40) or Type III, will be referred to as the remaining recovery; usually, heavy oils are naturally immobile but can be recovered when an agent is introduced to the tar-mat mix. In previous studies reported in the literature, an inorganic solvent has served as the laboratory agent, but in the present experiments, an organic solvent, toluene, was chosen to recover the remaining oil. The remaining oil yield after subtracting the extractable recovery from the residual recovering was 13.22%, an attractive prospect for EOR investments.

Figure 5.4 depicts a very clear toluene recovery trend; the higher the temperature of toluene, the more light oil (extractable) was produced, and the less heavy oil remained in the tar-mat mix.

Table 5.15 indicates that in the tar-mat's natural state, 14.77% of the original residual oil was available for recovery, but after increasing the temperature to 315 ˚C, only 3.57% of the oil remained, indicating that 11.2% of the total oil was produced successfully.

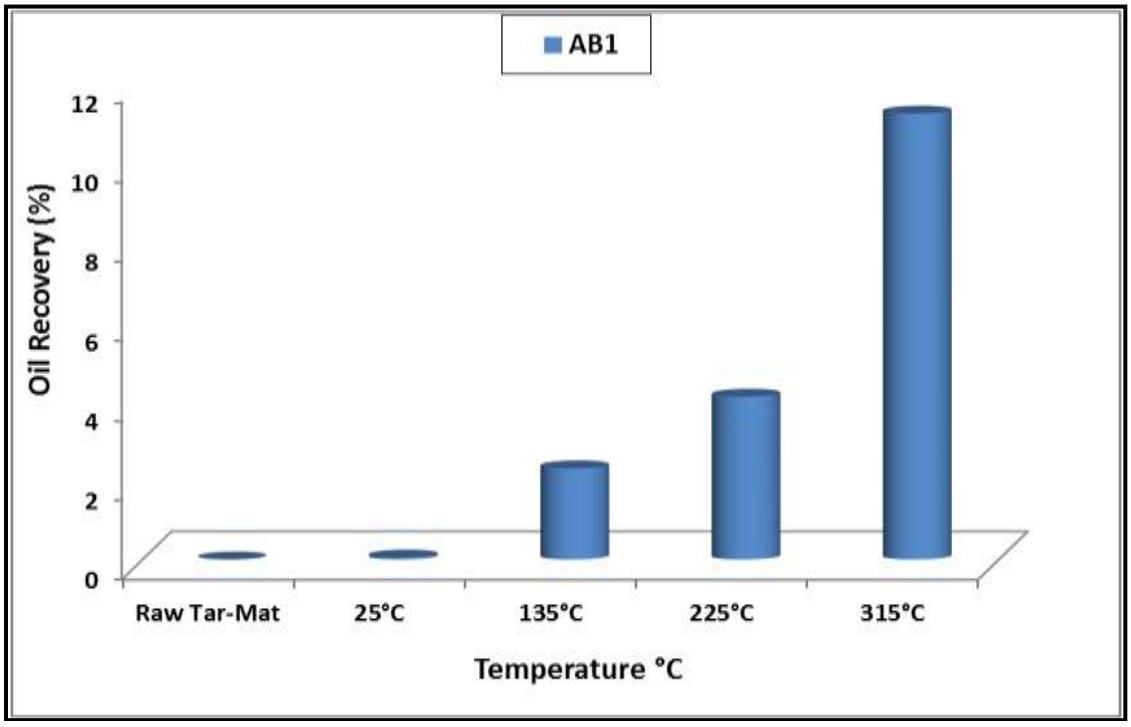

Figure 5.4. Effect of Temperature on Oil Recovery from Sample AB1 (Extracted by Toluene)

Table 5.15. Sample AB1 Recovery Schemes for Toluene at Different Temperatures

Sample	Temperature Setting (℃)	Type I (C1-C15) mg/g	Type I (C1-C15) %	Type II (C15-C40) mg/g	Type II (C15-C40) %	Type III (>C40) mg/g	Type III (>C40) %	Type IV (NSO) mg/g	Type IV (NSO) %	Total Oil mg/g	Total Oil %	Residual Recovery (%)	Extractable Recovery (%)	Remaining Recovery (%)	Maximum Recovery (%)
AB1	Raw Tar-Mat	0.77	0.18	4.44	1.04	51.86	12.17	369.19	86.61	426.3	100	14.77	1.55	13.22	0
	25°C	2.36	0.55	4.37	1.02	50.89	11.84	372.11	86.59	429.73	100	14.72	1.99	12.73	0.05
	135°C	9.38	1.93	3.59	0.74	44.05	9.06	428.94	88.27	485.96	100	12.48	3.28	9.20	2.29
	225°C	7.93	1.37	4.00	0.69	46.78	8.07	520.89	89.87	579.6	100	10.68	2.50	8.18	4.09
	315°C	6.69	0.42	4.10	0.26	46.17	2.91	1530.7	96.41	1587.7	100	3.57	0.78	2.79	11.2

5.4.1.2 Effect of toluene and temperature on oil recovery from sample AB2.

Figure 5.5 and Table 5.16 provides data showing the effect of toluene and the temperature on the recovery of oil from sample AB2. This sample had a residual recovery of 57.01%, which was divided into two categories, light oil (C1-C40) and heavy oil (>C40). Recovering the lighter oils required the use of an enhancement agent, which yielded 28.97% recovery. The heavy oils, while mostly immobile, were easily removed after adding some agent, such as toluene, which recovered 28.04% of the oil.

Figure 5.5 illustrates that more light oil was recovered as the temperature of toluene increased. Table 5.16 Figure 5.5 and indicate that residual oil that was not recoverable at low temperatures was significantly recovered at high temperatures (53.61%).

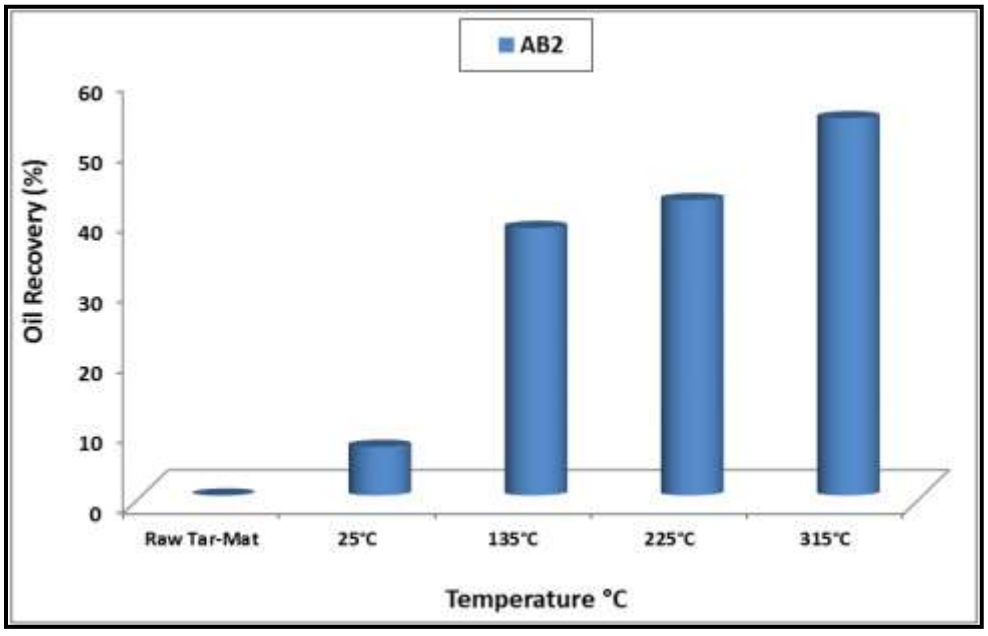

Figure 5.5. Effect of Temperature on Oil Recovery from Sample AB2 (Extracted by Toluene)

Table 5.16. Sample AB2 Recovery Schemes for Toluene at Different Temperatures

Sample	Temperature Setting (℃)	Type I (C1-C15) mg/g	Type I (C1-C15) %	Type II (C15-C40) mg/g	Type II (C15-C40) %	Type III (>C40) mg/g	Type III (>C40) %	Type IV (NSO) mg/g	Type IV (NSO) %	Total Oil mg/g	Total Oil %	Residual Recovery (%)	Extractable Recovery (%)	Remaining Recovery (%)	Maximum Recovery (%)
AB2	Raw Tar-Mat	5.46	4.55	16.85	14.05	30.43	25.37	67.21	56.03	119.95	100	57.01	28.97	28.04	0
	25°C	3.49	4.40	8.04	10.14	18.87	23.80	48.87	61.65	79.27	100	48.37	22.05	26.33	6.93
	135°C	0.45	1.02	1.32	2.98	5.86	13.24	36.64	82.76	44.27	100	19.01	5.18	13.83	38.01
	225°C	0.18	0.44	0.83	2.05	4.67	11.54	34.78	85.96	40.46	100	15.05	3.17	11.88	41.97
	315°C	0.52	0.25	1.45	0.71	5.23	2.56	197.45	96.48	204.65	100	3.41	1.10	2.31	53.61

5.4.1.3 Effect of toluene and temperature on oil recovery from sample AB3.

The recovery of oil from sample AB3 was affected by toluene as well as the temperature (Figure 5.6). According to Table 5.17, the residual recovery of AB3 was 58.62%. In the light oils, the recovery after the addition of an agent was found to be 25.77%. To enhance recovery in the heavy oil, toluene was added as an agent; adding this solvent resulted in the recovery of 32.85% of heavy oil, showing good prospects for investments in EOR techniques.

Figure 5.6 illustrates that as the temperature of toluene increased, more light oil was produced, and relatively little heavy oil remained in the original tar-mat mix. The results in Table 5.17 indicate that in the tar-mat's natural state, 58.62% of the original residual oil was available for recovery, but after increasing the temperature to 135 ˚C, only 16.82% of the oil remained, indicating that 41.8% of the total oil was produced successfully.

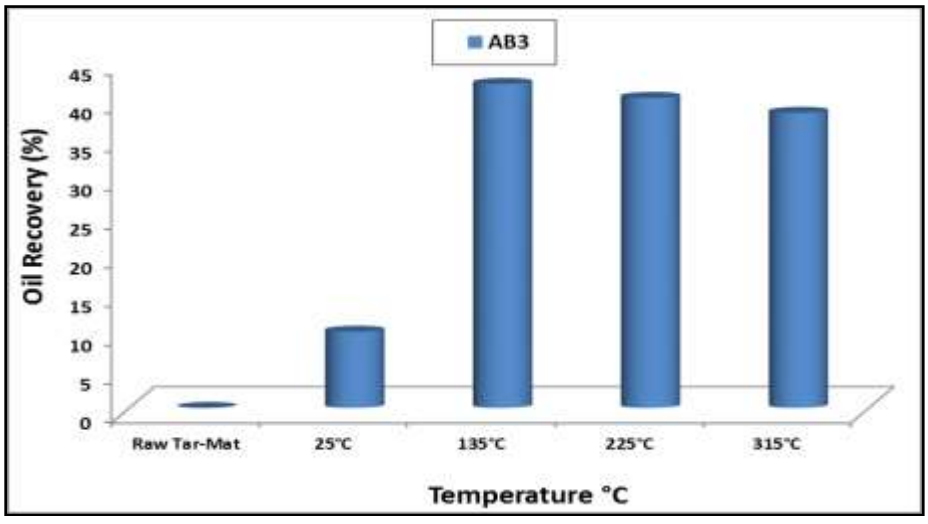

Figure 5.6. Effect of Temperature on Oil Recovery from Sample AB3 (Extracted by Toluene)

Table 5.17. Sample AB3 Recovery Schemes for Toluene at Different Temperatures

Sample	Temperature Setting (℃)	Type I (C1-C15) mg/g	Type I (C1-C15) %	Type II (C15-C40) mg/g	Type II (C15-C40) %	Type III (>C40) mg/g	Type III (>C40) %	Type IV (NSO) mg/g	Type IV (NSO) %	Total Oil mg/g	Total Oil %	Residual Recovery (%)	Extractable Recovery (%)	Remaining Recovery (%)	Maximum Recovery (%)
AB3	Raw Tar-Mat	7.12	5.26	14.55	10.76	37.47	27.70	76.14	56.28	135.28	100	58.62	25.77	32.85	0
	25°C	3.57	4.01	7.60	8.54	22.54	25.32	55.32	62.14	89.03	100	48.78	19.39	29.39	9.84
	135°C	0.14	0.33	0.51	1.20	5.85	13.74	36.07	84.73	42.57	100	16.82	1.99	14.83	41.80
	225°C	0.26	0.54	0.97	2.03	6.80	14.22	39.80	83.21	47.83	100	18.63	3.37	15.26	39.99
	315°C	0.12	0.41	0.39	1.34	4.65	15.96	23.98	82.29	29.14	100	20.55	2.33	18.22	38.07

5.4.1.4 Effect of toluene and temperature on oil recovery from sample AB4.

Figure 5.7 and Table 5.18 provides data showing the effect of toluene and the temperature on the recovery of oil from sample AB4. The residual recovery of AB4 when using toluene was 62.27%, as indicated in Table 5.18. Through extractable recovery, light oil was produced by applying an enhancement agent. The original recovery of sample AB4 was measured to be 25.76%. After the addition of toluene as a solvent, 36.51% of heavy oil was recovered, showing significant positive prospects for EOR investments.

Figure 5.7 illustrates that the higher the temperature of toluene, the more light oil (extractable) was produced, and the less heavy oil remained in the tar-mat mix. The results in Table 5.18 indicate that in the tar-mat's natural state, 62.27% of the original residual oil was available for recovery, but after increasing the temperature to 225 ˚C, only 15.04% of the oil remained, indicating that 47.23% of the total oil was produced successfully.

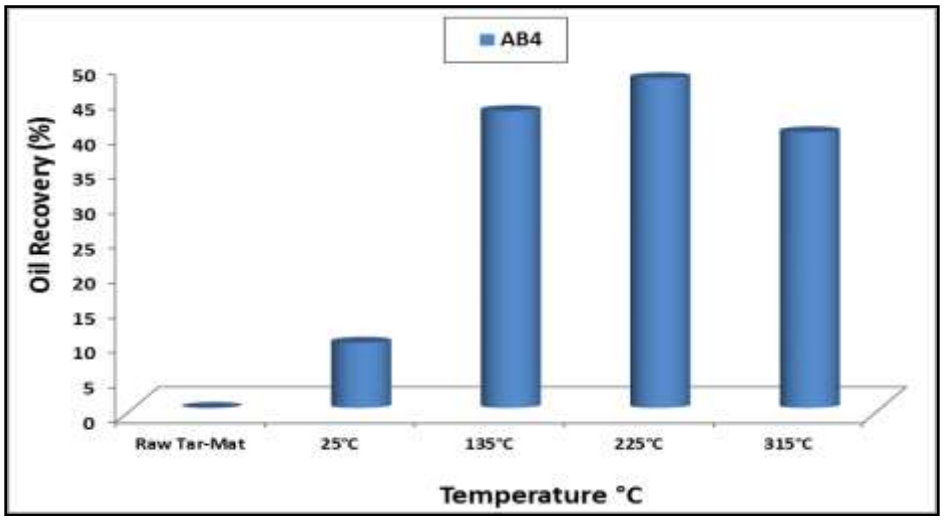

Figure 5.7. Effect of Temperature on Oil Recovery from Sample AB4 (Extracted by Toluene

Table 5.18. Sample AB4 Recovery Schemes for Toluene at Different Temperatures

Sample	Temperature Setting (℃)	Type I (C1-C15) mg/g	Type I (C1-C15) %	Type II (C15-C40) mg/g	Type II (C15-C40) %	Type III (>C40) mg/g	Type III (>C40) %	Type IV (NSO) mg/g	Type IV (NSO) %	Total Oil mg/g	Total Oil %	Residual Recovery (%)	Extractable Recovery (%)	Remaining Recovery (%)	Maximum Recovery (%)
AB4	Raw Tar-Mat	5.57	4.11	15.53	11.46	40.04	29.55	74.37	54.88	135.51	100	62.27	25.76	36.51	0
	25°C	3.10	3.99	7.86	10.10	20.47	26.31	46.36	59.60	77.79	100	52.93	22.14	30.79	9.34
	135°C	0.17	0.89	0.47	2.47	2.65	13.91	15.76	82.73	19.05	100	19.73	4.35	15.37	42.54
	225°C	0.16	0.51	0.55	1.77	3.59	11.54	26.81	86.18	31.11	100	15.04	2.89	12.15	47.23
	315°C	0.12	0.90	0.29	2.16	2.16	16.12	10.83	80.82	13.40	100	22.77	4.06	18.71	39.50

5.4.1.5 Effect of toluene and temperature on oil recovery from sample AB5. Toluene and the temperature also had an effect on the oil recovery from sample AB5 (Figure 5.8). Table 5.19 represents the toluene recovery scheme, indicating residual recovery of approximately 15.88%; this oil was categorized as heavy or light. In AB5, light oil accounted for 2.82%, and the heavy oil required the use of toluene as an enhancement agent. Residual recovery yielded 13.06% of the heavy oil, which represents a good prospect for EOR investments.

Figure 5.8 illustrates that the higher the temperature of the toluene, the more light oil (extractable) was produced, and the less heavy oil remained in the tar-mat mix. The results in Table 5.19 indicate that in the tar-mat's natural state, 15.88% of the original residual oil was available for recovery, but after increasing the temperature to 225 ˚C, only 4.61% of the oil remained, indicating that 11.27% of the total oil was produced successfully.

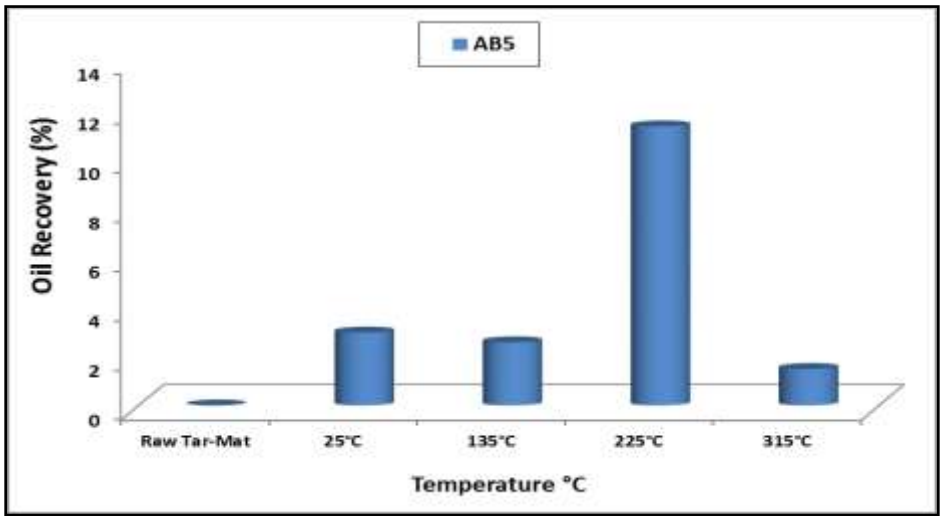

Figure 5.8. Effect of Temperature on Oil Recovery from Sample AB5 (Extracted by Toluene

Table 5.19. Sample AB5 Recovery Schemes for Toluene at Different Temperatures

Sample	Temperature Setting (℃)	Type I (C1-C15) mg/g	Type I (C1-C15) %	Type II (C15-C40) mg/g	Type II (C15-C40) %	Type III (>C40) mg/g	Type III (>C40) %	Type IV (NSO) mg/g	Type IV (NSO) %	Total Oil mg/g	Total Oil %	Residual Recovery (%)	Extractable Recovery (%)	Remaining Recovery (%)	Maximum Recovery (%)
AB5	Raw Tar-Mat	3.11	0.56	9.17	1.65	68.31	12.28	475.53	85.51	556	100	15.88	2.82	13.06	0
	25°C	4.22	0.63	8.09	1.22	68.22	10.25	584.89	87.90	665	100	12.94	2.30	10.63	2.94
	135°C	12.52	1.95	5.45	0.85	62.43	9.71	562.32	87.49	643	100	13.33	3.46	9.87	2.55
	225°C	7.73	0.49	4.37	0.28	60.68	3.84	1509.12	95.40	1582	100	4.61	0.89	3.72	11.27
	315°C	13.31	2.75	4.07	0.84	59.07	12.20	407.74	84.21	484	100	17.36	4.58	12.78	1.47

5.4.2. Hot Water. Hot water was applied at different temperatures to recover the oil from the tar-mat samples in this study.

5.4.2.1 Effect of hot water and temperature on oil recovery from sample AB1. Figure 5.9 shows the effect of hot water and temperature on the recovery of oil from sample AB1. As listed in Table 5.20, using the hot water recovery scheme, the residual recovery of AB1 was 14.77%, the extractable recovery was 1.55%, and the remaining recovery was 13.22%.

Figure 5.9 illustrates that water recovery worked best at around 135˚C, at which temperature water exists in its steam state, indicating that only steam was able to improve mobility in this type of treatment. With little improvement, water recovery produced less light oil (2.73%), but more heavy oil (13.93%) remained in the tar-mat mix than when using toluene recovery. The results in Table 5.20 indicate that in the tar-mat's natural state, 16.67% of the original residual oil was available for recovery, but after the treatment was applied at 135 ˚C, 13.93% of the oil remained, indicating that 2.73% of the total oil was produced successfully.

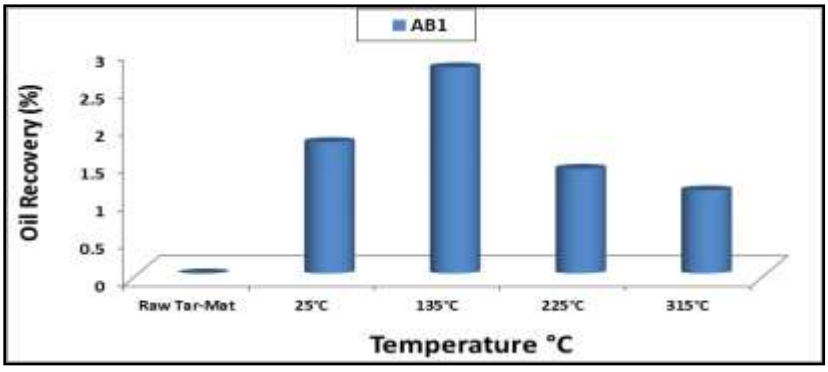

Figure 5.9. Effect of Temperature on Oil Recovery from Sample AB1 (Extracted by Hot Water)

Table 5.20. Sample AB1 Recovery Schemes for Water at Different Temperatures

Sample	Temperature Setting (℃)	Type I (C1-C15) mg/g	Type I (C1-C15) %	Type II (C15-C40) mg/g	Type II (C15-C40) %	Type III (>C40) mg/g	Type III (>C40) %	Type IV (NSO) mg/g	Type IV (NSO) %	Total Oil mg/g	Total Oil %	Residual Recovery (%)	Extractable Recovery (%)	Remaining Recovery (%)	Best Oil Recovery (%)
AB1	Raw Tar-Mat	0.77	0.18	4.44	1.04	51.86	12.17	369.19	86.61	426	100	14.77	1.55	13.22	0
	25°C	0.77	0.19	4.86	1.17	53.68	12.94	355.57	85.70	415	100	15.88	1.74	14.14	1.74
	135°C	2.38	0.45	8.99	1.68	69.11	12.93	454.11	84.95	535	100	16.67	2.73	13.93	2.73
	225°C	0.43	0.10	4.03	0.97	54.37	13.15	354.59	85.77	413	100	15.88	1.39	14.49	1.39
	315°C	0.53	0.10	4.11	0.78	56.75	10.78	465.08	88.34	526	100	12.65	1.10	11.54	1.10

5.4.2.2 Effect of hot water and temperature on oil recovery from sample AB2. Figure 5.10 shows the effect of hot water and temperature on the recovery of oil from sample AB2. According to Table 5.21, the residual recovery of AB2 was 57.01%, the extractable recovery was 28.97%, and the remaining recovery was 28.04%. Increasing the temperature produced few changes in the recovery trend.

Figure 5.10 illustrates that recovery using water was maximized at 225˚C, due in part to the fact that at this temperature, water exists in the form of steam. Changes in the temperature resulted in variations in the oil recovery trend, with more heavy oil than light oil being recovered. Water recovery produced less light oil (30.32%), but more heavy oil (35.84%) remained in the tar-mat mix than when using toluene recovery. According to the results in Table 5.21, 66.16% of the original residual oil was available for recovery, but after increasing the temperature to 225˚C, 30.32% of the oil remained, indicating that 26.99% of the total oil was produced successfully.

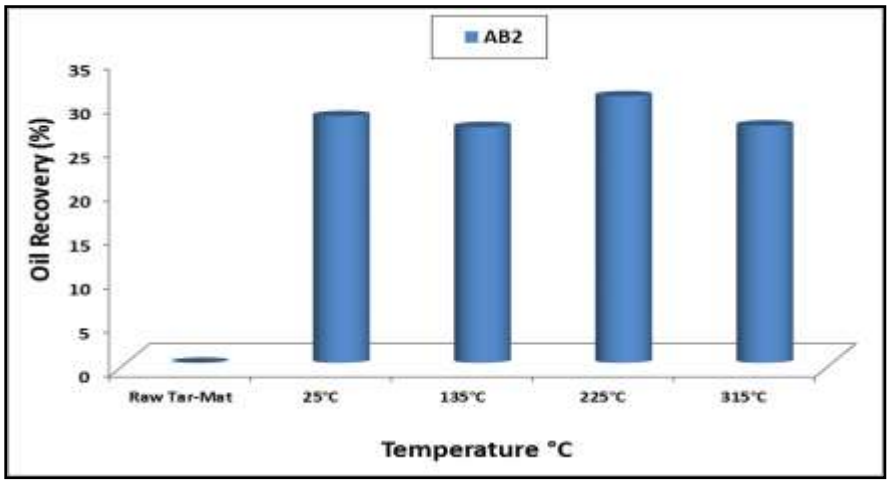

Figure 5.10. Effect of Temperature on Oil Recovery from Sample AB2 (Extracted by Hot Water)

Table 5.21. Sample AB2 Recovery Schemes for Water at Different Temperatures

Sample	Temperature Setting (°C)	Type I (C1-C15) mg/g	Type I (C1-C15) %	Type II (C15-C40) mg/g	Type II (C15-C40) %	Type III (>C40) mg/g	Type III (>C40) %	Type IV (NSO) mg/g	Type IV (NSO) %	Total Oil mg/g	Total Oil %	Residual Recovery (%)	Extractable Recovery (%)	Remaining Recovery (%)	Best Oil Recovery (%)
AB2	Raw Tar-Mat	5.46	4.55	16.85	14.05	30.43	25.37	67.21	56.03	120	100	57.01	28.97	28.04	0
	25°C	5.56	4.66	15.15	12.71	33.15	27.80	65.37	54.83	119	100	60.70	28.06	32.64	28.06
	135°C	5.66	4.32	15.26	11.64	39.84	30.40	70.28	53.63	131	100	64.87	26.82	38.05	26.82
	225°C	5.81	4.82	16.14	13.40	35.64	29.59	62.86	52.19	120	100	66.16	30.32	35.84	30.32
	315°C	5.76	4.41	16.02	12.28	36.52	27.99	72.19	55.32	130	100	60.22	26.99	33.23	26.99

5.4.2.3 Effect of hot water and temperature on oil recovery from sample AB3. Figure 5.11 shows the effect of hot water and temperature on the recovery of oil from sample AB3. According to Table 5.22, the recovery scheme using water in AB3 resulted in 58.62%, 25.77%, and 32.85% residual recovery, extractable recovery, and remaining recovery, respectively.

Figure 5.11 indicates that water recovery worked best at around 135˚C. With little improvement, water recovery produced less light oil (26.20%), but more heavy oil (34.97%) remained in the tar-mat mix. The results in Table 5.22 indicate that 61.17% of the original residual oil was available for recovery, but after the treatment was applied at 135 ˚C, 34.97% of the oil remained, indicating that 26.20% of the total oil was produced successfully.

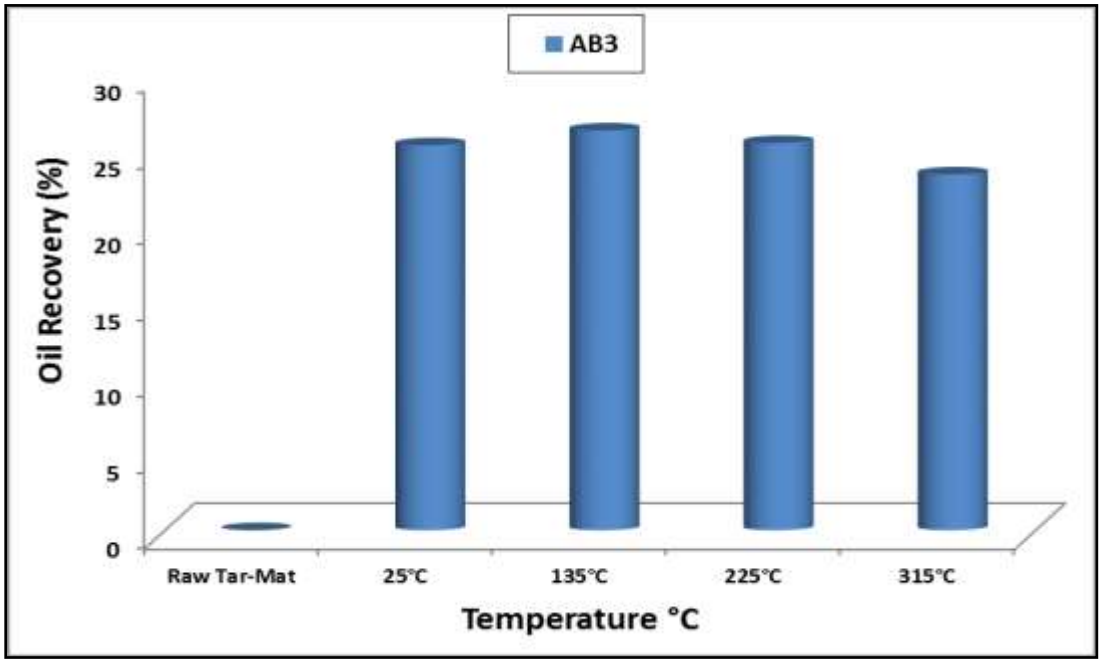

Figure 5.11. Effect of Temperature on Oil Recovery from Sample AB3 (Extracted by Hot Water

Table 5.22. Sample AB3 Recovery Schemes for Water at Different Temperatures

Sample	Temperature Setting (°C)	Type I (C1-C15) mg/g	Type I (C1-C15) %	Type II (C15-C40) mg/g	Type II (C15-C40) %	Type III (>C40) mg/g	Type III (>C40) %	Type IV (NSO) mg/g	Type IV (NSO) %	Total Oil mg/g	Total Oil %	Residual Recovery (%)	Extractable Recovery (%)	Remaining Recovery (%)	Best Oil Recovery (%)
AB3	Raw Tar-Mat	7.12	5.26	14.55	10.76	37.47	27.70	76.14	56.28	135	100	58.62	25.77	32.85	0
	25°C	6.80	5.03	14.45	10.69	37.23	27.55	76.67	56.73	135	100	57.84	25.24	32.60	25.24
	135°C	6.65	4.96	14.81	11.04	38.68	28.83	74.01	55.17	134	100	61.17	26.20	34.97	26.20
	225°C	5.97	4.57	14.36	10.98	37.44	28.63	73.00	55.82	131	100	60.05	25.38	34.67	25.38
	315°C	6.29	4.18	15.68	10.42	41.11	27.33	87.33	58.06	150	100	55.84	23.32	32.52	23.32

5.4.2.4 Effect of hot water and temperature on oil recovery from sample AB4. Figure 5.12 shows the effect of hot water and temperature on the recovery of oil from sampleAB4. Table 5.23 summarizes the results of the residual, extractable, and remaining recovery obtained from sample AB4. Increasing the temperature led to various changes that influenced the proportion of the different components.

Figure 5.12 illustrates that recovery was maximized at 135˚C. Water recovery produced less light oil (31.39%), but more heavy oil (35.61%) remained in the tar-mat mix than when using toluene recovery. According to Table 5.23, 67% of the residual oil was available for recovery, but after the treatment was applied at 135 ˚C, 35.61% of the oil remained, indicating that 31.39% of the total oil was produced successfully.

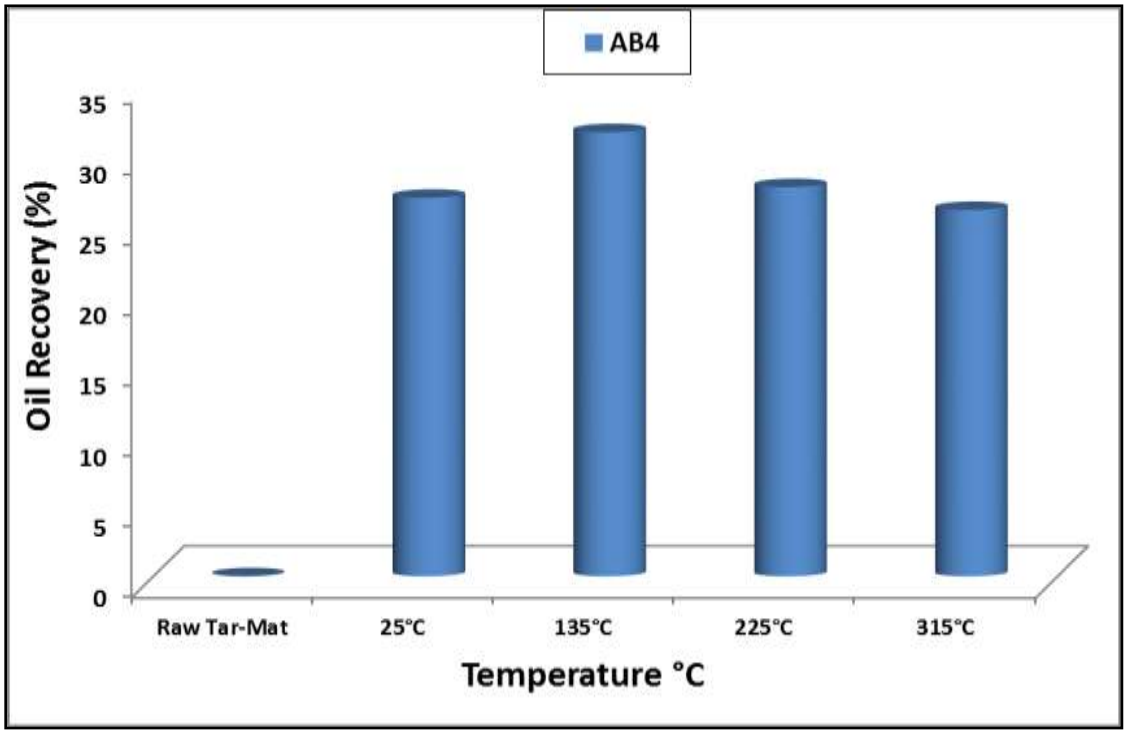

Figure 5.12. Effect of Temperature on Oil Recovery from Sample AB4 (Extracted by Hot Water)

Table 5.23. Sample AB4 Recovery Schemes for Water at Different Temperatures

Sample	Temperature Setting (°C)	Type I (C1-C15) mg/g	Type I (C1-C15) %	Type II (C15-C40) mg/g	Type II (C15-C40) %	Type III (>C40) mg/g	Type III (>C40) %	Type IV (NSO) mg/g	Type IV (NSO) %	Total Oil mg/g	Total Oil %	Residual Recovery (%)	Extractable Recovery (%)	Remaining Recovery (%)	Best Oil Recovery (%)
AB4	Raw Tar-Mat	5.57	4.11	15.53	11.46	40.04	29.55	74.37	54.88	136	100	62.27	25.76	36.51	0
	25°C	5.78	4.52	14.98	11.70	37.45	29.26	69.78	54.52	128	100	62.50	26.75	35.75	26.75
	135°C	6.22	5.30	15.94	13.57	34.70	29.54	60.59	51.59	117	100	67.00	31.39	35.61	31.39
	225°C	5.34	4.19	15.29	12.00	39.61	31.09	67.17	52.72	127	100	66.93	27.51	39.43	27.51
	315°C	5.74	4.10	16.01	11.43	41.88	29.90	76.44	54.57	140	100	62.98	25.89	37.08	25.89

5.4.2.5 Effect of hot water and temperature on oil recovery from sample AB5. Figure 5.13 shows the effect of hot water and temperature on the recovery of oil from sample AB5. As listed in Table 5.24, the residual recovery of AB5 was 15.88%, the extractable recovery was 2.82%, and the remaining recovery was 13.06%. Increasing the temperature produced slight changes in the recovery trend.

Figure 5.13 shows that water recovery worked best at 225˚C due to the increased mobility caused by the steam. With little improvement, water recovery produced less light oil (2.72%), but more heavy oil (14.32%) remained in the tar-mat mix. According to the results in Table 5.24, in the tar-mat's natural state, 17.03% of the original residual oil was available for recovery, but after the treatment was applied at 225 ˚C, 14.32% of the oil remained, indicating that 2.72% of the total oil was produced successfully.

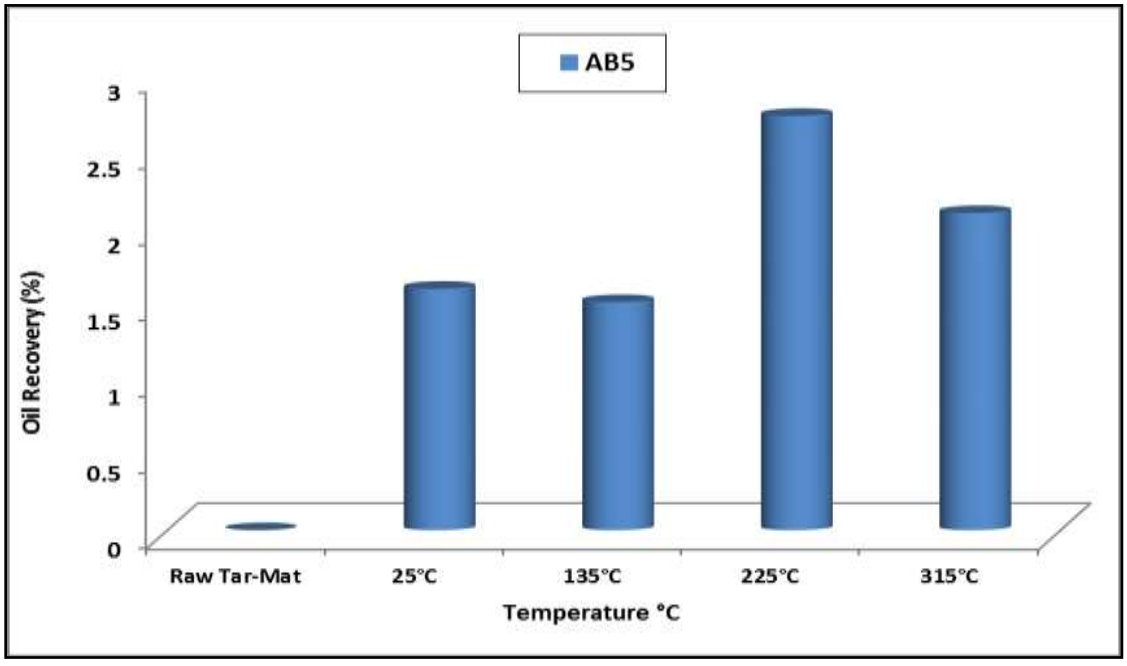

Figure 5.13. Effect of Temperature on Oil Recovery from Sample AB5 (Extracted by Hot Water)

Table 5.24. Sample AB5 Recovery Schemes for Water at Different Temperatures

Sample	Temperature Setting (°C)	Type I (C1-C15) mg/g	Type I (C1-C15) %	Type II (C15-C40) mg/g	Type II (C15-C40) %	Type III (>C40) mg/g	Type III (>C40) %	Type IV (NSO) mg/g	Type IV (NSO) %	Total Oil mg/g	Total Oil %	Residual Recovery (%)	Extractable Recovery (%)	Remaining Recovery (%)	Best Oil Recovery (%)
AB5	Raw Tar-Mat	3.11	0.56	9.17	1.65	68.31	12.28	475.53	85.51	556	100	15.88	2.82	13.06	0
	25°C	2.96	0.57	9.35	1.79	69.56	13.30	441.23	84.35	523	100	15.93	3.04	14.35	1.58
	135°C	0.52	0.13	4.28	1.04	54.03	13.09	354.03	85.75	413	100	15.86	1.50	14.37	1.50
	225°C	2.32	0.43	8.94	1.67	70.74	13.23	452.85	84.67	535	100	17.03	2.72	14.32	2.72
	315°C	2.26	0.33	9.09	1.34	70.84	10.41	598.62	87.93	681	100	12.97	2.08	10.89	2.08

5.4.3. Surfactant Solution. Surfactant was applied at various temperatures to recover the oil from the tar-mat samples in this study.

5.4.3.1 Effect of surfactant and temperature on oil recovery from sample AB1. Figure 5.14 shows the effect of surfactant and temperature on the recovery of oil from sample AB1. Table 5.25 indicates that the residual recovery of AB1 was 14.77%, the extractable recovery was 1.55%, and the remaining recovery was 13.22%.

As Figure 5.14 illustrates, surfactant solution recovery worked best when the temperature reached approximately 225˚C, which is beyond steam conditions; this result indicates that saturated surfactant-steam can improve the mobility of oil in this treatment method. With intermediate improvement, surfactant recovery produced less light oil (4.91%), and more heavy oil (19.54%) remained in the tar-mat mix. At 225 ˚C, 24.45% of the original residual oil was available for recovery, which decreased to 19.54% after the recovery method was applied, indicating that 4.91% of the total oil was produced successfully.

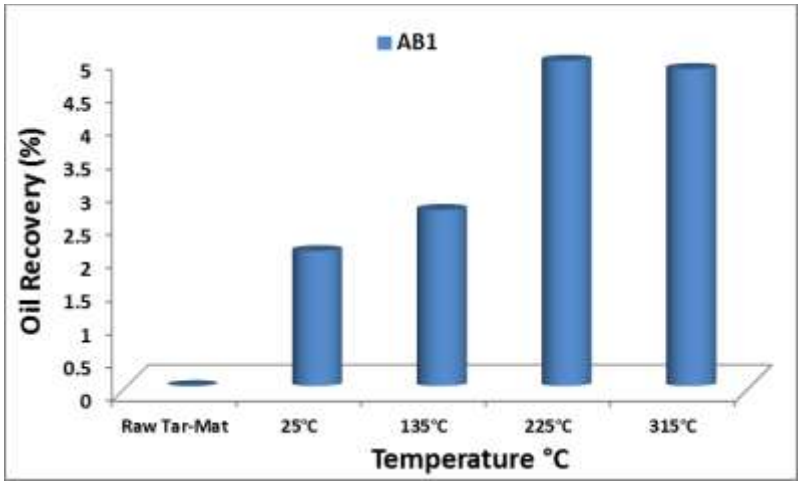

Figure 5.14. Effect of Temperature on Oil Recovery from Sample AB1 (Extracted by Surfactant)

Table 5.25. Sample AB1 Recovery Schemes for Surfactant at Different Temperatures

Sample	Temperature Setting (°C)	Type I (C1-C15) mg/g	Type I (C1-C15) %	Type II (C15-C40) mg/g	Type II (C15-C40) %	Type III (>C40) mg/g	Type III (>C40) %	Type IV (NSO) mg/g	Type IV (NSO) %	Total Oil mg/g	Total Oil %	Residual Recovery (%)	Extractable Recovery (%)	Remaining Recovery (%)	Best Oil Recovery (%)
AB1	Raw Tar-Mat	0.77	0.18	4.44	1.04	51.86	12.17	369.19	86.61	426	100	14.77	1.55	13.22	0
	25°C	1.24	0.24	7.20	1.38	59.24	11.33	455.02	87.05	523	100	14.04	2.04	12.01	2.04
	135°C	0.80	0.20	7.48	1.83	59.51	14.56	340.84	83.41	409	100	18.74	2.66	16.08	2.66
	225°C	2.84	0.63	13.52	2.98	78.85	17.37	358.74	79.03	454	100	24.45	4.91	19.54	4.91
	315°C	1.26	0.38	10.19	3.07	61.87	18.67	258.09	77.88	331	100	26.23	4.78	21.45	4.78

5.4.3.2 Effect of surfactant and temperature on oil recovery from sample AB2. Figure 5.15 shows the effect of surfactant and temperature on the recovery of oil from sample AB2. The results of oil recovery from sample AB2 are summarized in Table 5.26. As the temperature increased, the residual, extractable, and remaining recoveries increased, showing a clear recovery trend.

Figure 5.15 illustrates that this recovery method worked best when the temperature reached approximately 135˚C. Surfactant recovery produced less light oil (30.92%), and more heavy oil (37.70%) remained in the tar-mat mix. At 225˚C, 68.62% of the original residual oil was available for recovery, which decreased to 37.70% after the recovery method was applied, indicating that 30.92% of the total oil was produced successfully.

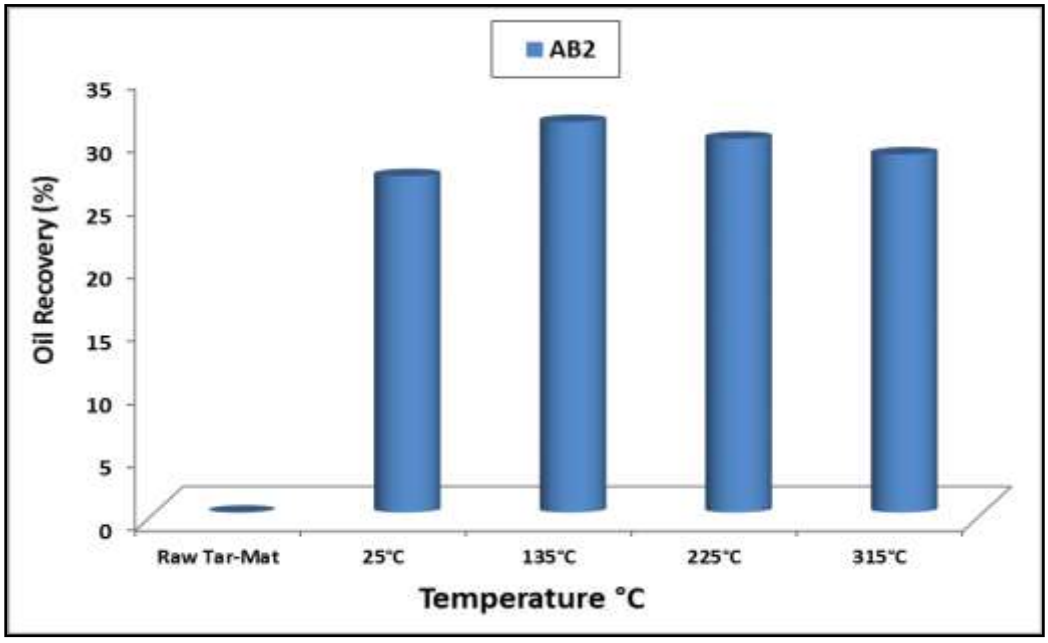

Figure 5.15. Effect of Temperature on Oil Recovery from Sample AB2 (Extracted by Surfactant)

Table 5.26. Sample AB2 Recovery Schemes for Surfactant at Different Temperatures

Sample	Temperature Setting (°C)	Type I (C1-C15) mg/g	Type I (C1-C15) %	Type II (C15-C40) mg/g	Type II (C15-C40) %	Type III (>C40) mg/g	Type III (>C40) %	Type IV (NSO) mg/g	Type IV (NSO) %	Total Oil mg/g	Total Oil %	Residual Recovery (%)	Extractable Recovery (%)	Remaining Recovery (%)	Best Oil Recovery (%)
AB2	Raw Tar-Mat	5.46	4.55	16.85	14.05	30.43	25.37	67.21	56.03	120	100	57.01	28.97	28.04	0
	25°C	5.99	4.61	15.77	12.13	35.01	26.93	73.23	56.33	130	100	57.89	26.63	31.26	26.63
	135°C	5.59	4.97	15.00	13.34	34.31	30.52	57.53	51.17	112	100	68.62	30.92	37.70	30.92
	225°C	4.83	4.46	13.72	12.66	34.73	32.06	55.06	50.82	108	100	70.81	29.59	41.23	29.59
	315°C	4.59	4.19	13.47	12.31	34.85	31.85	56.52	51.65	109	100	69.39	28.35	41.04	28.35

5.4.3.3 Effect of surfactant and temperature on oil recovery from sample AB3. Figure 5.16 shows the effect of surfactant and temperature on the recovery of oil from sample AB3. In the surfactant solution recovery scheme shown in Table 5.27, the residual recovery of AB3 was 58.62%, the extractable recovery was 25.77%, and the remaining recovery was 32.85%. Recovery increased after the temperature was increased.

As illustrated in Figure 5.16, the surfactant solution recovery worked best at 225˚C, which is beyond steam conditions; this result indicates that saturated surfactant-steam can improve the mobility of the oil in this treatment method. Surfactant recovery produced less light oil (27.7%), and more heavy oil (39.82%) remained in the tar-mat mix. At 225˚C, 67.52% of the original residual oil was available for recovery, which decreased to 39.82% after the recovery method was applied, indicating that 27.7% of the total oil was produced successfully.

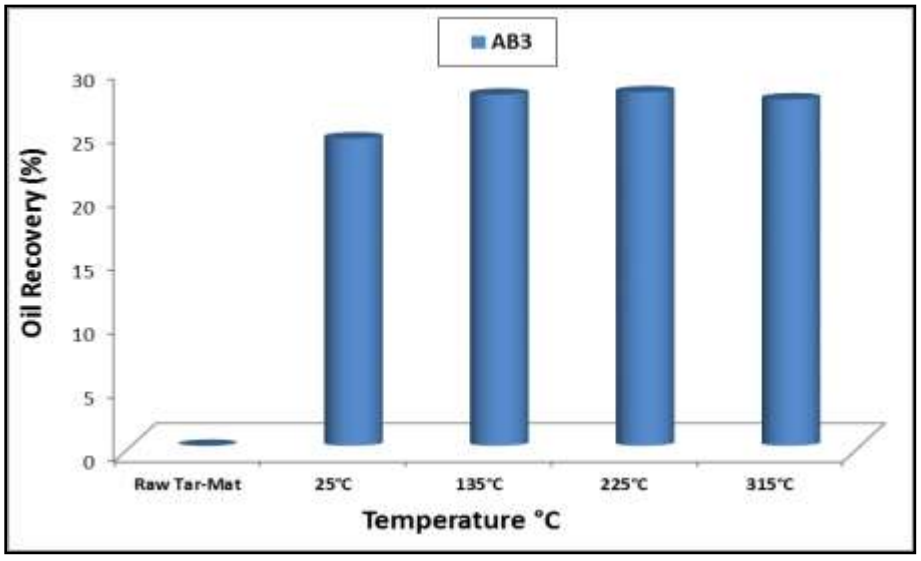

Figure 5.16. Effect of Temperature on Oil Recovery from Sample AB3 (Extracted by Surfactant)

Table 5.27. Sample AB3 Recovery Schemes for Surfactant at Different Temperatures

Sample	Temperature Setting (°C)	Type I (C1-C15) mg/g	Type I (C1-C15) %	Type II (C15-C40) mg/g	Type II (C15-C40) %	Type III (>C40) mg/g	Type III (>C40) %	Type IV (NSO) mg/g	Type IV (NSO) %	Total Oil mg/g	Total Oil %	Residual Recovery (%)	Extractable Recovery (%)	Remaining Recovery (%)	Best Oil Recovery (%)
AB3	Raw Tar-Mat	7.12	5.26	14.55	10.76	37.47	27.70	76.14	56.28	135	100	58.62	25.77	32.85	0
	25°C	7.35	5.00	15.21	10.34	38.57	26.21	86.01	58.46	147	100	54.43	24.08	30.35	24.08
	135°C	5.42	4.23	15.13	11.80	40.73	31.76	66.95	52.21	128	100	68.41	27.51	40.90	27.51
	225°C	6.10	4.84	14.37	11.41	39.41	31.29	66.08	52.46	126	100	67.52	27.70	39.82	27.70
	315°C	5.31	4.41	13.50	11.21	39.22	32.56	62.44	51.83	120	100	69.84	27.14	42.70	27.14

5.4.3.4 Effect of surfactant and temperature on oil recovery from sample AB4. Figure 5.17 shows the effect of surfactant and temperature on the recovery of oil from sample AB4. The results of the residual, extractable, and remaining oil recovery from sample AB4 appear in Table 5.28. Interestingly, gradually increasing the temperature resulted in a gradual increase in the oil recovery from the sample.

Figure 5.17 indicates that the surfactant solution recovery method worked best when the temperature reached approximately 135˚C. Surfactant recovery produced less light oil (28.30%), and more heavy oil (41.45%) remained in the tar-mat mix. At 135 ˚C, 69.74% of the original residual oil was available for recovery, which decreased to 41.45% after the recovery method was applied, indicating that 28.30% of the total oil was produced successfully.

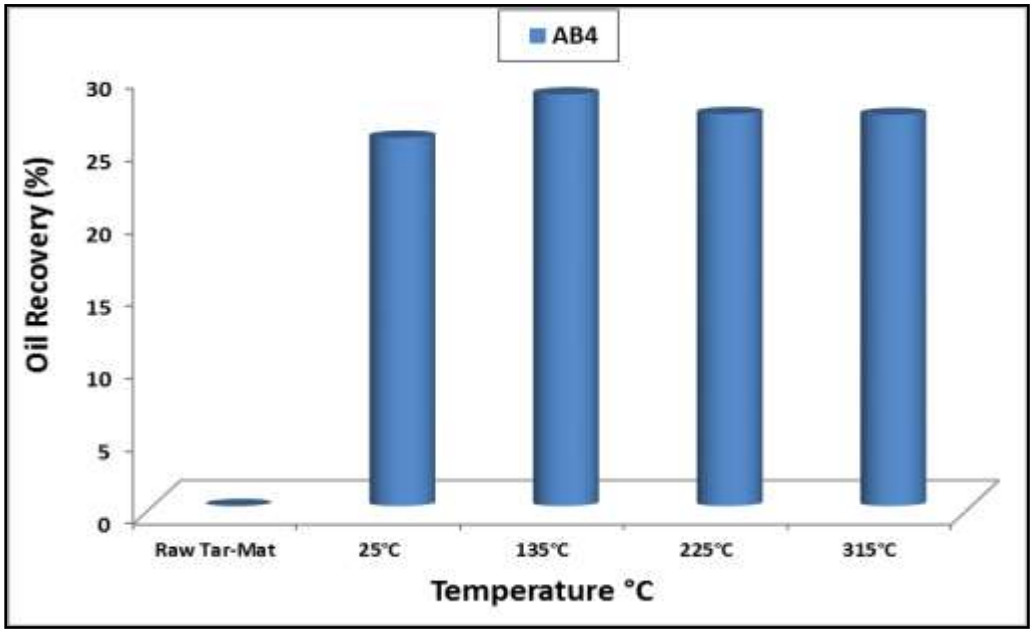

Figure 5.17. Effect of Temperature on Oil Recovery from Sample AB4 (Extracted by Surfactant)

Table 5.28. Sample AB4 Recovery Schemes for Surfactant at Different Temperatures

Sample	Temperature Setting (°C)	Type I (C1-C15) mg/g	Type I (C1-C15) %	Type II (C15-C40) mg/g	Type II (C15-C40) %	Type III (>C40) mg/g	Type III (>C40) %	Type IV (NSO) mg/g	Type IV (NSO) %	Total Oil mg/g	Total Oil %	Residual Recovery (%)	Extractable Recovery (%)	Remaining Recovery (%)	Best Oil Recovery (%)
AB4	Raw Tar-Mat	5.57	4.11	15.53	11.46	40.04	29.55	74.37	54.88	136	100	62.27	25.76	36.51	0
	25°C	6.30	4.42	15.98	11.22	40.00	28.09	80.11	56.26	142	100	58.98	25.32	33.66	25.32
	135°C	5.18	4.26	14.74	12.13	38.99	32.07	62.66	51.54	122	100	69.74	28.30	41.45	28.30
	225°C	4.61	3.80	14.28	11.76	39.14	32.24	63.36	52.20	121	100	68.90	26.95	41.95	26.95
	315°C	4.41	3.74	13.82	11.71	38.47	32.59	61.36	51.97	118	100	69.62	26.89	42.73	26.89

5.4.3.5 Effect of surfactant and temperature on oil recovery from sample AB5. Figure 5.18 shows the effect of surfactant and temperature on the recovery of oil from sample AB5. Table 5.29 summarizes the results of the residual, extractable, and remaining recovery obtained from sample AB5. These results make it quite evident that increasing the temperature resulted in increased oil recovery.

As illustrated in Figure 5.18, surfactant solution worked best at 315˚C, most likely due to an improvement in oil mobility. With intermediate improvement, surfactant recovery produced less light oil (5.41%), and more heavy oil (22.13%) remained in the tar-mat mix. At 315˚C, 27.54% of the original residual oil was available for recovery, which decreased to 22.13% after the recovery method was applied, indicating that 5.41% of the total oil was produced successfully.

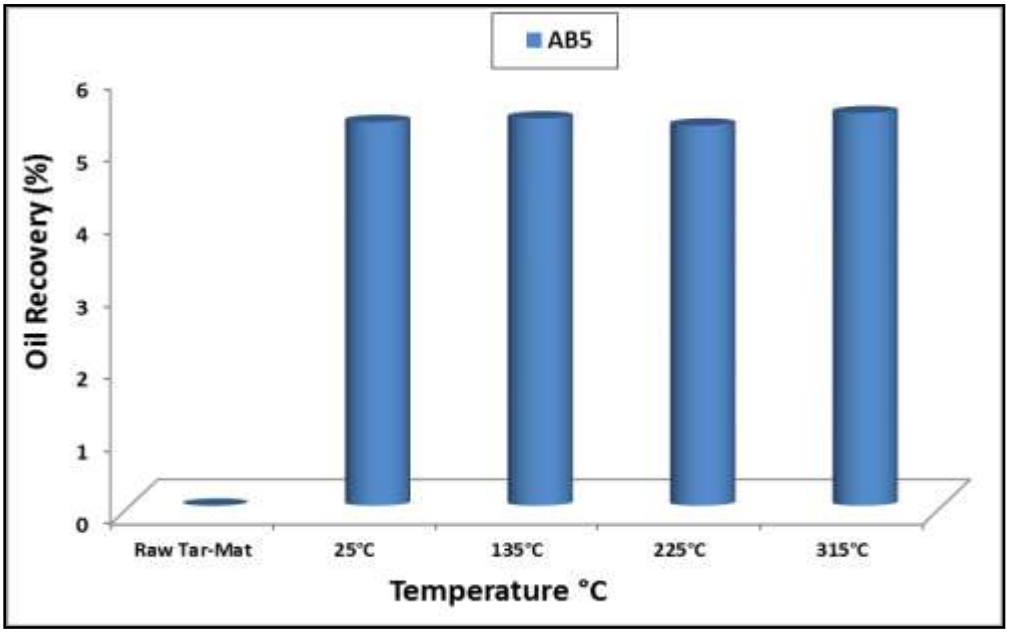

Figure 5.18. Effect of Temperature on Oil Recovery from Sample AB5 (Extracted by Surfactant)

Table 5.29. Sample AB5 Recovery Schemes for Surfactant at Different Temperatures

Sample	Temperature Setting (°C)	Type I (C1-C15) mg/g	Type I (C1-C15) %	Type II (C15-C40) mg/g	Type II (C15-C40) %	Type III (>C40) mg/g	Type III (>C40) %	Type IV (NSO) mg/g	Type IV (NSO) %	Total Oil mg/g	Total Oil %	Residual Recovery (%)	Extractable Recovery (%)	Remaining Recovery (%)	Best Oil Recovery (%)
AB5	Raw Tar-Mat	3.11	0.56	9.17	1.65	68.31	12.28	475.53	85.51	556	100	15.88	2.82	13.06	0
	25°C	3.71	0.90	12.17	2.95	74.47	18.03	322.58	78.12	413	100	25.72	5.28	20.43	5.28
	135°C	2.89	0.69	13.37	3.17	78.43	18.59	327.21	77.56	422	100	26.57	5.33	21.23	5.33
	225°C	2.71	0.62	13.92	3.17	81.58	18.56	341.25	77.65	439	100	26.44	5.23	21.21	5.23
	315°C	2.65	0.62	13.98	3.26	82.39	19.20	330.06	76.92	429	100	27.54	5.41	22.13	5.41

5.5. SUMMARY OF OIL RECOVERY FROM TAR-MAT SAMPLES BASED ON GEOCHEMISTY PYROLYSIS ANALYSIS

The maximum and best oil recoveries from the five tar-mat samples obtained by pyrolysis analysis are summarized in Table 5.30 through Table 5.32. The results indicate that toluene yielded the best oil recovery. The toluene recovered more oil as the temperature increased. Toluene yielded the highest recovery from samples AB2, AB3, and AB4, which had °API gravity greater than 3 °API. Samples AB1 and AB5, which had °API gravity lest then 2 °API, experienced the lowest oil recovery.

Surfactant yielded the second best oil recovery at 135 °C and 225 °C. Using surfactant solution at various temperatures to extract oil reduced the tar-mat and oil viscosity, which decreased the interfacial tension and thus the effect of the capillary forces; this, in turn, decreased the residual oil saturation. The recovery from samples AB2, AB3, and AB4 yielded the highest oil recovery at 135, 225, and 315°C, while recovery from samples AB1 and AB5 increased slightly at 135, 225, and 315°C.

Lastly, hot water recovery produced the least oil quality improvement of all the techniques. The highest recovery was obtained from samples AB2 at 225 °C and AB4 at 135 °C. This clearly occurred as a result of the reduced tar-mat and oil viscosities with temperature. Also, increasing the temperature reduces the interfacial tension, which further reduces the effect of the capillary forces. The reduction of capillary forces reduces the residual oil saturation, which increases the oil recovery.

Table 5.30. Summary of Maximum Oil Recovery from Five Tar-Mat Samples after the Extraction by Toluene at Different Temperatures

Sample	Type I (C1-C15) mg/g	Type I (C1-C15) %	Type II (C15-C40) mg/g	Type II (C15-C40) %	Type III (>C40) mg/g	Type III (>C40) %	Type IV (NSO) mg/g	Type IV (NSO) %	Total Oil mg/g	Total Oil %	Residual Recovery (%)	Extractable Recovery (%)	Remaining Recovery (%)	Maximum Recovery (%)	Comments
AB1	0.77	0.18	4.44	1.04	51.86	12.17	369.19	86.61	426.26	100	14.77	1.55	13.22	11.2	Toluene + 315°C
AB2	5.46	4.55	16.85	14.05	30.43	25.37	67.21	56.03	119.95	100	57.01	28.97	28.04	53.6	Toluene + 315°C
AB3	7.12	5.26	14.55	10.76	37.47	27.70	76.14	56.28	135.28	100	58.62	25.77	32.85	41.8	Toluene +135°C
AB4	5.57	4.11	15.53	11.46	40.04	29.55	74.37	54.88	135.51	100	62.27	25.76	36.51	47.23	Toluene +225°C
AB5	3.11	0.56	9.17	1.65	68.31	12.28	475.53	85.51	556.12	100	15.88	2.82	13.06	11.27	Toluene +225°C

Table 5.31. Summary of Best Oil Recovery from Five Tar-Mat Samples after the Extraction by Hot Water at Different Temperatures

Sample	Type I (C1-C15) mg/g	Type I (C1-C15) %	Type II (C15-C40) mg/g	Type II (C15-C40) %	Type III (>C40) mg/g	Type III (>C40) %	Type IV (NSO) mg/g	Type IV (NSO) %	Total Oil mg/g	Total Oil %	Residual Recovery (%)	Extractable Recovery (%)	Remaining Recovery (%)	Best Oil Recovery (%)	Comments
AB1	0.77	0.18	4.44	1.04	51.86	12.17	369.19	86.61	426.26	100	16.67	2.73	13.93	2.37	Water + 135°C
AB2	5.46	4.55	16.85	14.05	30.43	25.37	67.21	56.03	119.95	100	66.16	30.32	35.84	30.32	Water + 225°C
AB3	7.12	5.26	14.55	10.76	37.47	27.70	76.14	56.28	135.28	100	61.17	26.20	34.97	26.20	Water +135°C
AB4	5.57	4.11	15.53	11.46	40.04	29.55	74.37	54.88	135.51	100	67.00	31.39	35.61	31.39	Water +135°C
AB5	3.11	0.56	9.17	1.65	68.31	12.28	475.53	85.51	556.12	100	17.39	3.04	14.35	2.72	Water +225°C

Table 5.32. Summary of Best Oil Recovery from Five Tar-Mat Samples after the Extraction by Surfactant at Different Temperatures

Sample	Type I (C1-C15) mg/g	Type I (C1-C15) %	Type II (C15-C40) mg/g	Type II (C15-C40) %	Type III (>C40) mg/g	Type III (>C40) %	Type IV (NSO) mg/g	Type IV (NSO) %	Total Oil mg/g	Total Oil %	Residual Recovery (%)	Extractable Recovery (%)	Remaining Recovery (%)	Best Oil Recovery (%)	Comments
AB1	0.77	0.18	4.44	1.04	51.86	12.17	369.19	86.61	426.26	100	14.77	1.55	13.22	4.91	Surfactant + 225°C
AB2	5.46	4.55	16.85	14.05	30.43	25.37	67.21	56.03	119.95	100	57.01	28.97	28.04	30.92	Surfactant + 135°C
AB3	7.12	5.26	14.55	10.76	37.47	27.70	76.14	56.28	135.28	100	58.62	25.77	32.85	27.7	Surfactant + 225°C
AB4	5.57	4.11	15.53	11.46	40.04	29.55	74.37	54.88	135.51	100	62.27	25.76	36.51	28.3	Surfactant + 135°C
AB5	3.11	0.56	9.17	1.65	68.31	12.28	475.53	85.51	556.12	100	15.88	2.82	13.06	5.41	Surfactant + 315°C

5.6. EFFECT OF NSO ON OIL RECOVERY

According to the results in Section 5.5 (Table 5.30 through Table 5.32) and Figure 5.19 through Figure 5.21, after the extraction by toluene, hot water, and surfactant, the amount of NSO had an inverse relationship with oil recovery; as the amount of NSO increased, the oil recovery decreased.

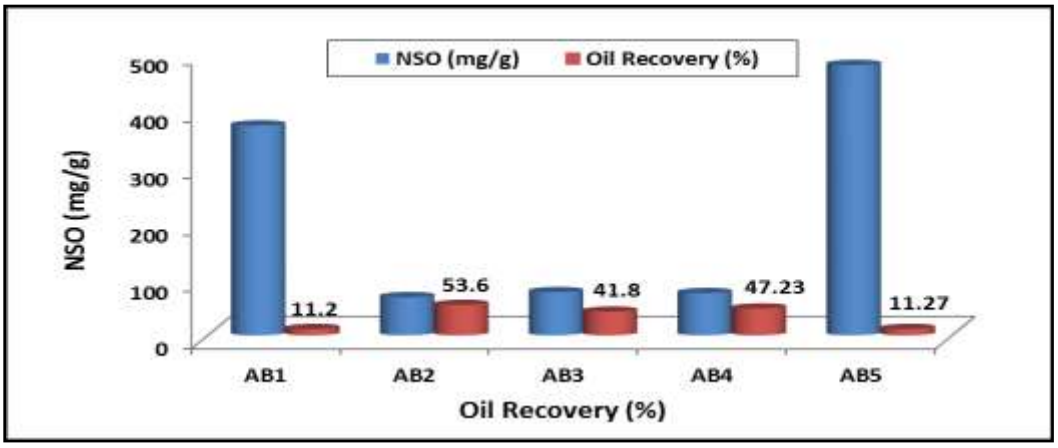

Figure 5.19. Effect of NSO on Oil Recovery after the Extraction by Toluene

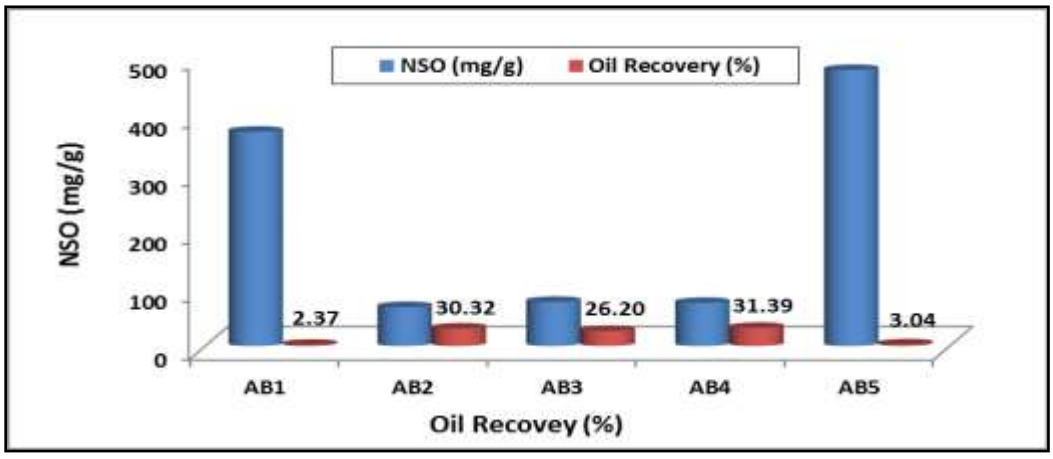

Figure 5.20. Effect of NSO on Oil Recovery after the Extraction by Hot Water

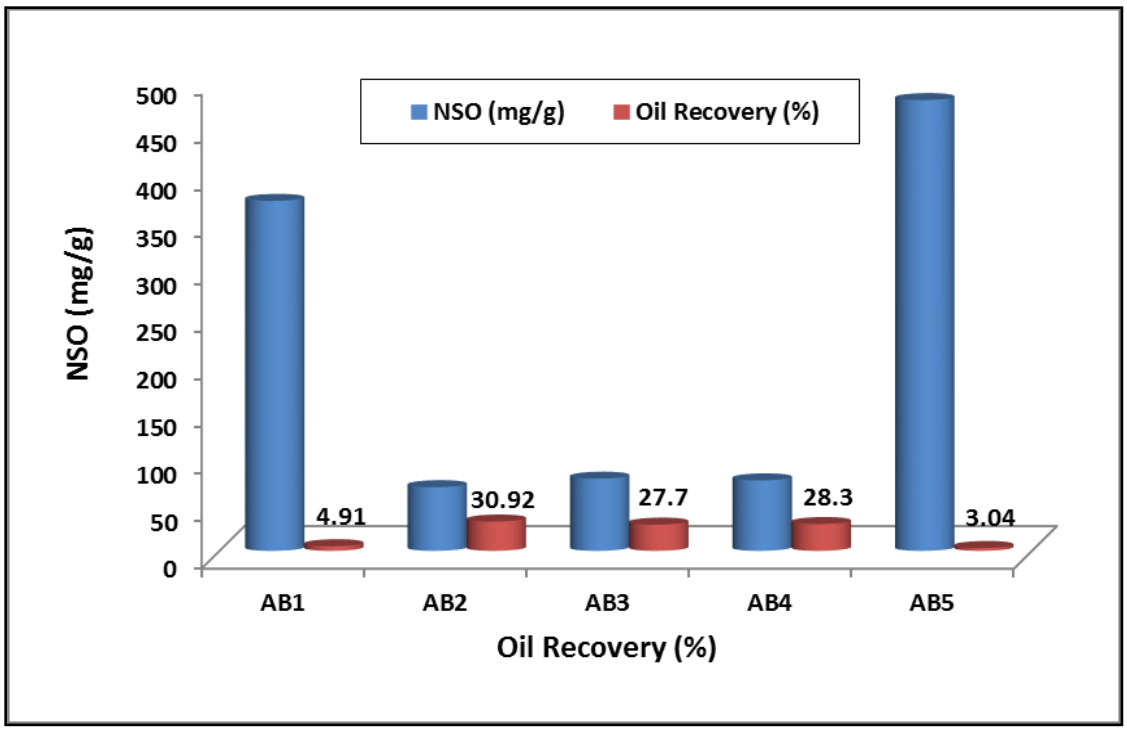

Figure 5.21. Effect of NSO on Oil Recovery after the Extraction by Surfactant

6. OIL RESERVES AND RECOVERY ECONOMICS

A simple economic analysis was conducted to evaluate the economic feasibility of extracting oil from tar-mat reservoir rocks using toluene, hot water, and surfactant solution.

6.1. SIMPLE ECONOMIC ANALYSIS FOR TAR-MAT ZONE AB1

Tar-mat zone AB1 hypothetically has the following characteristics: porosity of 0.349, water saturation of 0.2, a hypothetical field area of 1000 acres, a hypothetical tar-mat thickness of 74 feet, and a hypothetical formation volume factor of 0.992 reservoir barrels over stock tank barrels. The amount of tar-mat oil in place would be 161,579,119 barrels of immobile, solid-like, extremely heavy oil. If the oil price is assumed to be $100 per barrel, then Table 6.1 shows that the maximum profit would be achieved using toluene recovery at 315 ˚C because it recovers approximately 11.2% of the <5 ˚API extremely heavy oil; however, it would offer the least net profit among all three treatments if the average cost of toluene is considered to be $270 per barrel. Water recovery, on the other hand, would yield only 1.1% maximum recovery improvement at 135 ˚C, but would offer a better net profit than toluene treatment if the average cost of water is considered to be $43 per barrel, which is the least expensive option. The surfactant solution treatment would yield the best net profit among all three treatments if the average cost of surfactant and water is considered to be $54 per barrel, reaching its optimum net profit at 225 ˚C with 4.78% oil recovery.

Table 6.1. Simple Economic Analysis for Optimum Recovery Technique and Its Temperature – Extractable Recoveries for a Hypothetical Tar-Mat OOIP Case from Zone AB1

Zone	Reservoir Method	Tempearture Setting	Tar-Mat Density API	Extractable Recovery (%)	Hypothetical Amount of Oil Recovered, BBLs	Revenue with $100 BBL	Cost Method Recovery ($)	Net Profit After Technology Cost ($)
AB1	Toluene	315 °C	2	11.2	18,096,861	1,809,686,137	270	-3,076,466,433
	Water	135 °C	1.64	1.1	1,777,370	177,737,031	43	101,310,108
	Surfactant	225 °C	1.86	4.78	7,723,482	772,348,191	54	355,280,168

6.2. SIMPLE ECONOMIC ANALYSIS FOR TAR-MAT ZONE AB2

Tar-mat zone AB2 hypothetically has the following characteristics: porosity of 0.283, water saturation of 0.2, a hypothetical field area of 1000 acres, a hypothetical tar-mat thickness of 47 feet, and a hypothetical formation volume factor of 0.992 reservoir barrels over stock tank barrels. The amount of tar-mat oil in place would be 83,217,063 barrels of immobile, solid-like, extremely heavy oil. Table 6.2 shows that using hot water, the maximum profit would be achieved at 225 ˚C because it would yield 30.32% oil recovery improvement; this treatment would offer the best net profit among all three treatments if the average cost of water is assumed to be $43 per barrel. The surfactant would yield intermediate recovery potential, reaching its optimum net profit at 135 ˚C with 30.92% oil recovery. This treatment would offer good to marginal profit considering the average cost of surfactant and water to be $54 per barrel. Toluene would offer the best oil recovery at 315 ˚C, recovering approximately 53.6% of the oil, but it would offer the least net profit among all three treatments considering the average cost of toluene to be $270 per barrel.

Table 6.2. Simple Economic Analysis for Optimum Recovery Technique and Its Temperature – Extractable Recoveries for a Hypothetical Tar-Mat OOIP Case from Zone AB2

Zone	Reservoir Method	Tempearture Setting	Tar-Mat Density API	Extractable Recovery (%)	Hypothetical Amount of Oil Recovered, BBLs	Revenue with $100 BBL	Cost Method Recovery ($)	Net Profit After Technology Cost ($)
AB2	Toluene	315 °C	2.81	53.6	44,604,346	4,460,434,572	270	-7,582,738,772
	Water	225 °C	1.64	30.32	25,231,413	2,523,141,347	43	1,438,190,568
	Surfactant	135 °C	1.86	30.92	25,730,716	2,573,071,585	54	1,183,612,929

6.3. SIMPLE ECONOMIC ANALYSIS FOR TAR-MAT ZONE AB3

Tar-mat zone AB3 hypothetically has the following characteristics: 1000 acre field area, 0.35 porosity, 0.2 water saturation, 0.992 volume factor, and 23 foot thickness. The total tar-mat oil in place would be 50,364,435 barrels.

Table 6.3 shows that the maximum profit would be achieved using hot water at 135 ˚C because it would yield 26.2% oil recovery improvement and would offer the best net profit. The surfactant would yield intermediate recovery potential, reaching its optimum net profit at 225 ˚C with 27.7% oil recovery. Surfactant would offer good to marginal profit considering an average cost of surfactant and water to be $54 per barrel. Toluene offers the best oil recovery at 135 ˚C, recovering approximately 41.8% of the oil; however, it offers the least net profit among all three treatments considering an average cost of toluene to be $270 per barrel.

Table 6.3. Simple Economic Analysis for Optimum Recovery Technique and Its Temperature – Extractable Recoveries for a Hypothetical Tar-Mat OOIP Case from Zone AB3

Zone	Reservoir Method	Tempearture Setting	Tar-Mat Density API	Extractable Recovery (%)	Hypothetical Amount of Oil Recovered, BBLs	Revenue with $100 BBL	Cost Method Recovery ($)	Net Profit After Technology Cost ($)
AB3	Toluene	135 ℃	1.39	41.8	21,052,334	2,105,233,403	270	-3,578,896,785
	Water	135 ℃	3.95	26.2	13,195,482	1,319,548,210	43	752,142,480
	Surfactant	225 ℃	3.71	27.7	13,950,949	1,395,094,863	54	641,743,637

6.4. SIMPLE ECONOMIC ANALYSIS FOR TAR-MAT ZONE AB4

Zone AB4 hypothetically has the following characteristics: porosity of 0.357, water saturation of 0.2, a hypothetical field area of 1000 acres, thickness of 172 feet, and a hypothetical formation volume factor of 0.992 reservoir barrels over stock tank barrels. The oil in place of tar-mat zone AB4 would be 384,171,155 barrels.

The results in Table 6.4 indicate that the maximum profit would be achieved using hot water at 135 ˚C, which would yield 31.39% oil recovery improvement and offer the best net profit. In the case of surfactant treatment, 28.3% recovery would be achieved at 135 ˚C, offering the next best net profit after the water recovery method. Toluene would provide significant recovery of 47.23% at 225 ˚C, but it offers the least net profit among all three treatments considering an average cost of $270 per barrel.

Table 6.4. Simple Economic Analysis for Optimum Recovery Technique and Its Temperature – Extractable Recoveries for a Hypothetical Tar-Mat OOIP Case from Zone AB4

Zone	Reservoir Method	Tempearture Setting	Tar-Mat Density API	Extractable Recovery (%)	Hypothetical Amount of Oil Recovered, BBLs	Revenue with $100 BBL	Cost Method Recovery ($)	Net Profit After Technology Cost ($)
AB4	Toluene	225 ℃	1.81	47.23	181,444,036	18,144,403,643	270	-30,845,486,193
	Water	135 ℃	4.51	31.39	120,591,326	12,059,132,550	43	6,873,705,554
	Surfactant	135 ℃	3.66	28.3	108,720,437	10,872,043,682	54	5,001,140,094

6.5. SIMPLE ECONOMIC ANALYSIS FOR TAR-MAT ZONE AB5

Tar-mat zone AB5 hypothetically has the following characteristics: porosity of 0.098%, Sw of 0.2, a hypothetical field area of 1000 acres, thickness of 84 feet, and Bo of 0.994 reservoir barrels over stock tank barrels. The amount of tar-mat oil in place would be 51,399,482 barrels.

Table 6.5 shows that the highest oil recovery would be achieved using toluene at 225 ˚C, though this method would offer the least net profit among all three treatments considering the average cost of toluene to be $270 per barrel. Water recovery, on the other hand, would yield only 2.72% maximum recovery improvement at 225 ˚C but, being the least expensive option, offers the intermediate net profit among all three treatments. The surfactant treatment would yield the best net profit among all three treatments considering the average cost of surfactant and water to be $54 per barrel, reaching its optimum net profit at 315 ˚C with 5.41% oil recovery.

Table 6.5. Simple Economic Analysis for Optimum Recovery Technique and Its Temperature – Extractable Recoveries for a Hypothetical Tar-Mat OOIP Case from Zone AB5

Zone	Reservoir Method	Tempearture Setting	Tar-Mat Density API	Extractable Recovery (%)	Hypothetical Amount of Oil Recovered, BBLs	Revenue with $100 BBL	Cost Method Recovery ($)	Net Profit After Technology Cost ($)
AB5	Toluene	225 ℃	1.82	11.27	5,792,722	579,272,159	270	-984,762,670
	Water	225 ℃	1.62	2.72	1,398,066	139,806,590	43	79,689,756
	Surfactant	315 ℃	1.83	5.41	2,780,712	278,071,196	54	127,912,750

7. MODELING

7.1. API-NSO MODEL

According to Table 7.1 and Figure 7.1, the amount of NSO had an inverse relationship with the °API gravity; as the amount of NSO increased, the °API decreased. This relationship was based only on averaging five point samples. Therefore, a simple mathematical correlation for forecasting the °API was developed to predict the tar-mat oil density using measured NSO amounts (Eq. 27):

$$\text{Correlated API index} = 52.168 \times X^{\wedge(-0.584)} \quad (27)$$

Where

X represents the concentration of NSO, (mg/g).

Expanding Eq. 27 to other possible NSO measurements would yield useful information about a global spectrum of °API oil densities based on NSO concentration measurements for this particular formation (Table 7.2). Based on observation, the NSO concentration had a clear and more direct relationship (inversely proportional) to the °API density than to the sub-surface depth location for the tar-mat rock samples. This result highlights the role of the NSO concentration, but without deducting the relationship between the depth and API density. While measuring the NSO concentration will yield a useful hypothesis that confirms or expands the °API correlation, more oils at different densities need to be tested for NSO amounts to make this correlation solid and universal. A small disparity exists between actual measured °API values and mathematically predicted values because of the limited sample size (only 5 samples); more statistical measurements of samples will definitely improve the correlation.

Table 7.1. Results of NSO and °API Gravity from Five Initial Tar-Mat samples

Sample	NSO (mg/g)	°API
AB1	369.19	1.34
AB2	67.2	5.17
AB3	76.1	4.1
AB4	74.4	3.76
AB5	475.5	1.72

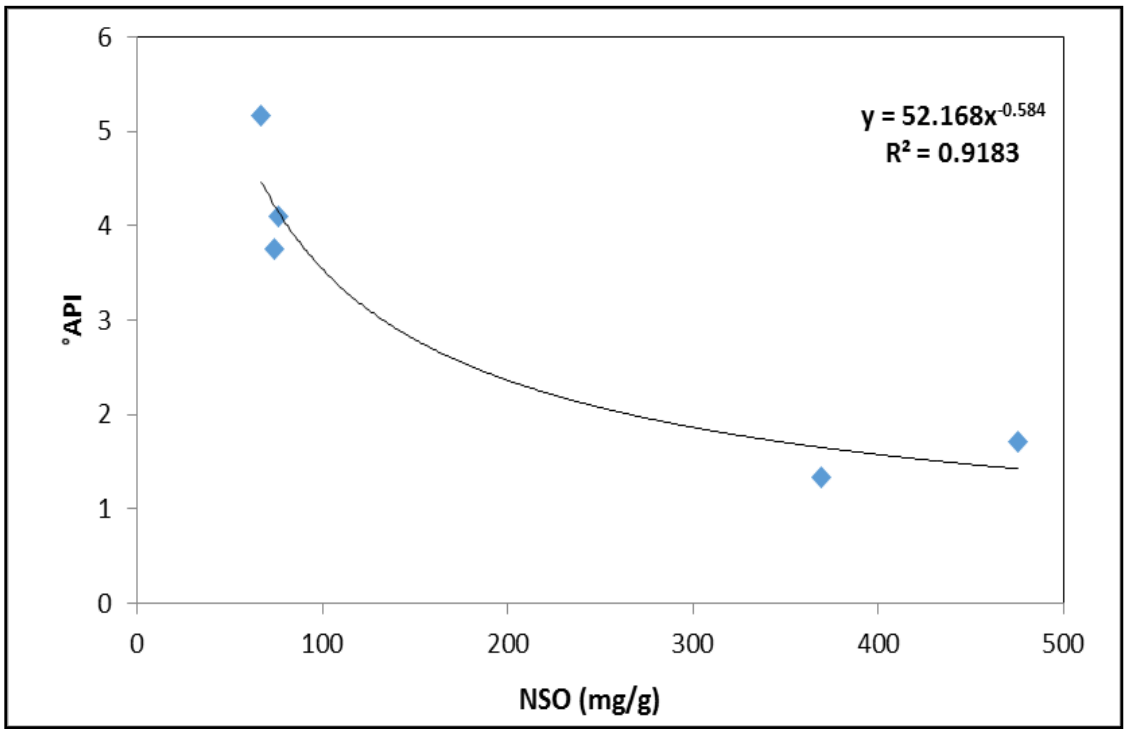

Figure 7.1. Calibration Curve of Rock-Eval 6 NSO Factor Versus Calculated API Gravity

Table 7.2. Results of Output Calculated °API Values from Assumed Input NSO Concentration Values Utilizing Equation 27

NSO (mg/g)	°API
1	52.17
1.5	41.17
2	34.80
2.5	30.55
3	27.46
4	23.22
5	20.38
10	13.60
15	10.73
20	9.07
50	5.31
75	4.19
100	3.54
125	3.11
150	2.80
175	2.56
200	2.36
250	2.07
275	1.96
300	1.87
350	1.70
400	1.58
450	1.47
500	1.38

The proposed model was created using Matlab software based on the equation obtained from the correlation between the NSO and API from the five initial tar-mat samples, as displayed in Figure 7.1. Codes were written based on Eq. 27 to calculate the °API gravity from the assumption data from additional tar-mat samples based on NSO measurements alone. Table 7.2 shows the assumed NSO data used in these written codes to calculate the °API gravity.

Figure 7.2 shows a crossplot of the correlation between the NSO and °API determined from the initial five tar-mat samples. Figure 7.3 shows a crossplot for the °API using measured NSO amounts. The Matlab program codes used to implement this model appear in Table C.1 (see Appendix C).

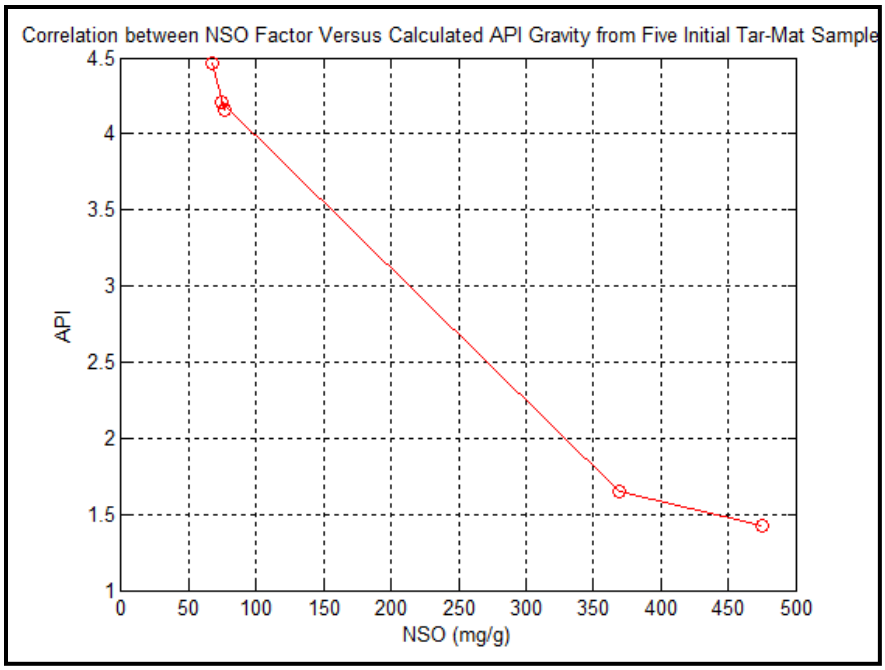

Figure 7.2. Crossplot of Measured NSO Amount Versus Calculated °API from Initial Five Tar-mat Samples Utilizing Eq. 27

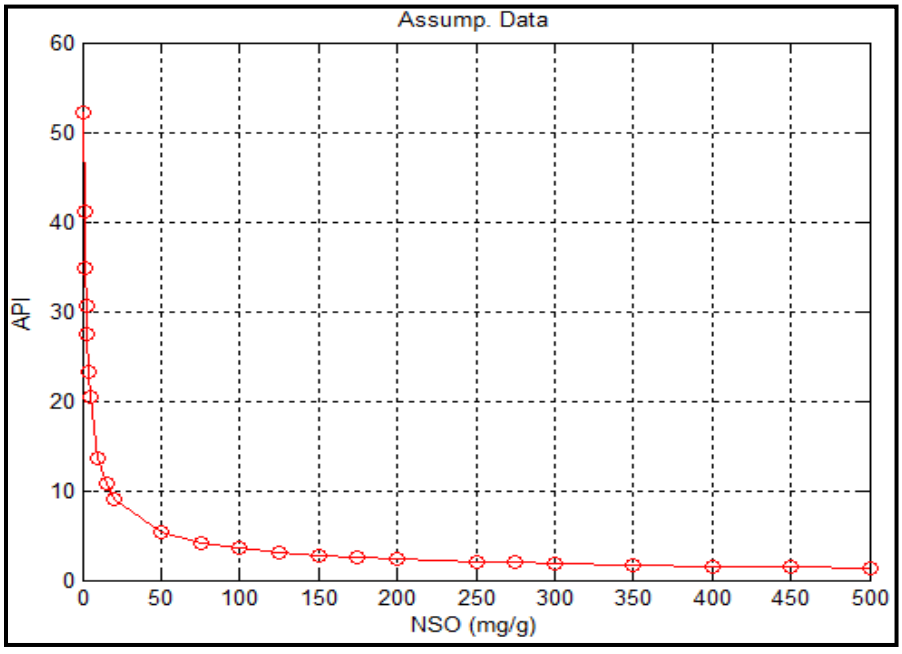

Figure 7.3. Crossplot of API Calculated Using Assumed NSO Amount Values Utilizing Eq. 27

7.2. H/C ASPECT RATIO MODEL

Table 7.3 summarizes the results of the API gravity and the hydrogen-to-carbon (H/C) ratio obtained from the five initial tar-mat samples.

Figure 7.4 shows an inverse relationship between the H/C ratio and °API; as the H/C ratio decreased, the °API increased. A simple mathematical correlation for forecasting the °API was obtained to predict the tar-mat oil density using measured H/C ratio amounts (Eq. 28):

$$\text{Correlated API index} = 1.847 \times X \wedge (-1.46) \tag{28}$$

Where

X represents the concentration of H/C ratio, (wt.%).

Table 7.3. Results of H/C Ratio and °API Gravity from Five Initial Tar-Mat Samples

Sample	°API	H/C Ratio (wt.%)
AB1	1.34	1.26
AB2	5.17	0.55
AB3	4.1	0.56
AB4	3.76	0.57
AB5	1.72	1.04

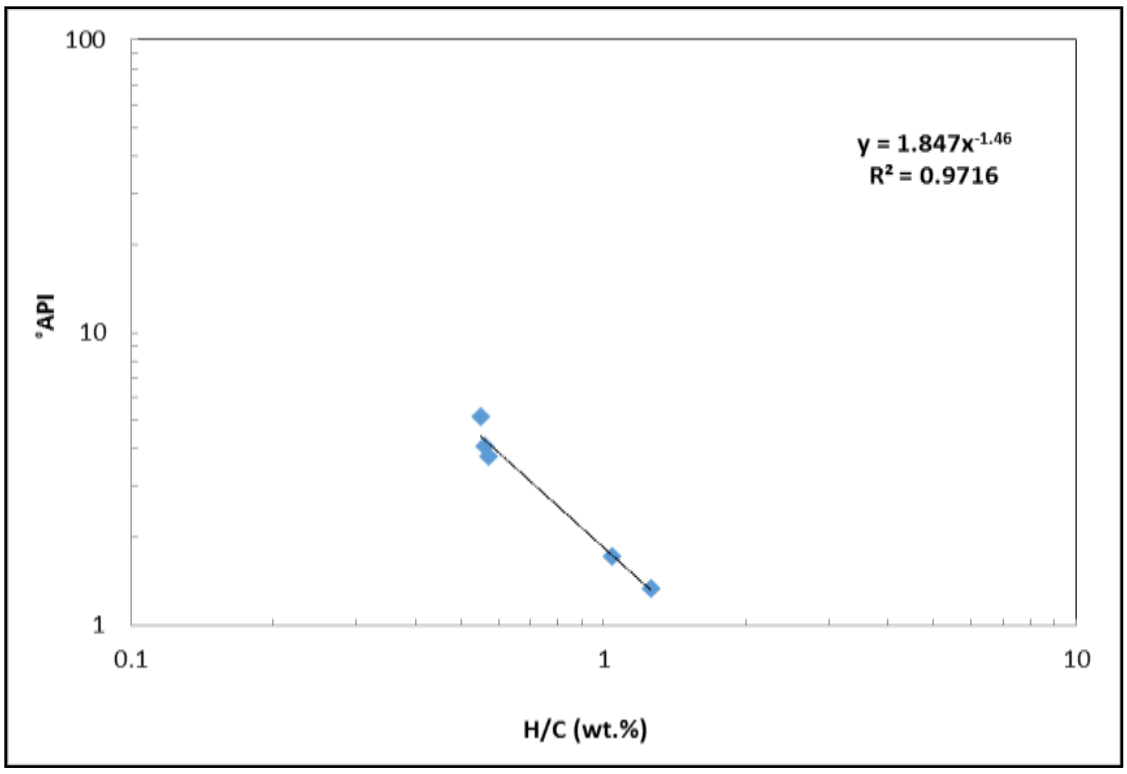

Figure 7.4. Calibration Curve of Elemental Analysis Ratio of H/C Versus Calculated API Gravity

Table 7.4 indicates the assumed data of other possible H/C ratios that could be achieved from other tar-mat samples to expand Eq. 28 in order to calculate the °API values based on the H/C ratio measurement. Matlab software was used to create the H/C ratio model that determines the value of the °API gravity from the tar-mat samples. This model was built based on Eq. 7.2, which was obtained from the correlation between the H/C ratio and °API from the five initial tar-mat samples, as displayed in

Figure 7.4. Basically, codes were written in Matlab software using Eq. 28 to calculate the °API gravity from other assumed H/C ratio data, as shown in Table 7.4.

Figure 7.5 illustrates the calculated °API values using Eq. 28 based on the H/C ratio from the five initial tar-mat samples.

Figure 7.6 shows the calculated °API gravity from other assumed H/C ratio data. The Matlab program codes used to implement this model in Table C.2 (see Appendix C).

Table 7.4. Results of Output Calculated °API Values from Assumed Input H/C Ratio Concentration Values Utilizing Eq. 28

H/C (wt.%)	°API
0.1	53.27
0.12	40.82
0.13	36.32
0.14	32.59
0.15	29.47
0.16	26.82
0.17	24.55
0.18	22.58
0.19	20.87
0.2	19.36
0.3	10.71
0.4	7.04
0.5	5.08
0.6	3.89
0.7	3.11
0.8	2.56
0.9	2.15
1	1.85
1.5	1.02
2	0.67

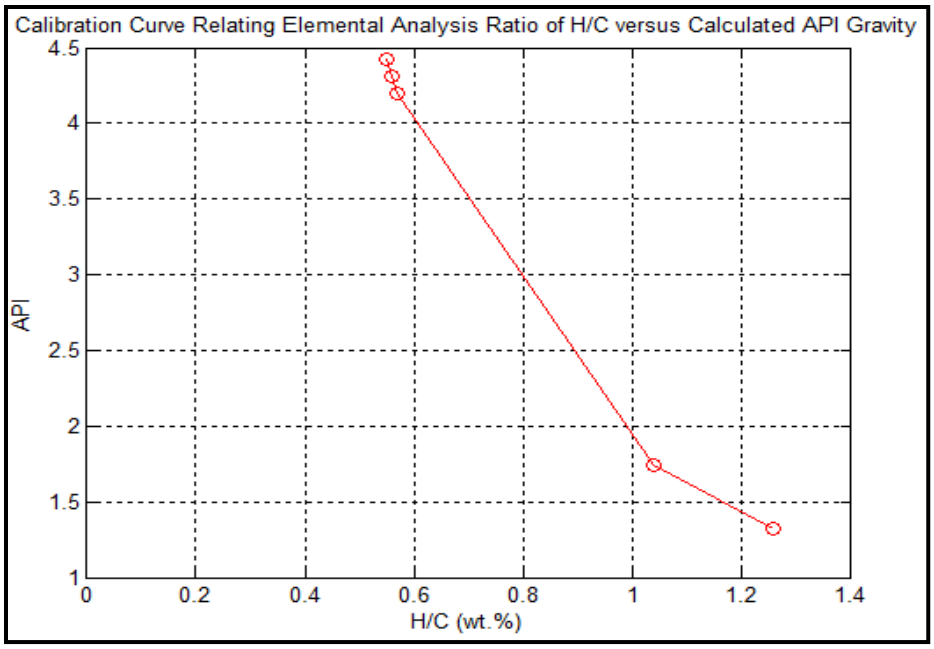

Figure 7.5. Crossplot of H/C Ratio Versus Calculated °API from Initial Five Tar-Mat Samples Utilizing Eq. 28

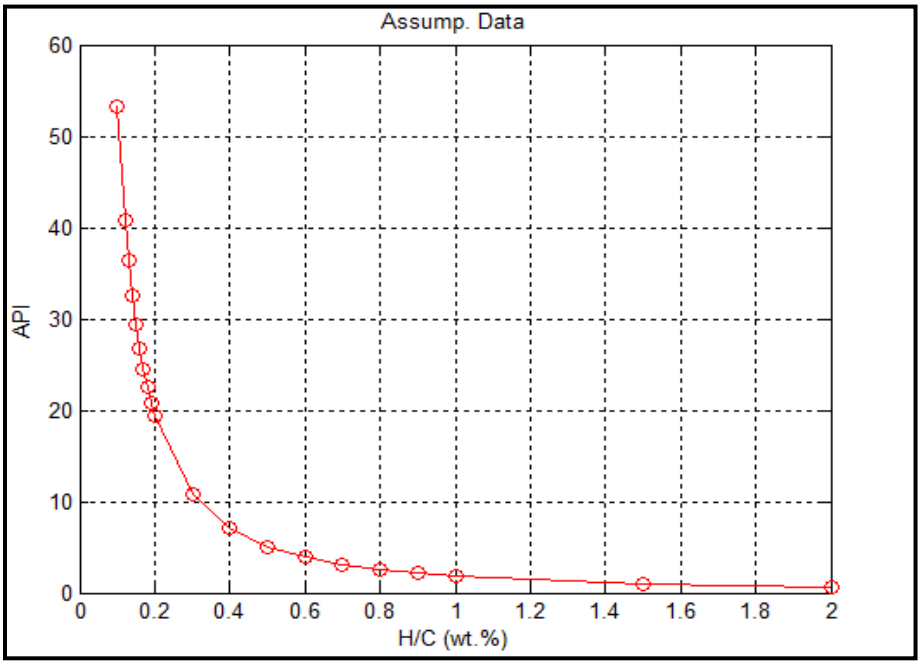

Figure 7.6. Crossplot of API Calculated Using Assumed H/C Ratio Values Utilizing Eq. 28

7.3. OIL RECOVERY MODEL

7.3.1. Model of the Effect of Temperature on Oil Extracted by Toluene. The results from the five initial tar-mat samples after the extraction by toluene using a Soxhlet extractor under different temperatures appear in Table 7.5. The oil recovery increased as the temperature increased. Matlab software was used in this model to calculate the oil recovery that can be obtained from the five tar-mat samples based on various assumed temperature values.

Table 7.5. Results of Oil Recovery from Five Initial Tar-Mat Samples under Four Different Temperatures (Extracted by Toluene)

Sample	T (°C)	Oil Recovery (%)
AB1	25	1.69
	135	2.63
	225	3.61
	315	6.57
AB2	25	13.86
	135	14.72
	225	16.70
	315	16.96
AB3	25	16.72
	135	23.10
	225	23.83
	315	29.32
AB4	25	15.31
	135	24.40
	225	29.93
	315	47.08
AB5	25	0.80
	135	2.48
	225	3.52
	315	6.09

Figures A.1 through A.5 (see Appendix A) illustrate the effect of various temperatures on oil recovery from the five initial tar-mat samples. The temperature had a proportional relationship with oil recovery; as the temperature increased, the oil recovery increased. This relationship was based only on four temperatures. Therefore, a simple mathematical correlation for forecasting oil recovery was created to predict the oil recovery from tar-mat samples AB1 through AB5 using various assumed temperatures (Eqs. 29-33). Exponential fitting gave the best fit for four temperatures versus the oil recovery from samples AB1 through AB5. The R^2 obtained from these correlations from samples AB1 through AB5 were 0.98, 0.93, 0.93, 0.98, and 0.96, respectively.

$$\text{Estimated Oil Recovery for Sample AB1} = 1.448e\wedge(0.0045\times X) \tag{29}$$

$$\text{Estimated Oil Recovery for Sample AB2} = 13.572e\wedge(0.0008\times X) \tag{30}$$

$$\text{Estimated Oil Recovery for Sample AB3} = 16.622e\wedge(0.0018\times X) \tag{31}$$

$$\text{Estimated Oil Recovery for Sample AB4} = 14.033e\wedge(0.0037\times X) \tag{32}$$

$$\text{Estimated Oil Recovery for Sample AB5} = 0.7766e\wedge(0.0068\times X) \tag{33}$$

Where, X represents the temperature, (°C).

Figures A.6 through A.10 (see Appendix A) illustrate the calculated oil recovery from samples AB1 through AB5 under four temperatures using Matlab software based on Eqs. 7.3 through 7.7. A small disparity existed between the actual measured oil recovery values and the mathematically predicted values because of the limited number of

temperatures used (only 4 different temperatures); more temperatures would definitely improve the correlation.

Figures A.11 through A.15 (see Appendix A) illustrate the calculated oil recovery from the five tar-mat samples based on different assumed temperature values. The results of these different assumed temperature values, obtained using the Matlab software model based on Eqs. 7.3 through 7.7 show the new possible calculated oil recovery that can be obtained from the five tar-mat samples.

Tables B.1 through B.5 (see Appendix B) present the output calculated oil recovery from samples AB1 through AB5 based on the assumed input temperature values utilizing Eqs. 29 through 33. The calculation was conducted using Matlab program codes, which were written based on the equations obtained from the correlation between the temperature and oil recovery from the five tar mat samples, as displayed in Figures A.1 through A.5.

The model showing the effect of the temperature on the calculated oil recovery from samples AB1 through AB5 was created using Matlab software. Codes were written based on the output assumed temperature values and the equations obtained from the correlations between the temperature and oil recovery (Figures A.1-A.5 in Appendix A). The Matlab program codes used to implement this model appear in Table C.3 (see Appendix C).

7.3.2. Model of the Effect of Temperature on Oil Extracted by Hot Water. Table 7.6 summarizes the results of oil recovery obtained from the five tar-mat samples. The results reveal a proportional relationship between the oil recovery and temperature;

the oil recovery increased as the temperature increased. A new model was created using Matlab software to calculate the oil recovery at different assumed temperatures values.

Table 7.6. Results of Oil Recovery from Five Initial Tar-Mat Samples under Four Different Temperatures (Extracted by Hot Water)

Sample	T (°C)	Oil Recovery (%)
AB1	25	0.65
	135	1.42
	225	1.57
	315	2.38
AB2	25	1.04
	135	3.19
	225	4.17
	315	4.12
AB3	25	1.87
	135	3.32
	225	3.73
	315	3.71
AB4	25	3.75
	135	4.34
	225	5.28
	315	6.23
AB5	25	0.48
	135	1.16
	225	2.17
	315	2.22

The results of the correlation between the four different temperatures and oil recovery from the five initial tar-mat samples appear in Figures A.16 through A.20 (see

Appendix A). The results indicate that the oil recovery increased as the temperature increased. Therefore, a simple mathematical correlation for oil recovery forecasting was created to predict the oil recovery from tar-mat samples AB1 through AB5 using various assumed temperature values (Eqs. 34-38). Power fitting gave the best fit for the four temperatures versus the oil recovery from samples AB1, AB2, AB3, and AB5. The R^2 obtained from these correlations from the five samples were 0.96, 0.93, 0.97, 0.97, and 0.97, respectively. On the other hand, exponential fitting gave the best fit for sample AB4, and the R^2 obtained from this fitting was 0.99.

$$\text{Estimated Oil Recovery for Sample AB1} = 0.1389 \times X \wedge (0.4732) \quad (34)$$

$$\text{Estimated Oil Recovery for Sample AB2} = 0.1686 \times X \wedge (0.5787) \quad (35)$$

$$\text{Estimated Oil Recovery for Sample AB3} = 0.761 \times X \wedge (0.2875) \quad (36)$$

$$\text{Estimated Oil Recovery for Sample AB4} = 3.5193e \wedge (0.0018 \times X) \quad (37)$$

$$\text{Estimated Oil Recovery for Sample AB5} = 0.062 \times X \wedge (0.6279) \quad (38)$$

Where, X represents the temperature, (°C).

Figures A.21 through A.25 (see Appendix A) illustrate the calculated oil recovery from samples AB1 through AB5 under four different temperatures. This calculation was conducted using Matlab software based on Eqs. 34-38. The results show a small disparity between the actual measured oil recovery values and the mathematically predicted values because of the limited number of temperatures used (only 4 different temperatures); however, more temperatures would definitely improve the correlation.

The oil recovery calculations based on the assumed temperature values appear in Figures A.26 through A.30 (see Appendix A). A Matlab software model was used to determine the possible oil recovery that could be obtained from samples AB1 through AB5. This model was built based on the equations obtained from the correlation between the four different temperatures and the oil recovery from samples AB1 through AB5, as displayed in Figures A.16 through A.20 (see Appendix A).

Tables B.6 through B.10 (see Appendix B) present the calculated oil recovery from samples AB1 through AB5 based on the assumed input temperature values utilizing Eqs. 7.8 through 7.12). The calculation of oil recovery from samples AB1 through AB5 was conducted using the Matlab software model.

The model showing the effect of the temperatures on the oil recovered using hot water was created using Matlab software. Codes were written based on the assumed input temperature values and equations obtained from the correlations between the temperature and oil recovery (Figures A.16-A.20 in Appendix A). The Matlab program codes used to implement this model appear in Table C.4 (see Appendix C).

7.3.3. Model of the Effect of Temperature on Oil Extracted by Surfactant Solution. The oil recovery results from the five initial tar-mat samples under four different temperatures appear in Table 7.7. The results show that the oil recovery from samples AB1 through AB5 increased as the temperature increased. A new model was built in Matlab to estimate the possible oil recovery that could be obtained from these samples assuming different temperatures values.

Table 7.7. Results of Oil Recovery from Five Initial Tar-Mat Samples under Four Different Temperatures (Extracted by Surfactant Solution)

Sample	T (°C)	Oil Recovery (%)
AB1	25	1.07
	135	2.07
	225	3.27
	315	3.30
AB2	25	2.28
	135	4.58
	225	5.98
	315	4.92
AB3	25	2.82
	135	3.96
	225	4.96
	315	5.36
AB4	25	4.33
	135	5.61
	225	6.61
	315	7.50
AB5	25	0.76
	135	1.76
	225	2.38
	315	3.12

Figures A.31 through A.35 (see Appendix A) illustrate the results of the correlation between the four different temperatures and oil recovery from samples AB1 through AB5. The results show a proportional relationship between the oil recovery and the four different temperatures; as the temperature increased, the oil recovery increased. Therefore, a simple mathematical correlation for oil recovery forecasting was created to predict the oil recovery from tar-mat samples AB1 through AB5 using various assumed temperature values (Eqs. 39-43). Power fitting provided a good fit for the relationship

between tar-mat samples AB1, AB2, AB3, and AB5, with R^2 equal to 0.97, 0.90, 0.98, and 0.99, respectively. On the other hand, exponential fitting provided the best fit for sample AB4, with an R^2 value of 0.99.

$$\text{Estimated Oil Recovery for Sample AB1} = 0.235 \times X \wedge (0.4648) \quad (39)$$

$$\text{Estimated Oil Recovery for Sample AB2} = 0.7552 \times X \wedge (0.3551) \quad (40)$$

$$\text{Estimated Oil Recovery for Sample AB3} = 0.1.2211 \times X \wedge (0.2536) \quad (41)$$

$$\text{Estimated Oil Recovery for Sample AB4} = 4.2246e \wedge (0.0019 \times X) \quad (42)$$

$$\text{Estimated Oil Recovery for Sample AB5} = 0.1281 \times X \wedge (0.5446) \quad (43)$$

Where, X represents the temperature, (°C).

The oil recovery results calculated using the Matlab software model from samples AB1-AB5 extracted by surfactant solution under four different temperatures appear in Figures A.36-A.40 (see Appendix A). The results indicate that a small disparity existed between the actual measured oil recovery values and the mathematically predicted values because of the limited number of temperatures used (only 4 different temperatures); more temperatures would definitely improve the correlation.

Figures A.41 through A.45 (see Appendix A) illustrate the calculated oil recovery from samples AB1 through AB5 based on the different assumed temperatures. The calculation was conducted using the Matlab software model to estimate the oil recovery that could be obtained from the five tar-mat samples. This model was built based on Eqs.

39 through 43 obtained from the relationship between the oil recovery and four different temperatures, as displayed in Figures A31 through A.35 (see Appendix A).

The results of the calculated oil recovery from samples AB1 through AB5 based on the assumed input temperature values and utilizing Eqs. 7.13 through 7.17 are summarized in Tables B.11 through B.15 (see Appendix B). The oil recovery from the five samples was calculated using the Matlab software model.

The Matlab codes used to implement this model appear in Table C.5 (see Appendix C). This model was built based on the assumed input temperatures and the equations obtained from the correlations between the temperature and oil recovery (Figures A.31-A.35).

8. CONCLUSIONS AND RECOMMENDATIONS

8.1. CONCLUSIONS

This work integrated several methods, such as elemental analysis, geochemistry pyrolysis analysis (Rock-Eval pyrolysis), and SARA analysis, to systematically characterize tar-mat reservoir rocks and to evaluate the effect of water, surfactant, and toluene on tar-mat recovery.

The following conclusions can be drawn from this study:

- The properties of the tar-mats in the selected carbonate reservoir varied with depth and area within the same field. This variation became more pronounced in the neighborhood of the tar/water contact.
- The CHNSO elemental analysis showed that the H/C ratio from the tar-mat samples increased as the API gravity decreased.
- The SARA analysis results showed that the content of saturates and aromatics was lower than the content of resin and asphaltenes in the tar-mat samples. The Colloid Instability Index (CII) of some samples exceeded 0.9, while in others, the value fell below 0.9, indicating that both stable and unstable oils exist in the formation.
- The Rock-Eval pyrolysis and TOC analysis results showed that the tar-mat samples were rich in organic matter and ranked as having very good to excellent potential for hydrocarbon production. The tested formation was composed of Types II and II/III kerogen of either land or marine origin capable of emitting oil and gas. The thermal maturity assessed from T_{max} and the productivity index indicated that the organic matter in this formation contains both mature and immature rocks.

- The results obtained by Rock-Eval 6 analysis revealed that the values of 10 parameters obtained from the tar-mat samples (HI, QI, BI, PI, PCI, PG, T_{max}, S1+ S2, and S1) increased as the thermal maturity of the organic materials in the tar-mat samples increased during the initial stage of thermal maturation. This increase was more noticeable in mature tar-mat samples AB2, AB3, AB4, and AB5.
- The API gravity value of the mature tar-mat rocks decreased with depth.
- The oil recovery increased as the temperature increased, while heavier compounds of NSO decreased. Toluene yielded the highest oil recovery in the samples that had high permeability and API values ranging from 3 to 5 ˚API. Surfactant solution yielded less oil recovery than toluene. The extraction by hot water yielded the lowest oil recovery from the tar-mat samples. The amount of oil extracted from the tar-mat samples by toluene, hot water, and surfactant solution reached as high as 47.1, 6.2, and 7.5%, respectively.
- After the extraction, toluene had the greatest impact on the tar-mat parameters obtained from elemental analysis and Rock-Eval 6 pyrolysis, while hot water and surfactant solution had only a slight impact on them.
- Based on the evaluation of organic matter, the samples collected from the five tar-mat cores in the Kuwaiti carbonate reservoir can be considered good source rock that can generate oil upon pyrolysis.
- Tar-mats are rich not only in asphaltenes, but also in a combination of asphaltenes, resins, and the unique new RAS peak, thus making their oil distinctly heavy. This RAS peak is a new peak that has not been reported previously in the literature for other extracts.

- The RAS peak is another tar-mat signature that fluctuates with the applied recovery method and temperature.
- Tar-mats have a large sulfur content, which may serve as a possible fingerprinting signature. Samples AB1 and AB5 had sulfur content as high as 7.96 and 5.24%, respectively.
- Four oil compositions were identified in the tar-mat samples. Type I (C1-C15) was considered a free-to-light oil, Type II (C15-C40) a light-to-medium oil, Type III (>C40) a heavy oil, and Type IV an insoluble and very solid-like oil that complicates conventional recovery.
- Types I and II were classified as one flow regime and termed the extractable or light oil of the tar-mat; Type III was considered a heavy oil requiring conventional recovery techniques to initiate mobility and was termed the remaining oil to be recovered. The summation of Types I, II, and III is referred to as the residual or absolute recovery.
- API-NSO and the H/C aspect ratio are new models that can contribute to API gravity prediction for solid tar-mats.

8.2. RECOMMENDATIONS

According to the results obtained from the investigation of tar-mat samples, the following recommendations are made for the extension of future study:

- To investigate the characterization of the tar-mat phase more thoroughly, the effective permeability and viscosity of tar in tar-mat zones must be investigated experimentally.

- In this work, oil recovery was conducted by a Soxhlet Extractor using powder samples. Core flooding methods can be applied to extract the oil from tar-mat cores to uncover more precise oil recovery trends.
- The oil recovery experiments were conducted at four temperatures over a constant amount of time (6 hours). Future oil recovery experiments could be conducted at various other temperatures and times. Also, investigations under reservoir conditions of temperature and pressure should be considered.
- The empirical model considered only the API gravity. Other configurations may be studied, such as the porosity, permeability, and viscosity, to formulate a better understanding.
- Different type and concentration of surfactant solutions could be applied for extracting the oil from tar-mat samples.

APPENDIX A.
EFFECT OF TEMPERATURE ON OIL RECOVERY

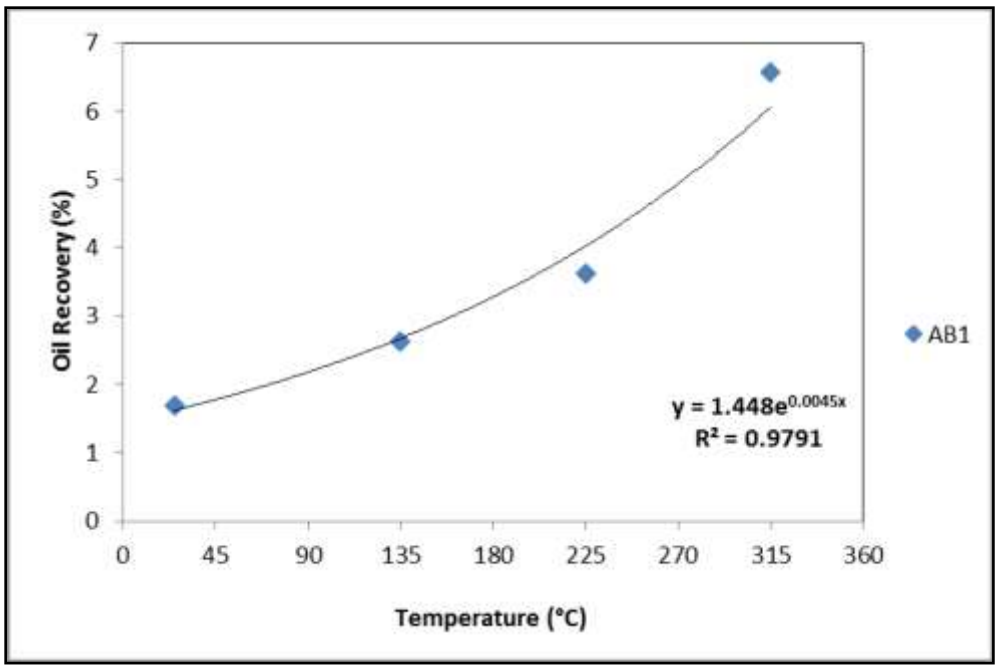

Figure A.1. Oil Recovery at Different Temperatures from Tar-Mat Sample AB1 (Extracted by Toluene)

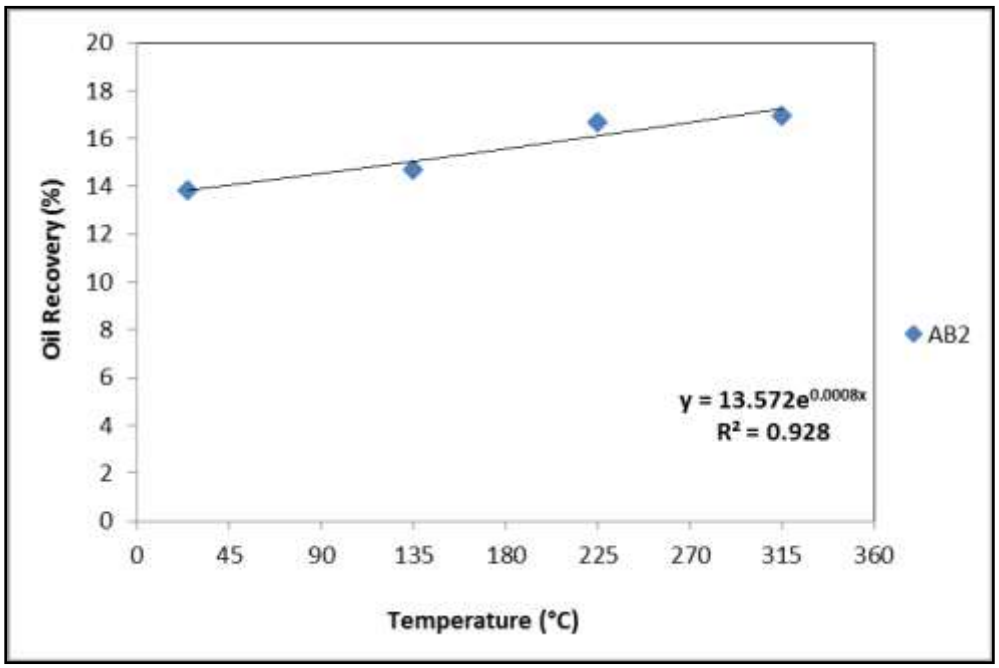

Figure A.2. Oil Recovery at Different Temperatures from Tar-Mat Sample AB2 (Extracted by Toluene)

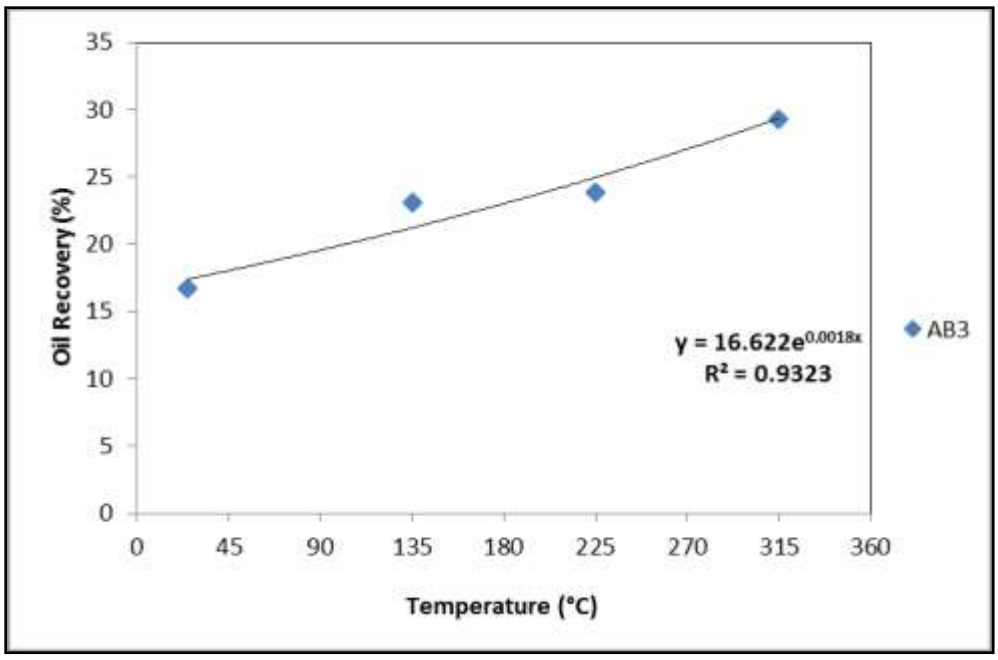

Figure A.3. Oil Recovery at Different Temperatures from Tar-Mat Sample AB3 (Extracted by Toluene)

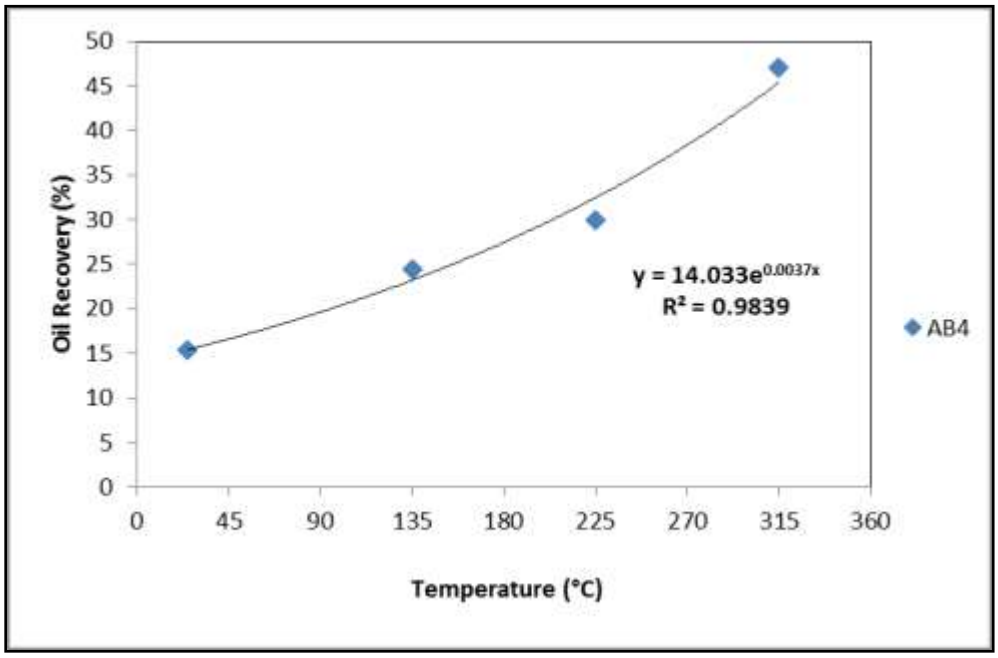

Figure A.4. Oil Recovery at Different Temperatures from Tar-Mat Sample AB4 (Extracted by Toluene)

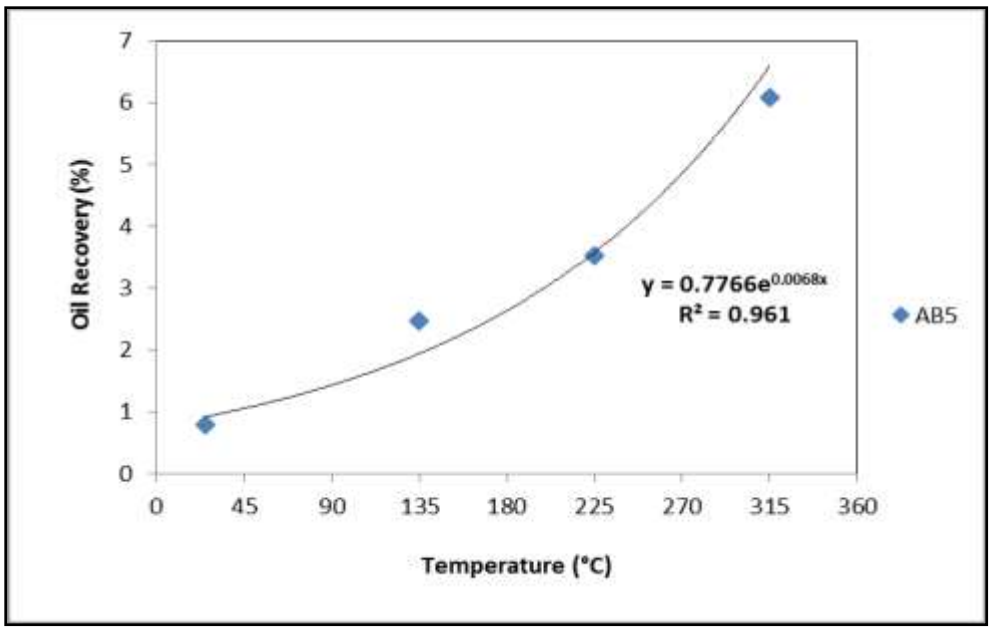

Figure A.5. Oil Recovery at Different Temperatures from Tar-Mat Sample AB5 (Extracted by Toluene)

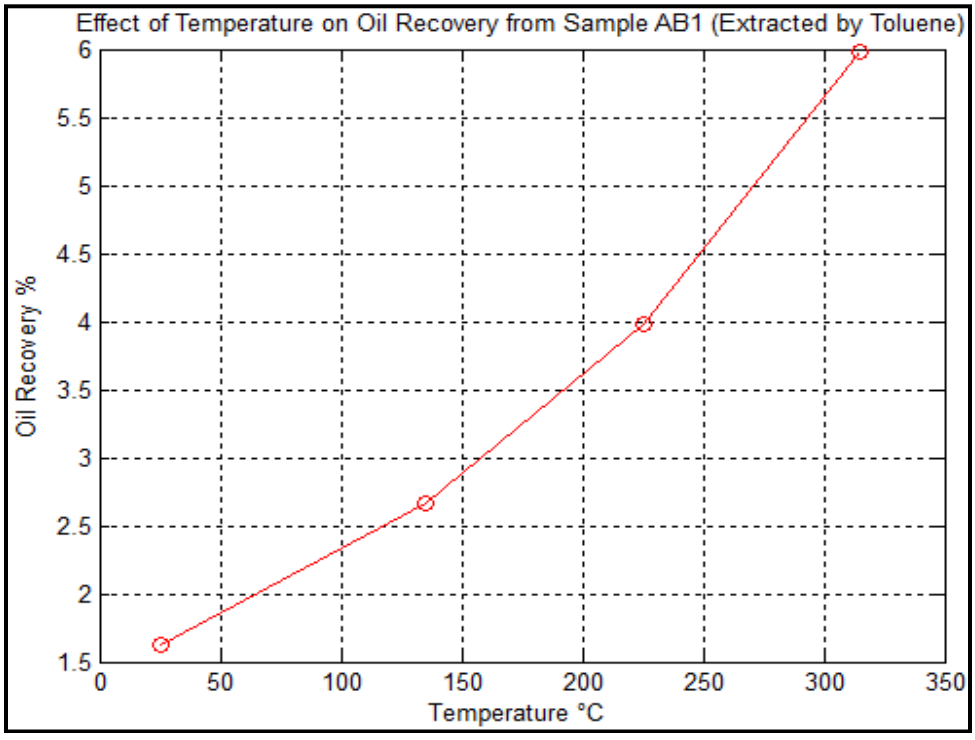

Figure A.6. Calculated Oil Recovery at Different Temperatures Utilizing Eq. 29 (Sample AB1)

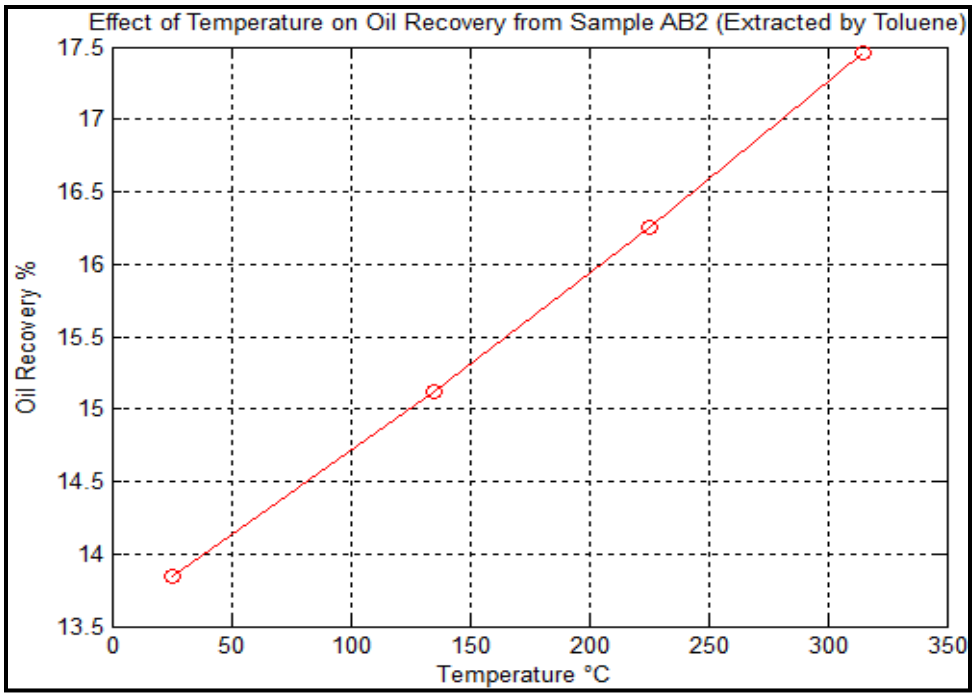

Figure A.7. Calculated Oil Recovery at Different Temperatures Utilizing Eq. 30 (Sample AB2)

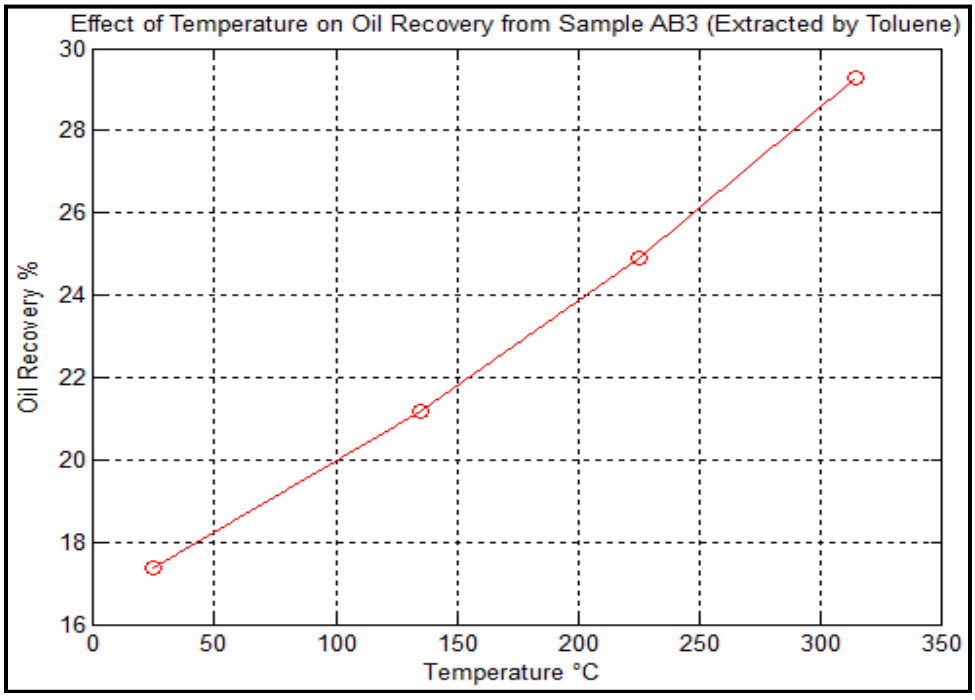

Figure A.8. Calculated Oil Recovery at Different Temperatures Utilizing Eq. 31 (Sample AB3)

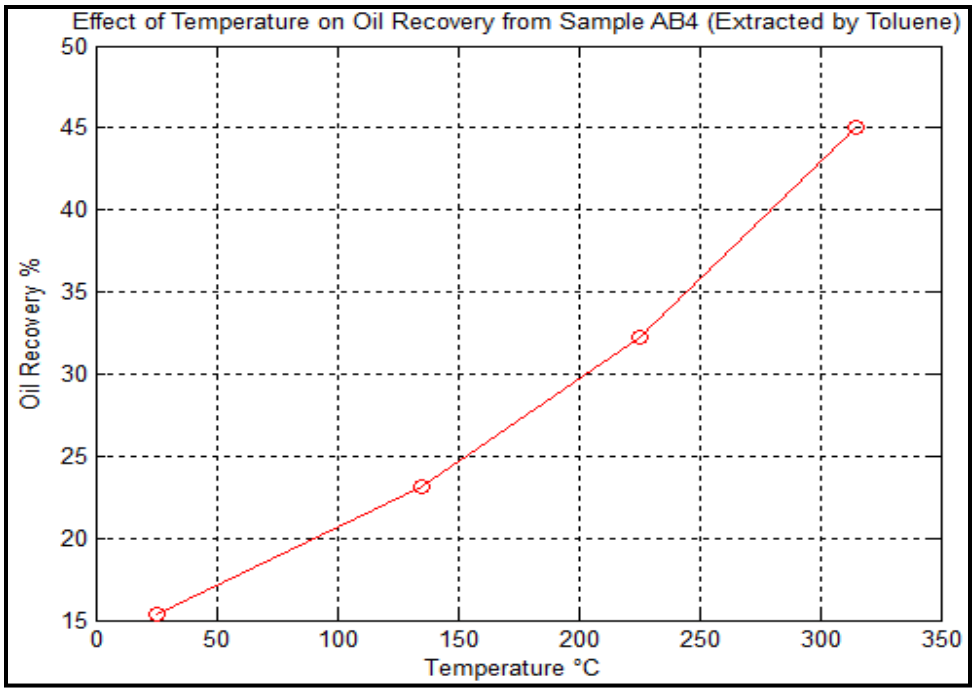

Figure A.9. Calculated Oil Recovery at Different Temperatures Utilizing Eq. 32 (Sample AB4)

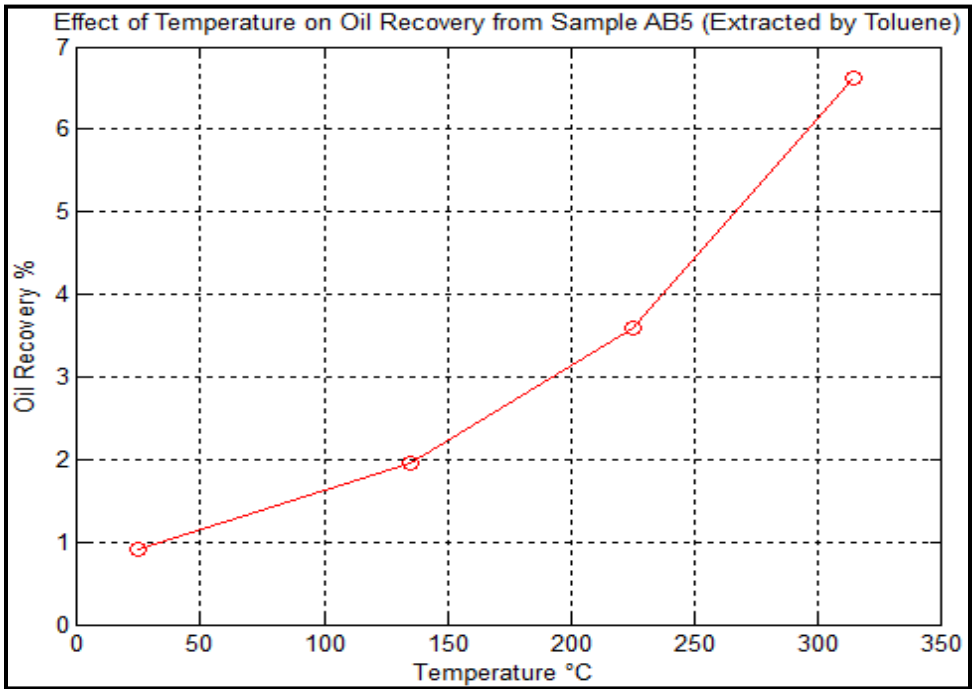

Figure A.10. Calculated Oil Recovery at Different Temperatures Utilizing Eq. 33 (Sample AB5)

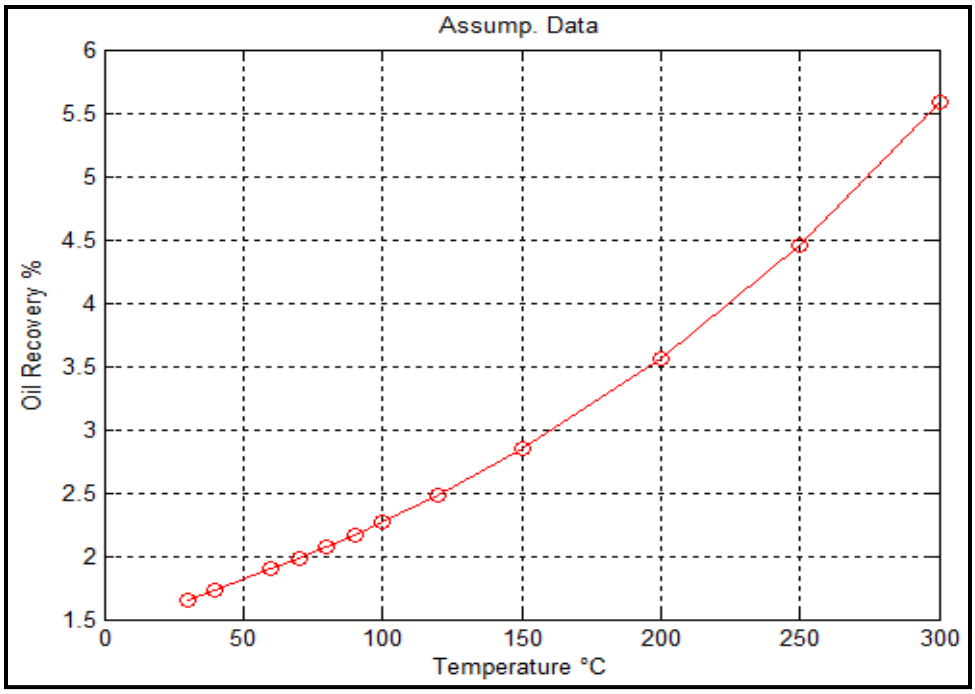

Figure A.11. Calculated Oil Recovery at Assumed Temperatures Utilizing Eq. 29 (Sample AB1)

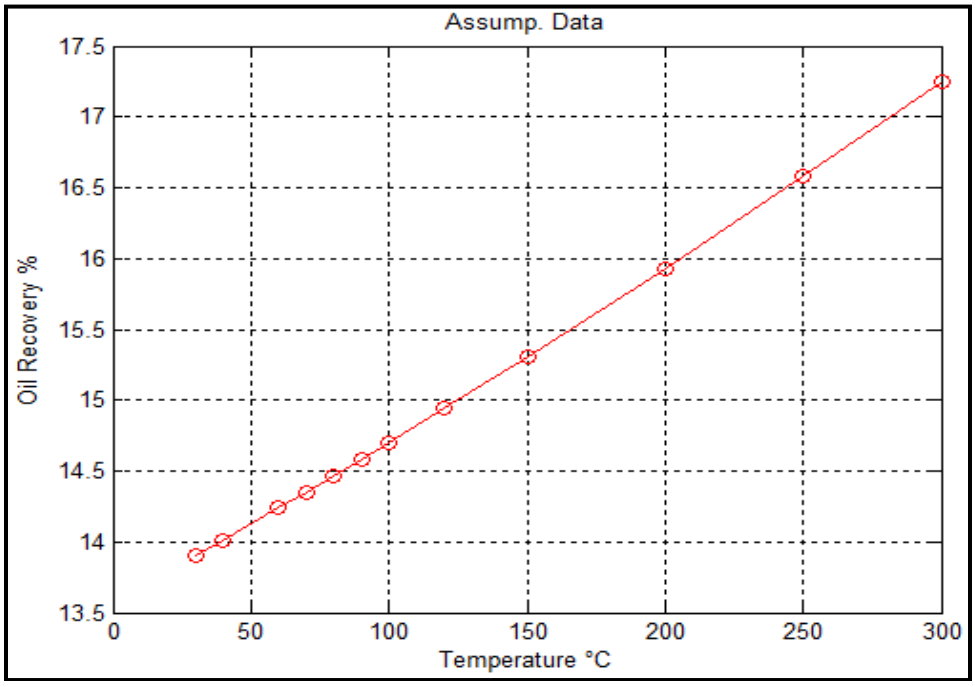

Figure A.12. Calculated Oil Recovery at Assumed Temperatures Utilizing Eq. 30 (Sample AB2)

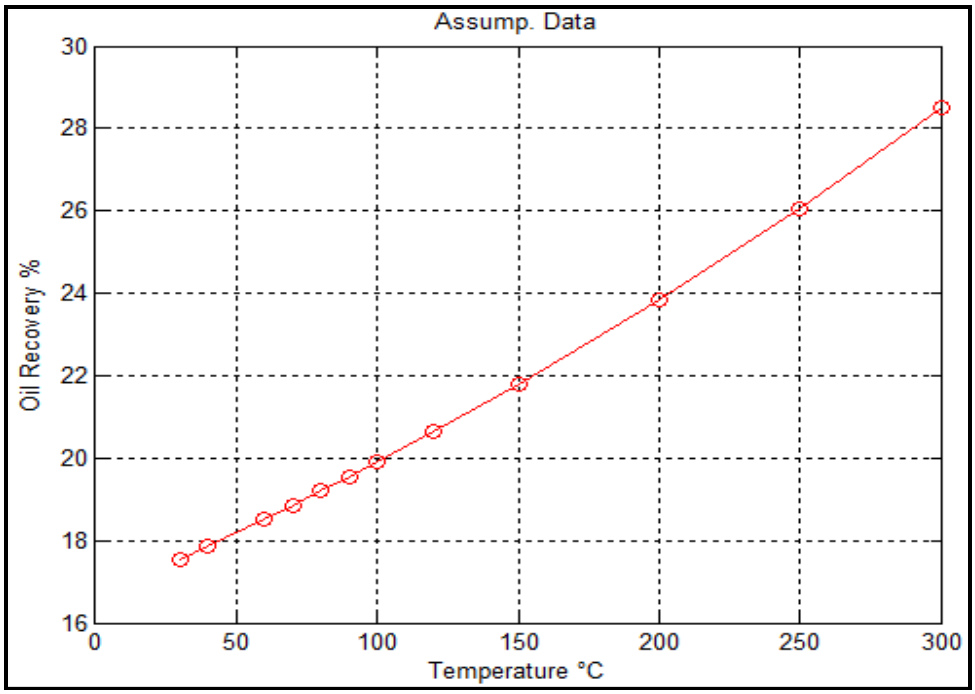

Figure A.13. Calculated Oil Recovery at Assumed Temperatures Utilizing Eq. 31 (Sample AB3)

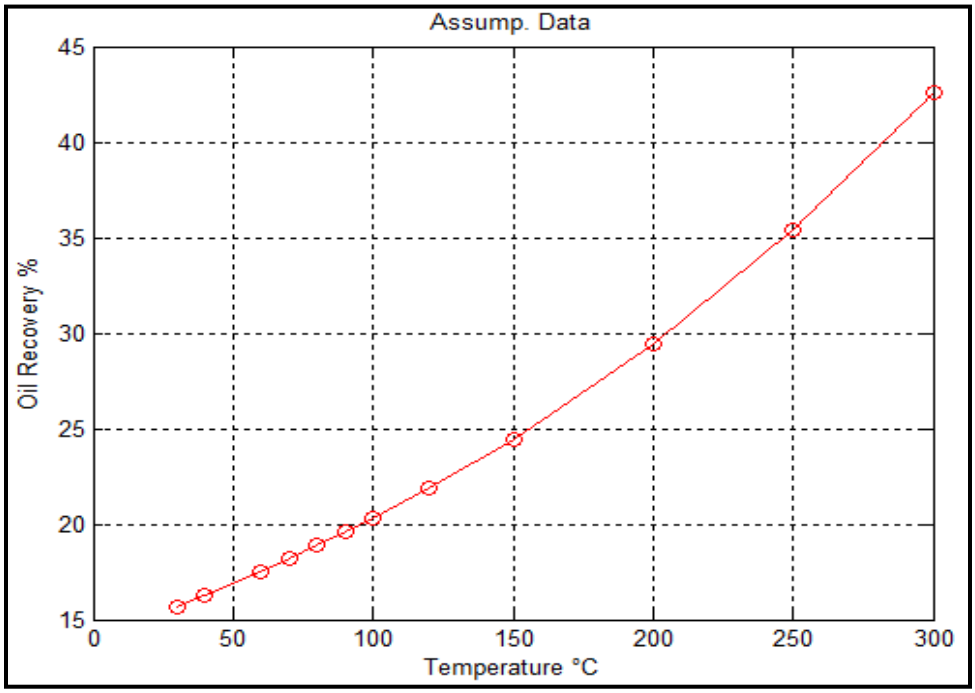

Figure A.14. Calculated Oil Recovery at Assumed Temperatures Utilizing Eq. 32 (Sample AB4)

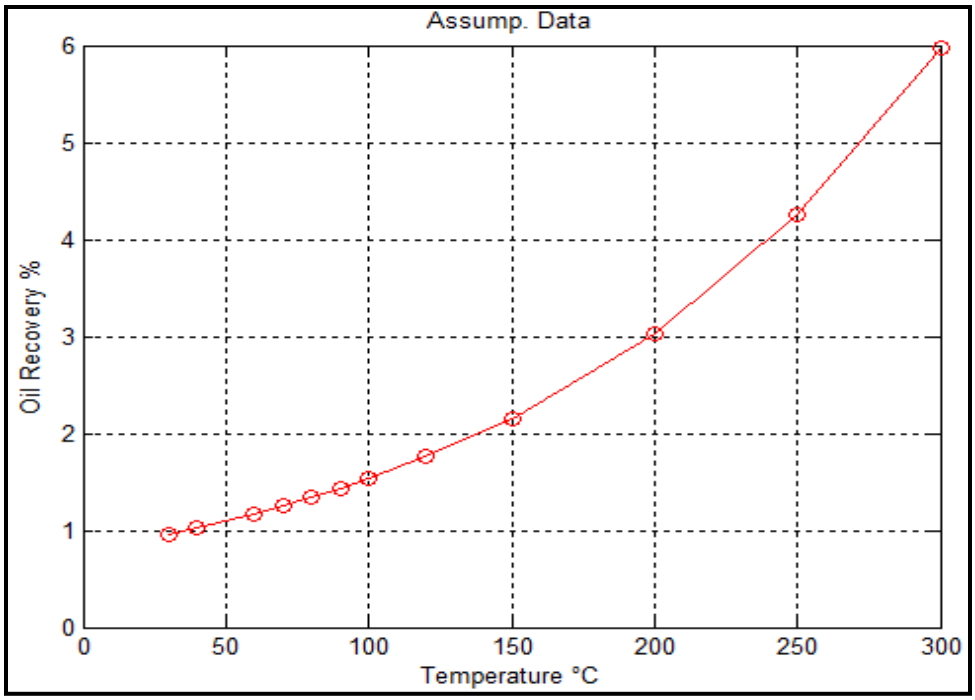

Figure A.15. Calculated Oil Recovery at Assumed Temperatures Utilizing Eq. 33 (Sample AB5)

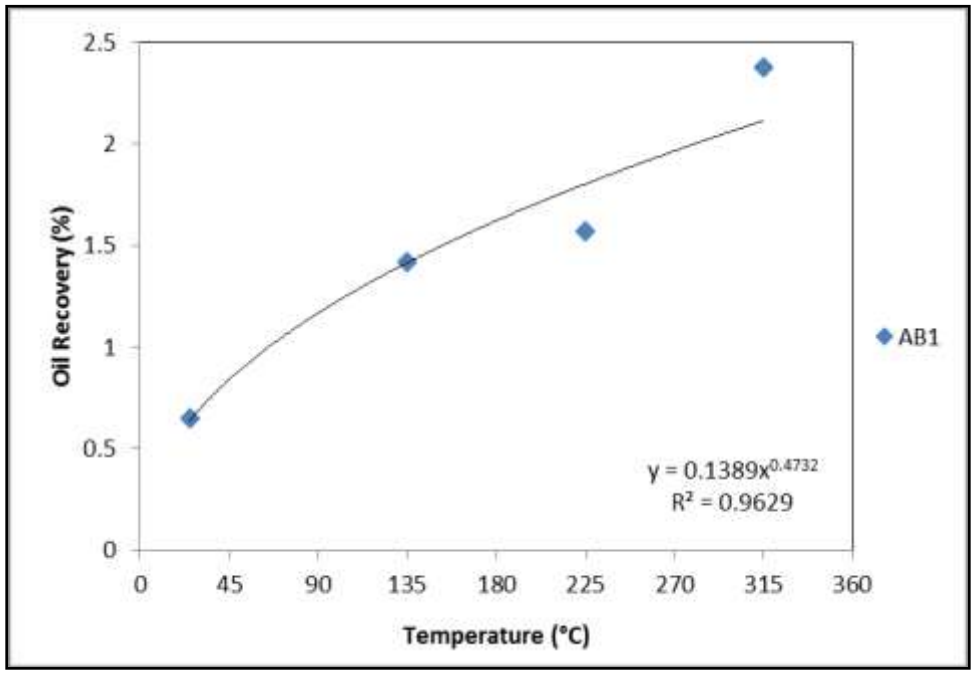

Figure A.16. Oil Recovery at Different Temperatures from Tar-Mat Sample AB1 (Extracted by Hot Water)

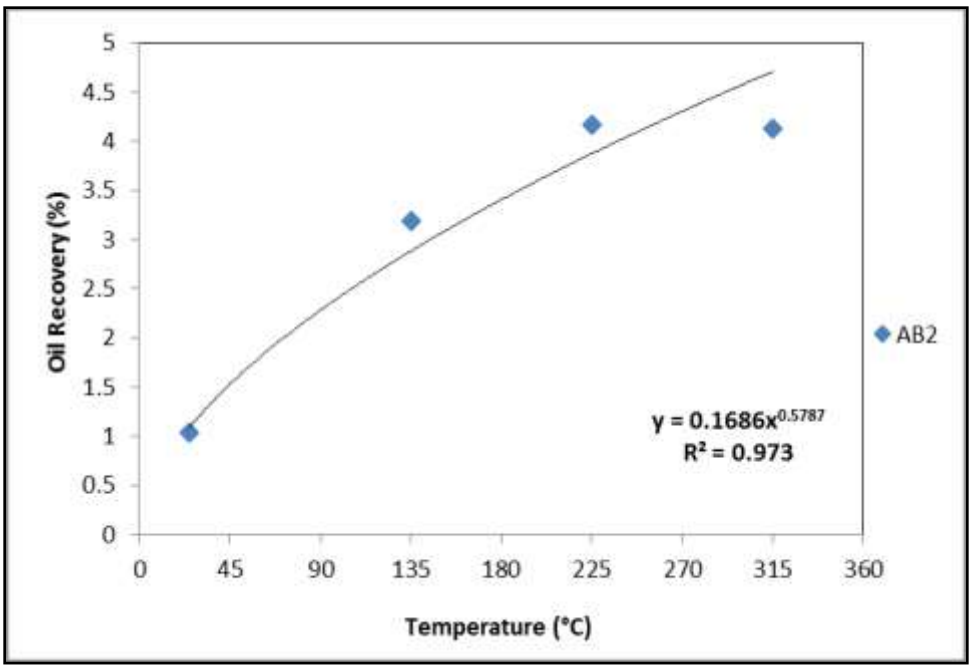

Figure A.17. Oil Recovery at Different Temperatures from Tar-Mat Sample AB2 (Extracted by Hot Water)

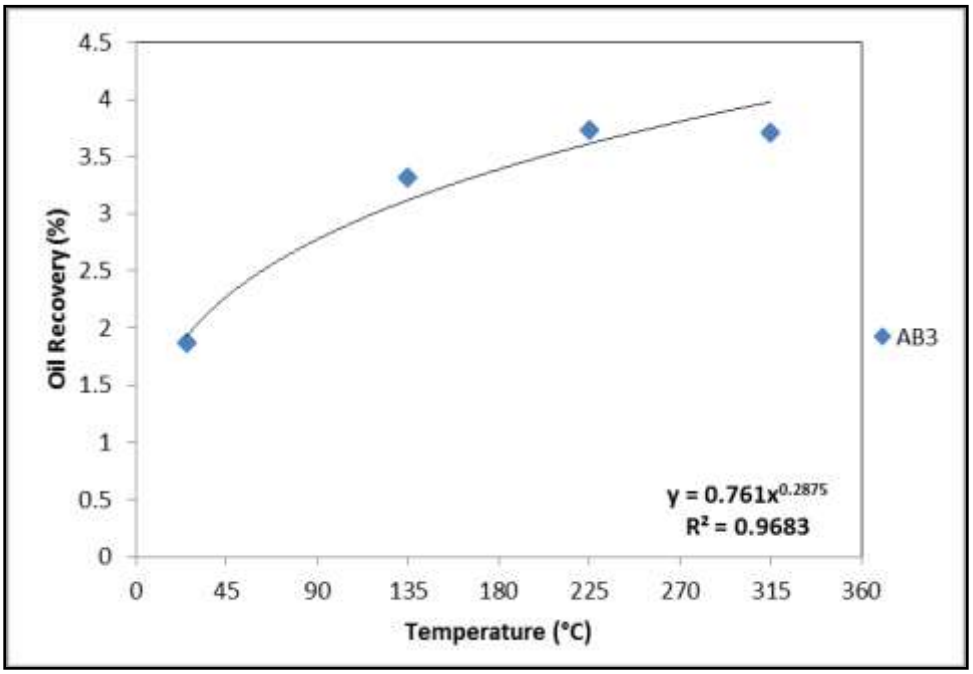

Figure A.18. Oil Recovery at Different Temperatures from Tar-Mat Sample AB3 (Extracted by Hot Water)

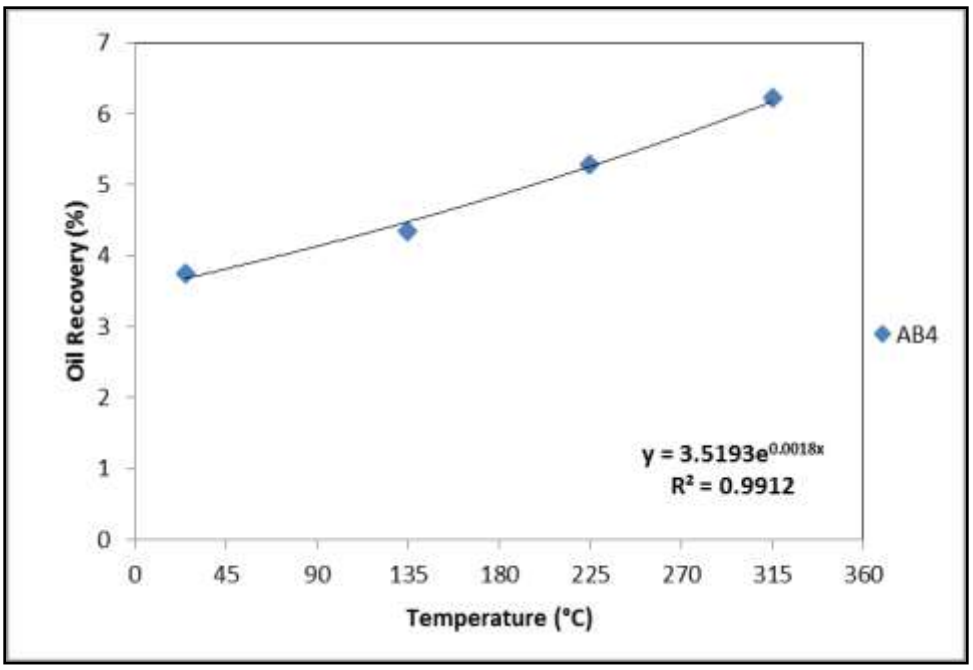

Figure A.19. Oil Recovery at Different Temperatures from Tar-Mat Sample AB4 (Extracted by Hot Water)

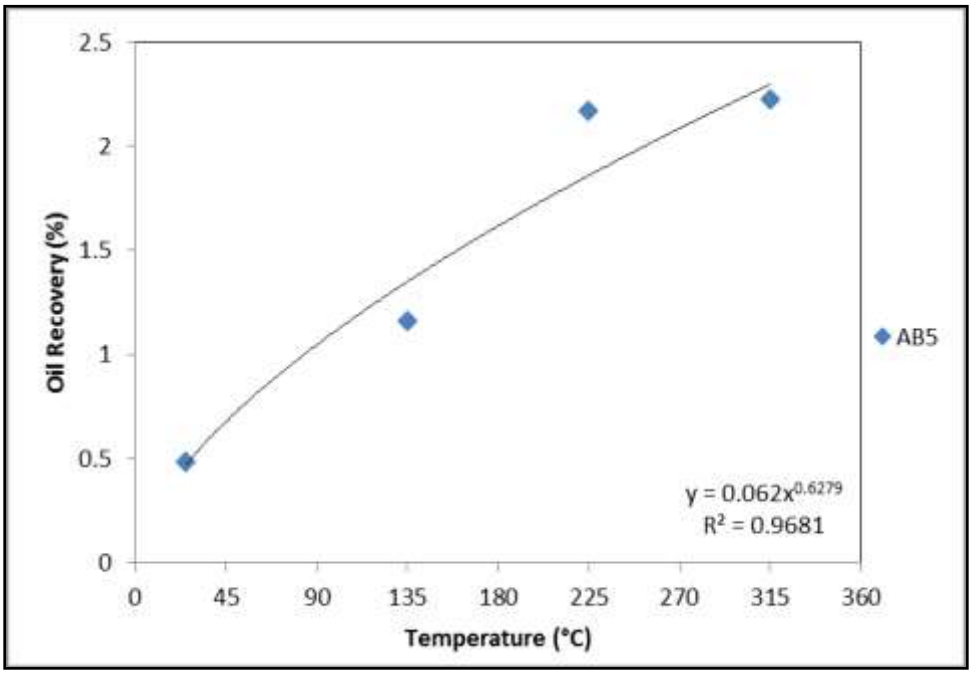

Figure A.20. Oil Recovery at Different Temperatures from Tar-Mat Sample AB5 (Extracted by Hot Water)

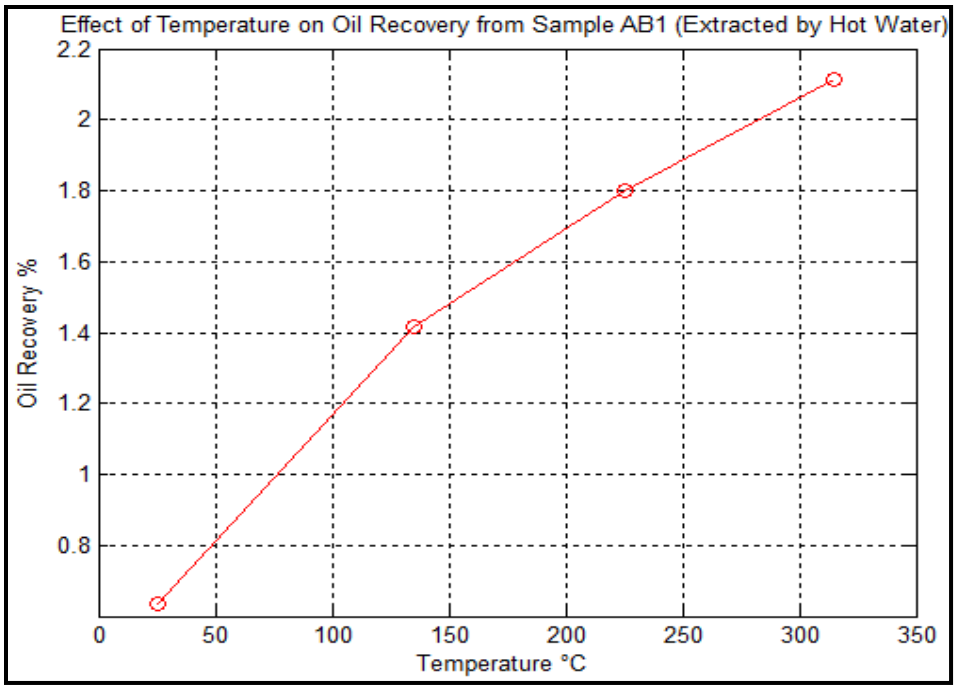

Figure A.21. Calculated Oil Recovery at Different Temperatures Utilizing Eq. 34 (Sample AB1)

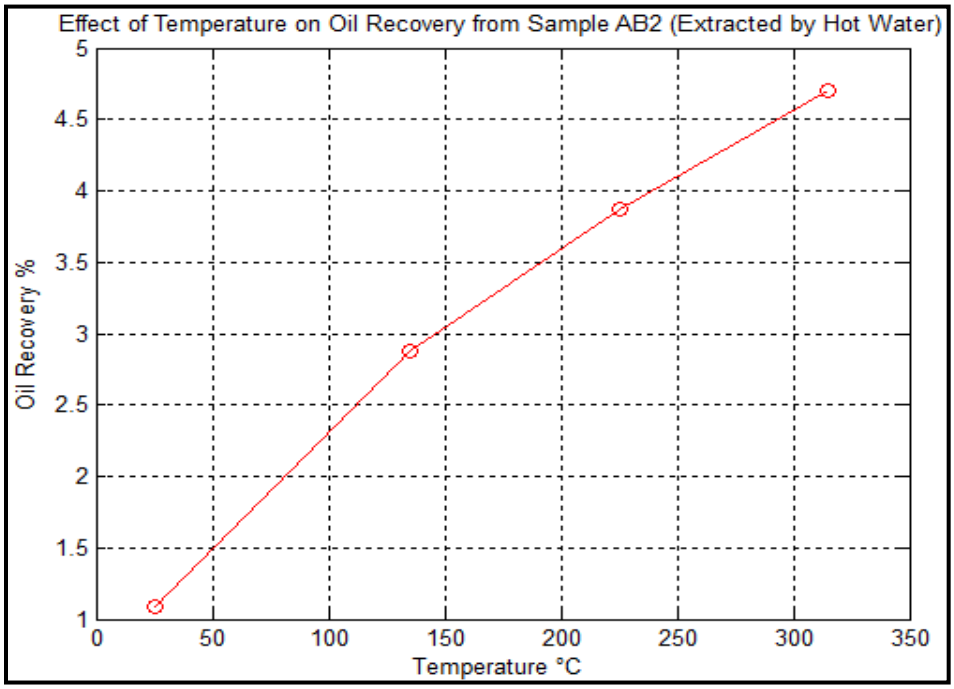

Figure A.22. Calculated Oil Recovery at Different Temperatures Utilizing Eq. 35 (Sample AB2)

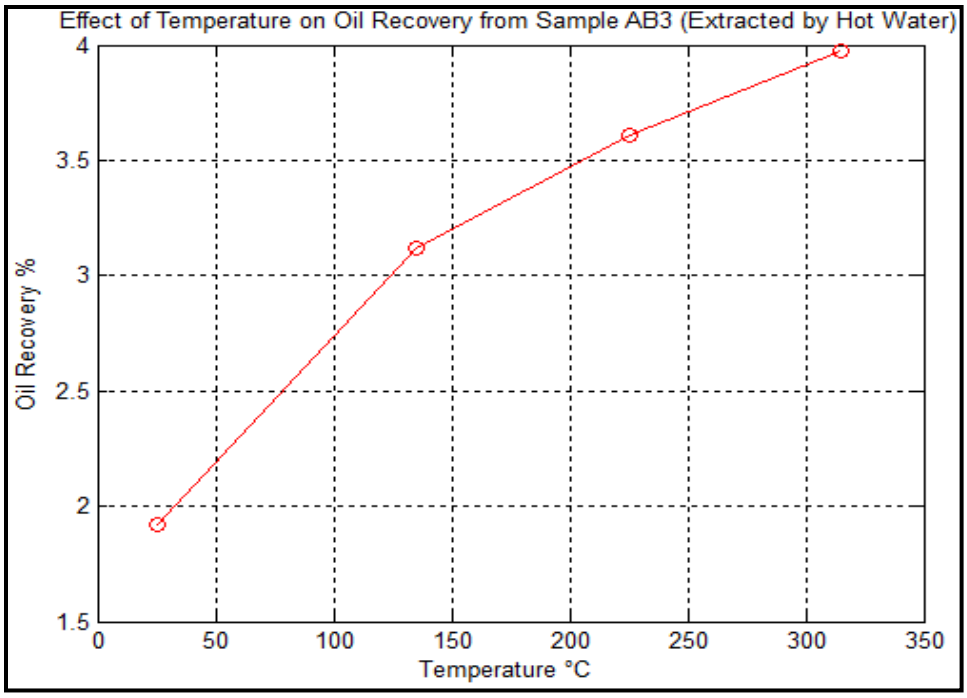

Figure A.23. Calculated Oil Recovery at Different Temperatures Utilizing Eq. 36 (Sample AB3)

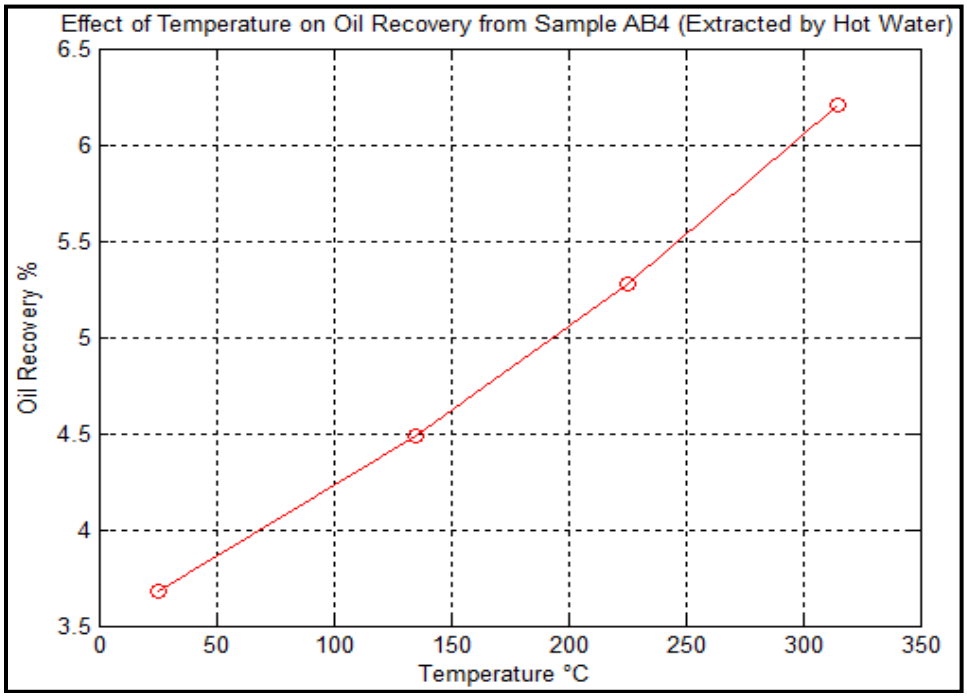

Figure A.24. Calculated Oil Recovery at Different Temperatures Utilizing Eq. 37 (Sample AB4)

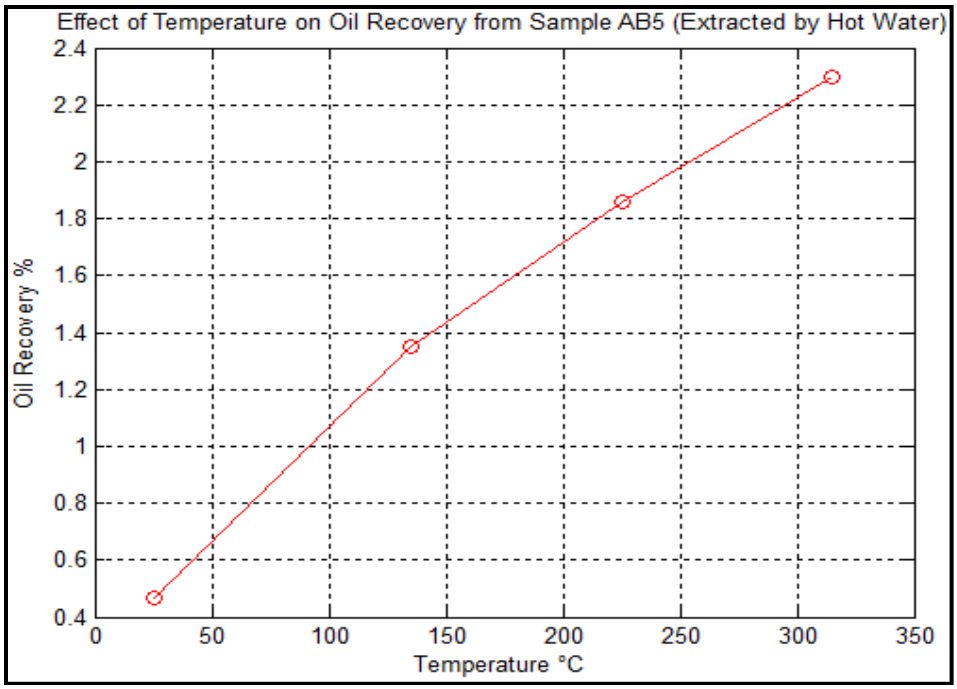

Figure A.25. Calculated Oil Recovery at Different Temperatures Utilizing Eq. 38 (Sample AB5)

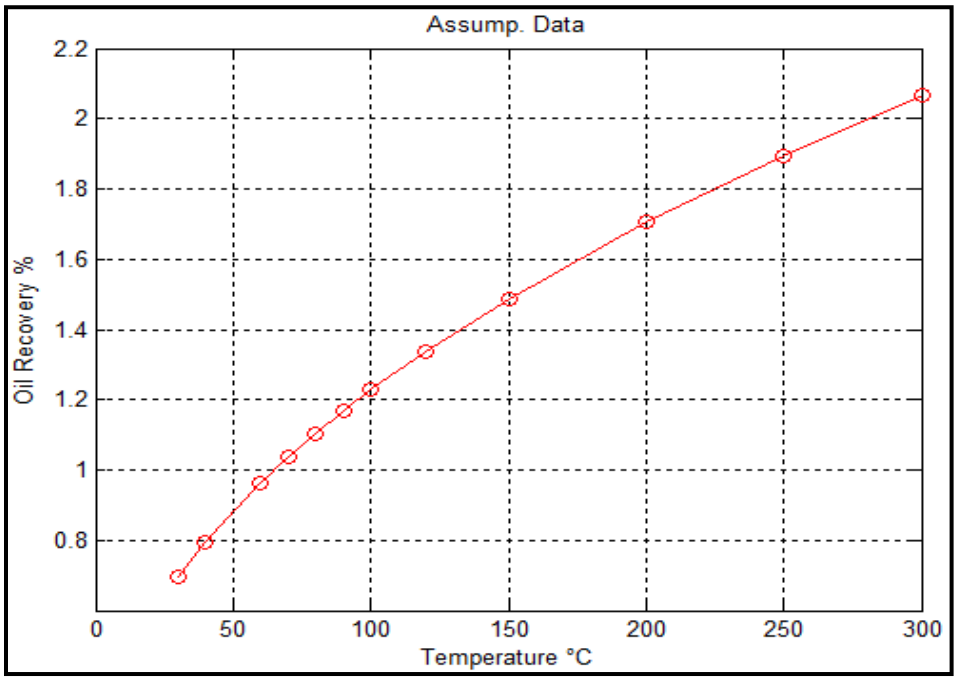

Figure A.26. Calculated Oil Recovery at Assumed Temperatures Utilizing Eq. 34 (Sample AB1)

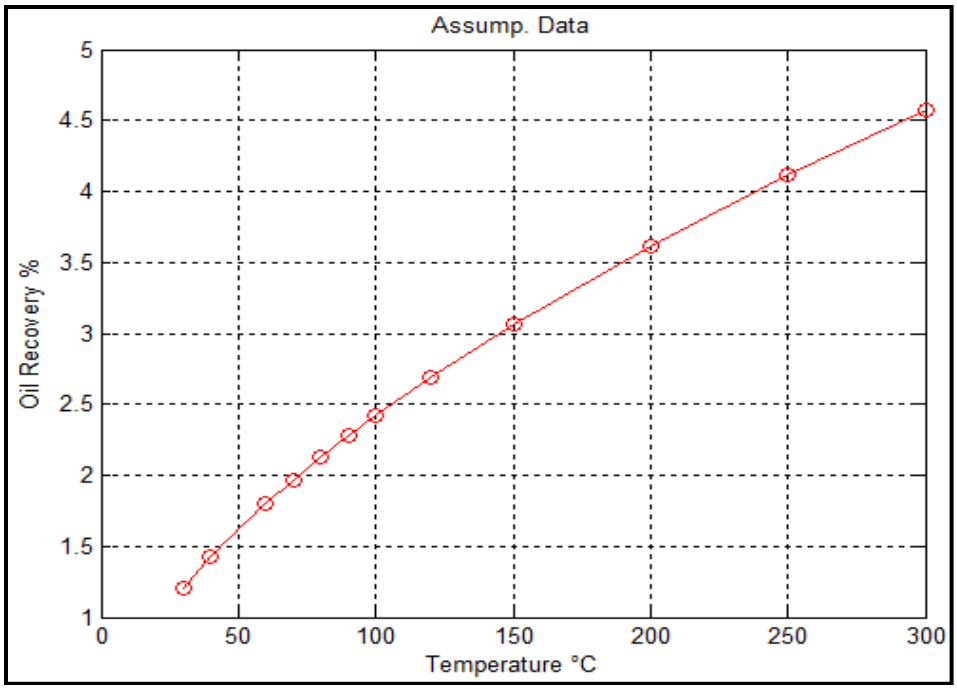

Figure A.27. Calculated Oil Recovery at Assumed Temperatures Utilizing Eq. 35 (Sample AB2)

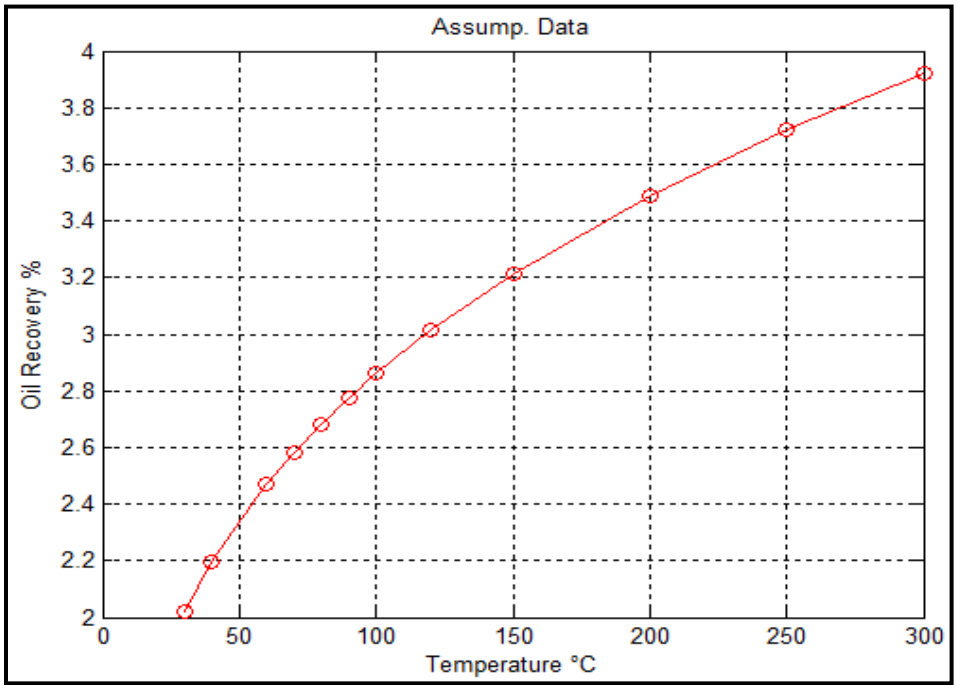

Figure A.28. Calculated Oil Recovery at Assumed Temperatures Utilizing Eq. 36 (Sample AB3)

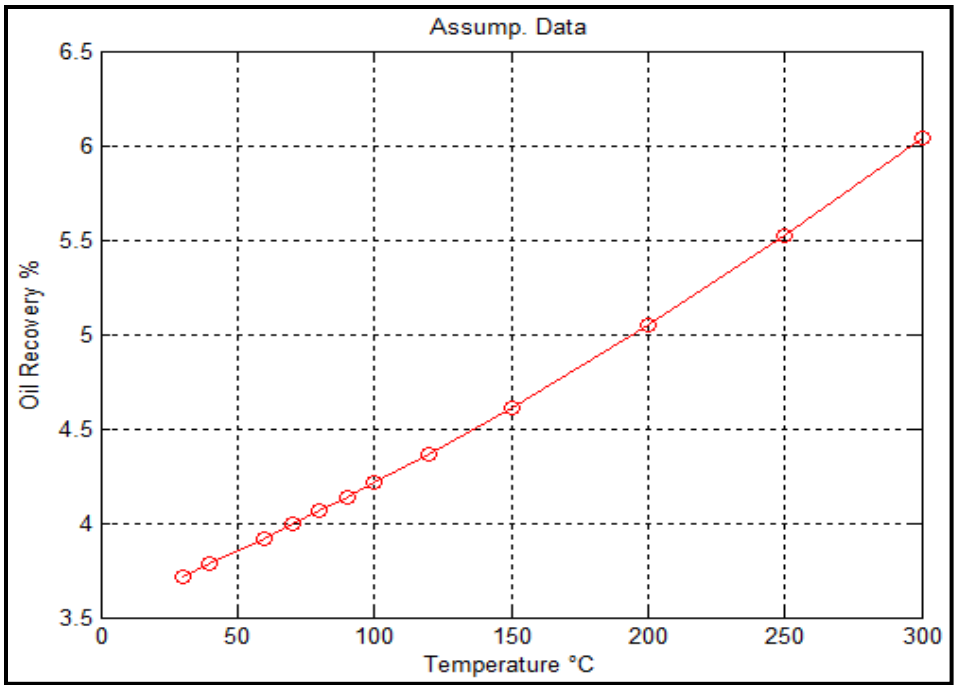

Figure A.29. Calculated Oil Recovery at Assumed Temperatures Utilizing Eq. 37 (Sample AB4)

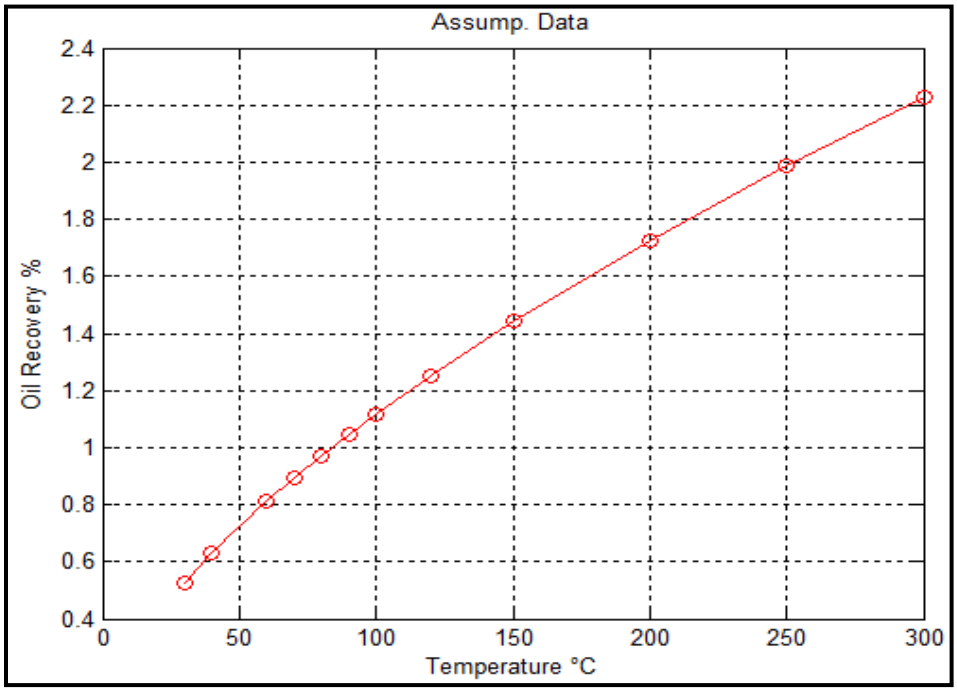

Figure A.30. Calculated Oil Recovery at Assumed Temperatures Utilizing Eq. 38 (Sample AB5)

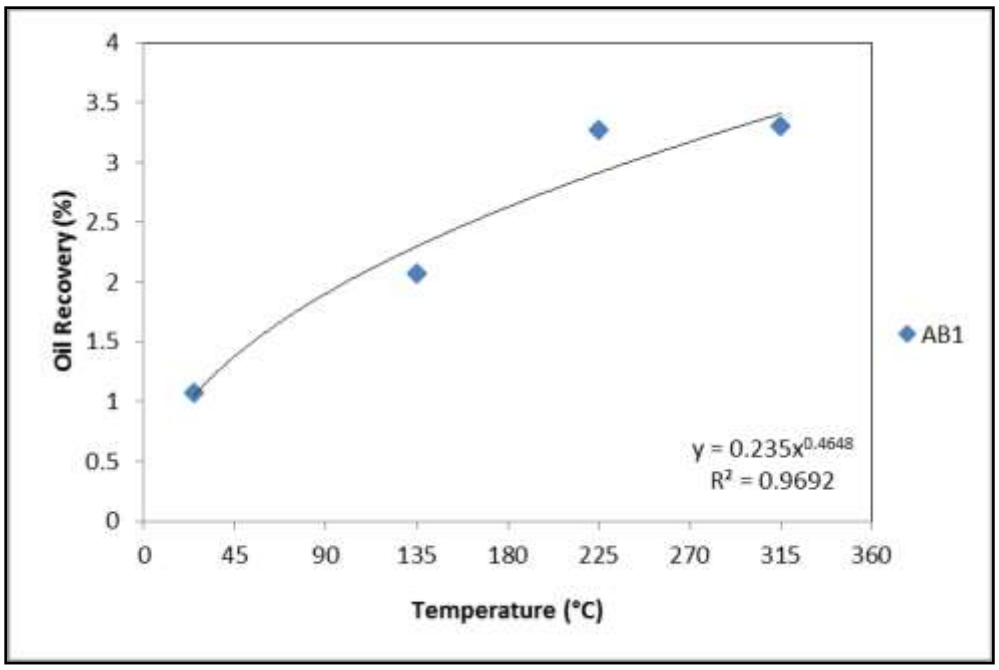

Figure A.31. Oil Recovery at Different Temperatures from Tar-Mat Sample AB1 (Extracted by Surfactant Solution)

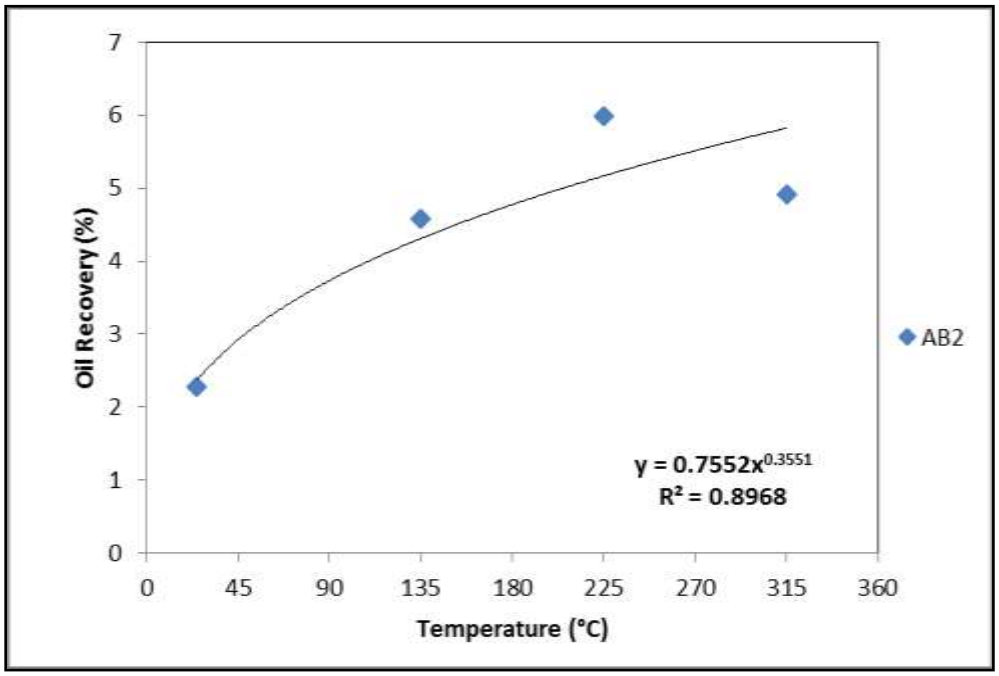

Figure A.32. Oil Recovery at Different Temperatures from Tar-Mat Sample AB2 (Extracted by Surfactant Solution)

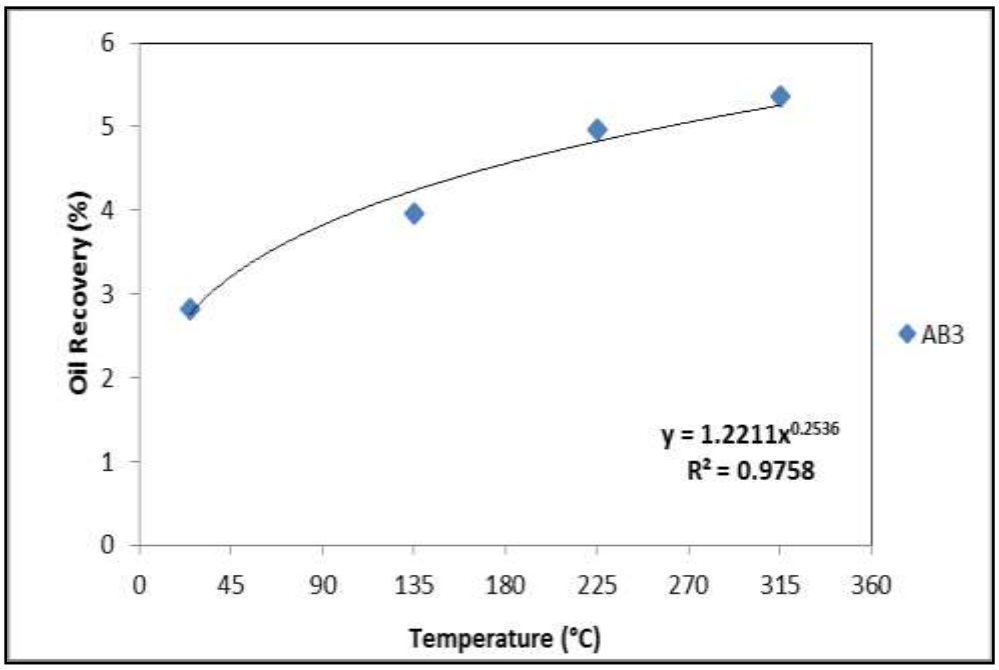

Figure A.33. Oil Recovery at Different Temperatures from Tar-Mat Sample AB3 (Extracted by Surfactant Solution)

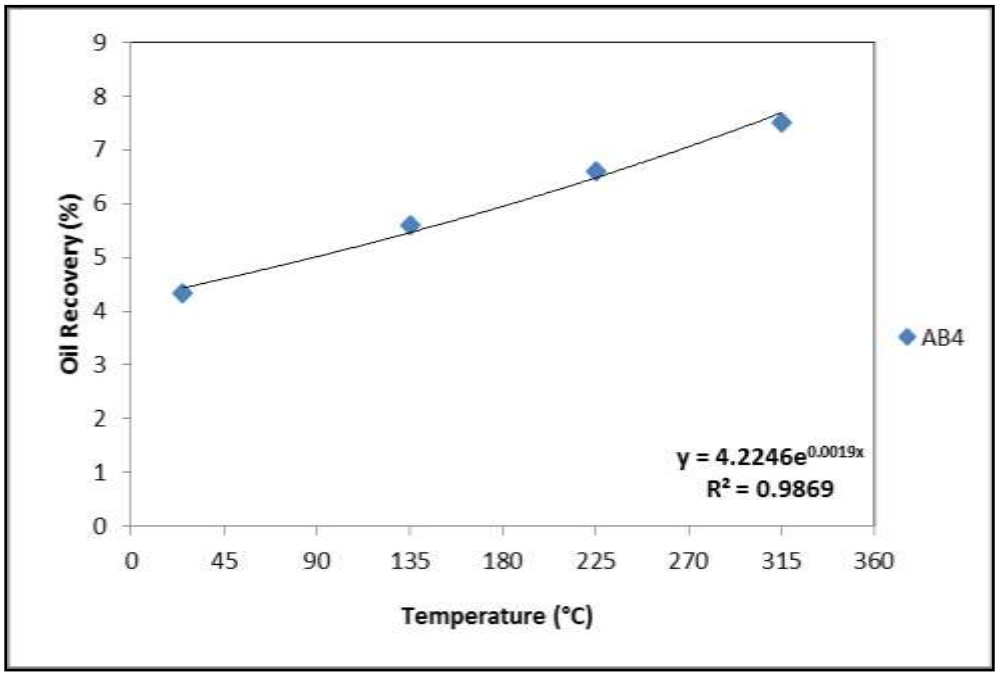

Figure A.34. Oil Recovery at Different Temperatures from Tar-Mat Sample AB4 (Extracted by Surfactant Solution)

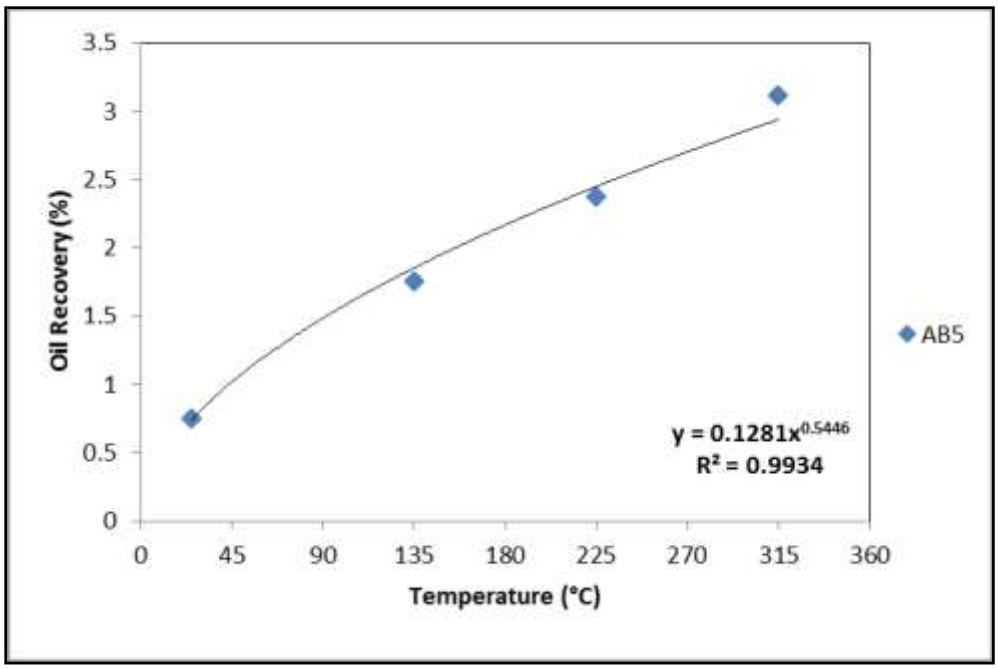

Figure A.35. Oil Recovery at Different Temperatures from Tar-Mat Sample AB5 (Extracted by Surfactant Solution)

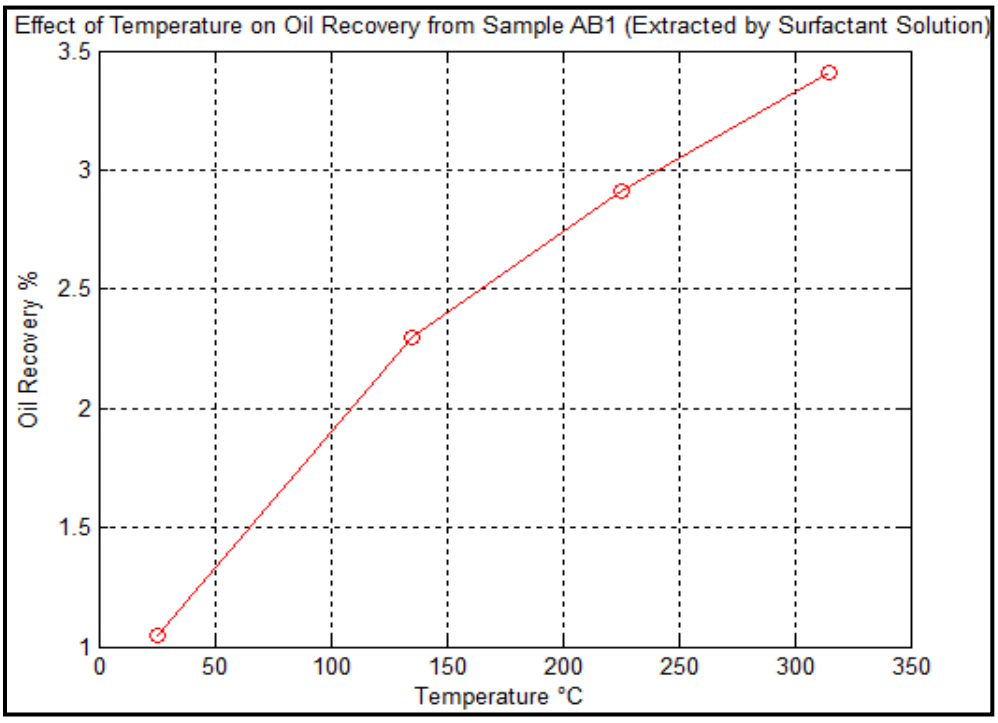

Figure A.36. Calculated Oil Recovery at Different Temperatures Utilizing Eq. 39 (Sample AB1)

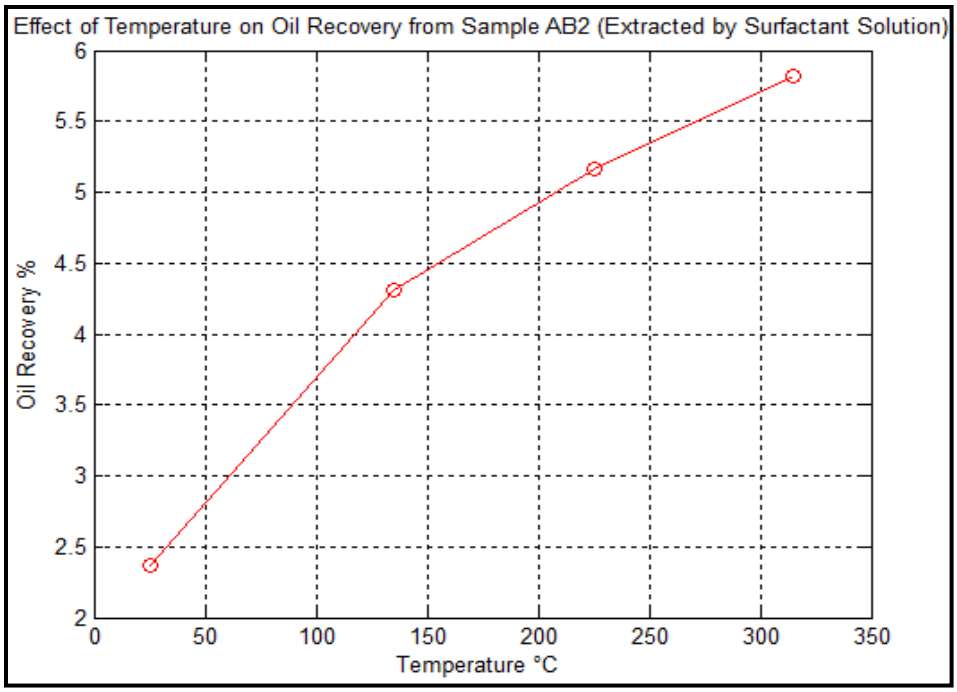

Figure A.37. Calculated Oil Recovery at Different Temperatures Utilizing Eq. 40 (Sample AB2)

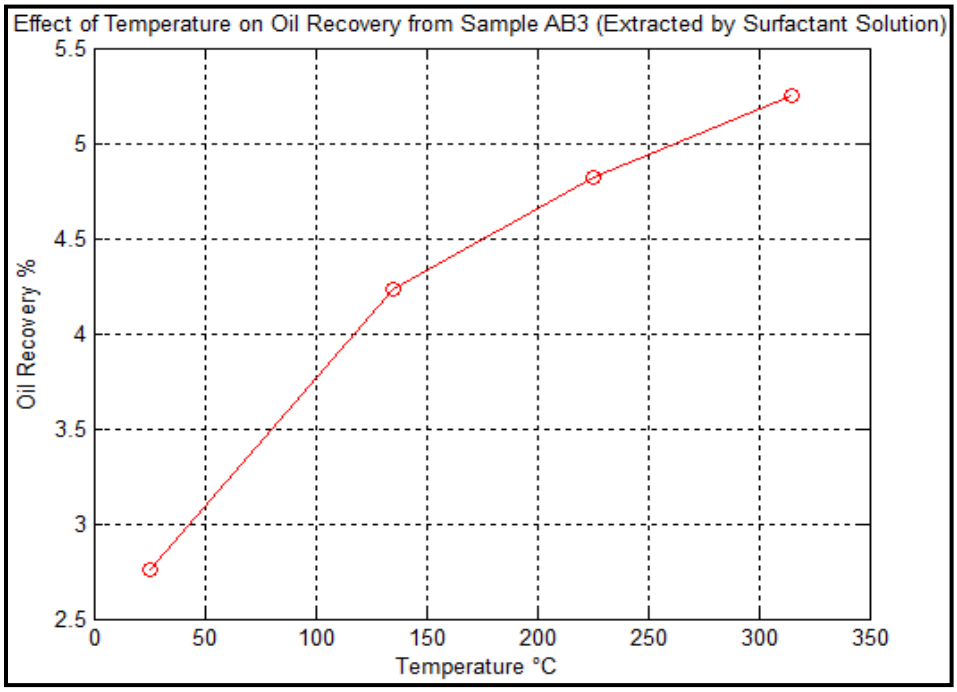

Figure A.38. Calculated Oil Recovery at Different Temperatures Utilizing Eq. 41 (Sample AB3)

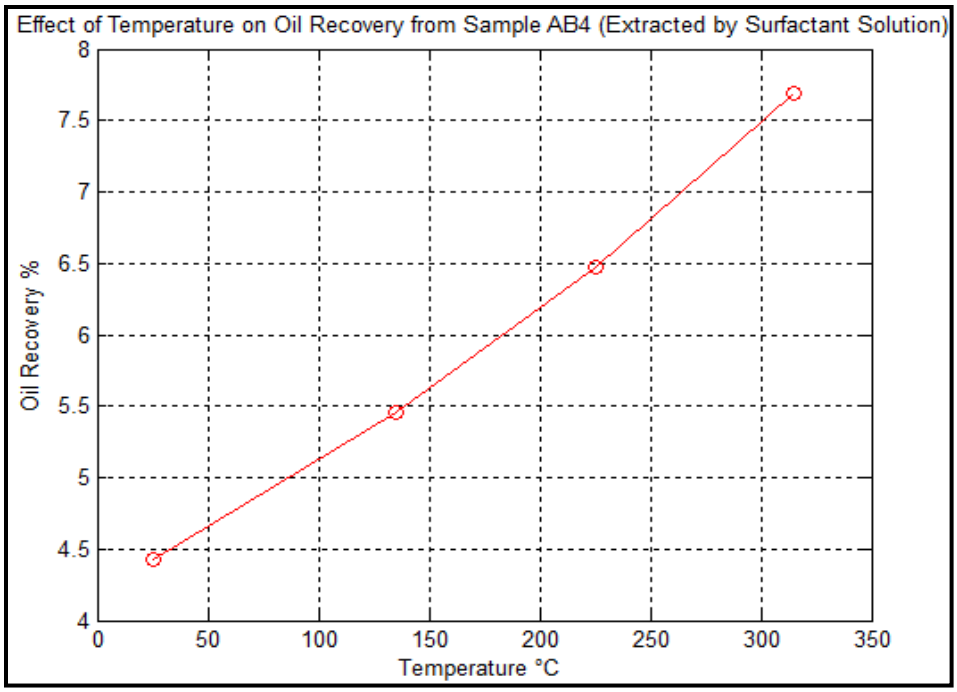

Figure A.39. Calculated Oil Recovery at Different Temperatures Utilizing Eq. 42 (Sample AB4)

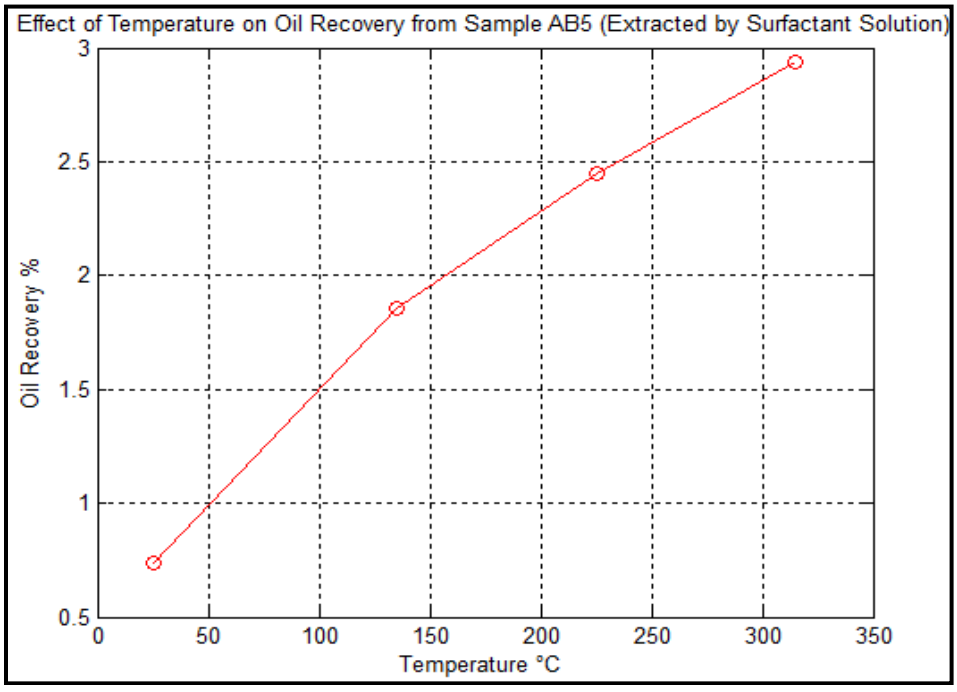

Figure A.40. Calculated Oil Recovery at Different Temperatures Utilizing Eq. 43 (Sample AB5)

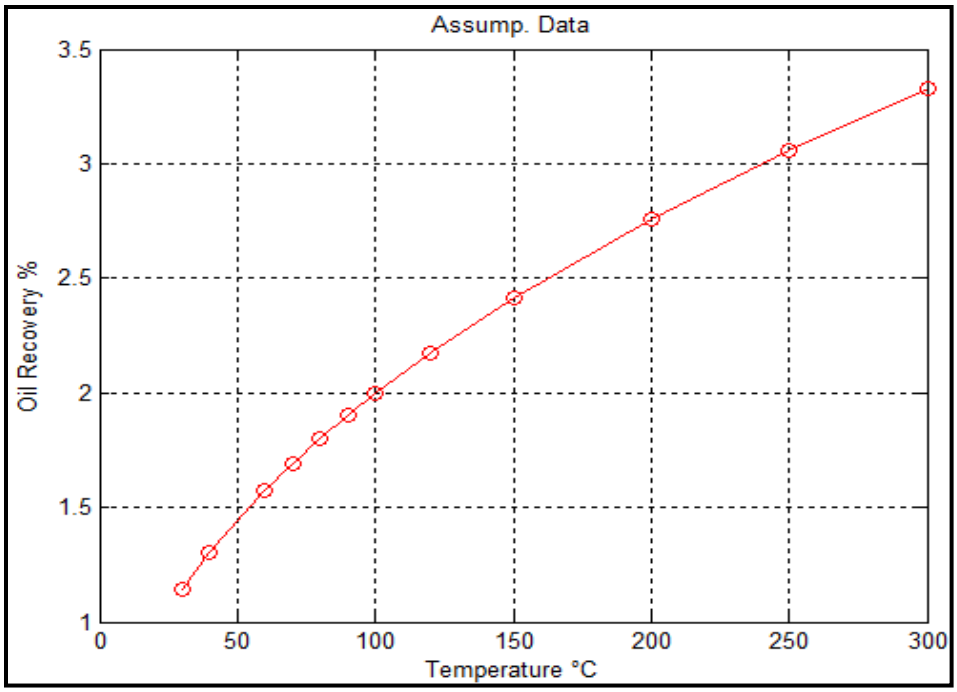

Figure A.41. Calculated Oil Recovery at Assumed Temperatures Utilizing Eq. 39 (Sample AB1)

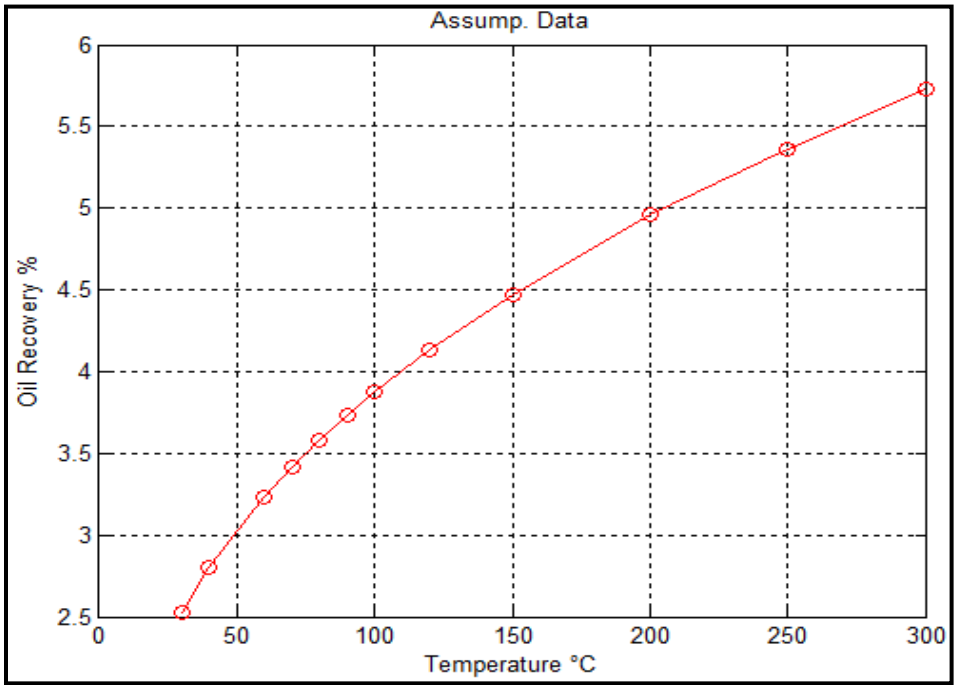

Figure A.42. Calculated Oil Recovery at Assumed Temperatures Utilizing Eq. 40 (Sample AB2)

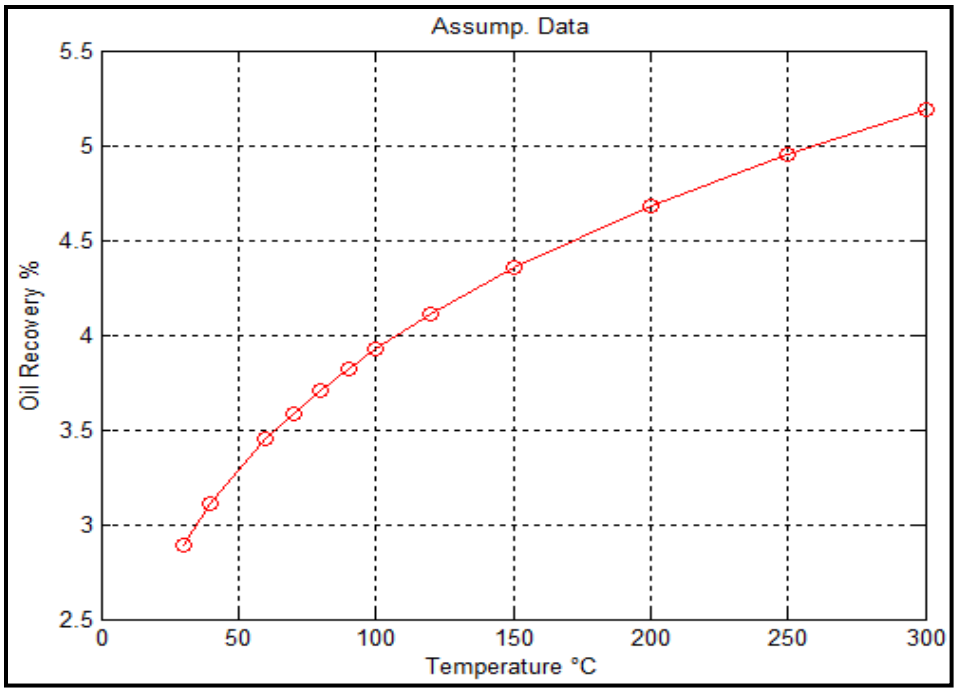

Figure A.43. Calculated Oil Recovery at Assumed Temperatures Utilizing Eq. 41 (Sample AB3)

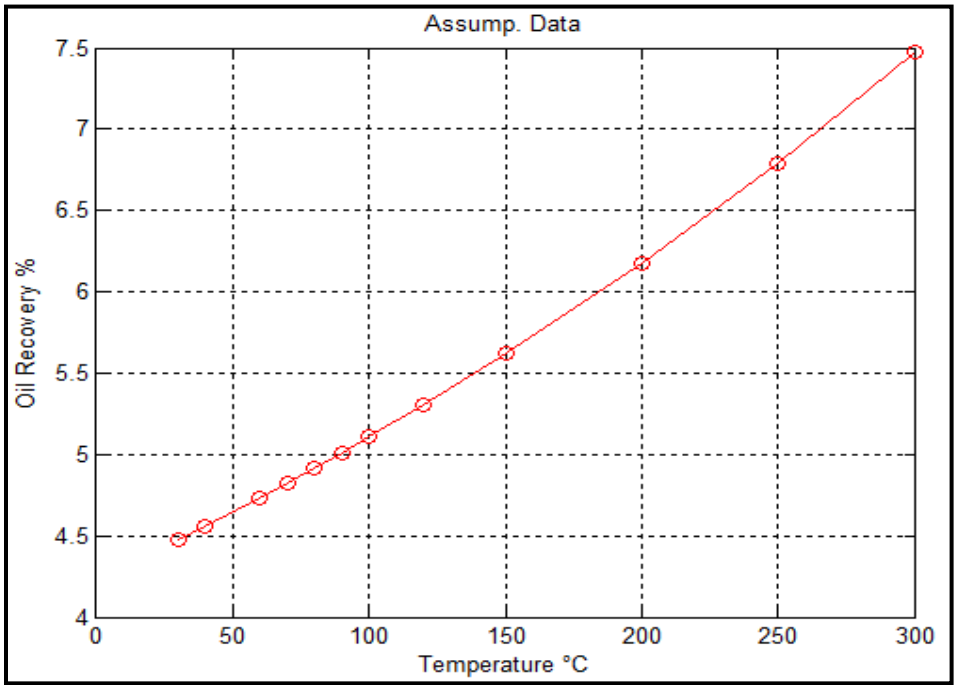

Figure A.44. Calculated Oil Recovery at Assumed Temperatures Utilizing Eq. 42 (Sample AB4)

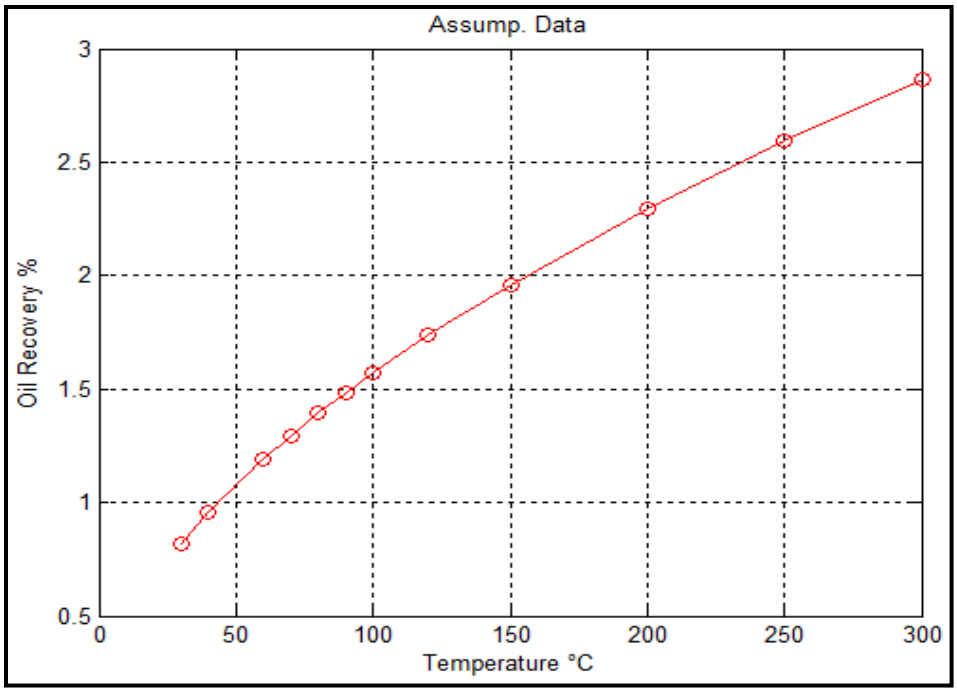

Figure A.45. Calculated Oil Recovery at Assumed Temperatures Utilizing Eq. 43 (Sample AB5)

APPENDIX B.

OIL RECOVERY CALCULATED RESULTS

Table B.1. Calculated Oil Recovery from Sample AB1 Based on Assumed Input Temperature Values Utilizing Eq. 29 (Extracted by Toluene)

Sample	T (°C)	Oil Recovery (%)
AB1	30	1.66
	40	1.73
	60	1.90
	70	1.98
	80	2.08
	90	2.17
	100	2.27
	120	2.48
	150	2.84
	200	3.56
	250	4.46
	300	5.59

Table B.2. Calculated Oil Recovery from Sample AB2 Based on Assumed Input Temperatures Values Utilizing Eq. 30 (Extracted by Toluene)

Sample	T (°C)	Oil Recovery (%)
AB2	30	13.90
	40	14.01
	60	14.24
	70	14.35
	80	14.47
	90	14.59
	100	14.70
	120	14.94
	150	15.30
	200	15.93
	250	16.58
	300	17.25

Table B.3. Calculated Oil Recovery from Sample AB3 Based on Assumed Input Temperature Values Utilizing Eq. 31 (Extracted by Toluene)

Sample	T (°C)	Oil Recovery
AB3	30	17.54
	40	17.86
	60	18.52
	70	18.85
	80	19.20
	90	19.55
	100	19.90
	120	20.63
	150	21.77
	200	23.82
	250	26.07
	300	28.52

Table B.4. Calculated Oil Recovery from Sample AB4 Based on Assumed Input Temperatures Values Utilizing Eq. 32 (Extracted by Toluene)

Sample	T (°C)	Oil Recovery (%)
AB4	30	15.68
	40	16.27
	60	17.52
	70	18.18
	80	18.87
	90	19.58
	100	20.32
	120	21.88
	150	24.44
	200	29.41
	250	35.39
	300	42.58

Table B.5. Calculated Oil Recovery from Sample AB5 Based on Assumed Input Temperature Values Utilizing Eq. 33 (Extracted by Toluene)

Sample	T (°C)	Oil Recovery (%)
AB5	30	0.95
	40	1.02
	60	1.17
	70	1.25
	80	1.34
	90	1.43
	100	1.53
	120	1.76
	150	2.15
	200	3.03
	250	4.25
	300	5.97

Table B.6. Calculated Oil Recovery from Sample AB1 Based on Assumed Input Temperature Values Utilizing Eq. 34 (Extracted by Hot Water)

Sample	T (°C)	Oil Recovery (%)
AB1	30	0.69
	40	0.80
	60	0.96
	70	1.04
	80	1.10
	90	1.17
	100	1.23
	120	1.34
	150	1.49
	200	1.70
	250	1.89
	300	2.06

Table B.7. Calculated Oil Recovery from Sample AB2 Based on Assumed Input Temperature Values Utilizing Eq. 35 (Extracted by Hot Water)

Sample	T (°C)	Oil Recovery (%)
AB2	30	1.21
	40	1.43
	60	1.80
	70	1.97
	80	2.13
	90	2.28
	100	2.42
	120	2.69
	150	3.06
	200	3.62
	250	4.12
	300	4.57

Table B.8. Calculated Oil Recovery from Sample AB3 Based on Assumed Input Temperature Values Utilizing Eq. 36 (Extracted by Hot Water)

Sample	T (°C)	Oil Recovery (%)
AB3	30	2.02
	40	2.20
	60	2.47
	70	2.58
	80	2.68
	90	2.77
	100	2.86
	120	3.01
	150	3.21
	200	3.49
	250	3.72
	300	3.92

Table B.9. Calculated Oil Recovery from Sample AB4 Based on Assumed Input Temperature Values Utilizing Eq. 37 (Extracted by Hot Water)

Sample	T (°C)	Oil Recovery (%)
AB4	30	3.71
	40	3.78
	60	3.92
	70	3.99
	80	4.06
	90	4.14
	100	4.21
	120	4.37
	150	4.61
	200	5.04
	250	5.52
	300	6.04

Table B.10. Calculated Oil Recovery from Sample AB5 Based on Assumed Input Temperature Values Utilizing Eq. 38 (Extracted by Hot Water)

Sample	T (°C)	Oil Recovery (%)
AB5	30	0.52
	40	0.63
	60	0.81
	70	0.89
	80	0.97
	90	1.05
	100	1.12
	120	1.25
	150	1.44
	200	1.73
	250	1.99
	300	2.23

Table B.11. Calculated Oil Recovery from Sample AB1 Based on Assumed Input Temperature Values Utilizing Eq. 39 (Extracted by Surfactant Solution)

Sample	T (°C)	Oil Recovery (%)
AB1	30	1.14
	40	1.31
	60	1.58
	70	1.69
	80	1.80
	90	1.90
	100	2.00
	120	2.18
	150	2.41
	200	2.76
	250	3.06
	300	3.33

Table B.12. Calculated Oil Recovery from Sample AB2 Based on Assumed Input Temperature Values Utilizing Eq. 40 (Extracted by Surfactant Solution)

Sample	T (°C)	Oil Recovery (%)
AB2	30	2.53
	40	2.80
	60	3.23
	70	3.41
	80	3.58
	90	3.73
	100	3.87
	120	4.13
	150	4.47
	200	4.96
	250	5.37
	300	5.72

Table B.13. Calculated Oil Recovery from Sample AB3 Based on Assumed Input Temperature Values Utilizing Eq. 41 (Extracted by Surfactant Solution)

Sample	T (°C)	Oil Recovery (%)
AB3	30	2.89
	40	3.11
	60	3.45
	70	3.59
	80	3.71
	90	3.82
	100	3.93
	120	4.11
	150	4.35
	200	4.68
	250	4.95
	300	5.19

Table B.14. Calculated Oil Recovery from Sample AB4 Based on Assumed Input Temperature Values Utilizing Eq. 42 (Extracted by Surfactant Solution)

Sample	T (°C)	Oil Recovery (%)
AB4	30	4.47
	40	4.56
	60	4.73
	70	4.83
	80	4.92
	90	5.01
	100	5.11
	120	5.31
	150	5.62
	200	6.18
	250	6.79
	300	7.47

Table B.15. Calculated Oil Recovery from Sample AB5 Based on Assumed Input Temperature Values Utilizing Eq. 43 (Extracted by Surfactant Solution)

Sample	T (°C)	Oil Recovery (%)
AB5	30	0.82
	40	0.96
	60	1.19
	70	1.30
	80	1.39
	90	1.49
	100	1.57
	120	1.74
	150	1.96
	200	2.29
	250	2.59
	300	2.86

APPENDIX C.

MAIN MATLAB PROGRAM CODES

C.1. MATLAB CODES FOR API-NSO MODEL

```
% °API calculation

clear all, clc


NSO1=[0 67.2 76.1 74.4 369.19 475.5]; % input data (mg/g)
NSO2=[1 1.5 2 2.5 3 4 5 10 15 20 50 75 100 125 150 175 ...
    200 250 275 300 350 400 450 500]; % input assumption data (mg/g)

C1=52.168; % Constant one (-)
C2=-0.584; % constant two (-)
API1=C1*NSO1.^C2 % calculate values for each input ( NSOl first input)
API2=C1*NSO2.^C2 % calculate values for each input ( NSO2 first input)


% Plotting Function to plot the °API Vs. NSO   %%

figure(1)
plot(NSO1,API1,'-or')
grid on
xlabel('NSO (mg/g)')
ylabel('API')
title('Correlation between NSO Factor versus Calculated API Gravity
from Five Initial Tar-Mat samples')

figure(2)
plot(NSO2,API2,'-or')
grid on
xlabel('NSO (mg/g)')
ylabel('API')
title('Assump. Data')
```

C.2. MATLAB CODES FOR H/C ASPECT RATIO MODEL

```
% °API calculation


clear all, clc


HC1=[0  0.55  0.56  0.57  1.04  1.26]; % input data ratio of Hydrogen to
Carbone(wt.%)
HC2=[0.1 0.12 0.13 0.14 0.15 0.16 0.17 0.18 0.19 0.2 0.3 0.4 ...
    0.5  0.6  0.7  0.8  0.9  1  2  3  4]; % input assumption data of Hydrogen
to Carbone ratio (wt.%)

C1=1.847; % Constant one (-)
C2=-1.46; % constant two (-)
API1=C1*HC1.^C2 % calculate values for each input ( H/Cl first input)
API2=C1*HC2.^C2 % calculate values for each input ( H/C2 first input)

% Plotting Function to plot the °API Vs. H/C   %%

figure(1)
plot(HC1,API1,'-or')
grid on
xlabel('H/C (wt.%)')
ylabel('API')
title('Calibration Curve Relating Elemental Analysis Ratio of H/C
versus Calculated API Gravity')

figure(2)
plot(HC2,API2,'-or')
grid on
xlabel('H/C (wt.%)')
ylabel('API')
title('Assump. Data')
```

C.3. MATLAB CODES FOR THE MODEL FOR THE EFFECT OF TEMPERATURE ON OIL RECOVERY BY TOLUENE

```
% Effect of temperature on oil recovery

clear all, clc

% Toluene Method

% Effect of Different temperatures on tar-mat sample AB1 with API
gravity (1.34 °API)

T1=[25 135 225 315]; % input data temperature used for extracting the
oil from Sample AB1(°C)
T2=[30 40 60 70 80 90 100 120 150 200 250 300]; % input assumed data of
different temperatures that can be applied to show the amount of oil
recovery can be produced(°C)

C1=1.448; % Constant one (-)
C2=0.0045; % constant two (-)
AB11=C1*exp(C2*T1) % calculate values for each input ( T1 first input)
AB12=C1*exp(C2*T2) % calculate values for each input ( T2 first input)

% Plotting Function to plot the Oil Recovery Vs. Temperature   %%

figure(1)
plot(T1,AB11,'-or')
grid on
xlabel('Temperature °C ')
ylabel('Oil Recovery %')
title('Effect of Temperature on Oil Recovery from Sample AB1 (Extracted
by Toluene)')

figure(2)
plot(T2,AB12,'-or')
grid on
xlabel('Temperature °C')
ylabel('Oil Recovery %')
title('Assump. Data')

% Sample AB2 with API gravity (5.17 °API)

T1=[25 135 225 315]; % input data temperature used for extracting the
oil from Sample AB2(°C)
T2=[30 40 60 70 80 90 100 120 150 200 250 300]; % input assumed data of
different temperatures that can be applied to show the amount of oil
recovery can be produced(°C)

C1=13.572; % Constant one (-)
C2=0.0008; % constant two (-)
AB21=C1*exp(C2*T1) % calculate values for each input ( T1 first input)
AB22=C1*exp(C2*T2) % calculate values for each input ( T2 first input)
```

```
% Plotting Function to plot the Oil Recovery Vs. Temperature   %%

figure(3)
plot(T1,AB21,'-or')
grid on
xlabel('Temperature °C ')
ylabel('Oil Recovery %')
title('Effect of Temperature on Oil Recovery from Sample AB2 (Extracted
by Toluene)')

figure(4)
plot(T2,AB22,'-or')
grid on
xlabel('Temperature °C')
ylabel('Oil Recovery %')
title('Assump. Data')

% Sample AB3 with API gravity (4.1 °API)

T1=[25 135 225 315]; % input data temperature used for extracting the
oil from Sample AB3(°C)
T2=[30 40 60 70 80 90 100 120 150 200 250 300]; % input assumed data of
different temperatures that can be applied to show the amount of oil
recovery can be produced(°C)

C1=16.622; % Constant one (-)
C2=0.0018; % constant two (-)
AB31=C1*exp(C2*T1) % calculate values for each input ( T1 first input)
AB32=C1*exp(C2*T2) % calculate values for each input ( T2 first input)

% Plotting Function to plot the Oil Recovery Vs. Temperature   %%

figure(5)
plot(T1,AB31,'-or')
grid on
xlabel('Temperature °C ')
ylabel('Oil Recovery %')
title('Effect of Temperature on Oil Recovery from Sample AB3 (Extracted
by Toluene)')

figure(6)
plot(T2,AB32,'-or')
grid on
xlabel('Temperature °C')
ylabel('Oil Recovery %')
title('Assump. Data')

% Sample AB4 with API gravity (3.76 °API)

T1=[25 135 225 315]; % input data temperature used for extracting the
oil from Sample AB4(°C)
T2=[30 40 60 70 80 90 100 120 150 200 250 300]; % input assumed data of
different temperatures that can be applied to show the amount of oil
recovery can be produced(°C)
```

```
C1=14.033; % Constant one (-)
C2=0.0037; % constant two (-)
AB41=C1*exp(C2*T1) % calculate values for each input ( T1 first input)
AB42=C1*exp(C2*T2) % calculate values for each input ( T2 first input)

% Plotting Function to plot the Oil Recovery Vs. Temperature   %%

figure(7)
plot(T1,AB41,'-or')
grid on
xlabel('Temperature °C ')
ylabel('Oil Recovery %')
title('Effect of Temperature on Oil Recovery from Sample AB4 (Extracted
by Toluene)')

figure(8)
plot(T2,AB42,'-or')
grid on
xlabel('Temperature °C')
ylabel('Oil Recovery %')
title('Assump. Data')

% Sample AB5 with API gravity (1.72 °API)

T1=[25 135 225 315]; % input data temperature used for extracting the
oil from Sample AB5(°C)
T2=[30 40 60 70 80 90 100 120 150 200 250 300]; % input assumed data of
different temperatures that can be applied to show the amount of oil
recovery can be produced(°C)

C1=0.7766; % Constant one (-)
C2=0.0068; % constant two (-)
AB51=C1*exp(C2*T1) % calculate values for each input ( T1 first input)
AB52=C1*exp(C2*T2) % calculate values for each input ( T2 first input)

% Plotting Function to plot the Oil Recovery Vs. Temperature   %%

figure(9)
plot(T1,AB51,'-or')
grid on
xlabel('Temperature °C ')
ylabel('Oil Recovery %')
title('Effect of Temperature on Oil Recovery from Sample AB5 (Extracted
by Toluene)')

figure(10)
plot(T2,AB52,'-or')
grid on
xlabel('Temperature °C')
ylabel('Oil Recovery %')
title('Assump. Data')
```

C.4. MATLAB CODES FOR THE MODEL FOR THE EFFECT OF TEMPERATURE ON OIL RECOVERY BY HOT WATER

```
% Effect of temperature on oil recovery

clear all, clc

% Hot Water Method

% Effect of Different temperatures on tar-mat sample AB1 with API
gravity (1.34 ˚API)

T1=[25 135 225 315]; % input data temperature used for extracting the
oil from Sample AB1(˚C)
T2=[30 40 60 70 80 90 100 120 150 200 250 300]; % input assumed data of
different temperatures that can be applied to show the amount of oil
recovery can be produced(˚C)

C1=0.1389; % Constant one (-)
C2=0.4732; % constant two (-)
AB11=C1*T1.^C2 % calculate values for each input ( T1 first input)
AB12=C1*T2.^C2 % calculate values for each input ( T2 first input)

% Plotting Function to plot the Oil Recovery Vs. Temperature   %%

figure(1)
plot(T1,AB11,'-or')
grid on
xlabel('Temperature ˚C ')
ylabel('Oil Recovery %')
title('Effect of Temperature on Oil Recovery from Sample AB1 (Extracted
by Hot Water)')

figure(2)
plot(T2,AB12,'-or')
grid on
xlabel('Temperature ˚C')
ylabel('Oil Recovery %')
title('Assump. Data')

% Sample AB2 with API gravity (5.17 ˚API)

T1=[25 135 225 315]; % input data temperature used for extracting the
oil from Sample AB2(˚C)
T2=[30 40 60 70 80 90 100 120 150 200 250 300]; % input assumed data of
different temperatures that can be applied to show the amount of oil
recovery can be produced(˚C)

C1=0.1686; % Constant one (-)
C2=0.5787; % constant two (-)
AB21=C1*T1.^C2 % calculate values for each input ( T1 first input)
AB22=C1*T2.^C2 % calculate values for each input ( T2 first input)
```

```
% Plotting Function to plot the Oil Recovery Vs. Temperature   %%

figure(3)
plot(T1,AB21,'-or')
grid on
xlabel('Temperature °C ')
ylabel('Oil Recovery %')
title('Effect of Temperature on Oil Recovery from Sample AB2 (Extracted
by Hot Water)')

 figure(4)
plot(T2,AB22,'-or')
grid on
xlabel('Temperature °C')
ylabel('Oil Recovery %')
title('Assump. Data')

% Sample AB3 with API gravity (4.1 °API)

T1=[25 135 225 315]; % input data temperature used for extracting the
oil from Sample AB3(°C)
T2=[30 40 60 70 80 90 100 120 150 200 250 300]; % input assumed data of
different temperatures that can be applied to show the amount of oil
recovery can be produced(°C)

C1=0.761; % Constant one (-)
C2=0.2875; % constant two (-)
AB31=C1*T1.^C2 % calculate values for each input ( T1 first input)
AB32=C1*T2.^C2 % calculate values for each input ( T2 first input)

% Plotting Function to plot the Oil Recovery Vs. Temperature   %%

figure(5)
plot(T1,AB31,'-or')
grid on
xlabel('Temperature °C ')
ylabel('Oil Recovery %')
title('Effect of Temperature on Oil Recovery from Sample AB3 (Extracted
by Hot Water)')

figure(6)
plot(T2,AB32,'-or')
grid on
xlabel('Temperature °C')
ylabel('Oil Recovery %')
title('Assump. Data')

% Sample AB4 with API gravity (3.76 °API)

T1=[25 135 225 315]; % input data temperature used for extracting the
oil from Sample AB4(°C)
T2=[30 40 60 70 80 90 100 120 150 200 250 300]; % input assumed data of
different temperatures that can be applied to show the amount of oil
recovery can be produced(°C)
```

```
C1=3.5193; % Constant one (-)
C2=0.0018; % constant two (-)
AB41=C1*exp(C2*T1) % calculate values for each input ( T1 first input)
AB42=C1*exp(C2*T2) % calculate values for each input ( T2 first input)

% Plotting Function to plot the Oil Recovery Vs. Temperature   %%

figure(7)
plot(T1,AB41,'-or')
grid on
xlabel('Temperature °C ')
ylabel('Oil Recovery %')
title('Effect of Temperature on Oil Recovery from Sample AB4 (Extracted
by Hot Water)')

figure(8)
plot(T2,AB42,'-or')
grid on
xlabel('Temperature °C')
ylabel('Oil Recovery %')
title('Assump. Data')

% Sample AB5 with API gravity (1.72 °API)

T1=[25 135 225 315]; % input data temperature used for extracting the
oil from Sample AB5(°C)
T2=[30 40 60 70 80 90 100 120 150 200 250 300]; % input assumed data of
different temperatures that can be applied to show the amount of oil
recovery can be produced(°C)

C1=0.062; % Constant one (-)
C2=0.6279; % constant two (-)
AB51=C1*T1.^C2 % calculate values for each input ( T1 first input)
AB52=C1*T2.^C2 % calculate values for each input ( T2 first input)

% Plotting Function to plot the Oil Recovery Vs. Temperature   %%

figure(9)
plot(T1,AB51,'-or')
grid on
xlabel('Temperature °C ')
ylabel('Oil Recovery %')
title('Effect of Temperature on Oil Recovery from Sample AB5 (Extracted
by Hot Water)')

figure(10)
plot(T2,AB52,'-or')
grid on
xlabel('Temperature °C')
ylabel('Oil Recovery %')
title('Assump. Data')
```

C.5. MATLAB CODES FOR THE MODEL FOR THE EFFECT OF TEMPERATURE ON OIL RECOVERY BY SURFACTANT SOLUTION

```
% Effect of temperature on oil recovery

clear all, clc

% Surfactant Solution Method

% Effect of Different temperatures on tar-mat sample AB1 with API
gravity (1.34 °API)

T1=[25 135 225 315]; % input data temperature used for extracting the
oil from Sample AB1(°C)
T2=[30 40 60 70 80 90 100 120 150 200 250 300]; % input assumed data of
different temperatures that can be applied to show the amount of oil
recovery can be produced(°C)

C1=0.235; % Constant one (-)
C2=0.4648; % constant two (-)
AB11=C1*T1.^C2 % calculate values for each input ( T1 first input)
AB12=C1*T2.^C2 % calculate values for each input ( T2 first input)

% Plotting Function to plot the Oil Recovery Vs. Temperature   %%

figure(1)
plot(T1,AB11,'-or')
grid on
xlabel('Temperature °C ')
ylabel('Oil Recovery %')
title('Effect of Temperature on Oil Recovery from Sample AB1 (Extracted
by Surfactant Solution)')

figure(2)
plot(T2,AB12,'-or')
grid on
xlabel('Temperature °C')
ylabel('Oil Recovery %')
title('Assump. Data')

% Sample AB2 with API gravity (5.17 °API)

T1=[25 135 225 315]; % input data temperature used for extracting the
oil from Sample AB2(°C)
T2=[30 40 60 70 80 90 100 120 150 200 250 300]; % input assumed data of
different temperatures that can be applied to show the amount of oil
recovery can be produced(°C)

C1=0.7552; % Constant one (-)
C2=0.3551; % constant two (-)
AB21=C1*T1.^C2 % calculate values for each input ( T1 first input)
```

```
AB22=C1*T2.^C2 % calculate values for each input ( T2 first input)

% Plotting Function to plot the Oil Recovery Vs. Temperature   %%

figure(3)
plot(T1,AB21,'-or')
grid on
xlabel('Temperature °C ')
ylabel('Oil Recovery %')
title('Effect of Temperature on Oil Recovery from Sample AB2 (Extracted
by Surfactant Solution)')

 figure(4)
plot(T2,AB22,'-or')
grid on
xlabel('Temperature °C')
ylabel('Oil Recovery %')
title('Assump. Data')

% Sample AB3 with API gravity (4.1 °API)

T1=[25 135 225 315]; % input data temperature used for extracting the
oil from Sample AB3(°C)
T2=[30 40 60 70 80 90 100 120 150 200 250 300]; % input assumed data of
different temperatures that can be applied to show the amount of oil
recovery can be produced(°C)

C1=1.2211; % Constant one (-)
C2=0.2536; % constant two (-)
AB31=C1*T1.^C2 % calculate values for each input ( T1 first input)
AB32=C1*T2.^C2 % calculate values for each input ( T2 first input)

% Plotting Function to plot the Oil Recovery Vs. Temperature   %%

figure(5)
plot(T1,AB31,'-or')
grid on
xlabel('Temperature °C ')
ylabel('Oil Recovery %')
title('Effect of Temperature on Oil Recovery from Sample AB3 (Extracted
by Surfactant Solution)')

figure(6)
plot(T2,AB32,'-or')
grid on
xlabel('Temperature °C')
ylabel('Oil Recovery %')
title('Assump. Data')

% Sample AB4 with API gravity (3.76 °API)

T1=[25 135 225 315]; % input data temperature used for extracting the
oil from Sample AB4(°C)
```

```
T2=[30 40 60 70 80 90 100 120 150 200 250 300]; % input assumed data of
different temperatures that can be applied to show the amount of oil
recovery can be produced(°C)
C1=4.2246; % Constant one (-)
C2=0.0019; % constant two (-)
AB41=C1*exp(C2*T1) % calculate values for each input ( T1 first input)
AB42=C1*exp(C2*T2) % calculate values for each input ( T2 first input)

% Plotting Function to plot the Oil Recovery Vs. Temperature   %%

figure(7)
plot(T1,AB41,'-or')
grid on
xlabel('Temperature °C ')
ylabel('Oil Recovery %')
title('Effect of Temperature on Oil Recovery from Sample AB4 (Extracted
by Surfactant Solution)')

figure(8)
plot(T2,AB42,'-or')
grid on
xlabel('Temperature °C')
ylabel('Oil Recovery %')
title('Assump. Data')

% Sample AB5 with API gravity (1.72 °API)

T1=[25 135 225 315]; % input data temperature used for extracting the
oil from Sample AB5(°C)
T2=[30 40 60 70 80 90 100 120 150 200 250 300]; % input assumed data of
different temperatures that can be applied to show the amount of oil
recovery can be produced(°C)

C1=0.1281; % Constant one (-)
C2=0.5446; % constant two (-)
AB51=C1*T1.^C2 % calculate values for each input ( T1 first input)
AB52=C1*T2.^C2 % calculate values for each input ( T2 first input)

% Plotting Function to plot the Oil Recovery Vs. Temperature   %%

figure(9)
plot(T1,AB51,'-or')
grid on
xlabel('Temperature °C ')
ylabel('Oil Recovery %')
title('Effect of Temperature on Oil Recovery from Sample AB5 (Extracted
by Surfactant Solution)')

figure(10)
plot(T2,AB52,'-or')
grid on
xlabel('Temperature °C')
ylabel('Oil Recovery %')
title('Assump. Data')
```

BIBLIOGRAPHY

Abu-Khamsin, S. A. (2002). Feasibility of In-Situ Combustion of Tar from a Tarmat Reservoir. *Journal of Petroleum Science & Technology*, 20:3&4, pp. 393-403.

Abu-Khamsin, S. A., Ayub, M., Al-Marhoun, M. A., and Menouar, H. (1993). Waterflooding in a Tarmat Reservoir Laboratory Model. *Journal of Petroleum Science & Engineering*, 9:3, pp. 251-261.

Acharya, U. B. (1987). Effect of Tarmat on Reservoir Behavior: Reservoir Simulation Case Studies. Proceeding of the Middle East Oil Show, Bahrain, 7-10 March, SPE 15690, http://dx.doi.org/10.2118/15690-MS.

Akkurt, R., Seifert, D., Al-Harbi, A., Al-Beaiji, T. M., Kruspe, T., Thern, H., and Kroken, A. (2008). Real-Time Detection of Tar in Carbonates Using LWD Triple Combo, NMR and Formation Tester in Highly-Deviated Wells. Proceeding of 49th Annual Logging Symposium, Austin, Texas, 25-28 May, SPWA-2008-XXX.

Al-Ali, Z. A. (1988). Improving Oil Recovery from Tarmat Reservoirs by Localized Communication. M.S. Thesis, King Fahad University of Petroleum and Minerals, Dahran, Saudi Arabia.

Al-Harthi, M., Al-Ali, M., and Gunarto, R. (2012). Tar Characterization for Optimum Reservoir Management Strategy. Proceeding of the SPE Saudi Arabia Section Technical Symposium and Exhibition, Al-Khobar, Saudi Arabia, 8-11 April, SPE 160891, http://dx.doi.org/10.2118/160891-MS.

Al-Kaabi, A. A., Menouar, H., Al-Marhoun, M. A., and Al-Hashim, H. S. (1988). Bottomwater Drive in Tarmat Reservoirs. SPEJ 3 (02): 395-400. http://dx.doi.org/10.2118/15687-PA.

Almutairi, S., Al-Obied, M. A., AlYami, I., Shebatalhamd, A., and Al-Shehri, D. A. (2012). Wormhole Propagation in Tar During Matrix Acidizing of Carbonate Formations. Proceeding of the SPE International Symposium and Exhibition on Formation Damage Control, Lafayette, Louisiana, USA, 15-17 February, SPE 151560, http://dx.doi.org/10.2118/151560-MS.

Al-Shehri, D. A., Kanfar, M., Al-Ansari Yusuf, S., and Syed, A. F. (2011). Utilizing NMR and Formation Pressure Testing While Drilling to Place Water Injectors Optimally in a Field in Saudi Arabia. Proceeding of the SPE Middle East Oil and Gas Show and Conference, Manama, Bahrain, 25-28 September, SPE 141783, http://dx.doi.org/10.2118/141783-MS.

Al-Umran, M. I., Al-Dossary, K. A., and Nasr-El-Din, H. A. (2005). Successful Treatment to Enhance the Performance of Horizontal Wells Drilling Near Tar-Mat Areas. Proceeding of the International Petroleum Technology Conference, Doha, Qatar, 21-23 November, IPTC 10188, http://dx.doi.org/10.2523/10188-MS.

Avramidis, P., and Zelilidis, A. (2007). Potential Source Rocks, Organic Geochemistry and Thermal Maturation in the Southern Depocenter (Kipourio-Grevena) of the Mesohellenic Basin, Central Greece. *International Journal of Coal Geology*, 71 (4), pp. 554-567. DOI: 10.1016/j.coal.2006.12.006.

Bashbush, J. L., Savage, W. K., Nagai, R. B., Ogimoto, T., Wakamiya, J., and Takizawa, H. (1983). A Reservoir Optimization Study-El Bunduq Field, Abu Dhabi, Qatar. Proceeding of the Middle East Oil Technical Conference and Exhibition, Bahrain, 14-17 March, SPE 11481, http://dx.doi.org/10.2118/11481-MS.

Carpentier, B., Arab, H., Pluchery, E. and Chautru, J. (2007). Tar Mats and Residual Oil Distribution in a Giant Oil Field Offshore Abu Dhabi. *Journal of Petroleum Science and Engineering* 58, pp. 472-490. DOI: 10.1016/j.petrol.2006.12.009.

Carpentier, B., Huc, A.-Y., Marquis, F., Badr, A. E. R., Al Aldarous, A. A., and Al-Baker, S. (1998). Distribution and Origin of a Tar Mat in the S. Field (Abu Dhabi, U.A.E.). Proceeding of the Abu Dhabi International Petroleum Exhibition and Conference, Abu Dhabi, United Arab Emirates, 11-14 November, SPE 49472, http://dx.doi.org/10.2118/49472-MS.

Chen, C., Guo, J., An, N., Ren, B., Li, Y., and Jiang, Q. (2013). Study of Asphaltene Deposition from Tahe Crude Oil. *Journal of Petroleum Science*, 10 (1). pp. 134 – 138. DOI: 10.1007/s12182-013-0260-y.

Clementz, D. M., Demaison, G. J. and Daly, A. R. (1979). Well Site Geochemistry by Programmed Pyrolysis. Proceedings of the 11th Annual Offshore Technology Conference, Houston, OTC 3410, v.1, 465-47, http://dx.doi.org/10.4043/3410-MS.

Cubitt, J. M., England, W. A., and Larter, S. (2004). Understanding Petroleum Reservoirs: Towards an Integrated Engineering and Geochemical Approach. Geol. Soc. Lond. Spec. Publ. 237.

Dembicki, J. H. (2009). Three Common Source Rock Evaluation Errors Made by Geologists During Prospect or Play Appraisals. AAPG Bulletin, v. 93, no. 3, p. 341-356. DOI: 10.1306/10230808076.

Dessort, D., Gelin, F., Duclerc, D., and Le-Van-Loi, R. (2012). Enhanced Assessment of the Distribution of Organic Matter in Unconventional Plays and Tarmat in Reservoirs Using a New Laser Pyrolysis Method on Core. Proceeding of the Abu Dhabi International Petroleum Exhibition and Conference, Abu Dhabi, United Arab Emirates, 11-14 November, SPE 161626, http://dx.doi.org/10.2118/161626-MS.

Dow, W. G., Allen, J. R. and Kuhnel, C. J. (2001). Determination of API Gravity from Very Small Samples of Oils, Tar Mats, and Solid Bitumens with the Rock-Eval 6 Instrument. In: Trindade, L. A. F., Macedo, A. C. & Barbanti, S. M. (eds.) New Perspectives on Organic Geochemistry for the Third Millennium. Proceedings, 7th Latin American Congress on Organic Geochemistry. Foz do Iguacu, Brazil, ALAGO, 22-26 October, 232-236.

Espitalie, J., La Porte, J. L., Madec, M., Marquis, F., Le Plat, P., Paulet, J. and Boutefeu, A. (1977). Rapid Method for Source Rocks Characterization and for Determination of Petroleum Potential and Degree of Evolution. Oil and Gas Science and Technology- Revue de l'Institut Français du Petrole, 32, 23-42.

Geologic Materials Center. (1990). Total Organic Carbon, Rock-Eval Pyrolysis, and Whole Oil Gas Chromatograms of Core from the Standard Alaska Production Co. Sag Delta 34633 No. 4 Well (11,637–12,129) and from the Shell Oil Co. OCS Y-0197 (Tern No. 3) Well (12,978-13,131): State of Alaska Geologic Materials Center Data Report no. 157, total of 4 pages in report < http://www.dggs.dnr.state.ak.us/webpubs/dggs/gmc/text/gmc157.PDF > Accessed 2/14/2010.

Ghasemi-Nejad, E., Head, M.J., and Naderi, M. (2009). Palynology and Petroleum Potential of the Kazhdumi Formation (Cretaceous: Albian–Cenomanian) in the South Pars Field, Northern Persian Gulf. *Journal of Marine and Petroleum Geology* 26:805–816. DOI: 10.1016/j.marpetgeo.2008.05.005.

Groune, K., Halim, M., Benmakhlouf, M., Arsalane, S., Lemee, L., and Ambles, A. (2013). Organic Geochemical and Mineralogical Characterization of the Moroccan Rif Bituminous Rocks. *J. Mater. Environ. Sci.*, 4(4), 472–481.

Haggag Amin, M., and Al-Yaaqoobi, A. (2008). Evaluation of the Bitumen Intervals in a Carbonate Reservoir, Case Study in Abu Dhabi Onshore Field, UAE. Proceeding of the Abu Dhabi International Petroleum Exhibition and Conference, Abu Dhabi, UAE, 3-6 November, SPE 117658, http://dx.doi.org/10.2118/117658-MS.

Harouaka, A. S., Asar, H. K., Al-Arfaj, A. A., Al-Husaini, A. H., and Nofal, W. A. (1991). Characterization of Tar from a Carbonate Reservoir in Saudi Arabia: Part I-Chemical Aspect. Proceeding of the SPE International Symposium on Oilfield Chemistry, Anaheim, California, 20-22 February, SPE 21004, http://dx.doi.org/10.2118/21004-MS.

Harouaka, A. S., Mtawaa, B., and Nofal, W. A. (2002). Characterization of Tar from a Carbonate Reservoir in Saudi Arabia: Physical Aspects. Proceeding of the Abu Dhabi International Petroleum Exhibition and Conference, Abu Dhabi, United Arab Emirates, 13-16 October, SPE 78538, http://dx.doi.org/10.2118/78538-MS.

Hirschberg, A. (1988). Role of Asphaltenes in Compositional Grading of a Reservoir's Fluid Column. SPEJ 40 (01): 89-94. http://dx.doi.org/10.2118/13171-PA.

Huc, A. Y., and Hunt, J. M. (1980). Generation and Migration of Hydrocarbons in Offshore South Texas Gulf Coast Sediments. *Journal of Geochemica et Cosmochimica Acta*, printed in Great Britain, v. 44, p. 1081-1089. DOI: 10.1016/0016-7037(80)90062-9.

Hunky, R. M., Wu, Y., Bai, B., and Dunn-Norman, S. (2010). An Experimental Study of Alkaline Surfactant Flooding for Ultra Shallow Heavy Oil Reservoirs. Proceeding of the SPE Western Regional Meeting, Anaheim, California, USA, 27-29 May, SPE 132537, http://dx.doi.org/10.2118/132537-MS.

Hunt, J. M. (1996). Petroleum Geochemistry and Geology. Second edition: New York, W. H. Freeman, and Company, 743 p.

Jarvie, D. M., Brenda, C., Bo, H. and John, B. (2001). Oil and Shale Gas from the Barnett Shale, Ft. Worth Basin, Texas, AAPG National Convention, June 3-6, Denver, CO, AAPG Bull. Vol. 85, No. 13 (Supplement), p. A100.

Jedaan, N. M. R., Fraisse, C. J., Pluchery, E., De Groen, V. L. N., Dessort, D., and Al Abdulmalik, A. (2007). Characterization, Origin and Repartition of Tar Mat in The Bul Hanine, Arab D Reservoir, Qatar. Proceeding of the International Petroleum Technology Conference, Dubai, United Arab Emarat, 4-6 December, IPTC11812, http://dx.doi.org/10.2523/11812-MS.

Larter, S. R., Adams, J., Gates, I. D., Bennett, B., and Huang, H. (2006). The Origin, Prediction and Impact of Oil Viscosity Heterogeneity on the Production Characteristics of Tar Sand and Heavy Oil Reservoirs. *Journal of Canadian Petroleum Technology* 47 (01), http://dx.doi.org/10.2118/08-01-52.

Moor, L. V. (1984). Significance, Classification of Asphaltic Material in Petroleum Exploration. *Oil & Gas Journal*, v. 82, no. 41 (October 8), p. 109-112.

Nascimento, J.d. D. S. and Gomes, R. M. R. (2004). Tar Mats Characterization from NMR and Conventional Logs, Case Studies in Deepwater Reservoirs, Offshore Brazil. Presented at the SPWLA 45th Annual Logging Symposium, Noordwijk, The Netherlands, 6–9 June. SPWLA-2004-FF.

Newberry, M. E., and Barker, K. M. (2000). Organic Formation Damage Control and Remediation. Proceeding of the SPE International Symposium on Formation Damage Control, Lafayette, Louisiana, 23-24 February, SPE 58723, http://dx.doi.org/10.2118/58723-MS.

Okasha, T. M., Menouar, H. K., and Abu-Khamsin, S. A. (1998). Oil Recovery from Tarmat Reservoirs Using Hot Water and Solvent Flooding. *Journal of Canadian petroleum technology*, 37(4), 33-40. http://dx.doi.org/10.2118/98-04-03.

Osman, M. E. S. (1985). An Approach to Predict Tarmat Breakdown in Minagish Reservoir in Kuwait. SPEJ 37 (11): 2071-2075. http://dx.doi.org/10.2118/11492-PA.

Osman, M. E. S. (1988). Prediction of Tarmat Behavior under Water Injection in the Presence of Two Parallel Faults. Proceeding of the Society of Petroleum Engineers, SPE 17115.

Panuganti, S. R., Vargas, F. M. and Chapman, W. G. (2011). Modeling of Reservoir Connectivity and Tar-Mat Using Gravity-Induced Asphaltene Compositional Grading. *Journal of Energy Fuels*, 26 (5), pp. 2548–2557. DOI**:** 10.1021/ef201280d.

Peters, K. E. (1986). Guidelines for Evaluating Petroleum Source Rock Using Programmed Pyrolysis: AAPG Bulletin, v. 70, no. 3, p. 318-329.

Peters, K. E., and Cassa, M. R. (1994). Applied Source Rock Geochemistry, Chapter 5, in Magoon, L.B., and W.G. Dow, eds., The Petroleum System - From Source to Trap: AAPG Memoir 60, p. 93–120.

Pineda-Flores, G. and Mestahoward, A. M. (2001). Petroleum Asphaltenes: Generated Problematic and Possible Biodegradation Mechanisms. *Journal of Review Latinoam Microbiologia*, 43, 143-150.

Reed, S. and Ewan, H. M. (1986). Geochemical Report, Norse Hydro A/S, 6407/7-1, http://www.npd.no/engelsk/cwi/pbl/geochemical_pdfs/474_7.pdf, Accessed February 8, 2010.

Richardson, J. G., Harris, D. G., Rossen, R. H., and Van Hee, G. (1978). The Effect of Small, Discontinuous Shales on Oil Recovery. SPEJ 30 (11): 1531-1537. http://dx.doi.org/10.2118/6700-PA.

Saenger, A., Cécillon, L., Sebag, D., and Brun, J.-J. (2013). Soil Organic Carbon Quantity, Chemistry and Thermal Stability in a Mountainous Landscape: A Rock–Eval Pyrolysis Survey. *Journal of Organic Geochemistry* 54, pp. 101–114, http://dx.doi.org/10.1016/S0146-6380 (12)00258-6.

Saint, C., Glowig, T., Swain, A. S. S., Al-Khaldi, N. A., Al Otaibi, M. H., Al Ghareeb, A. Aziz, and Al Bader, A. B. (2013). Hydrocarbon Mobility Steering for Optimum Placement of a Power Water Injector above Tar Mats - A Case Study from a Light Oil Carbonate Reservoir in the Middle East. Proceeding of the SPE Middle East Oil and Gas Show and Conference, Manama, Bahrain, 10-13 March, SPE 164282, http://dx.doi.org/10.2118/164282-MS.

Shaaban, F., Lutz, R., Littke, R., Bueker, C., and Odisho, K. (2006). Source-Rock Evaluation and Basin Modelling in NE Egypt (NE Nile Delta and Northern Sinai). *Journal of Petroleum Geology*, v. 29, issue 2, p. 103-124.

Shamaldeen, S. M., and Ali, S. M. F. (1985, January 1). An Experimental Study of Techniques for Increasing Oil Recovery from Oil Reservoirs with Tar Barriers. Proceeding of the Middle East Oil Technical Conference and Exhibition, Bahrain, 11-14 March, SPE 13705, http://dx.doi.org/10.2118/13705-MS.

Spiro, B. (1991). Effects of Minerals on Rock Eval Pyrolysis of Kerogen. *Journal of Thermal Analysis*, v. 37, pp. 1513-1552.

Sykes, R., and Snowdon, L. R. (2002). Guidelines for Assessing the Petroleum Potential of Coaly Source Rocks Using Rock-Eval Pyrolysis. *Journal of Organic Geochemistry*, v. 33, p. 1441-1455. DOI: 10.1016/S0146-6380(02)00183-3.

Tissot, B. P., and Welte, D. H. (1984). Petroleum Formation and Occurrence. 2nd Revised and Enlarged Edition: Berlin Heidelberg New York, Tokyo, Springer-Verlag, p. 699.

Tobey, M. H., Halpern, H. I., Cole, G. A., Lynn, J. D., Al-Dubaisi, J. M., and Sese, P. C. (1993). Geochemical Study of Tar in the Uthmaniyah Reservoir. Proceeding of the Middle East Oil Show, Bahrain, 3-6 April, SPE 25609, http://dx.doi.org/10.2118/25609-MS.

Tripathy, B. (1985). Water Influx Characteristics of Tar Barriers - Their Impact on Injector Locations. Society of Petroleum Engineers, SPE 15203.

Tripathy, B. (1988). Analysis and Evaluation of Alternative Concepts in Modeling Tarmats to Conform to Laboratory Investigations and Field Conditions. SPEJ 3 (04): 1109-1113. http://dx.doi.org/10.2118/15689-PA.

Van Krevelen, D. W. (1993). Coal: Typology – Chemistry –Physics – Constitution, 3rd ed. Elsevier Science, Amsterdam, 979 pp.

Waxman, M. H., Closmann, P. J., and Deeds, C. T. (1980). Peace River Tar Flow Experiments under in Situ Conditions. Proceeding of the SPE Annual Technical Conference and Exhibition, Dallas, Texas, 21-24 September, SPE 9511, http://dx.doi.org/10.2118/9511-MS.

Wilhelms, A. and Larter, S. R. (1994). Origin of Tar Mats in Petroleum Reservoirs. Part 1: Introduction and Case Studies. *Journal of Marin and Petroleum Geology*, v. 11, p. 418-441. DOI: 10.1016/0264-8172(94)90077-9.

Wilhelms, A. and Larter, S. R. (1994). Origin of Tar Mats in Petroleum Reservoirs. Part II: Formation Mechanisms for Tar Mats. *Journal of Marin and Petroleum Geology*, v. 11, p. 442-456. DOI: 10.1016/0264-8172(94)90078-7.

Yen, A., Yin, Y. R., and Asomaning, S. (2001). Evaluating Asphaltene Inhibitors: Laboratory Tests and Field Studies. Proceeding of the SPE International Symposium on Oilfield Chemistry, Houston, Texas, 13-16 February, SPE 65376, http://dx.doi.org/10.2118/65376-MS.

Zuo, J. Y., Mullins, O. C., Mishra, V., Garcia, G., Dong, C., Zhang, D., Pang, J. (2012). Asphaltene Grading, Flow Assurance and Tar Mats in Oil Reservoirs. *Journal of Energy & Fuels*, 26 (3), 1670−1680. Doi/10.1021/ef201218m.

VITA

Abdullah Almansour was born in Najran, Saudi Arabia. Abdullah obtained his bachelor's degree in petroleum geology from King Abdulaziz University in Jeddah-Saudi Arabia in 2004. He earned his master's degree in Information Technology from western Oregon University in 2008.

Abdullah has been working for C.A.T Oil Company in Saudi Arabia for more than one year in Uthmaniyah oil field. Abdullah worked at Saudi Geophysical Company as a petroleum engineer for more than one year.

In 2009, Abdullah has been working at King Abdulaziz City for Science and Technology as academic researcher at oil and gas institute.

In 2010, Abdullah was awarded the King Abdulaziz City for Science and Technology to fund his PhD work at Missouri University of Science and Technology.

PUBLICATIONS:

1. Almansour, A., Al-Bazzaz, W., Saraswathy, G., Almohsin, A., & Bai, B. (2014). Characterization of Next-Generation Heavy Oil of Tar Mats in Carbonate Reservoirs and Understanding Its Role in Reserve Estimation and Oil Recovery Economics. Proceeding of the SPE Saudi Arabia Section Technical Symposium and Exhibition, Al-Khobar, Saudi Arabia, 21-24 April, SPE 172243.

2. Almansour, A. O., Al-Bazzaz, W. H., Saraswathy, G., Sun, Y., Bai, B., & Flori, R. E. (2014). Investigation of the Physical and Chemical Genesis of Deep Tar-Mat Oil and Its Recovery Potential under Different Temperatures. Proceeding of the SPE Heavy Oil Conference, Alberta, Canada, 10-12 June, SPE 170059.

3. Muhammed, F. A., Bai, B., Imqam, A., & Almansour, A. O. (2014). Preformed Particle Gel-Enhanced Surfactant Imbibition for Improving Oil Recovery in Fractured Carbonate Reservoirs. Proceeding of the SPE Heavy Oil Confer
   Alberta, Canada, 10-12 June, SPE 170067.